



Universiteit  
Leiden  
The Netherlands

## Transfer of "goods" from plants to humans: Fundamental and applied biochemical investigations on retaining glycosidases

Kytidou, K.

### Citation

Kytidou, K. (2020, June 25). *Transfer of "goods" from plants to humans: Fundamental and applied biochemical investigations on retaining glycosidases*. Retrieved from <https://hdl.handle.net/1887/123040>

Version: Publisher's Version

License: [Licence agreement concerning inclusion of doctoral thesis in the Institutional Repository of the University of Leiden](#)

Downloaded from: <https://hdl.handle.net/1887/123040>

**Note:** To cite this publication please use the final published version (if applicable).

Cover Page



Universiteit Leiden



The handle <http://hdl.handle.net/1887/123040> holds various files of this Leiden University dissertation.

**Author:** Kytidou, K.

**Title:** Transfer of goods from plants to humans: Fundamental and applied biochemical investigations on retaining glycosidases

**Issue Date:** 2020-06-25

---

# Transfer of “*goods*” from plants to humans

---

Fundamental and applied biochemical investigations on retaining glycosidases

*Kassiani Kytidou*

**Transfer of “goods” from plants to humans: Fundamental and applied biochemical investigations on retaining glycosidases**

***Kassiani Kytidou***

Doctoral thesis, Leiden University 2020

Cover design: Nicola Francesco Toro

Cover description: Crystal structure of alpha galactosidase, A1.1; PDB ID: 6F4C and *Nicotiana benthamiana* plant.

Layout: Kassiani Kytidou

Printing: Ipskamp printing, the Netherlands

© 2020, Kassiani Kytidou. All rights reserved. No part of this book may be reproduced, stored in a retrieval system or transmitted in any form or by any means, without prior permission of the author.

# Transfer of “goods” from plants to humans: Fundamental and applied biochemical investigations on retaining glycosidases

Proefschrift

ter verkrijging van  
de graad van Doctor aan de Universiteit Leiden,  
op gezag van Rector Magnificus prof.mr. C.J.J.M. Stolker,  
volgens besluit van het College voor Promoties  
te verdedigen op donderdag 25 Juni 2020  
klokke 11:15 uur

door

Kassiani Kytidou  
(Κασσιανή Κυτιδου)

geboren te Thessaloniki, Greece

in 1989

# Promotiecommissie

Promotor: Prof. dr. J.M.F.G. Aerts

Co-promotor: Dr. R.G. Boot

Overige leden: Prof. dr. M. van der Stelt  
Prof. dr. J. Brouwer  
Prof. dr. A.H. Meijer  
Prof. dr. C.J.M. de Vries,  
(University van Amsterdam)  
Dr. H.J. Bosch,  
(Wageningen University and Research Center)

*To my unofficial lab partners,  
Dimitris and Foivos*

*To my family,*





# Table of contents

|  |            |
|--|------------|
| <b>List of abbreviations and acronyms</b>  | <b>8</b>   |
| <b>List of activity-based probes coding</b>  | <b>9</b>   |
| <b>Chapter 1</b>   | <b>11</b>  |
| General Introduction and Scope of the thesis   |            |
| <b>Chapter 2</b>   | <b>33</b>  |
| Plant glycosides and glycosidases: a treasure-trove for therapeutics   |            |
| <b>Chapter 3</b>   | <b>81</b>  |
| Human alpha galactosidases transiently produced in <i>Nicotiana benthamiana</i> leaves: new insights in substrate specificities with relevance for Fabry disease |            |
| <b>Chapter 4</b>   | <b>121</b> |
| <i>Nicotiana benthamiana</i> $\alpha$ -galactosidase A1.1 can functionally complement human $\alpha$ -galactosidase A deficiency associated with Fabry disease   |            |
| <b>Chapter 5</b>   | <b>167</b> |
| $\alpha$ -D-Gal-cyclophellitol cyclosulfamidate and Gal-DNJ stabilize therapeutic lysosomal $\alpha$ -galactosidase A and <i>Nicotiana benthamiana</i> , A1.1    |            |
| <b>Chapter 6</b>   | <b>191</b> |
| Cross species investigations with activity-based probes; Future prospects  |            |
| <b>Chapter 7</b>   | <b>219</b> |
| Diagnosis with activity-based probes of inherited glycosidase deficiencies using urine samples   |            |
| <b>Chapter 8</b>   | <b>233</b> |
| General discussion and perspectives for future research  |            |
| <b>Summary</b>   | <b>249</b> |
| <b>Samenvatting</b>  | <b>254</b> |
| <b>Acknowledgements</b>  | <b>258</b> |
| <b>Curriculum vitae</b>  | <b>260</b> |
| <b>Publications</b>  | <b>261</b> |

# List of Abbreviations and acronyms

FD = Fabry disease  
ERT = Enzyme replacement therapy  
 $\alpha$ -GAL A or GLA = human alpha galactosidase  
( $\alpha$ -)NAGA(L) =  $\alpha$ -N-acetyl-galactosaminidase  
( $\alpha$ -)NAGAEL = modified  $\alpha$ -N-acetyl-galactosaminidase  
 $\alpha$ -GAL = any alpha galactosidase, including plant enzymes  
4MU = 4-Methylumbelliferyl  
ABP = Activity-based probe  
CBB = Coomassie brilliant blue  
ConA = Concanavalin A  
Gb3 = globotriaosylceramide  
GlcCer = glucosylceramide  
Cer = ceramide  
lysoGb3 = globotriaosylsphingosine  
LacCer = lactosylceramide  
lysoLacCer = lactosylsphingosine  
mAb = monoclonal antibodies  
Gal-DNJ = deoxygalactonojirimycin  
GBA = human lysosomal glucocerebrosidase  
GAA = human lysosomal alpha glucosidase  
 $\beta$ GLUR = human lysosomal beta glucuronidase  
 $\alpha$ MAN = human alpha mannosidase  
 $\alpha$ FUC = human alpha fucosidase  
 $\beta$ GAL = human beta galactosidase  
HPSE = Heparanase  
MPR = Mannose-6-phosphate receptor  
Man-6-P = Mannose-6-phosphate moieties  
MR = Molecular Replacement  
PD = Parkinson disease  
GD = Gaucher disease  
SDS-PAGE = sodium dodecyl sulfate polyacrylamide gel electrophoresis  
HPLC = High Performance Liquid Chromatography  
LC-MS/MS = Liquid chromatography–mass spectrometry with two mass spectrometers in tandem  
HRP = horseradish peroxidase  
NBD = nitrobenzoxadiazole  
NBD-Gb3 = NBD-C12-globotriaosylceramide  
PBS = Phosphate buffered saline  
DAPI = 4',6'-diamidino-2-phenylindole  
BY2 cells = Bright Yellow 2 *Nicotiana tabacum* cells  
BSA = Bovine serum albumin

RT = real time

A1.1 = *Nicotiana benthamiana* alpha galactosidase, identified in current thesis

B56 = *Nicotiana tabacum* beta glucosidase, identified in current thesis

## List of activity-based probes coding

TB474 = Cy5 labelled alpha galactosidase activity-based probe

ME741 = Biotinylated alpha galactosidase activity-based probe

ME569 = Cy5 labelled epoxide beta glucosidase activity-based probe

ME869 = TAMRA/Biotinylated labelled epoxide beta glucosidase activity-based probe

JJB111 = Biotinylated labelled aziridine beta glucosidase activity-based probe

JJB367 = Cy5 labelled aziridine beta glucosidase activity-based probe

JJB75 = Bodipy-red labelled aziridine beta glucosidase activity-based probe

TB652 = Cy5 labelled aziridine beta galactosidase activity-based probe

JJB381 = Cy5 labelled aziridine alpha fucosidase activity-based probe

JJB383 = Cy5 labelled aziridine alpha glucosidase activity-based probe

JJB392 = Cy5 labelled aziridine beta glucuronidase activity-based probe

KY358 = aziridine beta glucosidase activity-based probe

MDW944 = Bodipy-red labelled epoxide beta glucosidase activity-based probe

TB482 = Cy5 labelled aziridine alpha mannosidase activity-based probe

TB434 = Cy5 labelled aziridine beta mannosidase activity-based probe



# Chapter 1

---

General introduction and  
Scope of the thesis

---



## Introduction

### Lysosomal enzymes and their function

In 1955 Christian de Duve and colleagues were the first to observe the existence of distinct membrane-enclosed acidic cellular organelles, that were named lysosomes to reflect their “lytic” nature (Appelmans et al. 1955). Lysosomes fulfil various functions ranging from turnover of endogenous macromolecules from the extracellular space and the cell itself to the supply of the cytosol with vital nutrients and degradation of pathogens (Parkinson-Lawrence et al. 2010). Degradation of very different macromolecules such as sphingolipids, glycogen, mucopolysaccharides and glycoproteins takes place in lysosomes. Macromolecular substrates for degradation are delivered into lysosomes via endocytic and autophagy pathways (Futerman and van Meer 2004). Lysosomes contain over 60 soluble acid hydrolases mediating fragmentation of macromolecules to building blocks that are exported to the cytosol via transporters in the lysosomal membrane (Platt 2014). The lysosomal membrane contains several heavily glycosylated integral membrane proteins with function in transport, interactions with the cytosol, endosomes and autophagosomes and provide stability and integrity of the organelles (Schwake et al. 2013).

Lysosomal hydrolases are glycoproteins containing N-linked glycans. Exceptions to this are the enzymes lysozyme and chitotriosidase, specialized endoglycosidases of phagocytes (Bussink et al. 2006). Lysosomal proteins are all synthesized at the endoplasmic reticulum (ER). Co-translationally, the newly formed polypeptides enter the lumen of the ER and specific asparagine residues become N-glycosylated. After correct folding, newly formed lysosomal proteins are transported to the Golgi apparatus which they traverse from *cis* to *trans* structures (Neufeld et al. 1975). The N-glycans of integral lysosomal membrane proteins and the lysosomal  $\beta$ -glucosidase (glucocerebrosidase, GBA) are modified from high mannose-type structures to sialylated hybrid type- and complex type-structures (Aerts et al. 1988; Saftig and Klumperman 2009). The soluble lysosomal proteins undergo another unique modification of their N-glycans in the Golgi apparatus, i.e. in a two-step process mannose-6-phosphate (M6P) moieties are generated in their high mannose-type N-glycans (Neufeld et al. 1975). Binding to mannose-6-phosphate receptors governs the sorting of soluble lysosomal proteins from other glycoproteins destined for secretion. Bound to M6P receptor lysosomal proteins are delivered to late endosomes from which their final destination, the lysosome, is reached (Braulke and Bonifacio 200). M6P-mediated sorting also plays a role in re-uptake of secreted lysosomal proteins. Following binding to M6P receptors at the plasma of various cell

types, endocytosis ensures their delivery to lysosomes (Neufeld et al. 1975; Vellodi 2005).

### **Lysosomal storage disorders: therapies and diagnosis**

In 1963 Henri Hers was the first to demonstrate that Pompe disease, also known as glycogen storage disease type II, is caused by deficient activity of the lysosomal  $\alpha$ -glucosidase (GAA, EC 3.2.1.3) (Hers 1963). Deficiency of this enzyme encoded by the *GAA* gene (locus 17q25.3) leads to accumulation of glycogen in the lysosomes of heart and skeletal muscle cells of Pompe patients, causing cardiac and respiratory failures (Van der Ploeg and Reuser 2008). Following the seminal discovery of the molecular basis of Pompe disease, identified are over 60 inherited diseases characterized by a defect in some function of lysosomes (Vellodi 2005; Ballabio and Gieselmann 2009; Cox and Cachón-González 2012). In a large number of these lysosomal storage diseases (LSDs) the primary cause is a mutation in a gene encoding a lysosomal hydrolase resulting in deficient enzymatic activity in lysosomes, so-called lysosomal enzymopathies (Figure 1) (Ballabio and Gieselmann 2009). LSDs can be also due to defects in non-enzymatic proteins in and beyond lysosomes. For example, there are LSDs originating from defects in lysosomal activator proteins (Gm2 activator protein and several saposin fragments of prosaposin) assisting lysosomal enzymes in their activity towards substrates (Sandhoff and Harzer 2013). Other LSDs are caused by primary defects in lysosomal membrane proteins, either acting as transporters or mediating interaction with other organelles (Schwake et al. 2013). Specific LSDs stem from inherited defects in proteins involved in transport of lysosomal proteins to lysosomes. Examples in this respect are deficiencies in enzymes involved in the generation of M6P sorting signal, defects in CLN8, an ER protein governing transport of newly formed lysosomal enzymes from the ER to the Golgi apparatus, and defects in LIMP-2, the membrane receptor transporting newly formed GBA from the ER to lysosomes (Reczek et al. 2007; Braulke and Bonifacino 2009; Di Ronza et al. 2018).



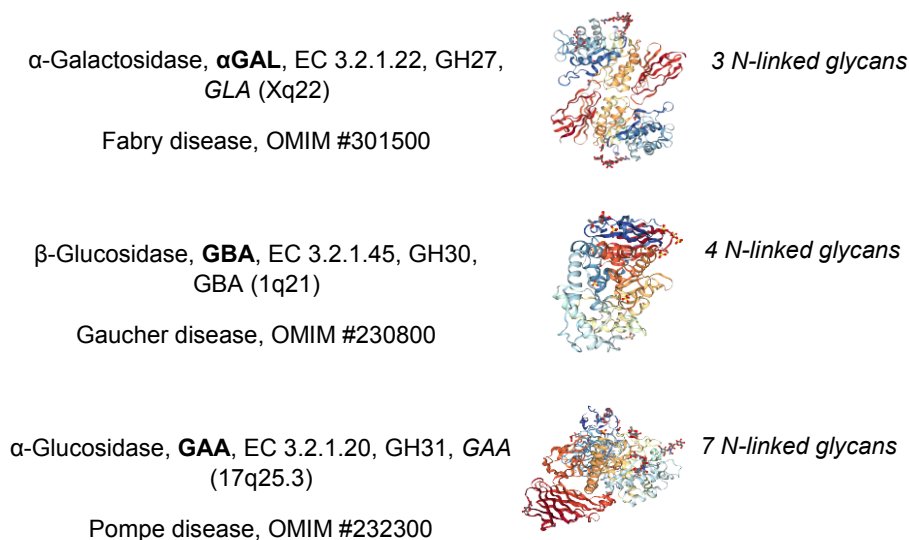


**Figure 1. Examples of 3 different lysosomal enzymes and the diseases caused by their dysfunction.** The PDB-IDs of the enzymes  $\alpha$ Gal, GBA and GAA are 1R46, 1OGS and 5KZW, respectively.

One group of LSDs concerns lysosomal accumulation of glycosphingolipids (Aerts et al. 2017; Marques and Saftig 2019) (Sandhoff and Harzer 2013). Common glycosphingolipidoses are Fabry disease (FD) and Gaucher disease (GD) (Ferraz et al. 2014). Fabry disease (FD) is an X-linked disorder caused by mutations in the gene *GLA* (locus Xq22.1) that encodes the lysosomal hydrolase  $\alpha$ -galactosidase A ( $\alpha$ GAL, EC 3.2.1.22) (Brady et al. 1967; Ferraz et al. 2014). Fabry disease is characterized by intralysosomal accumulation of globotriaosylceramide (Gb3), also known as ceramidetrihexoside (Charles C. Sweeley and Bernard Klionsky 1963). The clinical expression of FD is very heterogenous (Desnick et al. 2003). Males with classic FD develop at young age angiokeratoma, acroparasthesias, corneal opacity and anhidrosis followed by renal, cardiovascular and neurological impairments later in life. Atypical variants of FD are recognized, manifesting not as multi-system disease but involving only single organs such as kidney and heart. It has also become apparent that a large proportion of female carriers of mutant *GLA* develop an ameliorated form of Fabry disease. All these phenotypic manifestations together make Fabry disease a relatively common disorder.

Gaucher disease is caused by deficiency of the lysosomal acid- $\beta$ -glucosidase (GBA, EC.3.2.1.45), encoded by the *GBA* gene (locus 1q21) (Brady et al. 1966; Beutler and Grabowski 2001). GBA is responsible for the lysosomal hydrolysis

of glucosylceramide (GlcCer) into ceramide and glucose, the penultimate step in glycosphingolipid degradation. GD patients characteristically develop lipid-laden tissue macrophages that accumulate in spleen, liver and bone marrow. These Gaucher cells are thought to underly the characteristic hepatomegaly, splenomegaly and impaired hematopoiesis and associated cytopenia in Gaucher patients (Beutler and Grabowski 2001; Ferraz et al. 2014). Other common symptoms of GD patients are skeletal deterioration and gammopathies. The manifestation of GD is remarkably diverse and different phenotypes are discerned (Beutler and Grabowski 2001). The common variant among Caucasians, type 1 GD, does not involve prominent symptoms in the central nervous system (CNS). More rare and severe are the acute neuronopathic variant (type 2 GD) and sub-acute neuronopathic variant (type 3 GD) manifesting at infantile and juvenile age respectively. The most extreme form of GD is the collodion baby with a fatal abnormality in skin permeability at birth. In recent years it has become apparent that carriers of a mutant GBA allele are at increased risk for developing Parkinson disease (Siebert et al. 2014).

GD has been the frontrunner among LSDs in the development of effective rational therapeutic interventions. In the 70's, Roscoe Brady conceived enzyme replacement therapy (ERT) to treat type 1 GD (Brady 2003; Aerts and Cox 2018). This approach is based on chronic supplementation of enzyme to relevant cells by means of intravenous infusions. Uptake of lysosomal enzyme and delivery to lysosomes in ERT is mediated by cellular lectin receptors. In the case of type 1 GD supplementation of macrophages with GBA is needed. For this purpose, a recombinant GBA containing N-glycans with terminal mannose groups is employed allowing selective uptake via the mannose receptor (MR) expressed at the surface of tissue macrophages (Barton et al. 1991). In the case of other LSDs, such as FD and Pompe disease, where multiple cells develop lysosomal storage, therapeutic recombinant enzymes contain N-glycans with M6P to allow uptake via M6P receptors. A drawback of the ERT approach is that (neutralizing) antibodies against the infused recombinant enzyme may develop in patients that lack endogenous protein. This complication commonly occurs in infantile Pompe disease patients and males with classic Fabry disease (Linthorst et al. 2004; De Vries et al. 2016).

For some LSDs bone marrow transplantation is used as intervention. However, difficulties in the availability of suitable donors constitutes a major hurdle for this approach. Other therapeutic approaches for glycosphingolipidoses involve reduction of the glycosphingolipid substrates by inhibiting key enzymes involved in their biosynthesis. This substrate reduction therapy (SRT) was again first developed for type 1 GD (Cox et al. 2000; Aerts

et al. 2006). Presently two inhibitors of glucosylceramide synthase (Miglustat and Eliglustat) are registered for SRT of type 1 GD (Shayman and Larsen 2014). Another considered intervention is enzyme enhancement therapy (EET), also known as pharmacological chaperone therapy (PCT). Here, small compounds entering the catalytic pocket (commonly inhibitors) are used to assist proper folding in the ER of amenable mutant enzymes and thus increase degradative capacity in lysosomes. Actively studied in clinical trials as chaperone for GBA is Ambroxol (Maegawa et al. 2009; Narita et al. 2016) and Migalastat (deoxygalactonojirimycin) is already registered as chaperone for GLA to treat FD patients (Müntze et al. 2019). Finally, gene therapy, even though still in experimental stages, prompts great expectation as cure of LSDs since it aims at life-long correction of the impaired glycosidase in patients' cells. A major challenge for all therapy approaches is the prevention and correction of abnormalities in the CNS. In addition, it is increasingly realized that early intervention is desired since parts of the pathology in various LSDs seem irreversible (Ramaswami et al. 2019).

The diagnosis of LSDs is therefore receiving considerable attention and newborn screening is in place in some countries, or seriously considered, for some of these disorders. Traditionally diagnosis relied on examination of biopsies, but nowadays laboratory tests are increasingly used. DNA sequencing is broadly applied for several LSDs; however, this also leads to the detection of individuals with alterations of unknown significance. In the case of lysosomal enzymopathies measurement of residual enzymatic activity with chromogenic or fluorogenic artificial substrates is employed to demonstrate deficiency. Increasingly use is made of LC-MS/MS to demonstrate specific metabolite abnormalities. The detection of sphingoid bases derived from primary accumulating glycosphingolipids is found to have high diagnostic sensitivity for several glycosphingolipidoses (Aerts et al. 2011; Mirzaian et al. 2017). Examples are the markedly elevated glucosylsphingosine (GlcSph) and globotriaosylceramide (lysoGb3) in GD and FD, respectively (Aerts et al. 2008; Dekker et al. 2011). Dried blood spots are nowadays commonly used for routine enzyme activity and metabolite analysis. Plasma and urine samples are also used for detection of biomarker proteins stemming from storage cells (Aerts et al. 2011). Combining various tests mentioned above offers the most reliable laboratory confirmation for an LSD.

## **Glycosidases in plants and humans**

The use of plants as medication for various diseases has a long history. Several plant-derived compounds have been identified over the years as therapeutic agents. Many of these are glycoconjugates. For example, aspirin, one of the most popular pain killers that also reduces inflammation and fever, is based on minor modification of salicylic acid from *Salix alba*, *Spirea* and *Betula* (Friend 1974). Chapter 2 of this thesis provides a detailed review of this topic. Glycoconjugates are ongoingly synthesized and degraded, involving glycosyltransferases and glycoside hydrolases, respectively. All organisms contain multiple glycoside hydrolases (GHs, glycosidases) that hydrolyse specific glycosidic bonds in glycoconjugates. Glycosidases have important functions, for example in lysosomal metabolism of glycolipids in animals, catabolism of cell wall polysaccharides in plants and biomass conversion by microorganisms (Ketudat Cairns and Esen 2010). The name of glycosidases, e.g.  $\beta$ -glucosidase, reveals their preference for hydrolysis of specific glycosides.

Glycosidases are alternatively classified based on their amino acid sequence and structural similarity, as in the Carbohydrate Active EnZymes (CAZy) repository (Lombard et al. 2013). More than 150 GH families are listed in the CAZy database, revealing the plethora of glycosidases among various organisms. In addition, glycosidases are classified based on their reaction mechanism, according to the stereochemical outcome of the hydrolysis reaction, into inverting or retaining enzymes (Koshland 1953; Sinnott 1990). Moreover, the glycosidases are characterized as *exo* or *endo* enzymes, depending on their ability to cleave at the end or in the middle of a carbohydrate chain (Davies and Henrissat 1995; Lairson et al. 2008).

### **Mode of Action: catalytic mechanism and structure**

Two carboxyl-exposing residues like glutamic acid (Glu) and aspartic acid (Asp) (Glu/Glu, Asp/Asp or Glu/Asp), present in the active site of both inverting and retaining enzymes, are taking part in the hydrolysis of the glycosidic bond (Koshland 1953). The inverting reaction is a single step reaction, and it occurs when a water molecule is activated by the one carboxylic group at the active site which is acting as a base and attacks the water molecule at its anomeric centre (Guce et al. 2010). Simultaneously, the second carboxylic group enables the departure of the leaving group via acid catalysis. In the case of retaining glycosidases, a double displacement mechanism is employed. At first, a nucleophilic attack is happening to the anomeric centre and results at the formation of a glycosyl-enzyme intermediate (Koshland 1953). Then, the deprotonated carboxylate acts as a base and uses a water molecule, to hydrolyze the intermediate giving the reaction product (Figure 2).

GHs are grouped into structurally similar families that can be further sub-grouped into clans. For instance,  $\beta$ -glycosidases, that belong to GH families 1, 5, 30 (like the human GBA1), 35, 59, fall into the clan A of hydrolases with a catalytic ( $\beta/\alpha$ )<sub>s</sub> TIM barrel domain (Ben Bdira et al. 2018). GH116 enzymes, like the cytosolic human GBA2 enzyme, belong to clan O and they have a ( $\alpha/\alpha$ )<sub>s</sub> catalytic domain. The majority of  $\beta$ -glycosidases have two glutamic acid amino acids at their active site, acting as their catalytic residues. Alpha galactosidases and glucosidases are listed in families 27, 31 and 36 and belong to clan D, with a ( $\beta/\alpha$ )<sub>s</sub> TIM barrel domain (Fujimoto et al. 2003; Guce et al. 2010). The enzymes' active site is composed of two aspartic acid residues. In general, the active site of most glycosidases is rather conserved among species. Interestingly, the human enzymes such as GBA1 and  $\alpha$ GAL enzymes are physiological dimers whereas research on plant enzymes reveals that they are mostly presented as monomers (Kytidou et al. 2018).

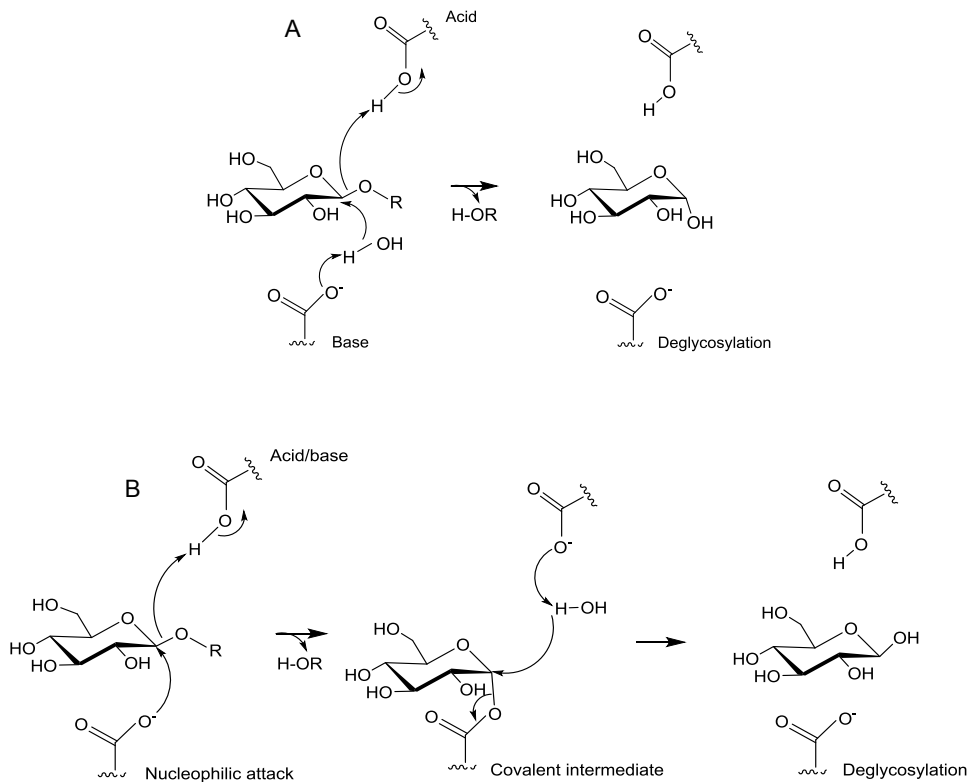


**Figure 2. Inverting (A) vs Retaining (B) reaction mechanism of glycosidases.**

### **Ubiquitous glycosidases in plants**

Plants contain numerous carbohydrate active enzyme encoded genes, more than any other organism (Coutinho et al. 2003). For instance, *Arabidopsis* has over 400 different genes coding for glycosidases (Husaini et al. 2018). These include several  $\alpha$ - and  $\beta$ -glucosidases, galactosidases and xylosidases. Their main function is the hydrolysis of glycosidic bonds between carbohydrates or another type of aglycone. The enzymes play various roles in processes in the plant cell, such as cell wall degradation, lignification, inactivation of phytohormones and activation of chemical defense compounds like cyanogenic glycosides (Ketudat Cairns and Esen 2010). Interestingly, some plant glycosidases are known to also act as transglycosidases, i.e. attaching sugar moieties from donor to acceptor molecules, forming new glycosides (Morant et al. 2008). As the matrix of the cell wall is of great complexity, the different glycosidases have inter connected roles and specificities. Therefore, there are many examples of plant glycosidases acting as trans enzymes *in vitro*. For instance, the linamarase from *Manihot esculenta* (cassava) which is acting on specific cyanogenic glucosides, is used for industrial applications for the production of alkyl  $\beta$ -glucosides (Svasti et al. 2003). In the case of human enzymes, transglycosylation activity have been proposed for chitotriosidase using as acceptor molecules sugars and also for the human GBA enzyme having acceptor molecules retinol or sterol (Vanderjagt et al. 1994; Aguilera et al. 2003). Akiyama and Marques also described the formation of cholesterol glucoside by the transglucosylation activity of the human GBA 1 and 2 enzymes (Akiyama et al. 2013; Marques et al. 2016a). Important to mention that such specificities are not yet reported to happen *in vivo*.

### **New tools exploring glycosidases: activity-based probes**

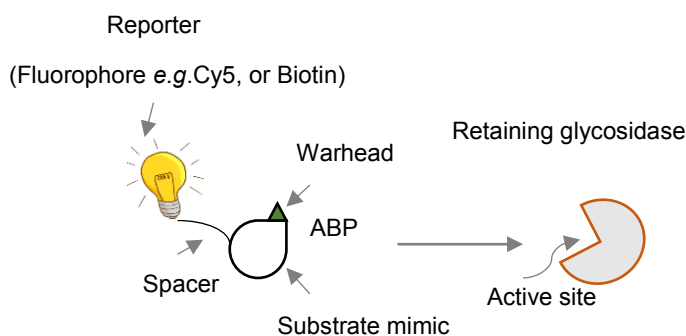
In 2010, Witte et al. were among the first to report the design of a fluorescent activity-based probes, APBs, visualizing active GBA molecules in complex biological samples (Witte et al. 2010). The ABPs for GBA have two structural elements: (1) the cyclophellitol-type “warhead” that covalently binds to the catalytic nucleophile of the enzyme, and (2) a variable reporter group which allows visualization of bound enzyme or its enrichment for identification through proteomics. The reporter group is linked to the warhead via a spacer (Kallemeijn et al. 2014; Willems et al. 2014c, d) (Figure 3). With biotin as reporter group, ABPs can be used for streptavidin-mediated enrichment, followed by identification of bound protein with proteomics.

The first described ABP for GBA consisted of a cyclophellitol with attached at C6 the spacer and reporter group (Witte et al. 2010). A hydrophobic extension at this position of cyclophellitol increases markedly the affinity for GBA and

renders specificity (Kuo et al. 2019; Artola et al. 2019). Other  $\beta$ -glucosidases do not react with this ABP. Next, a cyclophellitol-aziridine type ABP was designed with the spacer and reporter attached to the nitrogen (Kallemeijn et al. 2012). This type of ABP reacts with all retaining  $\beta$ -glucosidases in class: GBA, cytosol-faced GBA2, cytosolic GBA3 and lactase phlorizin hydrolase (LPH) (Kallemeijn et al. 2012).

After the generation of ABPs for  $\beta$ -glucosidases, a plethora of ABPs was developed for other retaining glycosidases by changing the cyclophellitol configuration. ABPs (usually cyclophellitol-aziridine type) are now available for the detection of  $\alpha$ -galactosidases,  $\beta$ -galactosidases,  $\alpha$ -fucosidases,  $\beta$ -glucuronidases,  $\alpha$ -glucosidases,  $\alpha$ -iduronidases  $\alpha$ -mannosidases, and  $\beta$ -mannosidases (Willems et al. 2014a, b; Jiang et al. 2015, 2016; Marques et al. 2016b; Wu et al. 2017; Artola et al. 2018).

### A. Approach



### B. ABP library

| Targeting enzymes        | Literature  |
|--------------------------|---|
| $\beta$ -glucosidases    | Witte <i>et al.</i> 2010, Kallemeijn <i>et al.</i> 2012 |
| $\alpha$ -galactosidases | Willems <i>et al.</i> 2014, Kytidou <i>et al.</i> 2017  |
| $\alpha$ -fucosidases    | Jiang <i>et al.</i> 2015                                |
| $\alpha$ -iduronidases   | Artola <i>et al.</i> 2018                               |
| $\alpha$ -glucosidases   | Jiang <i>et al.</i> 2016                                |
| $\beta$ -glucuronidases  | Wu <i>et al.</i> 2017                                   |
| $\beta$ -galactosidases  | Marques <i>et al.</i> 2016b, not published              |
| $\alpha$ -mannosidases   | Not published   |
| $\beta$ -mannosidases    | Not published   |

## C. Mechanism

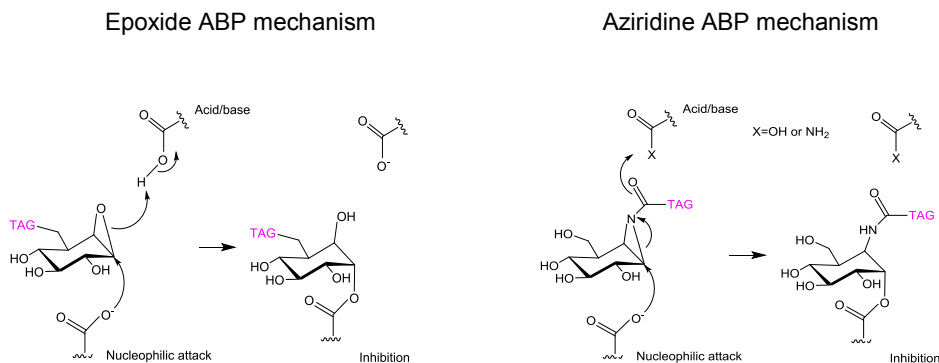


**Figure 3. Activity-based probe (ABP) technology.** A. ABP approach. B. ABP library. C. Reaction mechanism of epoxide and aziridine activity-based probes.

Several applications for glycosidase ABPs in both fundamental research and diagnosis of lysosomal diseases have meanwhile been developed (Kuo et al. 2018). Firstly, the ABPs can be used to label active enzyme molecules and visualize these upon SDS-PAGE by fluorescence scanning. Thus, the MW of the target enzyme is detected and maturation by proteolytic processing or modification of N-glycans can be observed (Witte et al. 2010; Jiang et al. 2016). Secondly, the amphiphilicity of ABPs allows passage of membranes and the labeling of active enzymes *in situ* (Witte et al. 2010; Kallemeijn et al. 2012). Recently, correlative light electron microscopy (CLEM) was successfully used to visualize the location of active GBA molecules in individual lysosomes and the delivery of exogenous therapeutic enzyme to these organelles in cultured cells expressing mannose receptor (Van Meel et al. 2019). Infusion of ABPs in mice has allowed the detection of active enzyme molecules in various visceral tissues (Kallemeijn et al. 2012). The fluorophore in the ABP prevents effective passage across the blood-brain barrier. Labeling of GBA in the brain was accomplished by *i.c.v.* administration of ABP in rodents (Herrera Moro Chao et al. 2015). Another application concerns the convenient screening of libraries for inhibitors of the target glycosidases (Lahav et al. 2017). This method is based on detecting the competition of ABP labeling of a target enzyme by an inhibitory compound blocking the active site. Along the same line, the *in-situ* target engagement of cyclophellitol and conduritol B-epoxide (CBE), two suicide inhibitors of GBA, was recently determined (Kuo et al. 2019). Analyzed was possible interaction of cyclophellitol (CP) and CBE with the off-target enzymes Gba2,  $\beta$ -glucuronidase and retaining  $\alpha$ -glucosidases GAA and GANAB after



administration of the inhibitors to cultured cells or zebrafish larvae. The investigation revealed that CP inhibits GBA2 on a par with GBA and is therefore not suitable to generate a genuine GD model. Examination of mice exposed to relative low dose CBE administrations showed that GBA was selectively inhibited under these conditions (Kuo et al. 2019).

A great advantage of ABPs is that they label retaining glycosidases cross-species as the result of conservation of catalytic pockets. This enables the use of such inhibitors not only for the detection of human hydrolases but also for the study of plant, bacterial and fungal enzymes. A recent study revealed the successful use of ABPs in detection and identification of  $\beta$ -xylosidases and endo- $\beta$ -1,4-xylanases in secretome of *Aspergillus niger*, for research of biomass breakdown (Schröder et al. 2019). Comparable examples are reported regarding use of ABPs in plant science. The van den Hoorn laboratory used  $\beta$ - and  $\alpha$ -glucosyl configured cyclophellitol ABPs in several plant species to identify various enzymes (Chandrasekar et al. 2014; Husaini et al. 2018). The  $\beta$ -glucosyl configured ABPs epoxide and aziridine were also used in plants during these experiments, data presented at chapter 6. In addition, the use of  $\alpha$  galactosidase ABPs in plants is described in this thesis chapters 3 and 4.

Together with the enormous progress in the use of ABPs in cells and organisms, the cyclophellitol-type inhibitors have proved to be valuable in biochemical investigations and crystallography, providing further understanding of mechanism of the glycosidases (Jiang et al. 2015; Ben Bdira et al. 2016, 2018; Wu et al. 2017). Finally, the application of ABPs for diagnosis of corresponding lysosomal diseases holds great promise (Aerts et al. 2011, this thesis, chapters 7 and 8).

## Scope of the thesis

This thesis reports the study of retaining glycosidases in humans and plants. The major goal of the performed investigations has been to increase fundamental knowledge on the enzymes to contribute to translation into improved diagnosis and treatment of LSDs caused by deficiencies in lysosomal glycosidases. The first part of this thesis pays special attention to plants as platform for the production of recombinant enzymes for use in human glycosidases as well as source of endogenous enzymes with potential medical application. The second section is focused on the diagnostic value of the activity-based probes as used towards urine and cultured cell materials.

At **chapter 1** a brief introduction on the lysosomal storage disorders and glycosidases, both in human and plants, is presented. **Chapter 2** reviews glycosylated metabolites from plants and their metabolizing enzymes. Discussed are the medical applications of plant glycoconjugates, with special emphasis to glycosylated lipids. The features of metabolizing plant  $\beta$ -glucosidases and glucosyltransferases are described. The reaction mechanisms of glycosidases are discussed in detail and new chemical biology tools employed to investigate retaining glucosidases, so-called activity-based probes (ABPs) are introduced. The emerging use of plants as production platforms for therapeutic glycosidases is described.

Recombinant human glycosidases are presently used to treat patients with corresponding enzyme deficiencies. Traditionally, therapeutic enzymes employed in ERT were produced with cDNA technology in cultured Chinese hamster ovary (CHO) cells. More recently, alternative production platforms, including plants, have been used. **Chapter 3** reports an investigation on the use of *Nicotiana benthamiana* as production platform (Figure 4) of three recombinant human  $\alpha$ -galactosidases:  $\alpha$ -galactosidase A (deficient in the lysosomal storage disorder Fabry disease),  $\alpha$ -*N*-acetyl-galactosaminidase and a modified  $\alpha$ -*N*-acetyl-galactosaminidase with increased  $\alpha$ -galactosidase activity. The feasibility of production of human  $\alpha$ -galactosidases *in planta* was studied and the efficacy of the recombinant enzymes to correct cultured fibroblasts of Fabry patients was examined.

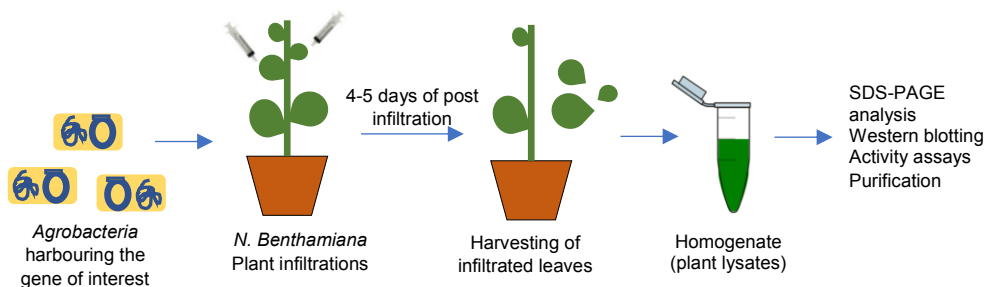


**Figure 4. Overview of transient overexpression of proteins in *N.benthamiana* leaves.**

The abundant presence of endogenous  $\alpha$ -galactosidase in *Nicotiana benthamiana* was observed with activity-based probe labeling. **Chapter 4** concerns an investigation on a novel  $\alpha$ -galactosidase, named A1.1, from *Nicotiana benthamiana*. It was studied to which extent the enzyme resembles the human counterparts. In this analysis use was made of N-glycan detection and crystallography. The potential value of plant A1.1 to Fabry disease was examined by studying correction of stored glycolipids in cultured fibroblasts of Fabry patients.

Knowledge on the reaction itinerary led to the design of a new close mimic of the transition state, cyclosulfamidate. In **chapter 5**, the design of the cyclophellitol cyclosulfamidate is described and the outcome of studies on the ability of the compound to stabilize human and plant  $\alpha$ -galactosidases in human serum and culture media is described. The findings with cyclosulfamidate are compared to those with deoxy-galactonojirimycin, a registered chaperone for human  $\alpha$ -galactosidase A and the treatment of amenable Fabry patients.

In the last decade ABPs labeling various glycosidases have been designed and applied. The first ones involved cyclophellitol scaffold modified to fluorescently label retaining  $\beta$ -glucosidases. Since ABPs can be applied cross species to identify target glycosidases, the thesis reports a pilot investigation on plant  $\beta$ -glucosidase and the fungal  $\alpha$ -galactosidase from Beano supplement. **Chapter 6**, reports the visualization of retaining  $\beta$ -glucosidases in tobacco BY2 cell cultures via the use of activity-based probes. The identified enzymes belonged to GH families, 5, 3 and 17. Interestingly, some of the identified candidates showed activity towards the human lipid accumulated in Gaucher disease, GlcCer. Further, the presence of the fungal (*Asperigillus niger*)  $\alpha$ -galactosidase in the dietary supplement Beano was detected via the use of activity-based probes. The dietary enzyme which is used to improve the digestion process, was also *in vitro* active against the Gb3 lipid, accumulated in Fabry disease.

The ability to visualize active glycosidase molecules with fluorescent ABPs has potential diagnostic applications regarding inherited defects in enzymes underlying lysosomal storage diseases. Urine is known to contain considerable amounts of lysosomal glycosidases and to be a useful source for diagnosis of lysosomal glycosidase deficiencies. **Chapter 7** concerns an investigation with cultured cells and urine samples regarding the diagnostic potential of ABPs visualizing distinct glycosidases. The findings of this thesis investigation are discussed in view of the literature and future research prospects are put forward in the discussion (**chapter 8**). Further, in **chapter 8**, the urinary activity-based protein profiling of patients experiencing kidney failures, such as diabetes, is being described. In more detail, detection of urinary heparanase in relation to kidney failure diseases is also discussed.

The main results of the conducted investigation are presented in the **Summary**.

## References

- Aerts JMFG, Cox TM (2018) Roscoe O. Brady : Physician whose pioneering discoveries in lipid biochemistry revolutionized treatment and understanding of lysosomal diseases. *Blood Cells, Mol Dis* 68:4–8. doi: <https://doi.org/10.1016/j.bcmd.2016.10.030>
- Aerts JMFG, Ferraz MJ, Mirzaian M, et al (2017) Lysosomal Storage Diseases. For Better or Worse: Adapting to Defective Lysosomal Glycosphingolipid Breakdown. In eLS, John Wiley & Sons, Ltd (Ed.). doi:10.1002/9780470015902.a0027592
- Aerts JMFG, Groener JE, Kuiper S, et al (2008) Elevated globotriaosylsphingosine is a hallmark of Fabry disease. *Proc Natl Acad Sci U S A* 105:2812–2817. doi: 10.1073/pnas.0712309105
- Aerts JMFG, Hollak CEM, Boot RG, et al (2006) Substrate reduction therapy of glycosphingolipid storage disorders. *J Inherit Metab Dis* 29:449–456. doi: 10.1007/s10545-006-0272-5
- Aerts JMFG, Kallemeijn WW, Wegdam W, et al (2011) Biomarkers in the diagnosis of lysosomal storage disorders: proteins, lipids, and inhibitors. *J Inherit Metab Dis* 34:605–619. doi: 10.1007/s10545-011-9308-6
- Aerts JMFG, Schram A, Strijland A, et al (1988) Glucocerebrosidase, a lysosomal enzyme that does not undergo oligosaccharide phosphorylation. *Biochim Biophys Acta - Gen Subj* 964:303–308. doi: [https://doi.org/10.1016/0304-4165\(88\)90030-X](https://doi.org/10.1016/0304-4165(88)90030-X)
- Aguilera B, Ghauharali-van der Vlugt K, Helmond MTJ, et al (2003) Transglycosidase Activity of Chitotriosidase: Improved enzymatic assay for the human macrophage chitinase. *J Biol Chem* 278:40911–40916. doi: 10.1074/jbc.M301804200
- Akiyama H, Kobayashi S, Hirabayashi Y, Murakami-Murofushi K (2013) Cholesterol glucosylation is catalyzed by transglucosylation reaction of  $\beta$ -glucosidase 1. *Biochem Biophys Res Commun* 441:838–843. doi: <https://doi.org/10.1016/j.bbrc.2013.10.145>
- Appelmans F, Wattiaux R, De Duve C (1955) Tissue fractionation studies. 5. The association of acid phosphatase with a special class of cytoplasmic granules in rat liver. *Biochem J* 59:438–445.
- Artola M, Kuo C-L, Lelieveld LT, et al (2019) Functionalized Cyclophellitols Are Selective Glucocerebrosidase Inhibitors and Induce a Bona Fide Neuropathic Gaucher Model in Zebrafish. *J Am Chem Soc* 141:4214–4218. doi: 10.1021/jacs.9b00056
- Artola M, Kuo C-L, McMahon SA, et al (2018) New Irreversible  $\alpha$ -L-iduronidase Inhibitors and Activity-Based Probes. *Chemistry* 24:19081–19088. doi: 10.1002/chem.201804662
- Ballabio A, Gieselmann V (2009) Lysosomal disorders: From storage to cellular damage. *Biochim Biophys Acta - Mol Cell Res* 1793:684–696. doi: <https://doi.org/10.1016/j.bbamcr.2008.12.001>

- Barton NW, Brady RO, Dambrosia JM, et al (1991) Replacement Therapy for Inherited Enzyme Deficiency — Macrophage-Targeted Glucocerebrosidase for Gaucher's Disease. *N Engl J Med* 324:1464–1470. doi: 10.1056/NEJM199105233242104
- Ben Bdira F, Artola M, Overkleeft HS, et al (2018) Distinguishing the differences in  $\beta$ -glycosylceramidase folds, dynamics, and actions informs therapeutic uses. *J Lipid Res* 59:2262–2276. doi: 10.1194/jlr.R086629
- Ben Bdira F, Jiang J, Kallemeijn W, et al (2016) Hydrophobic Interactions Contribute to Conformational Stabilization of Endoglycoceramidase II by Mechanism-Based Probes. *Biochemistry* 55:4823–4835. doi: 10.1021/acs.biochem.6b00363
- Beutler, E. and Grabowski GA (2001) Gaucher disease. In: Scriver, C.R., Beaudet, A.L., Sly, W.S., and Valle, D., Eds., 8th edn. McGraw-Hill, New York 3635-3668.
- Brady RO (2003) Enzyme replacement therapy: conception, chaos and culmination. *Philos Trans R Soc London Ser B Biol Sci* 358:915–919. doi: 10.1098/rstb.2003.1269
- Brady RO, Gal A.E, Bradley RM, et al (1967) Enzymatic Defect in Fabry's Disease. *N Engl J Med* 276:1163–1167. doi: 10.1056/NEJM196705252762101
- Brady RO, Kanfer JN, Bradley RM, Shapiro D (1966) Demonstration of a deficiency of glucocerebroside-cleaving enzyme in Gaucher's disease. *J Clin Invest* 45:1112–1115. doi: 10.1172/JCI105417
- Braulke T, Bonifacino JS (2009) Sorting of lysosomal proteins. *Biochim Biophys Acta - Mol Cell Res* 1793:605–614. doi: <https://doi.org/10.1016/j.bbamcr.2008.10.016>
- Bussink AP, Van Eijk M, Renkema GH, et al (2006) The Biology of the Gaucher Cell: The Cradle of Human Chitinases. In: *A Survey of Cell Biology*. Academic Press, 252:71–128. doi: [https://doi.org/10.1016/S0074-7696\(06\)52001-7](https://doi.org/10.1016/S0074-7696(06)52001-7)
- Chandrasekar B, Colby T, Emran Khan Emon A, et al (2014) Broad-range Glycosidase Activity Profiling. *Mol Cell Proteomics* 13:2787–2800. doi: 10.1074/mcp.O114.041616
- Charles C. Sweeley and Bernard Klionsky (1963) Fabry's Disease: Classification as a Sphingolipidosis and Partial Characterization of a Novel Glycolipid. *J Biol Chem* 238:3148–3150.
- Coutinho PM, Stam M, Blanc E, Henrissat B (2003) Why are there so many carbohydrate-active enzyme-related genes in plants? *Trends Plant Sci* 8:563–565. doi: <https://doi.org/10.1016/j.tplants.2003.10.002>
- Cox T, Lachmann R, Hollak C, et al (2000) Novel oral treatment of Gaucher's disease with N-butyldeoxynojirimycin (OGT 918) to decrease substrate biosynthesis. *Lancet* 355:1481–1485. doi: [https://doi.org/10.1016/S0140-6736\(00\)02161-9](https://doi.org/10.1016/S0140-6736(00)02161-9)
- Cox TM, Cachón-González MB (2012) The cellular pathology of lysosomal diseases. *J Pathol* 226:241–254. doi: 10.1002/path.3021
- Davies G, Henrissat B (1995) Structures and mechanisms of glycosyl hydrolases. *Structure* 3:853–859. doi: [https://doi.org/10.1016/S0969-2126\(01\)00220-9](https://doi.org/10.1016/S0969-2126(01)00220-9)

- De Vries JM, Kuperus E, Hoogeveen-Westerveld M, et al (2016) Pompe disease in adulthood: effects of antibody formation on enzyme replacement therapy. *Genet Med* 19:90–97. doi: 10.1038/gim.2016.70
- Dekker N, van Dussen L, Hollak CEM, et al (2011) Elevated plasma glucosylsphingosine in Gaucher disease: relation to phenotype, storage cell markers, and therapeutic response. *Blood* 118:e118–e127. doi: 10.1182/blood-2011-05-352971
- Desnick RJ, Brady RO, Barranger J, et al (2003) Fabry Disease, an Under-Recognized Multisystemic Disorder: Expert Recommendations for Diagnosis, Management, and Enzyme Replacement Therapy. *Ann Intern Med* 138:338–346. doi: 10.7326/0003-4819-138-4-200302180-00014
- Di Ronza A, Bajaj L, Sharma J, et al (2018) CLN8 is an endoplasmic reticulum cargo receptor that regulates lysosome biogenesis. *Nat Cell Biol* 20:1370–1377. doi: 10.1038/s41556-018-0228-7
- Ferraz MJ, Kallemeijn WW, Mirzaian M, et al (2014) Gaucher disease and Fabry disease: New markers and insights in pathophysiology for two distinct glycosphingolipidoses. *Biochim Biophys Acta - Mol Cell Biol Lipids* 1841:811–825. doi: <https://doi.org/10.1016/j.bbalip.2013.11.004>
- Friend DG (1974) Aspirin: The Unique Drug. *JAMA Surg* 108:765–769. doi: 10.1001/archsurg.1974.01350300009004
- Fujimoto Z, Kaneko S, Momma M, et al (2003) Crystal structure of rice  $\alpha$ -galactosidase complexed with D-galactose. *J Biol Chem* 278:20313–20318. doi: 10.1074/jbc.M302292200
- Futerman AH, Van Meer G (2004) The cell biology of lysosomal storage disorders. *Nat Rev Mol Cell Biol* 5:554–565. doi: 10.1038/nrm1423
- Guce AI, Clark NE, Salgado EN, et al (2010) Catalytic Mechanism of Human  $\alpha$ -Galactosidase. *J Biol Chem* 285:3625–3632. doi: 10.1074/jbc.M109.060145
- Herrera Moro Chao D, Kallemeijn WW, Marques ARA, et al (2015) Visualization of Active Glucocerebrosidase in Rodent Brain with High Spatial Resolution following In Situ Labeling with Fluorescent Activity Based Probes. *PLoS One* 10:e0138107. doi: 10.1371/journal.pone.0138107
- Hers HG (1963) alpha-Glucosidase deficiency in generalized glycogenstorage disease (Pompe's disease). *Biochem J* 86:11–16. doi: 10.1042/bj0860011
- Husaini AM, Morimoto K, Chandrasekar B, et al (2018) Multiplex Fluorescent, Activity-Based Protein Profiling Identifies Active  $\alpha$ -Glycosidases and Other Hydrolases in Plants. *Plant Physiol* 177:24–37. doi: 10.1104/pp.18.00250
- Jiang J, Kallemeijn WW, Wright DW, et al (2015) In vitro and in vivo comparative and competitive activity-based protein profiling of GH29  $\alpha$ -l-fucosidases. *Chem Sci* 6:2782–2789. doi: 10.1039/C4SC03739A
- Jiang J, Kuo C-L, Wu L, et al (2016) Detection of Active Mammalian GH31  $\alpha$ -Glucosidases in Health and Disease Using In-Class, Broad-Spectrum Activity-Based Probes. *ACS Cent Sci* 2:351–358. doi: 10.1021/acscentsci.6b00057

- Kallemeijn WW, Li K-Y, Witte MD, et al (2012) Novel Activity-Based Probes for Broad-Spectrum Profiling of Retaining  $\beta$ -Exoglucosidases In Situ and In Vivo. *Angew Chemie Int Ed* 51:12529–12533. doi: 10.1002/anie.201207771
- Kallemeijn WW, Witte MD, Wennekes T, Aerts JMFG (2014) Chapter 4 - Mechanism-Based Inhibitors of Glycosidases: Design and Applications. In: Horton DBT-A in CC and B (ed). Academic Press, 71:297–338. doi: <https://doi.org/10.1016/B978-0-12-800128-8.00004-2>
- Ketudat Cairns JR, Esen A (2010)  $\beta$ -Glucosidases. *Cell Mol Life Sci* 67:3389–3405. doi: 10.1007/s00018-010-0399-2
- Koshland DE (1953) Stereochemistry and the mechanism of enzymatic reactions. *Biol Rev* 28:416–436. doi: 10.1111/j.1469-185X.1953.tb01386.x
- Kuo C-L, Kallemeijn WW, Lelieveld LT, et al (2019) In vivo inactivation of glycosidases by conduritol B epoxide and cyclophellitol as revealed by activity-based protein profiling. *FEBS J* 286:584–600. doi: 10.1111/febs.14744
- Kuo C-L, van Meel E, Kytidou K, et al (2018) Activity-Based Probes for Glycosidases: Profiling and Other Applications. *Methods Enzymol.* 598:217-235. doi: 10.1016/bs.mie.2017.06.039.
- Kytidou K, Beekwilder J, Artola M, et al (2018) *Nicotiana benthamiana*  $\alpha$ -galactosidase A1.1 can functionally complement human  $\alpha$ -galactosidase A deficiency associated with Fabry disease. *J Biol Chem* 293:10042–10058. doi: 10.1074/jbc.RA118.001774
- Lahav D, Liu B, van den Berg RJBHN, et al (2017) A Fluorescence Polarization Activity-Based Protein Profiling Assay in the Discovery of Potent, Selective Inhibitors for Human Nonlysosomal Glucosylceramidase. *J Am Chem Soc* 139:14192–14197. doi: 10.1021/jacs.7b07352
- Lairson LL, Henrissat B, Davies GJ, Withers SG (2008) Glycosyltransferases: Structures, Functions, and Mechanisms. *Annu Rev Biochem* 77:521–555. doi: 10.1146/annurev.biochem.76.061005.092322
- Linthorst GE, Hollak CEM, Donker-Koopman WE, et al (2004) Enzyme therapy for Fabry disease: Neutralizing antibodies toward agalsidase alpha and beta. *Kidney Int* 66:1589–1595. doi: <http://dx.doi.org/10.1111/j.1523-1755.2004.00924.x>
- Lombard V, Golaconda Ramulu H, Drula E, et al (2013) The carbohydrate-active enzymes database (CAZy) in 2013. *Nucleic Acids Res* 42:D490–D495. doi: 10.1093/nar/gkt1178
- Maegawa GHB, Tropak MB, Buttner JD, et al (2009) Identification and Characterization of Ambroxol as an Enzyme Enhancement Agent for Gaucher Disease. *J Biol Chem* 284:23502–23516. doi: 10.1074/jbc.M109.012393
- Marques ARA, Mirzaian M, Akiyama H, et al (2016a) Glucosylated cholesterol in mammalian cells and tissues: formation and degradation by multiple cellular  $\beta$ -glucosidases. *J Lipid Res.* 57:451-463 doi: 10.1194/jlr.M064923
- Marques ARA, Willems LI, Herrera Moro D, et al (2016b) A Specific Activity-Based Probe to Monitor Family GH59 Galactosylceramidase, the Enzyme Deficient in Krabbe Disease. *ChemBioChem.* 18:402-412. doi: 10.1002/cbic.201600561



- Marques ARA, Saftig P (2019) Lysosomal storage disorders – challenges, concepts and avenues for therapy: beyond rare diseases. *J Cell Sci* 132:jcs.221739. doi: 10.1242/jcs.221739
- Mirzaian M, Ferraz MJ, Oussoren SV, et al (2017) Simultaneous quantitation of sphingoid bases by UPLC-ESI-MS/MS with identical <sup>13</sup>C-encoded internal standards. *Clin Chim Acta*. 466:178-184. doi: 10.1016/j.cca.2017.01.014
- Morant AV, Jørgensen K, Jørgensen C, et al (2008)  $\beta$ -Glucosidases as detonators of plant chemical defense. *Phytochemistry* 69:1795–1813. doi: <https://doi.org/10.1016/j.phytochem.2008.03.006>
- Müntze J, Gensler D, Maniuc O, et al (2019) Oral Chaperone Therapy Migalastat for Treating Fabry Disease: Enzymatic Response and Serum Biomarker Changes After 1 Year. *Clin Pharmacol Ther* 105:1224–1233. doi: 10.1002/cpt.1321
- Narita A, Shirai K, Itamura S, et al (2016) Ambroxol chaperone therapy for neuronopathic Gaucher disease: A pilot study. *Ann Clin Transl Neurol* 3:200–215. doi: 10.1002/acn3.292
- Neufeld EF, Lim TW, Shapiro LJ (1975) Inherited Disorders of Lysosomal Metabolism. *Annu Rev Biochem* 44:357–376. doi: 10.1146/annurev.bi.44.070175.002041
- Parkinson-Lawrence EJ, Shandala T, Prodoehl M, et al (2010) Lysosomal Storage Disease: Revealing Lysosomal Function and Physiology. *Physiology* 25:102–115. doi: 10.1152/physiol.00041.2009
- Platt FM (2014) Sphingolipid lysosomal storage disorders. *Nature* 510:68-75. doi: 10.1038/nature13476.
- Ramaswami U, Bichet DG, Clarke LA, et al (2019) Low-dose agalsidase beta treatment in male pediatric patients with Fabry disease: A 5-year randomized controlled trial. *Mol Genet Metab* 127:86–94. doi: <https://doi.org/10.1016/j.ymgme.2019.03.010>
- Reczek D, Schwake M, Schröder J, et al (2007) LIMP-2 Is a Receptor for Lysosomal Mannose-6-Phosphate-Independent Targeting of  $\beta$ -glucocerebrosidase. *Cell* 131:770–783. doi: 10.1016/j.cell.2007.10.018
- Saftig P, Klumperman J (2009) Lysosome biogenesis and lysosomal membrane proteins: trafficking meets function. *Nat Rev Mol Cell Biol* 10:623–635. doi: 10.1038/nrm2745
- Sandhoff K, Harzer K (2013) Gangliosides and Gangliosidoses: Principles of Molecular and Metabolic Pathogenesis. *J Neurosci* 33:10195 LP – 10208. doi: 10.1523/JNEUROSCI.0822-13.2013
- Schröder SP, de Boer C, McGregor NGS, et al (2019) Dynamic and Functional Profiling of Xylan-Degrading Enzymes in *Aspergillus* Secretomes Using Activity-Based Probes. *ACS Cent Sci* 5:1067–1078. doi: 10.1021/acscentsci.9b00221
- Schwake M, Schröder B, Saftig P (2013) Lysosomal Membrane Proteins and Their Central Role in Physiology. *Traffic* 14:739–748. doi: 10.1111/tra.12056
- Shayman JA, Larsen SD (2014) The development and use of small molecule inhibitors

- of glycosphingolipid metabolism for lysosomal storage diseases. *J Lipid Res* 55:1215–1225. doi: 10.1194/jlr.R047167
- Siebert M, Sidransky E, Westbroek W (2014) Glucocerebrosidase is shaking up the synucleinopathies. *Brain* 137:1304–1322. doi: 10.1093/brain/awu002
- Sinnott ML (1990) Catalytic mechanism of enzymic glycosyl transfer. *Chem Rev* 90:1171–1202. doi: 10.1021/cr00105a006
- Svasti J, Phongsak T, Sarnthima R (2003) Transglucosylation of tertiary alcohols using cassava beta-glucosidase. *Biochem Biophys Res Commun* 305:470–475. doi: 10.1016/s0006-291x(03)00793-9
- Van der Ploeg AT, Reuser AJJ (2008) Pompe's disease. *Lancet* 372:1342–1353. doi: [https://doi.org/10.1016/S0140-6736\(08\)61555-X](https://doi.org/10.1016/S0140-6736(08)61555-X)
- Van Meel E, Bos E, van der Lienden MJC, et al (2019) Localization of Active Endogenous and Exogenous GBA by Correlative Light-Electron Microscopy in Human Fibroblasts. *Traffic*. 20:346-356. doi: 10.1111/tra.12641.
- Vanderjagt DJ, Fry DE, Glew RH (1994) Human glucocerebrosidase catalyses transglucosylation between glucocerebroside and retinol. *Biochem J* 300:309 LP – 315. doi: 10.1042/bj3000309
- Vellodi A (2005) Lysosomal storage disorders. *Br J Haematol* 128:413–431. doi: 10.1111/j.1365-2141.2004.05293.x
- Willems LI, Beenakker TJM, Murray B, et al (2014a) Potent and Selective Activity-Based Probes for GH27 Human Retaining  $\alpha$ -Galactosidases. *J Am Chem Soc* 136:11622–11625. doi: 10.1021/ja507040n
- Willems LI, Beenakker TJM, Murray B, et al (2014b) Synthesis of  $\alpha$ - and  $\beta$ -Galactopyranose-Configured Isomers of Cyclophellitol and Cyclophellitol Aziridine. *European J Org Chem* 2014:6044–6056. doi: 10.1002/ejoc.201402589
- Willems LI, Jiang J, Li KY, et al (2014c) From covalent glycosidase inhibitors to activity-based glycosidase probes. *Chem - A Eur J* 20:10864–10872. doi: 10.1002/chem.201404014
- Willems LI, Overkleeft HS, van Kasteren SI (2014d) Current Developments in Activity-Based Protein Profiling. *Bioconjug Chem* 25:1181–1191. doi: 10.1021/bc500208y
- Witte MD, Kallemeijn WW, Aten J, et al (2010) Ultrasensitive in situ visualization of active glucocerebrosidase molecules. *Nat Chem Biol* 6:907–913. doi: 10.1038/nchembio.466
- Wu L, Jiang J, Jin Y, et al (2017) Activity-based probes for functional interrogation of retaining  $\beta$ -glucuronidases. *Nat Chem Biol* 13:867–873. doi: 10.1038/nchembio.2395

# Chapter 2

---

Plant glycosides and glycosidases: a treasure-trove for therapeutics.

---

*Kassiani Kytidou, Marta Artola, Herman S. Overkleeft, Johannes M.F.G Aerts*

*This work has been published in *Frontiers Plant Science* (2020); 11:357.  
doi: 10.3389/fpls.2020.00357*



## **Abstract**

Plants contain numerous glycoconjugates that are metabolized by specific glucosyltransferases and hydrolyzed by specific glycosidases, some also catalyzing synthetic transglycosylation reactions. The documented value of plant-derived glycoconjugates to beneficially modulate metabolism is first addressed. Next, focus is given to glycosidases, the central theme of the review. The therapeutic value of plant glycosidases is discussed as well as the present production in plant platforms of therapeutic human glycosidases used in enzyme replacement therapies. The increasing knowledge on glycosidases, including structure and catalytic mechanism, is described. The novel insights have allowed the design of functionalized highly specific suicide inhibitors of glycosidases. These so-called activity-based probes allow unprecedented visualization of glycosidases cross-species. Here special attention is paid on the use of such probes in plant science that promote the discovery of novel enzymes and the identification of potential therapeutic inhibitors and chaperones.

## Introduction

Plant metabolites and their glycosylation. Plants provide nutrition and the human body has evolved to thrive optimally on this nourishment. Besides the nutritional value, plant-derived food influences the microbiome in the gastrointestinal tract with physiological effects (Theilmann et al., 2017). Plants produce a huge variety of secondary metabolites that can be decorated with sugars, i.e. glycosylated (Jones and Vogt 2001; Gachon et al., 2005; Wink, 2015). Specific plant glycosyltransferases using nucleotide-sugars as donors can attach specific sugar moieties to an acceptor molecule (Henrissat and Davies, 2000; Jones and Vogt, 2001). Glycosyl hydrolases, so-called glycosidases, remove specific sugar moieties. Most of these enzymes are retaining exo-glycosidases (Coutinho et al., 2003). Some of these glycosidases are also able to synthetically transglycosylate in the presence of high concentrations of an acceptor molecule, a reaction implying the transfer of a sugar moiety from a substrate to an acceptor molecule (Morant et al., 2008).

Glycosylation of metabolites in plants serves multiple purposes. Upon glycosylation, hydrophobic metabolites become more water-soluble which improves their bio-distribution and metabolism (Kren and Martinkova, 2001; Pandey et al., 2014). Increased solubility and amphiphilicity of glycosylated metabolites may assist their transport across cell membranes (Vetter, 2000). The attachment of sugars to small metabolites raises their molecular weight and melting point. This allows synthesis and storage of precursors of volatile compounds that can be released on demand after hydrolysis (Ohgami et al., 2015). The stability of glycosylated metabolites may depend on the position where the sugar moiety is attached, for example the 6-O-glucosides of ascorbic acid are chemically less stable than the 2-O-glucoside form or non-glycosylated ascorbic acid (Jones and Vogt, 2001). Furthermore, detoxification of harmful molecules can take place through glycosylation. Glycosylation may generate a non-toxic agent that later can be re-activated and used as aglycone in defense against parasites and plant-eating organisms such as herbivores. Examples are cyanogenic glycosides produced by plants. These consist of an  $\alpha$ -hydroxynitrile group attached to a sugar moiety, often a D-glucose (Vetter, 2000). Release of cyanohydrin aglycone leads to spontaneous transformation to the corresponding ketone or aldehyde and release of hydrogen cyanide (prussic acid) (Cressey and Reeve, 2019). Hydrolysis of cyanogenic glycosides can be mediated by endogenous  $\beta$ -glucosidases when brought into contact with the substrate upon damaging of plant cells (Cressey and Reeve 2019). Additionally, hydrolysis may take place by the gut microbiome during digestion of plant material. The first identified cyanogenic glycoside was amygdalin isolated from

almonds in 1830 (Robiquet and Bourtron-Charland, 1830). Cyanogenic glycosides are ubiquitous in plants, being identified in more than 2500 species (Vetter, 2000). The sugars attached to the aglycone may vary from a disaccharide to monosaccharide, usually glucose (Vetter, 2000; Haque and Bradbury, 2002; Cressey and Reeve, 2019). Cassava, *M. esculenta*, produces the cyanogenic glycosides linamarin and lotaustralin and consumption may cause severe pathology (Kamalu, 1991; Kamula, 1993). Finally, another example of regulating biological activity by glycosylation is provided by glycosylated phytohormones such as abscisic acid (ABA), auxin (IAA), cytokinins (CKs), brassinosteroids (BRs), salicylic acid and gibberellin that regulate growth, development, and responses to environmental stresses (Gachon et al., 2005). Glycosylation of phytohormones usually leads to inactive storage forms of plant hormones that can be hydrolyzed for activation, allowing rapid responses and maintaining the hormonal homeostasis (Kren and Martinkova, 2001; Stupp et al., 2013; Pandey et al., 2014).

In this review we pay attention to the natural occurrence of glycosides in plants with emphasis to glycolipids and touch upon their metabolizing enzymes. We address the use of plant lipids for therapeutic purposes as well as their potential harmful effects. Described is the increasing use of plants as production platforms for therapeutic enzymes, in particular glycosidases for the treatment of lysosomal storage disorders. Finally, we discuss the recent design of unprecedented tools to study glycosidases, cross-species. These so-called activity-based probes (ABPs) are modified cyclophellitols that allow in situ visualization of their target glycosidases. ABPs label glycosidases cross-species due to the highly conserved catalytic pockets and find many applications like discovery of glycosidases in several organisms, diagnosis of inherited lysosomal glycosidase deficiencies, visualization of tissue distribution and subcellular localization of endogenous and exogenous (therapeutic) glycosidases and the identification of therapeutic inhibitors and chaperones.

## Beneficial glycosylated plant metabolites

**Plant-derived agents and human health.** Balanced consumption of vegetables is nowadays in the center of attention, particularly prompted by the worldwide epidemic of obesity and associated health problems. There is considerable interest in plant products from practitioners of regular medicine and pharmaceutical industry. Of note, the first generation of pharmaceuticals largely consisted of plant-derived products or minor chemical modifications thereof (Friend, 1974). The longstanding popularity of natural plant products

with alternative medicine advocates stems in many cases from ancient use of such materials in traditional medicine.

The chemical structure of plant glycosides determines their biological action(s) and bioavailability (uptake). In this respect, attention is first paid to glycosylated flavonoids.

**Glycosylated flavonoids.** The predominant polyphenols in food (i.e. fruits, vegetables, nuts) and beverages (i.e. tea, wine) are flavonoids (Pandey and Rizvi, 2009; Pan et al., 2010). Plant flavonoids can be categorized into subclasses: flavonols, isoflavonols, flavones, flavanones, flavanols (catechins) and anthocyanidins (Ross and Kasum, 2002; Xiao et al., 2014). Daily consumption of several milligrams of flavonoids (25 mg to 1 g/day) is common (Hertog et al., 1993; Tsuda et al., 1999; Ross and Kasum, 2002).

Many plant flavonoids (see Figure 1 for general structures) are glycosylated (Day et al., 1998; Tohge et al., 2017). Glycosides are linked to the phenolic hydroxyls, via  $\alpha$ - or  $\beta$ -D-glycosidic linkages (Murota and Terao, 2003). This type of modification may involve a single oligosaccharide or in some cases a polysaccharide moiety (Xiao et al., 2014). Commonly reported benefits of flavonoid glycosides are anti-oxidants and anti-inflammatory activities which find application in prevention and disease management (Lin and Harnly, 2007; Xiao et al., 2014). To illustrate this, some examples of each subclass are here discussed.

Flavonols are characterized by a phenolic substitution at position 2 of its 3-hydroxyflavone backbone. Quercetin is a flavonol present in plants, fruits and vegetables. It can occur as diverse glucosylated forms: for example quercetin-4'-O- $\beta$ -D-glucoside or quercetin-3,4'-O- $\beta$ -D-glucoside are predominant in onion with the glucose attached at the 3 or/and 4' position of the phenol respectively (Murota and Terao, 2003) (Figure 1A). It has been suggested that phenolic hydroxyl groups contribute to the free radical scavenging activity of the molecules (Bors et al., 1990). The health benefits of quercetin are generally attributable to its anti-oxidant action positively impacting on glutathione and reactive oxygen species (Xu et al., 2019). The anti-oxidant action is in part mediated by the modulation of enzymes associated with oxidative stress like acetylcholinesterase and butyrylcholinesterase (Xu et al., 2019). Kaempferol, present in broccoli, apples, tea, strawberries and beans, is another flavonol with reported antioxidant and anti-inflammatory properties (Chen and Chen, 2013).

Whereas flavonols have an OH group at C-3, the flavones bear a hydrogen in that position (Figure 1B). Apigenin and luteolin are flavones found in plant food. Apigenin occurs in a wide variety of vegetables and fruits such as parsley, celery, chamomile, oranges, thyme, onions, honey and spices, as well as beverages derived from plants such as tea, beer and wine. It exists largely as



C-glycosylated form, being more stable and reactive than the O-glycosylated counterparts. Apigenin is found to be absorbed as glycosylated structure and to exert antioxidant, anti-inflammatory and anti-cancer effects. For instance, glycosylated forms of apigenin with various pharmacological activities are apigenin 6-C-glucoside (isovitexin), apigenin 8-C-glucoside (vitexin), apigenin 7-O-glucoside and apigenin 7-O-neohesperidoside (rhoifolin) (He et al., 2016). Luteolin, present in carrots, peppers, celery, olive oil, peppermint, thyme, rosemary and oregano, is reported to have antioxidant effects and it is assumed to inhibit angiogenesis, induce apoptosis and thereby prevent carcinogenesis in vivo (Lin et al., 2008). Well known glycosylated forms of luteolin in citrus fruits are luteolin 7-O-rutinoside and lucenin-2 (luteolin 6,8-di-C-glucoside). Furthermore, cynaroside, the 7-O-glucoside derivative of luteolin, is found in *Lonicera japonica* Thunb. and *Angelica keiskei*. and also shows anti-oxidant and anti-inflammatory activity (Lin et al., 2008; Lopez-Lazaro, 2009; Chen et al., 2012; Nho et al., 2018).

Isoflavones bear a phenolic moiety at position 3 instead of 2 (Figure 1C). Genistein, an isoflavone found predominantly in soy, and together with its glycosylated form genistin, is reported to provide multiple health benefits. Several studies demonstrated that genistein has anti-diabetic effects, in particular through direct positive effects on  $\beta$ -cells and glucose-stimulated insulin secretion. In addition, protection against apoptosis is reported, independent of its function as an estrogen receptor agonist, antioxidant action, and inhibition of tyrosine kinase activity (Fotsis et al., 1993; Record et al., 1995; Allred et al., 2001; Pandey et al., 2014).

Flavanones are characterized by a saturated C2-C3 bond in the C ring and normally occur as a racemic mixture (Figure 1D). Hesperidin, a 7-O-rutinoside flavone, is a natural product with a wide range of biological effects, in particular it presents inhibitory effect against the development of neurodegenerative diseases (Hajjalyani, 2019). Hesperidin, a dietary flavanone, and its aglycone hesperetin, are found predominantly in citrus fruits such as oranges and lemons. These compounds are considered to exert beneficial anti-inflammatory and anti-oxidative action (De Souza et al., 2016).

Flavanols (a.k.a. catechins) have a 2-phenyl-3,4-dihydro-2H-chromen-3-ol skeleton and are mainly found in tea. Contrary to other flavonoids, flavanols are often not glycosylated and their glycosylation normally decreases anti-oxidant activity (Plumb et al., 1998). The beneficial effects of green tea have been attributed to its high content of polyphenolic catechins, including catechin (C), (-)-epicatechin (EC), (-)-epigallocatechin (EGC), (-)-epicatechin-3-gallate (ECG), and (-)-epigallocatechin-3-gallate (EGCG) (Figure 1E). Among them, EGCG is the polyphenolic catechin with the highest antioxidant effect as

reactive oxygen species (ROS) scavenger and metal ion chelator, and it finds application in prevention of disease caused by oxidative stress, such as cancer, cardiovascular diseases, neurodegenerative disease, neuropathic pain and diabetes (Roghani and Baluchnejadmojarad, 2009; Xifró et al., 2015).

Anthocyanidins possess a 2-phenylchromenylium ion backbone and are the deglycosylated version of anthocyanins (Figure 1F). Anthocyanins are abundant pigments in many red berries with documented antioxidant action. Examples are cyanidin-3-O-rutinoside and cyanidin-3,5-O-diglucoside (Feng et al., 2016). Likewise, anti-inflammatory properties are reported for the anthocyanidin malvidin-3'-O- $\beta$ -D-glucoside and malvidin-3'-O- $\beta$ -D-galactoside in blueberries by blocking the NF- $\kappa$ B pathway mechanism (Huang et al., 2014).

To which extent glycosylation of flavonoids contributes to their beneficial action is not always well understood. Glycosylation of flavonoids might favor bioavailability and uptake into the body. One advantage of glycosylation is that it can stabilize the molecules, preserving their structural integrity and therefore enabling their accumulation. In addition, glycosylation serves as a transport signal among the different compartments of the plant cell. For example, cyanogenic glucosides are transported only in their glycosylated form (Jones and Vogt, 2001). Flavonoid glycosides may be converted to their aglycons prior to absorption by intestinal epithelial cells. However, some glycosylated flavonoids are apparently also absorbed as such (for example, cyanidin-3-O- $\beta$ -D-glucoside and glycosylated apigenin) (Murota and Terao, 2003; Xiao et al., 2014; Xio et al., 2016). The linked sugar moiety, the type of linkage (O- versus C-) and the position of the glycoside attachment may influence the bioactivity of a flavanoid. An example of the latter forms the inferior free radical scavenging of quercetin-4'-O- $\beta$ -D-glucoside compared to quercetin-3-O- $\beta$ -D-glucoside (Yamamoto et al., 1999). This difference is due to the fact that the flavonoids' free radical scavenging activity depends on phenolic hydroxyl groups which act as electron donors. In particular, a catechol moiety with two neighboring hydroxyls has high electron donation ability (Murota and Terao, 2003). The antioxidant activities of glycosylated flavonoids can partly be also attributed to their chelation action, with the catechol group also playing a key role in the process (Murota and Terao, 2003). Interestingly, C-glycosylation enhances some of the beneficial traits of flavonoids such as their antioxidant and anti-diabetic activities. O-glycosylation is reported to reduce flavonoid bioactivity and absorption (Hostetler et al., 2012; Xiao et al., 2014).

The anti-inflammatory effects of flavonoids can be attributed to reduction of cytokine-induced inflammation by the inhibition of tumor necrosis factor- $\alpha$  (TNF- $\alpha$ ) signalling and reduced expression of pro-inflammatory genes by down-regulation of NF- $\kappa$ B (Ramos, 2007; Pan et al., 2010; Huang et al., 2014). An

example is provided by the anti-inflammatory flavonol kaempferol which is present in broccoli, tea and vegetables. During osteoporosis, pro-inflammatory cytokines, e.g. TNF- $\alpha$ , are expressed and cause bone disruption and further cytokine production. Kaempferol antagonizes the TNF- $\alpha$  induced production of interleukin-6 (IL-6) and monocyte chemotactic protein-1 (MCP1a), as well as the RANKL triggered osteoclast precursor cell differentiation (Pang et al., 2006; Pan et al., 2010). Another example is the anti-inflammatory effect of glycosylated anthocyanins present in blueberries, malvidin-3-O-glucoside and malvidin-3-O- $\beta$ -D-galactoside. These molecules reduce the levels of MCP1, intercellular adhesion and vascular cell adhesion molecule-1 at protein and mRNA level in endothelial cells through the inhibition of TNF- $\alpha$ . In addition, they block the NF- $\kappa$ B pathway by affecting I $\kappa$ B $\alpha$  degradation and the nuclear translocation of p65 (Huang et al., 2014).

For many flavonoids miscellaneous anti-cancer effects have been reported. The presumed modes of action of flavonoids as anti-cancer agents are diverse and the role of glycosylation in such anti-tumor effect is often not well understood. Examples of flavonoids with reported anti-tumor action are kaempferol (Ramos, 2007; Chen and Chen, 2013), peonidin 3-O- $\beta$ -D-glucoside, genistein, genistin and EGCG (Fotsis et al., 1993; Record et al., 1995; Allred et al., 2001; Pandey et al., 2014; Xifró et al., 2015). Genistein and genistin are however also reported to stimulate breast cancer cells in vivo at very low concentrations (nM range), acting as estrogen agonists in mice mammary glands (Allred et al., 2001). Daidzin of soybeans is another well-studied isoflavone 7-O- $\beta$ -D-glucoside with similar anti-cancer properties as genistein. Anti-cancer action has also been documented during the last decades for apigenin, hesperidin and its aglycone hesperetin (Madunić et al., 2018).

Plant-derived cardiac glycosides are secondary metabolites consisting of a steroid backbone functionalized with a lactone ring at the 17- $\beta$  position and a sugar moiety at the 3- $\beta$  position (Figure 1G). Cardiac glycosides can be classified as cardenolides or bufadienolides depending on the 5- or 6-membered lactone ring, respectively. Cardenolides are known since ancient times for their positive effects on cardiac arrhythmia, congestive heart failure and atrial fibrillation (Nesher et al., 2007). Their main role as antiarrhythmic agents is based on their ability to inhibit the Na<sup>+</sup>/K<sup>+</sup> ATPase ion pump, thus increasing intracellular potassium concentrations (Kelly, 1990; Kepp et al., 2012; Patel, 2016). In response to this, intracellular calcium increases which promotes more efficient myocardial contraction and improves cardiac pump activity (Newman et al., 2008). Well known examples of therapeutic cardiac glycosides are digoxin and digitoxin from the foxglove plant *Digitalis*. Even though the positive effects of cardiac glycosides are well established, dose-dependent toxicity remains an

issue (Ehle et al., 2011). Bufadienolides are present in very low amounts in plants and are prominent in animals such as the toad (*Bufo*), fireflies (*Photinus*) and snake (*Rhabdophis*) (Steijn and Van Heerder, 1998).

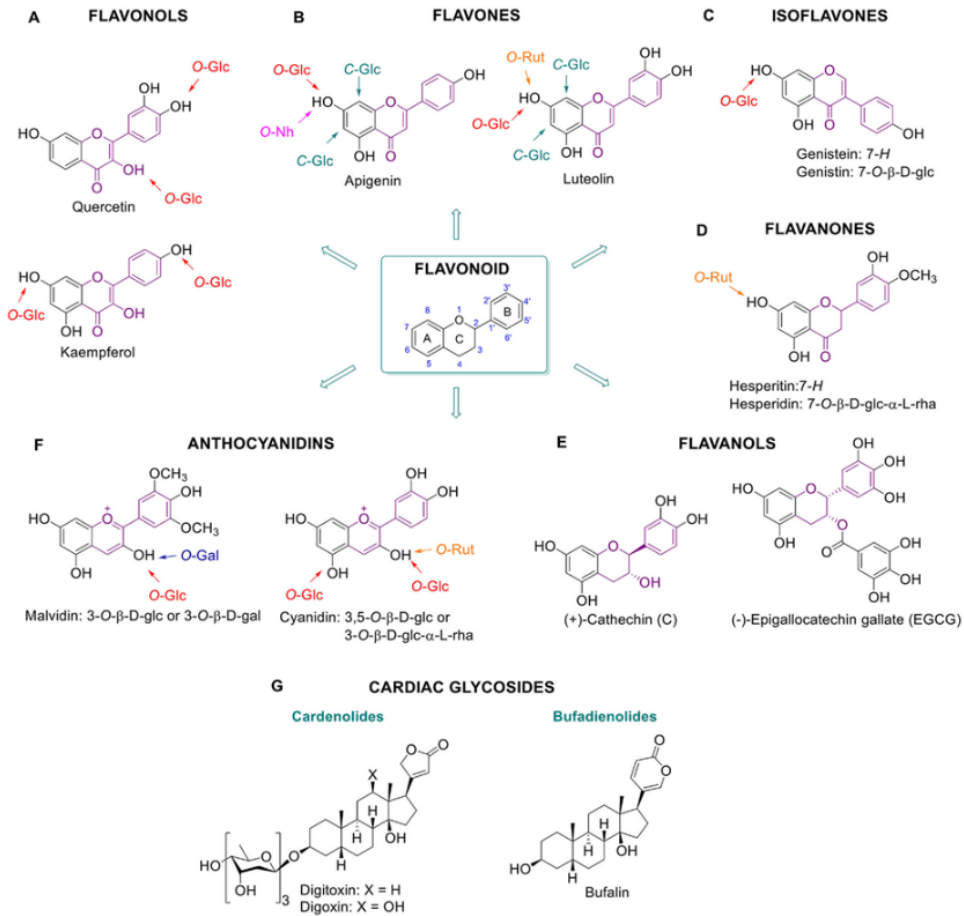


**Figure 1. Glycosylated plant metabolites beneficial for humans.** Flavonoids and some of their glycoside metabolites: flavonols (A), flavones (B), isoflavones (C), flavanones (D), flavanols (E) and anthocyanidins (F). Chemical structures of cardiac glycosides (G). Note: bufalin is an animal-derived cardiac glycoside.

## Glycosylated lipids

**Diacylglycerols.** Plants contain diverse glycosylated lipids. Galactosylated diacylglycerols are ubiquitous glycolipids in plants. They are predominantly

found in photosynthetic tissues, such as the leaf. In particular, chloroplast thylakoid membranes contain high quantities of monogalactosyldiacylglycerol (MGDG) and digalactosyldiacylglycerol (DGDG) (see figure 2A for the chemical structure and cellular localization) (Hölzl and Dörmann, 2019). For instance, MGDG and DGDG account to 36% and 20%, respectively, of spinach chloroplast glycerolipids. Less abundant are the acidic sulfoquinovosyldiacylglycerol (5%), and other glycerophospholipids (Wintermans, 1960). Of note, the existence of acylated MGDG (acylMGDG) has also been documented by Nilsson et al. (Nilsson et al., 2015) and their concentration is increased during environmental stresses such as frost. Glucosylated diacylglycerols are far rarer than galactosylated counterparts in plants and animals. 1,2-Di-O-acyl-3-O- $\beta$ -D-glucopyranosyl-sn-glycerol has however been found in rice bran (Holst, 2008).

**Sphingolipids.** Glycosylated sphingolipids (glycosphingolipids) in which sugar(s) are attached to ceramide are very abundant in animal cells. Distinct sphingolipids exist in plants (see figure 2B for the chemical structure and cellular localization). Plants produce, like animals, the simple glycosphingolipid glucosylceramide (GlcCer) where glucose is  $\beta$ -linked to a phytoceramide that differs from animal ceramide in the composition of the sphingosine moiety (also referred as long-chain base (LCB)) (Spassieva and Hille, 2003; Pata et al., 2010; Ali et al., 2018; Huby et al., 2019). Another glycosylated sphingolipid in plants is glucosylinositol phosphoryl ceramide (GIPC) (Ali et al., 2018). Whereas in animals the major sphingosine base is C18 LCB, in plants over 9 different LCBs have been identified. In addition, the presence of dienes in the plant sphingosine bases is rather common (Pruett et al., 2008; Ali et al., 2018). Plant LCBs can occur in very low concentrations in cells, but they are mainly present as backbones of ceramides that further contain linked fatty acid chains (C16-C26). The ceramides are next glycosylated forming GlcCer and/or glucosylinositol phosphoryl ceramides (GIPC) (Ali et al., 2018). In plants, elongation of glucosylceramide to oligoglycosylceramides occurs with either mannosyl or galactosyl units (Lynch and Dunn, 2004). In the common mannosyl series in higher plants, up to four mannosyl units may be added via  $\beta$ 1 $\rightarrow$ 4 linkages. Oligoglycosylceramides are present in the endoplasmic reticulum (ER), Golgi apparatus, vacuole membrane and plasma membrane. Sphingolipids and their glycosylated forms together with plant sterols are important constituents of the lipid rafts of the plasma membrane (Msanne et al., 2015). The complex GCIPC are considered as the equivalents of complex glycosphingolipids like gangliosides in animal cells (Gronnier et al., 2016; Cacas et al., 2016). They play important roles in regulation of cellular processes, such as cell wall formation, programmed cell death, drought and salt tolerance (Ali et al., 2018).

**Phytosterols (plant sterols and stanols).** Phytosterols, also known as xenosterols, are essential components of plant cells that are predominantly found in cell membranes (Hartmann, 1998). They include plant sterols and stanols (saturated sterols without double bonds in the sterol ring) (see figure 2C for chemical structure and cellular localization). Their chemical structure consists of a sterol body; a cyclopentano-perhydro-phenanthrene ring system (formed by four rigid rings) with a hydroxyl group at position C-3 and a side chain attached to the carbon C-17 (Figure 2C). Differences in the nature of the side chain gives a plethora of diverse sterols in plants, accounting to more than 260 different ones, as described over the last decades (Vanmierlo et al., 2015). The most abundant phytosterols in human diet are  $\beta$ -sitosterol, campesterol, campestanol and stigmasterol. Their structure is similar to the structure of the mammalian sterol, cholesterol. Phytosterols structurally differ from cholesterol only at the length and saturation of their aliphatic side chain. For instance, campesterol has an additional methyl group at its side chain, at C-24 position (Mamode Cassim et al., 2019). It is important to mention that plants also contain small amounts of cholesterol (Hartmann, 1998). Phytosterols are mainly found in vegetable oils, seeds and nuts and in less extent in fruits and vegetables (Amiot et al., 2011). Phytosterols play important roles in several biological processes. For instance, campesterol is found to act as a precursor at the biosynthesis of brassinosteroids, hormones that regulate plant growth, development and morphogenesis. In addition,  $\beta$ -sitosterol and stigmasterol are mainly involved in the maintenance of cell membranes, and together with sphingolipids, form the lipid rafts (Amiot et al., 2011; Ferrer et al., 2017). Phytosterols are also involved in responses to biotic and abiotic stresses (Ferrer et al., 2017). A characteristic example is the formation of stigmasterol in *Arabidopsis* leaves after inoculation with specific bacteria. In general, plant sterols play a key role in the innate immunity of plants against bacterial infections via regulating the nutrient efflux in the apoplast (Griebel and Zeier, 2010; Wang et al., 2012). In addition, tolerance to aluminum is shown to be influenced positively by the high sterol and low phospholipid contents in the root tip of plants. This results in a less negatively charged plasma membranes, tolerating better aluminum (Wagatsuma et al., 2014). At last, drought tolerance is also associated with sterol composition of the plants as studied via using the drought hypersensitive/squalene epoxidase 1- 5 mutants in *Arabidopsis* (Posé et al., 2009).

**Glucosylated phytosterols and medicinal properties.** Conjugated forms of phytosterols occur. Examples are the steryl glycosides (SG) (sometimes referred to as sterolins) and their acylated forms; the acyl steryl glycosides (ASG). In plant SG, the sugar moiety, often a glucose, is attached at the C-3 hydroxyl

group of the sterol. When the sugar moiety is further acylated with a fatty acid at the primary alcohol (C-6 carbohydrate numbering), ASG is formed (Grille et al., 2010; Nyström et al., 2012) (Figure 2C). The first glycosylated plant sterol to be purified was ipuranol from the olive tree in 1908. A few years later it was identified as  $\beta$ -sitosterol-D-glycoside. ASGs were next discovered in lipid extracts of soybean seeds and potato tubers (Grille et al., 2010). Plant glycolipids occur in different amounts and in different composition among plant species even in different tissues from the same plant. High levels of SG and ASG occur in *Solanum* species, accounting to more than 50 % of the total sterol levels (Nyström et al., 2012; Ferrer et al., 2017). SG and ASG levels are high in fruit, vegetable juices, beer, wine as well as in tomatoes and potatoes (Declodt et al., 2018).

SGs and ASGs play important roles in biological processes such as maintenance of the plasma membrane organization and they allow adaptive responses to environmental changes (Mamode Cassim et al., 2019). Several studies using forward and reverse genetic approaches have revealed the important role of SGs and ASGs in plants during different environmental stresses. An example is provided by transgenic *Arabidopsis* and tobacco plants, overexpressing a sterol glycosyltransferase from *W. somnifera*, showing increased tolerance towards salt, heat and cold. Furthermore, downregulation of the same gene product results in increased susceptibility to plant pathogens (reviewed in Ferrer et al. 2017). SGs and ASGs are also present in pollen and phloem sap of *Arabidopsis*. It has been hypothesized that SGs act as primers of cellulose synthesis (Ferrer et al., 2017). The attached sugar to the sterol increases drastically the hydrophilicity of phytosterols and might increase the ability to interact with proteins embedded in membranes as well as with other glycolipids in lipid rafts. The same has been proposed for the amphiphilic cardiac glycosides ouabain and digitalin (Tabata et al., 2008).

Phytosterols are nowadays widely used as food additives aiming to lower plasma LDL cholesterol and reduce cholesterol absorption in humans. Already in the early 1950s, intake of plant sterols was reported to reduce the total plasma cholesterol and LDL-cholesterol and cholesterol absorption efficiency (Peterson, 1951). After this, a vast number of studies and clinical trials demonstrated cholesterol-lowering effects of a phytosterol-rich diet. This led to the industrial production of phytosterol enriched food products such as margarines and yogurts (Abumweis and Jones, 2008; Amiot et al., 2011; Trautwein et al., 2018; Nakano et al., 2019). It is generally accepted that 1-3 g of a daily dose of phytosterols leads to a 10-15% decrease of total cholesterol levels and also decreases plasma LDL-cholesterol (Patel et al., 2018; Nakano et al., 2019).

The metabolic response to phytosterols varies among individuals (Jones, 2015). This can be due to genetic differences, for example in genes encoding ApoE and CYP7A1. Of particular interest in this connection are also ATP-binding cassette (ABC) subfamily G member 5 (ABCG5) and member 8 (ABCG8), which are proteins involved in phytosterol transport. Mutations in ABCG5 or ABCG8 cause sitosterolemia, a devastating disease first described by Bhattacharyya and Connor in 1974 (Bhattacharyya and Connor, 1974; Tada et al., 2018; Plat et al., 2019). The ABCG5 and ABCG8 proteins act as heterodimers, forming together with other proteins a functional sterol transport complex, and are expressed in hepatocytes, gallbladder epithelium, and enterocytes. ABCG5/ABCG8 excretes phytosterols and other xenosterols from cells, even better than cholesterol. Impaired ABCG5/ABCG8 leads to accumulation of phytosterols in the body causing macrothrombocytopenia, platelet dysfunction, liver disease, cholesterol accumulation with xanthoma formation and atherosclerosis (Silbernagel et al., 2013; Patel et al., 2018).

Little is still known on the impact of SGs and ASGs on the human body. The  $\beta$ -sitosterol- $\beta$ -D-glycoside (BSSG) is relatively abundant in the human diet (Decloedt et al., 2018). Both  $\beta$ -sitosterol (BSS) and its glycosylated form are found in human plasma and tissues in very low levels, at 800-1000 less compared to endogenous cholesterol (Pegel, 1997). It has been shown that upon chronic high intake plant sterols accumulate in the brain (Vanmierlo et al., 2012; Saeed et al., 2015). Even though the mammalian blood brain barrier (BBB) is not, or very poorly, permeable to cholesterol, studies have shown that phytosterols like sitosterol and campesterol are able to cross the BBB in mice.

BSS and BSSG are proposed to exert beneficial anti-inflammatory actions and to reduce mild hypercholesterolemia (Bouic et al., 1999). Bouic et al. observed that administering a mixture of BSS/BSSGs to marathon runners had a positive effect on the immune system under physical stress conditions (Bouic et al., 1999). On the other hand, BSSGs were also found to be toxic to motor neurons in vitro (Tabata et al., 2008). The exposure to high amounts of BSSGs amounts present in the seed of the cycad tree (*Cycas micronesica*) has been speculated to underly the historical high prevalence of the neurodegenerative disease amyotrophic lateral sclerosis–parkinsonism dementia complex (ALS–PDC) at the island of Guam (Tabata et al., 2008). Indeed, feeding of BSSGs to rats is found to cause several neurological signs and defects resembling those occurring in Parkinson disease patients, such as  $\alpha$ -synuclein aggregates, motor abnormalities and striatal dopamine loss (Shen et al., 2010; Van Kampen et al., 2014; Kampen et al., 2015; Franco et al., 2018). Van Kampen and co-workers successfully induced Parkinsonism in Sprague Dawley rats by feeding them with BSSG for 4 months (Van Kampen et al., 2014).



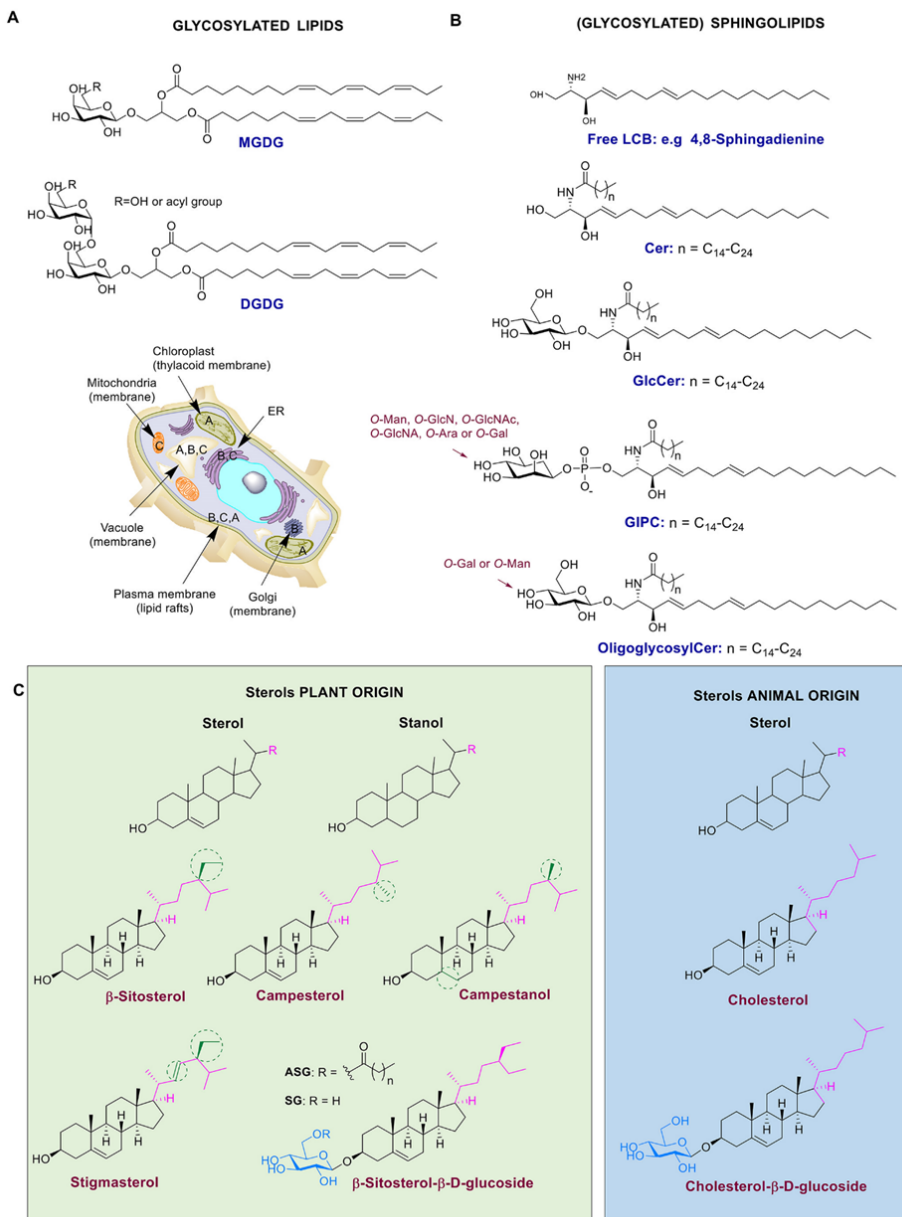


**Figure 2. Different classes of plant lipids and their localization in the plant cell.** A. Chemical structures of plant glycosylated lipids: monogalactosyldiacylglycerol (MGDG) and digalactosyldiacylglycerol (DGDG). B. Chemical structures of plant (glycosyl) sphingolipids: long-chain base (LCB) 4,8-sphingadienine, ceramide (Cer), glucosylceramide (GlcCer), glucosylinositol phosphoryl ceramides (GIPC) and oligoglycosylceramide. C. Chemical structures of plant sterols (green) versus the animal counterparts (blue). Plant cell image illustrating the localization of lipid classes: A. stands for MGDG and DGDG, B. for plant (glycosyl) sphingolipids and C. for plant sterols.

## Absorption and metabolism of plant glycoconjugates

Knowledge on the absorption and metabolism of individual plant glycoconjugates is warranted to better understand their mechanism of action. It appears that upon ingestion the fate of individual glycoconjugates may fundamentally differ.

**Uptake of glycosylated flavonoids.** For decades it was widely believed that prior to uptake in the body glycosylated flavonoids, such as quercitrin, rutin and robinin, common components of human diets, were first deglycosylated by intestinal glycosidases and bacterial enzymes in the intestine (Griffiths and Barrow, 1972; Bokkenheuser et al., 1987). Only the produced aglycones would be partially absorbed in the large intestine (Walle, 2004). Following uptake, flavonoids are glucuronidated, O-methylated or sulphated in the liver. Part of them are subsequently excreted into the bile and undergo enterohepatic cycling to finally being eliminated by renal excretion (Murota and Terao, 2003). An example of such metabolism is that of the flavanone hesperidin, mainly found in citrus fruits such as oranges and lemons. Hesperidin (hesperetin with a linked rutinoside moiety) is absorbed as the aglycone hesperetin, after removal of the glucose moiety by intestinal bacteria. However, rapid absorption of  $\alpha$ -glucosylated hesperidin (G-hesperidin) containing an additional linked  $\alpha$ -glucosyl moiety has been observed, possibly due to its high-water solubility (De Souza et al., 2016). It has become apparent that deglycosylation of some flavonoids may not depend on intestinal bacteria. Saliva has been also suggested to play a role in the hydrolysis of the dietary flavonoids. Browning et al. in 2005 performed a study on different glycosylated flavonoids like quercitrin, rutin, isoquercitrin, spiraeoside, genistin, naringin and phloridzin (Browning et al., 2005). Their findings suggest that saliva enzymes may hydrolyze the glycosylated flavonoids, in particular, glucosides. For instance, quercetin 4-glucoside and genistein 7-glucoside, found in high amounts in dietary products, are rapidly hydrolyzed in the oral cavity. Saliva is also suggested to already hydrolyze quercetin glucosides (Hirota et al., 2001).

Dietary glycosylated anthocyanins, such as cyanidin-3-glucoside and cyanidin-3,5-diglucoside, are absorbed in intact form (Miyazawa et al., 1999). Quercetin glycosides are known to be taken up in the small intestine via the sodium dependent glucose transporter SGLT1 (Hollman et al., 1995; Walgren et al., 1998; Walgren et al., 2000). Phloridzin, the glucoside of the flavonoid phloretin, was also found to be transported by SGLT1 (Walle and Walle, 2003). Takahashi et al. recently observed that intestinal absorption of galactosylated-cyanidin is inferior to that of the glucosylated one (Takahashi et al., 2019). Of note, absorbed glycosylated anthocyanins may pass the BBB and reach

different brain regions like the cortex and hippocampus (Milbury et al., 2002; Milbury and Kalt, 2010; Zhang et al., 2019). Phloridzin and other flavonoid glycosides (quercetin and genistein) have also been identified as substrates for efflux by the multidrug resistance-associated protein transporters MRP1 and MRP2 (Walle and Walle, 2003). Thus, dietary glycosylated anthocyanins seem to manage to reach visceral tissues and the brain by hijacking glucose transporters and are actively removed by MRPs.

**Uptake of (glycosylated) phytosterols.** In the lumen of the intestine the poorly water-soluble phytosterols are incorporated into micelles that allow close contact with the surface of enterocytes (Gylling et al., 2014). Next, phytosterols are thought to be internalized by the mucosal intestinal cells via the Niemann–Pick C1-Like1 (NPC1L1)-transporter. Subsequently, plant sterols are re-secreted into the lumen of the intestine via ABCG5/ABCG8 transporter complex (as discussed in section 3). In the liver, the ABCG5/ABCG8 complex mediates efflux of plant sterols into bile (Gylling et al., 2014). Plant sterols manage to pass the BBB and therefore potentially may influence brain function (Jansen et al., 2006; Vanmierlo et al., 2012). This notion raises considerations regarding excessive consumption of olive oil containing high amounts of plant sterols. The poor solubility of phytosterol in both water and oil limits absorption. Esterification of phytosterols increases their solubility in oil and margarine (Ostlund, 2004). Regarding glycosylated phytosterols it is clear that these reach tissues, including the brain (see section 3). Relatively little is however known with respect to transporter proteins involved in the uptake glycosylated sterols. They have been reported to be absorbed intact and exert as such their effects (Lin et al., 2009; Lin et al., 2011).

## Plant $\beta$ -glucosidases and glucosyltransferases

**Classification of glycosidases.** All domains of living organisms contain multiple glycoside hydrolases (GHs, glycosidases). These enzymes play a variety of functions, including the lysosomal metabolism of glycolipids in animals, the catabolism of cell wall polysaccharides in plants and biomass conversion in microorganisms (Leah et al., 1995; Ketudat Cairns and Esen, 2010). More than 160 GH families have been listed in the Carbohydrate Active EnZymes (CAZy) database using a classification system based on amino acid sequence and secondary structure similarities (Henrissat, 1991; Ben Bdira et al., 2018). This classification system is regularly updated and new families are continuously discovered. Additionally, the enzymes are classified based on their reaction mechanism, according to the stereochemical outcome of the hydrolytic reaction, into inverting or retaining enzymes (Koshland, 1953; Sinnott, 1990). Moreover,

glycosidases are also classified as exo- or endo-enzymes, depending on their ability to cleave at the end or in the middle of a carbohydrate chain.

Plants contain numerous carbohydrate active enzyme-encoding genes, more than any other organism. For instance, *Arabidopsis* contains over 400 different genes encoding glycosidases (Husaini et al., 2018). This complexity stems from gene duplications and has likely been promoted by the increasingly complex plant cell wall structure, as described for *Arabidopsis* by Bowers et al. (Bowers et al., 2003). Some proteins, based on homology designated as glycosidases or glycosyltransferases might have further evolved to act on different types of substrates or to fulfill other non-enzymatic functions (Coutinho et al., 2003). An example is the soybean hydroxyisourate hydrolase. Even though the enzyme has a highly conserved retaining  $\beta$ -glucosidase active site, it catalyzes the hydrolysis of 5-hydroxyisourate (Raychaudhuri and Tipton, 2003). Therefore, caution when talking about plant glycosidases and glycosyltransferases is necessary.

Particularly ubiquitous in plants are  $\beta$ -glucosidases. Most plant  $\beta$ -glucosidases (E.C.3.2.1.21) are mainly classified in the glycoside hydrolase family 1 (GH1) of the CAZy database. However, some plant  $\beta$ -glucosidases are grouped in GH families 5 and 30. They all fall in GH Clan A, and contain similar ( $\beta/\alpha$ )8-barrel structures. They consistently share an active site with two catalytic residues (Morant et al., 2008; Ketudat Cairns and Esen, 2010). Their main activity, even though it is not restricted, accounts to the hydrolysis of the  $\beta$ -glucosidic bond between carbohydrates or between a sugar and an aglycone moiety.

Plant  $\beta$ -glucosidases play a number of important biological roles. For instance, they are involved in cell wall degradation during endosperm germination (Leah et al., 1995). The enzymes together with other plant and microbial glycosidases and glycanases degrade the plant cell wall, leading to formation of intermediates for cell wall lignification (Dharmawardhana et al., 1995; Escamilla-Treviño et al., 2006). Over different enzymes have been reported taking a part in this process (Mohnen, 2008). Furthermore,  $\beta$ -glucosidases are involved in activation of phytohormones (Kristoffersen et al. 2000; Lee et al. 2006). They participate in plant defence mechanisms via activating several chemical defence compounds, like phytohormones, flavonoids and cyanogenic glucosides (Nisius, 1988; Poulton, 1990; Suzuki et al., 2006; Morant et al., 2008). For instance, a cyanogenic glucosidase (linamarase) from cassava and white clove is able to cleave glucosides from glucosylated cyanosides releasing toxic HCN as a defence mechanism (Oxtoby et al., 1991; Hughes et al., 1992). In addition, a  $\beta$ -glucosidase from maize was found to be active towards cytokinin-O-glucosides and kinetin-N3-glucoside, releasing

active cytokinin (Brzobohaty et al. 1993). Furthermore, they are reported to release volatiles like flower scents from their glycoside storage forms (Sarry and Günata, 2004). Due to the high number of different plant glycosides, it is very likely that plant glycosidases play other roles that are yet to be discovered.

**Catalytic mechanism of glycosidases.** Two carboxyl-exposing residues in the active site of both inverting and retaining  $\beta$ -glycosidases enzymes take part in the hydrolysis of the glycosidic bond (Koshland, 1953). In the case of inverting enzymes, these two groups are separated at a distance of 6-12 Å, whereas in retaining enzymes, this is  $\sim 5$  Å. The inverting reaction is a single step reaction; a direct displacement of the aglycone, where one carboxylic group is acting as the base and it activates a water molecule that hydrolyses the glycosidic bond through a nucleophilic attack at the anomeric centre (Guce et al., 2010) and at the same time, the second carboxylic acid facilitates the departure of the leaving group via acid catalysis. On the contrary, retaining glycosidases employ a double displacement mechanism (Koshland, 1953). The reaction initiates with the nucleophilic attack to the anomeric center, resulting in a glycosyl-enzyme covalent intermediate. Then, the deprotonated carboxylate acts as a base and deprotonates a water molecule, that now plays the role of a nucleophile, to hydrolyze the covalent intermediate giving the reaction product. The transfer of a released sugar from a substrate to an acceptor other than a water molecule is called transglycosylation, and has been observed for several retaining glycosidases (Hehre, 2001; Sinnott, 1990). The acceptor molecules can be sugars, as in the case of chitotriosidase (Aguilera et al., 2003), but also retinol or sterol in the case of glucocerebrosidase, the human  $\beta$ -glucosidase (Vanderjagt et al., 1994). Akiyama and Marques reported the use of glucosylceramide as sugar donor in the formation of cholesterol glucoside via  $\beta$ -glucosidase mediated transglycosylation (Akiyama et al., 2013; Marques et al. 2016a). Several examples of transglycosylation activity of plant and bacterial glycosidases have also been reported (Crout and Vic, 1998; Morant et al., 2008).

**Glycosyltransferases.** The carbohydrate active enzyme (CAZy) database currently contains 110 glycosyltransferases (GTs). In plants, GTs have many functions, for example in the biosynthesis of glycosylated metabolites, oligosaccharides, polysaccharides (cellulose, hemicelluloses, and pectins among others) and glycoproteins in the plant cell membrane (Hansen et al., 2012). The polysaccharides and other glycans are mainly synthesized by glycosyltransferases (GTs; EC 2.4.x.y). Most GTs (Leloir GTs) transfer a sugar residue from an activated nucleotide sugar to a specific acceptor molecule, with high specificity for the sugar donor and the acceptor substrates (Breton et al., 2005). GTs are classified as retaining or inverting depending on whether

glycosylation results in net retention or inversion of stereochemistry at the anomeric carbon of the donor substrate. GTs are classified in the CAZy database into families on the basis of amino acid sequence similarities (Cantarel et al., 2009). Two major folds of structures of nucleotide–sugar-dependent GTs solved to date are observed, termed GT-A and GT-B (Hansen et al., 2010). Many GT-Bs are independent of a metal ion for catalysis, whereas most GT-A enzymes contains a conserved DxD motif that coordinates the phosphate atoms of the nucleotide donors via coordination of a divalent cation, usually Mn<sup>2+</sup> or Mg<sup>2+</sup> (Breton et al., 2005). Besides glycosyltransferases using sugar mono- or diphosphonucleotide donors, known as Leloir type GTs, two additional group of glucosyltransferases occur: non-Leloir-type GTs which employ sugar lipid phosphates, pyrophosphates or polyprenol phosphates as donors, and non-activated acyl-glucose dependent glucosyltransferases. This last group of enzymes are transglucosidases related to GH1 family hydrolases. One example of this is the rice  $\beta$ -glucosidase Os9BGlu31 that uses glucopyranosides as well 1-O-acyl glucose esters as sugar donors in synthetic reactions (Luang et al., 2013; Komvongsa et al., 2015).

## **New tools to explore “plant” glycosidases; Activity based probes (ABPs) for retaining glycosidases**

Detailed knowledge on the reaction mechanism of retaining glycosidases has allowed the generation of ABPs, a new class of versatile research tools (for a recent review see Wu, 2009).

**ABPs, principles and applications through time.** The idea to exploit covalent inhibitors of active enzymes as ABPs was firstly put forward for esterases by Ostrowski et al. in 1961 (Ostrowski and Barnard, 1961). The concept was further pioneered by Cravatt and co-workers for several enzyme classes. Now, ABPs have been designed for kinases, proteases, serine hydrolases, lipases and glycosidases (Cravatt et al., 2008; Witte et al., 2010; Witte et al., 2011; Serim et al., 2012; Baggelaar et al. 2013).

In the case of retaining glycosidases, the use of irreversible inhibitors optimally mimicking the oxocarbenium ion-like transition state of the target enzyme has promoted the design of diverse ABPs. Withers et al. first proposed the use of fluorinated inhibitors for targeting human  $\beta$ -glucosidase (Wicki et al., 2002; Goddard-Borger et al., 2010). Chauvigné-Hines and co-workers generated difluoromethylphenyl aglycone, N-halogenated glycosylamine, and 2-deoxy-2-fluoroglucoside activity-based probes to identify reactive glycosidases in the cellulosomal secretome of *Clostridium thermocellum* (Chauvigné-Hines et al.,

2012). Their study identified a wide number of cellulases, xylanases, hemicellulases and carbohydrate active enzymes. More specific, they were able to identify both inverting and retaining enzymes that were listed in different GH families. Some of them play an important role in the degradation of cellulose: GH9 (inverting) cellulase enzymes, a number of GH5 (retaining) endoglucanases, and GH10 and GH11 (retaining) xylanases (Chauvigné-Hines et al., 2012).

The first retaining  $\beta$ -glucosidase for which a high affinity and highly selective ABP was designed has been human glucocerebrosidase. A decade ago, Witte et al. demonstrated that cyclophellitol based ABPs irreversibly bind and enable identification of GBA (human lysosomal  $\beta$ -glucosidase; glucocerebrosidase) in complex biological samples, such as cell lysates, cell cultures and laboratory animals (Witte et al., 2010). This ABP has meanwhile found important applications in studies on Gaucher disease, an inherited lysosomal storage disorder caused by GBA deficiency. Its use for diagnostic purposes holds great promise (Aerts et al., 2011). The glucosyl-configured cyclophellitol ABP binds covalently to the catalytic nucleophile, Glu-340, of the human GBA enzyme (Figure 3A). In addition to the cyclophellitol sugar, the probes contain a reporter group, that can be a fluorophore and/or biotin, attached via a linker to the C-6 position of the functionalized cyclophellitol, enabling the visualization and/or identification of active enzyme molecules (Witte et al., 2010).

Next, a different class of ABPs was designed by Overkleeft for retaining  $\beta$ -glucosidases based on the use of cyclophellitol-aziridine scaffolds (Kallemeijn et al., 2012) (Figure 3A and B). Subsequently, by variation of the configuration of cyclophellitol-aziridine a series of new probes were developed for other retaining glycosidases. Detection of active  $\alpha$ -D-galactosidase (Willems et al., 2014a),  $\beta$ -D-galactosidase (Marques et al., 2016b),  $\alpha$ -L-fucosidase (Jiang et al., 2015),  $\alpha$ -D-glucosidases (Jiang et al., 2016),  $\beta$ -D-glucuronidase (Wu et al., 2017),  $\alpha$ -L-iduronidase (Artola et al., 2018) and  $\alpha$ -L-arabinofuranosidases (McGregor et al., 2020) was achieved with these types of ABPs. Through changing the reporter group into a biotin, the probes can be used for streptavidin-mediated enrichment, followed by proteomics identification of labelled proteins using LC-MS/MS (Jiang et al., 2016). Meanwhile, many research applications for glycosidase ABPs have been found. The amphiphilic nature of glycosidase ABPs enables them to penetrate cells and organisms, allowing in situ labelling of active enzyme molecules in lysosomes. Intravenous infusion of mice with ABPs resulted in specific labeling of GBA in various tissues (Kallemeijn et al., 2012). More recently, the same ABPs were employed to very sensitively visualize active GBA molecules in lysosomes of cells by correlative light electron

microscopy (CLEM) (Van Meel et al., 2019). Visualization of GBA in the brain of mice was also achieved after intracerebroventricular administration of the ABP (Herrera Moro Chao et al., 2015). Application of ABPs in studies with zebrafish models of GBA enzyme deficiency have been recently described (Artola et al., 2019; Lelieveld et al. 2019). In addition,  $\beta$ -D-glucuronidase ABPs have recently been employed in fecal samples to study the anticancer Irinotecan drug toxicity driven by gut microbial enzymes (Jariwala, et al. 2020).

**ABPs in plant science.** Plant scientists interested in hydrolases have to deal with a huge number of genes encoding potential glycosidases. Moreover, transcript expression levels do not always correlate with actual active enzyme levels. Therefore, methods for conveniently monitoring distinct active glycosidases are in great demand to establish the functional proteome of different plant species. ABPs provide a novel toolbox for this purpose which has been successfully applied in plant science during the last decade (van der Hoorn and Morimoto, 2016). Enzymes of several families have been identified and functionally characterized using ABPs, such as serine hydrolases (Kaschani et al., 2009), papain-like cysteine proteases (Richau et al., 2012) and cysteine proteases (Lu et al., 2015). In addition, retaining glycosidases of different plant species have been characterized and identified (Chandrasekar et al., 2014; Husaini et al., 2018; Kytidou et al., 2018-chapter 4). The use of ABPs as functional tool for studying retaining glycosidases in plants was first reported by the group of van der Hoorn in 2014. The chemical structures of ABPs used in this research are depicted in Figure 3B. An overview is provided in Figure 3C of key publications describing specific applications of ABPs in research using several plant species.

The  $\beta$ -D-glucose configured cyclophellitol-aziridines JJB70 conjugated with a BODIPY green fluorophore and JJB111 conjugated with a biotin was combined with proteomic analysis of targeted protein to study glycosidases in *Arabidopsis thaliana* total leaf samples and in *N. benthamiana* apoplast samples (Chandrasekar et al., 2014). KY371 probe, which does not contain any reporter group, was applied as competitor to ensure that protein labeling was specific. The investigation revealed that the aziridine type  $\beta$ -glucosidase ABPs present a broad activity, enabling identification of not only  $\beta$ -glucosidases but also myrosinases, xylosidases, and galactosidases. Importantly, very high (micromolar) concentrations of ABP were used in the study which favors detection of different classes of glycosidases. The identified proteins are members of seven different retaining glycosidase families (Chandrasekar et al., 2014). Of note, no cellulases were identified. The main identified proteins were the  $\beta$ -thioglucoside glucohydrolase TGG2 (68-kDa signal) and TGG1 (75-kDa signal). Both enzymes are myrosinases and catalyze the conversion of



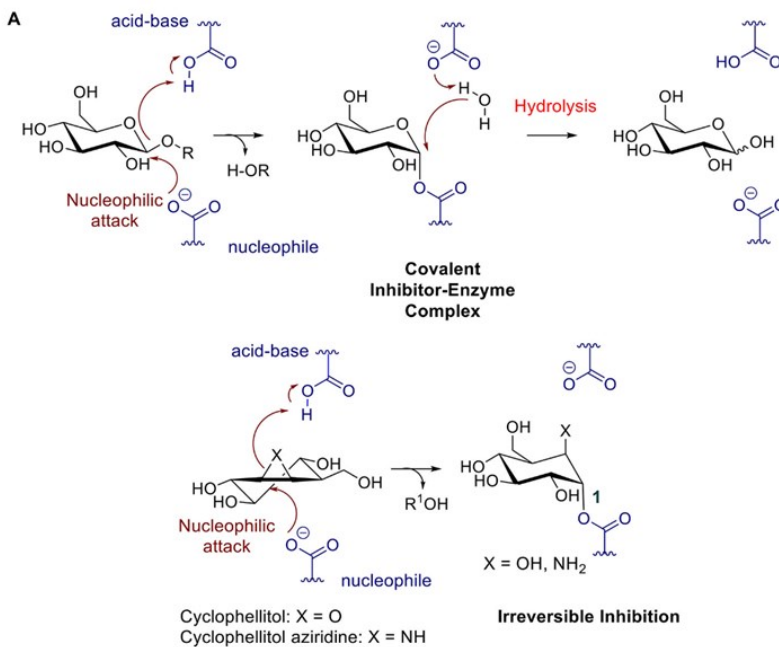
glucosinolates during attack of invaders. Interestingly, yet uncharacterized glycosidases, one of which was previously classified as pseudogene (TGG3), were identified in the study. An investigation with the ABP of secreted proteins by *N. benthamiana* cells led to the identification a wide range of putative xylosidases, galactosidases, glucanases, and heparanase. In addition, in situ labeling of active glycosidases present in Arabidopsis cell cultures revealed that ABPs (KY371 and JJB70) can penetrate living plant cells and therefore can be fortuitously also used to generate knock out models. Furthermore, van Hoorn and colleagues explored the presence of glycosidases in different (tissues of) plant species like *Brassica napus*, *Brassica oleracea*, *Brassica rapa*, *Brassica pekinensis*, *Triticum monococcum*, *Zea mays*, *Avena sativa* and *Nicotiana benthamiana* via in-gel imaging (Chandrasekar et al. 2014) (see Figure 3C).

Next, Daneri-Castro et al. used ABPs to identify and characterize enzymes that are secreted by the aleurone layer during barley germination and are induced or not by gibberellic acid (GA). They employed different ABP classes and thus were able to identify putative aleurains, cathepsin-B-like proteases and serine hydrolases. JJB70 ABP, targeting active retaining glycosidases, was used to demonstrate the presence of a putative xylanase in barley aleurone by competing the labeling with xylose (Daneri-Castro et al., 2016). More recent, ABPs targeting  $\alpha$ -glucosidases have been used in investigations on *Arabidopsis* and saffron crocus (*Crocus sativus*) (Husaini et al. 2018). Interestingly, using the  $\alpha$ -glucosidase ABP (JJB383) evidence was obtained that during stigma development in saffron glycosidases are involved in the conversion of picrocrocin into safranal. Furthermore, during Fox infection the enzyme AGLU1 was detected to be present in the apoplast. In the same study, parallel analysis of both  $\alpha$ - and  $\beta$ -glucosidases was performed, enabling simultaneous identification of different enzyme classes (Husaini et al., 2018). In conclusion, ABPs find very broad applications in investigations on plant metabolism and physiology.

ABPs have also already been successfully used to monitor recombinant active enzyme during transient expressions in *N. benthamiana* plants. Human  $\alpha$ -galactosidases have been produced in *N. benthamiana* leaves and in HEK293 cell cultures (Kytidou et al., 2017-chapter 3). Recombinant protein was detected and quantified using the  $\alpha$ -galactosyl configured cyclophellitol-aziridine TB474 containing a Cy5 fluorophore (Kytidou et al., 2017). This detection method is superior to western-blot since it allows selective detection of active enzyme molecules. Based on previous investigations, it might be concluded that ABPs can be applied as an easy quantitative method to follow the production of biopharmaceuticals in recombinant systems. In addition, the use of the biotinylated ABP, ME741, enabled the identification of a novel *N. benthamiana*

galactosidase, named A1.1. The enzyme was then overexpressed in *N. benthamiana* leaves, purified and further biochemically characterized. One of the most important findings was that A1.1 proves to be able to hydrolyze human glycosphingolipids in vitro and in situ and might find applications in the treatment of Fabry disease, caused by deficiency of the human  $\alpha$ -galactosidase (Kytidou et al., 2018, chapter 4). Therapeutic application of a plant enzyme, discovered with an ABP, for treatment of a human metabolic disease can be thus be envisioned (Figure 3B and C).

The specificity of ABP labeling of glycosidases can be fine-tuned by the assay conditions (e.g. variation of pH), concentration of probe and use of competitive inhibitors. The ABPs can in principle be used to visualize glycosidases during physiological processes of interest such as plant development, seed germination, cell wall formation and different responses to biotic and abiotic stresses.



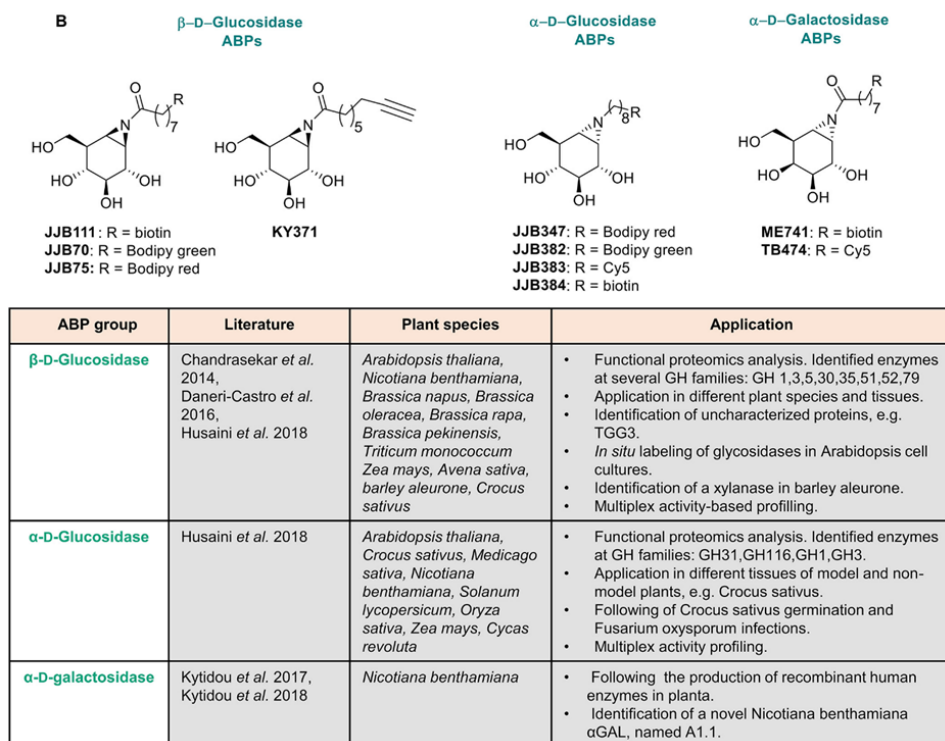


**Figure 3. Activity based probes mechanism and use in plant science.** A. Mechanism of aziridine and epoxide activity-based probes. B. Structures of ABPs used in plant science. C. Summary of published ABPs used in plant research. Presented are key publications describing specific applications in plant species.

## Production of therapeutic (human) glycosidases in plants

**History.** Production of biopharmaceutical proteins in plants is undertaken since the early 2000s. It gained great attention due to the advantages in economy, safety and scalability with several examples of in planta recombinant protein productions over the last decades (Westerhof *et al.*, 2014; Wilbers *et al.*, 2017). The first plant-produced protein was the human growth hormone, in 1986, in tobacco cell cultures (Fischer *et al.*, 2004). After that, a vast number of different proteins have been produced in planta, demonstrating the viability of such methods for industrial and pharmaceutical uses (Hidalgo *et al.*, 2018; Kopertekh and Schiemann, 2019). A recent example is the large-scale production of the drug ZMapp in 2014 in tobacco leaves for use against Ebola

virus (Yao et al., 2015). This review focuses on the production of therapeutic human glycosidases in plants for the treatment of lysosomal diseases.

**Lysosomal enzymes and their production in plants.** Lysosomal diseases are inherited metabolic diseases caused by dysfunction of lysosomal hydrolases. A possible therapy for these diseases involves replacement of deficient enzymes by their normal equivalents. Supplementation of patient cells is envisioned following intravenous administration (infusion) of recombinant enzyme. This concept was developed and pioneered by Brady and is known as enzyme replacement therapy (ERT) (Brady, 2003; Desnick and Schuchman, 2012; Aerts and Cox, 2018). The uptake of the recombinant enzyme preparations is usually mediated by mannose receptors (MR) which are present in the surface of the targeted cells and also via mannose-6-phosphate receptors (M6PR) and the asialoglycoprotein receptor (Ashwell-Morell receptor; AMR) (Figure 4) (Coutinho et al., 2012; Shen et al., 2016; Tian et al., 2019). Examples of such disorders and their corresponding impaired glycosidase are Gaucher disease and  $\beta$ -glucocerebrosidase (GBA), Fabry disease and  $\alpha$ -galactosidase ( $\alpha$ GAL), Pompe disease and  $\alpha$ -glucosidase (GAA) and Krabbe disease and  $\beta$ -galactocerebrosidase (GALC).

The production of the lysosomal human GBA enzyme in carrot cells by Shaaltiel and colleagues in 2007 can be considered as a hallmark in the production of pharmaceutical glycosidases in plants for the treatment of lysosomal diseases (Shaaltiel et al., 2007). The plant produced enzyme, ELELYSO (taliglucerase alfa) (Protalix BioTherapeutics), was approved by the FDA in May 2012. The enzyme is targeted to the vacuoles of carrot cells via the insertion of a chitinase (“GLLVDTM”) vacuole signal peptide. The recombinant enzyme has high mannose terminal N-glycans that mediate uptake by macrophages (Shaaltiel et al., 2007). It was firstly demonstrated that the plant specific N-glycans on the plant produced recombinant GBA are not immunogenic, a crucial finding. Production of human GBA enzyme in transgenic, complex-glycan-deficient, *Arabidopsis* seeds, has also been achieved (He et al., 2011). The produced enzyme in the latter case does not contain any targeting signal to the vacuole. Active GBA has recently also been produced in root cultures of *Nicotiana tobacco* (Naphatsamon et al., 2018). Finally, GBA enzyme with high mannose N-glycans (gnt1-GBA) was produced in mutant rice (Jung et al., 2019).

Another human lysosomal hydrolase produced in plants is  $\alpha$ -galactosidase A. The production of this enzyme for therapy of Fabry disease was firstly accomplished in tobacco cell cultures in 2015 (Kizhner et al., 2015; Ruderfer et al., 2018; Schiffmann et al., 2019). The protein, pegunidalsidase alfa, PRX-102 (Protalix BioTherapeutics), is currently in clinical trials and it is produced in

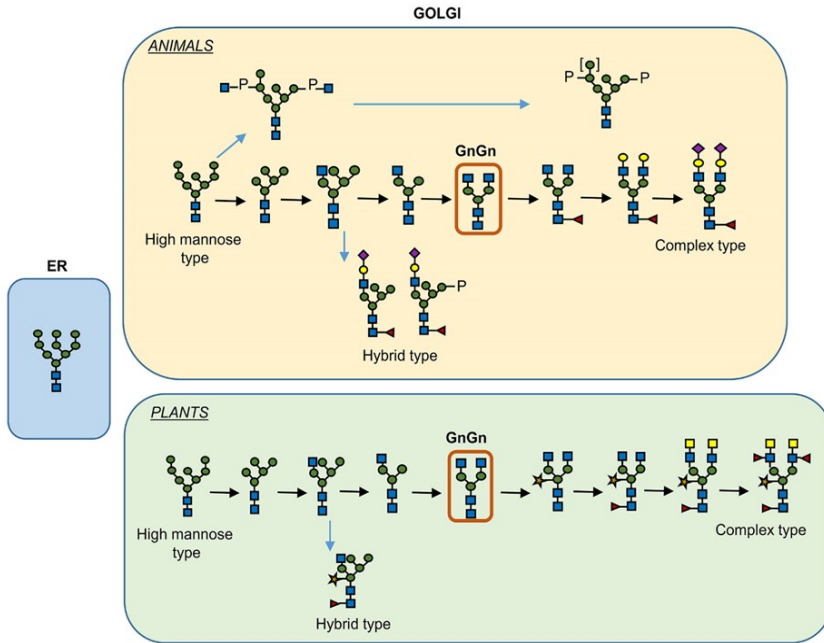
large scale at ProCellEx plant cell-based protein expression platform (Ruderfer et al., 2018). Interestingly, the recombinant protein is chemically modified with a bifunctional PEG polymer to form stable dimers. Such modification improves the enzyme's stability in plasma and its pharmacokinetic properties (Ruderfer et al., 2018). PRX-102 is found superior in stability than the current available recombinant enzymes for treatment of Fabry disease (agalasidase beta, Fabrazyme and agalsidase alpha, Replagal) which are both produced in mammalian cell culture systems. Of note, no M6P residues are present in the N-linked glycans of pegunidalsidase alfa. A mannose enriched human  $\alpha$ -galactosidase A was produced in 2016 in moss cell cultures (Shen et al., 2016). The enzyme was found to be effectively targeted through the MR pathway to defective organs such as heart and kidney.  $\alpha$ -Galactosidase was also produced transiently in *N. benthamiana* leaves for research purposes (Kytidou et al., 2017). In parallel, in the same platform human  $\alpha$ -N-acetylgalactosaminidase and a mutated form with increase  $\alpha$ -galactosidase activity was generated (Tajima et al., 2009; Kytidou et al., 2017). Finally, a modified fragment of human  $\alpha$ -glucosidase (GAA) has been produced in plant chloroplasts to induce tolerance against human GAA in Pompe disease patients receiving ERT (Su et al., 2015). Future investigations will demonstrate clinical benefit of this approach.

**N-glycoengineering.** The feasibility to manipulate and humanize the N-glycosylation pathway of plants offers a great advantage in the production of biopharmaceuticals (Castilho and Steinkellner, 2012; Bosch et al., 2013). N-glycosylation of glycoproteins in plants and mammals is identical up to the formation of the vital intermediate "GlcNAc2Man3GlcNAc2" N-glycan (GnGn structure) in medial-Golgi apparatus (Figure 4A) (Gomord et al., 2010). Further modification of the GnGn structure takes place in mammals in trans-Golgi apparatus, resulting in complex and highly heterogenic N-glycan structures whereas in plants further modifications are not as frequent and mainly include the addition of  $\beta$  (1,2)-xylose and  $\alpha$  (1,3)-fucose residues at core GnGn structure (Gomord and Faye, 2004). Additionally, high mannose, paucimannosidic structures and also Lewis-X epitopes are frequently observed in N-glycans of plant glycoproteins. Even though core fucosylation may occur in mammals this involves addition of  $\alpha$ (1,6)-linked fucose residues (Bosch et al., 2013). Several examples of N-glycoengineering plants to reach a human like N-glycan profile have been reported and reviewed (Castilho and Steinkellner, 2012; Bosch et al., 2013). Using reverse genetics (CRISPR/cas9 knock out, RNAi methods), plants were generated lacking endogenous activities such as the ones of  $\beta$  (1,2)-xylosyltransferase and core  $\alpha$  (1,3)-fucosyltransferase responsible for attaching plant-specific residues to core glycan structures (Jansing et al., 2019). This was

first accomplished in *Arabidopsis thaliana* plants followed by *Nicotiana benthamiana*, *Lemna minor*, and the moss *Physcomitrella patens* and rice cells (Strasser et al., 2004; Schähs et al., 2007; Loos et al., 2011; Castilho and Steinkellner, 2012; Bosch et al., 2013).

During ERT of patients suffering from glycosidase deficiencies, intravenously infused recombinant enzymes are endocytosed via lectin-mediated pathways. In the case of Gaucher disease, ERT is highly successful since the recombinant enzyme is targeted efficiently to macrophages (the primary storage cells) via MR-mediated uptake (see above and Figure 4B). In other LSDs however, several cell types are affected and need to be supplemented with therapeutic enzyme. For this reason, use of the ubiquitous M6PR uptake is envisioned and recombinant enzyme with a high M6P content in their N-glycans are produced (Schiffmann et al., 2001; Eng et al., 2001; Kroos et al., 2012; Ferraz et al., 2014). Thus, the N-glycan profile of the therapeutic enzyme plays a key role in its availability, targeting and bioactivity. The  $\alpha$ -galactosidase produced in moss by Shen et al. is claimed to be endocytosed by many cell types via mannose-lectin mediated uptake. The enzyme has high mannose N-glycans that lack the plant specific  $\alpha$  (1,3)-fucose and  $\beta$  (1,2)-xylose residues (Shen et al., 2016).

**A** N-glycosylation pathway of newly synthesized proteins in animals and plants



**B** Lectin-mediated uptake of lysosomal enzymes

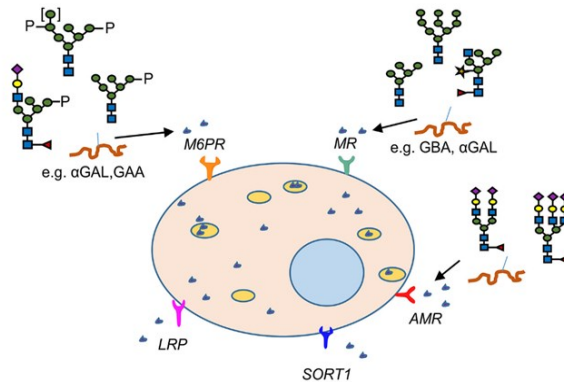


**Figure 4. Plant and human N-glycosylation pathways: importance in production of pharmaceuticals.** A. N-linked glycosylation pathway of proteins produced in plants and humans. B. The lectin mediated uptake of recombinant enzymes from cells for the treatment of LSDs.

## **ABPs: linking retaining glycosidases with small compound interactors of their catalytic pockets.**

The previous sections of this review largely focused on glycosylated metabolites on the one hand and retaining glycosidases on the other hand. In addition, the design and application of ABP reacting in a mechanism-based manner with the catalytic nucleophile of specific glycosidases was introduced. In this section, the use of ABPs to 'bridge' glycosidases with interacting small compounds is discussed.

The great value of ABPs to identify, purify and characterize glycosidases from various plants has been addressed in the previous sections. Some of these enzymes might find future applications as drugs or in industrial processes. Another application for ABPs warrants discussion. By virtue, ABPs can be also used to identify small compounds that interact with the catalytic pocket of the reactive glycosidase. Such interactors, (substrates, inhibitors), will compete with the ABP for occupancy of the pocket and the subsequent labeling of the enzyme (Figure 5). This concept can for example be exploited to screen different plant extracts or selected compounds (glycosylated plant sterols and flavonoids) for interaction with (plant or human) glycosidases as revealed by the competition of labeling of the glycosidase with the corresponding ABP. Proof of principle for such screens has already been obtained. In this manner, inhibitors have been identified for the human non-lysosomal glucosylceramidase GBA2, an enzyme that is difficult to purify to homogeneity in active form. Lahav et al. used a fluorescent polarization activity-based protein profiling (ABPP) assay where they successfully screened a library of 350+ iminosugars for potential GBA2 inhibitors using a lysate of cells over-expressing GBA2 and the appropriate glucosidase ABP (Lahav et al., 2017). In the same manner, complex biological samples can be screened on the presence of potential substrates for a glycosidase competing with ABP labelling. One further application along the same line is the use of cell-permeable ABP labeling of a glycosidase to identify the in-situ inhibition of a target glycosidase by an administered inhibitor. An example of such application is provided by a recent study identifying in intact cells and zebrafish the  $\beta$ -glucosidase target engagement of condurititol B-epoxide and cyclophellitol analogues (Kuo et al., 2019; Artola et al., 2019).

In conclusion, ABPs will not only be of value to study their target glycosidases but also interactors of their catalytic pockets.



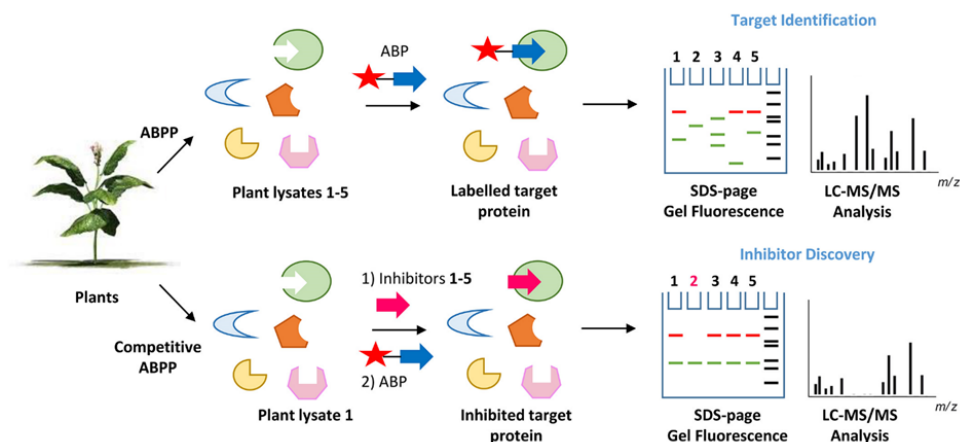


**Figure 5. Principle of activity-based protein profiling for target identification and competitive activity-based protein profiling for the screening of glycosidase inhibitors.** The competition of ABP labelling of a glycosidase by agents interacting with its pocket (inhibitors, substrates) can be conveniently and sensitively assessed. Note: there is no need for a pure enzyme, when visualizing labelled glycosidase using SDS-PAGE and fluorescence scanning.

## Summary and Perspectives

Natural plant-derived glycosides are used for various therapeutic purposes. Increased knowledge of beneficial/toxic effects is warranted. This is particularly relevant for plant sterols for which beneficial and potentially harmful effects have been reported. Better insight is needed regarding the biological effects, bioavailability and metabolism of glycosylated sterols prior to any clinical use in prevention/treatment of diseases. This may also hold for other plant metabolites. The therapeutic value of infusion of glycosidases in treatment of inherited deficiencies in man has been demonstrated for a number of diseases. In recent years, production of such glycosidase increasingly occurs in plant platforms that offer several advantages. Importantly, the N-glycan composition of plant-produced recombinant enzymes can be very well controlled using genetically modified plants. The ubiquitous plant glycosidases themselves might conceivably find therapeutic applications in humans and might have potential to treat inherited glycosidase deficiencies in man (Kytidou et al., 2018:chapter 4). Overall, activity-based probes may help to identify plant glycosidases of interest.

## References

- AbuMweis, S.S., Jones, P.J.H. (2008). Cholesterol-lowering effect of plant sterols. *Curr. Atheroscler. Rep.* 10:467-472. doi: <https://doi.org/10.1007/s11883-008-0073-4>
- Aerts, J.M.F.G., Cox, T.M., (2018). Roscoe O. Brady: Physician whose pioneering discoveries in lipid biochemistry revolutionized treatment and understanding of lysosomal diseases. *Blood Cells, Mol Dis* 68:4–8. doi: <https://doi.org/10.1016/j.bcmd.2016.10.030>
- Aerts, J.M.F.G., Kallemeijn, W.W., Wegdam, W., et al (2011). Biomarkers in the diagnosis of lysosomal storage disorders: proteins, lipids, and inhibitors. *J Inher Metab Dis* 34:605–619. doi: [10.1007/s10545-011-9308-6](https://doi.org/10.1007/s10545-011-9308-6)
- Aguilera, B., Ghauharali-van der Vlugt, K., Helmond, M.T.J., et al (2003). Transglycosidase Activity of Chitotriosidase: Improved enzymatic assay for the human macrophage chitinase. *J Biol Chem* 278:40911–40916. doi: [10.1074/jbc.M301804200](https://doi.org/10.1074/jbc.M301804200)
- Akiyama, H., Kobayashi, S., Hirabayashi, Y., Murakami-Murofushi, K. (2013). Cholesterol glucosylation is catalyzed by transglucosylation reaction of  $\beta$ -glucosidase 1. *Biochem Biophys Res Commun* 441:838–843. doi: <https://doi.org/10.1016/j.bbrc.2013.10.145>
- Ali, U, Li H, Wang, X, Guo, L (2018), Emerging Roles of Sphingolipid Signaling in Plant Response to Biotic and Abiotic Stresses. *Mol Plant* 11:1328–1343. doi: [10.1016/j.molp.2018.10.001](https://doi.org/10.1016/j.molp.2018.10.001)
- Amiot, M.J., Knol, D., Cardinault, N., et al. (2011). Phytosterol ester processing in the small intestine: impact on cholesterol availability for absorption and chylomicron cholesterol incorporation in healthy humans. *J Lipid Res* 52:1256–1264. doi: [10.1194/jlr.M013730](https://doi.org/10.1194/jlr.M013730)
- Artola, M., Kuo, C-L., Lelieveld L.T., et al (2019). Functionalized Cyclophellitols Are Selective Glucocerebrosidase Inhibitors and Induce a Bona Fide Neuropathic Gaucher Model in Zebrafish. *J Am Chem Soc* 141:4214–4218. doi: [10.1021/jacs.9b00056](https://doi.org/10.1021/jacs.9b00056)
- Artola, M., Kuo, C-L., McMahon, S.A., et al. (2018). New Irreversible  $\alpha$ -l-Iduronidase Inhibitors and Activity-Based Probes. *Chemistry* 24:19081–19088. doi: [10.1002/chem.201804662](https://doi.org/10.1002/chem.201804662)
- Baggelaar, M.P., Janssen F.J., van Esbroeck, A.C.M., et al. (2013). Development of an Activity-Based Probe and In Silico Design Reveal Highly Selective Inhibitors for Diacylglycerol Lipase- $\alpha$  in Brain. *Angew Chemie Int Ed* 52:12081–12085. doi: [10.1002/anie.201306295](https://doi.org/10.1002/anie.201306295)
- Ben Bdira, F., Artola, M., Overkleeft H.S., et al. (2018). Distinguishing the differences in  $\beta$ -glycosylceramidase folds, dynamics, and actions informs therapeutic uses. *J Lipid Res* 59:2262–2276. doi: [10.1194/jlr.R086629](https://doi.org/10.1194/jlr.R086629)
- Bhattacharyya, A.K., Conno, W.E. (1974). Beta-sitosterolemia and xanthomatosis. A newly described lipid storage disease in two sisters. *J Clin Invest* 53:1033–1043.

doi: 10.1172/JCI107640

- Bokkenheuser, V.D., Shackleton, C.H., Winter, J. (1987). Hydrolysis of dietary flavonoid glycosides by strains of intestinal *Bacteroides* from humans. *Biochem. J.* 248:953–956. <https://doi.org/10.1042/bj2480953>
- Bors, W., Heller, W., Michel, C., Saran, M. Bors W, Heller W, Michel C, Saran M. (1990). Flavonoids as antioxidants: determination of radical-scavenging efficiencies. *Methods Enzymol.* 186:343-55. doi: [https://doi.org/10.1016/0076-6879\(90\)86128-I](https://doi.org/10.1016/0076-6879(90)86128-I)
- Bosch, D., Castilho, A., Loos A., et al. (2013). N-glycosylation of plant-produced recombinant proteins. *Curr Pharm Des* 19:5503—5512. doi: 10.2174/1381612811319310006
- Bouic, P.J., Clark, A., Lamprecht, J., et al. (1999). The effects of B-sitosterol (BSS) and B-sitosterol glucoside (BSSG) mixture on selected immune parameters of marathon runners: inhibition of post marathon immune suppression and inflammation. *Int J Sports Med* 20:258—262. doi: 10.1055/s-2007-971127
- Bowers, J.E., Chapman, B.A., Rong, J., Paterson, A.H. (2003). Unravelling angiosperm genome evolution by phylogenetic analysis of chromosomal duplication events. *Nature* 422:433–438. doi: 10.1038/nature01521
- Brady, R.O. (2003). Enzyme replacement therapy: conception, chaos and culmination. *Philos Trans R Soc London Ser B Biol Sci* 358:915–919. doi: 10.1098/rstb.2003.1269
- Breton, C., Šnajdrová, L., Jeanneau, C., et al. (2005). Structures and mechanisms of glycosyltransferases. *Glycobiology* 16:29R-37R. doi: 10.1093/glycob/cwj016
- Browning, A.M., Walle, U.K., Walle, T., et al. (2005). Flavonoid Glucosides Are Hydrolyzed and Thus Activated in the Oral Cavity in Humans. *J Nutr* 135:48–52. doi: 10.1093/jn/135.1.48
- Brzobohaty, B., Moore, I., Kristoffersen, P., et al. (1993). Release of active cytokinin by a beta-glucosidase localized to the maize root meristem. *Science* (80- ) 262:1051 LP – 1054. doi: 10.1126/science.8235622
- Cacas, J-L., Buré, C., Grosjean, K., et al. (2016). Revisiting Plant Plasma Membrane Lipids in Tobacco: A Focus on Sphingolipids. *Plant Physiol* 170:367 LP – 384. doi: 10.1104/pp.15.00564
- Cantarel, B.L., Coutinho, P.M., Rancurel, C., et al. (2009). The Carbohydrate-Active EnZymes database (CAZy): an expert resource for Glycogenomics. *Nucleic Acids Res* 37:D233–D238. doi: 10.1093/nar/gkn663
- Castilho A, Steinkellner H (2012). Glyco-engineering in plants to produce human-like N-glycan structures. *Biotechnol J* 7:1088–1098. doi: 10.1002/biot.201200032
- Chandrasekar, B., Colby, T., Emran Khan Emon, A., et al. (2014). Broad-range Glycosidase Activity Profiling. *Mol Cell Proteomics* 13:2787–2800. doi: 10.1074/mcp.O114.041616
- Chauvigné-Hines, L.M., Anderson, L.N., Weaver, H.M., et al. (2012). Suite of Activity-

- Based Probes for Cellulose-Degrading Enzymes. *J Am Chem Soc* 134:20521–20532. doi: 10.1021/ja309790w
- Chen, A.Y., Chen, Y.C. (2013). A review of the dietary flavonoid, kaempferol on human health and cancer chemoprevention. *Food Chem* 138:2099–2107. doi: 10.1016/j.foodchem.2012.11.139
- Chen, Z., Tu, M., Sun, S., et al. (2012). The Exposure of Luteolin Is Much Lower than That of Apigenin in Oral Administration of Flos Chrysanthemi Extract to Rats. *Drug Metab Pharmacokinet* 27:162–168. doi: 10.2133/dmpk.DMPK-11-RG-081
- Allred, C.D., Ju, Y.H., Allred, F.K., et al. (2001). Dietary genistin stimulates growth of estrogen-dependent breast cancer tumors similar to that observed with genistein. *Carcinogenesis* 22:1667–1673. doi: 10.1093/carcin/22.10.1667
- Coutinho, M.F., Prata, M.J., Alves, S. (2012) A shortcut to the lysosome: The mannose-6-phosphate-independent pathway. *Mol Genet Metab* 107:257–266. doi: <https://doi.org/10.1016/j.ymgme.2012.07.012>
- Coutinho, P.M., Stam, M., Blanc, E., Henrissat, B. (2003). Why are there so many carbohydrate-active enzyme-related genes in plants? *Trends Plant Sci* 8:563–565. doi: <https://doi.org/10.1016/j.tplants.2003.10.002>
- Cravatt, B.F., Wright, A.T., Kozarich, J.W. (2008). Activity-Based Protein Profiling: From Enzyme Chemistry to Proteomic Chemistry. *Annu Rev Biochem* 77:383–414. doi: 10.1146/annurev.biochem.75.101304.124125
- Cressey, P., Reeve, J. (2019). Metabolism of cyanogenic glycosides: A review. *Food Chem Toxicol* 125:225–232. doi: <https://doi.org/10.1016/j.fct.2019.01.002>
- Crout, D.H.G., Vic, G. (1998). Glycosidases and glycosyl transferases in glycoside and oligosaccharide synthesis. *Curr Opin Chem Biol* 2:98–111. doi: [https://doi.org/10.1016/S1367-5931\(98\)80041-0](https://doi.org/10.1016/S1367-5931(98)80041-0)
- Daneri-Castro, S.N., Chandrasekar, B., Grosse-Holz, F.M., et al. (2016). Activity-based protein profiling of hydrolytic enzymes induced by gibberellic acid in isolated aleurone layers of malting barley. *FEBS Lett* 590:2956–2962. doi: 10.1002/1873-3468.12320
- Day, A., Dupont, M.S., Ridley, S., et al. (1998). Deglycosylation of flavonoid and isoflavonoid glycosides by human small intestine and liver beta-glucosidase activity. *FEBS Lett* 436:71–75. doi: [https://doi.org/10.1016/S0014-5793\(98\)01101-6](https://doi.org/10.1016/S0014-5793(98)01101-6)
- De Souza, V.T., De Franco, É.P.D., De Araújo, M.E.M.B., et al. (2016). Characterization of the antioxidant activity of aglycone and glycosylated derivatives of hesperetin: an in vitro and in vivo study. *J Mol Recognit* 29:80–87. doi: 10.1002/jmr.2509
- Declodt, I.A., Van Landschoot, A., Watson, H., et al. (2017). Plant-Based Beverages as Good Sources of Free and Glycosidic Plant Sterols. *Nutrients* 10:E21. doi: 10.3390/nu10010021.
- Desnick, R.J., Schuchman, E.H. (2012). Enzyme Replacement Therapy for Lysosomal Diseases: Lessons from 20 Years of Experience and Remaining Challenges. *Annu*

- Rev Genomics Hum Genet 13:307–335. doi: 10.1146/annurev-genom-090711-163739
- Dharmawardhana, D.P., Ellis, B.E., Carlson, J.E. (1995). A [beta]-Glucosidase from Lodgepole Pine Xylem Specific for the Lignin Precursor Coniferin. *Plant Physiol* 107:331-339. doi: 10.1104/pp.107.2.331
- Ehle, M., Patel, C, Giugliano, R.P. (2011). Digoxin: Clinical Highlights : A Review of Digoxin and Its Use in Contemporary Medicine. *Crit Pathw Cardiol* 10:93–98. doi: 10.1097/HPC.0b013e318221e7dd.
- Eng, C.M., Guffon, N., Wilcox, W.R., et al. (2001). Safety and efficacy of recombinant human alpha-galactosidase A replacement therapy in Fabry's disease. *N Engl J Med* 345:9-16. doi: 10.1056/nejm200107053450102
- Escamilla-Treviño, L.L., Chen, W., Card, M.L., et al. (2006). Arabidopsis thaliana β-Glucosidases BGLU45 and BGLU46 hydrolyse monolignol glucosides. *Phytochemistry* 67:1651–1660. doi: <https://doi.org/10.1016/j.phytochem.2006.05.022>
- Feng, C., Su, S., Wang, L., et al. (2016).. Antioxidant capacities and anthocyanin characteristics of the black-red wild berries obtained in Northeast China. *Food Chem.* 204:150-158. doi:10.1016/j.foodchem.2016.02.122.
- Ferraz, M.J., Kallemeijn, W.W., Mirzaian, M., et al. (2014). Gaucher disease and Fabry disease: New markers and insights in pathophysiology for two distinct glycosphingolipidoses. *Biochim Biophys Acta* 1841:811–825. doi: <https://doi.org/10.1016/j.bbali.2013.11.004>
- Ferrer A., Altabella T., Arró M., Boronat A. (2017). Emerging roles for conjugated sterols in plants. *Prog. Lipid Res.* 67:27–37. doi: 10.1016/j.plipres.2017.06.002.
- Fischer, R., Stoger, E., Schillberg, S., et al. (2004). Plant-based production of biopharmaceuticals. *Curr Opin Plant Biol* 7:152–158. doi: 10.1016/j.pbi.2004.01.007
- Fotsis, T., Pepper, M., Adlercreutz, H., et al. (1993). Genistein, a dietary-derived inhibitor of in vitro angiogenesis. *Proc Natl Acad Sci* 90:2690-2694. doi: 10.1073/pnas.90.7.2690
- Franco, R., Sánchez-Arias, J.A., Navarro, G., Lanciego, JL. (2018). Glucocerebrosidase Mutations and Synucleinopathies. Potential Role of Sterylglucosides and Relevance of Studying Both GBA1 and GBA2 Genes. *Front Neuroanat* 12:52. doi: 10.3389/fnana.2018.00052
- Friend, D.G. (1974). Aspirin: The Unique Drug. *Arch Surg.* 1974 Jun;108(6):765-769. doi: 10.1001/archsurg.1974.01350300009004
- Gachon, C.M.M., Langlois-Meurinne, M., Saindrenan, P. (2005). Plant secondary metabolism glycosyltransferases: the emerging functional analysis. *Trends Plant Sci* 10:542–549. doi: <https://doi.org/10.1016/j.tplants.2005.09.007>
- Goddard-Borger, E.D., Wennekes, T., Withers, S.G. (2010). Getting lucky in the lysosome. *Nat Chem Biol* 6:881. doi: 10.1038/nchembio.470

- Gomord, V., Faye, L. (2004). Posttranslational modification of therapeutic proteins in plants. *Curr Opin Plant Biol* 7:171–181. doi: 10.1016/j.pbi.2004.01.015
- Gomord, V., Fitchette A.C., Menu-Bouaouiche, L., et al. (2010). Plant-specific glycosylation patterns in the context of therapeutic protein production. *Plant Biotechnol J* 8:564–587. doi: 10.1111/j.1467-7652.2009.00497.x
- Griebel, T., Zeier, J. (2010). A role for  $\beta$ -sitosterol to stigmasterol conversion in plant–pathogen interactions. *Plant J* 63:254–268. doi: 10.1111/j.1365-313X.2010.04235.x
- Griffiths, L.A., Barrow, A. (1972). Metabolism of flavonoid compounds in germ-free rats. *Biochem. J.* 130:1161–1162. doi: 10.1042/bj1301161
- Grille, S., Zaslowski, A., Thiele, S., et al. (2010). The functions of steryl glycosides come to those who wait: Recent advances in plants, fungi, bacteria and animals. *Prog Lipid Res* 49:262–288. doi: 10.1016/j.plipres.2010.02.001
- Gronnier, J., Germain, V., Gouguet, P., et al. (2016). GIPC: Glycosyl Inositol Phospho Ceramides, the major sphingolipids on earth. *Plant Signal Behav* 11:e1152438. doi: 10.1080/15592324.2016.1152438
- Guce, A.I., Clark, N.E., Salgado, E.N., et al. (2010). Catalytic Mechanism of Human  $\alpha$ -Galactosidase. *J Biol Chem* 285:3625–3632. doi: 10.1074/jbc.M109.060145
- Gylling, H., Plat, J., Turley, S., et al. (2014). Plant sterols and plant stanols in the management of dyslipidaemia and prevention of cardiovascular disease. *Atherosclerosis* 232:346–360. doi: <https://doi.org/10.1016/j.atherosclerosis.2013.11.043>
- Hajjalyani, M., Hosein Farzaei, M., Echeverría, J., et al. (2019). Hesperidin as a Neuroprotective Agent: A Review of Animal and Clinical Evidence. *Molecules*. 24:E648. doi: 10.3390/molecules24030648.
- Hansen, S., Harholt, J., Oikawa, A., Scheller, H. (2012). Plant Glycosyltransferases Beyond CAZy: A Perspective on DUF Families. *Front Plant Sci* 3:59. doi: 10.3389/fpls.2012.00059
- Hansen, S.F., Bettler, E., Rinnan Å., et al. (2010). Exploring genomes for glycosyltransferases. *Mol BioSyst* 6:1773–1781. doi: 10.1039/C000238K
- Hartmann, M-A. (1998). Plant sterols and the membrane environment. *Trends Plant Sci* 3:170–175. doi:10.1016/S1360-1385(98)01233-3.
- Haque, R.M., Bradbury, H.J. (2002). Total cyanide determination of plants and foods using the picrate and acid hydrolysis methods. *Food Chem* 77:107–114. doi: [https://doi.org/10.1016/S0308-8146\(01\)00313-2](https://doi.org/10.1016/S0308-8146(01)00313-2)
- He, M., Min, J-W., Kong, W-L., et al. (2016). A review on the pharmacological effects of vitexin and isovitexin. *Fitoterapia* 115:74–85. doi: 10.1016/j.fitote.2016.09.011
- He, X., Galpin, J.D., Tropak, M.B., et al. (2011). Production of active human glucocerebrosidase in seeds of *Arabidopsis thaliana* complex-glycan-deficient (cgl) plants. *Glycobiology* 22:492–503. doi: 10.1093/glycob/cwr157

- Hehre, E.J. (2001). Glycosyl transfer: a history of the concept's development and view of its major contributions to biochemistry. *Carbohydr Res* 331:347–368. doi: [https://doi.org/10.1016/S0008-6215\(01\)00042-8](https://doi.org/10.1016/S0008-6215(01)00042-8)
- Henrissat, B. (1991). A classification of glycosyl hydrolases based on amino acid sequence similarities. *Biochem J* 280:309-316. doi: 10.1042/bj2800309
- Henrissat, B., Davies, G.J. (2000). Glycoside Hydrolases and Glycosyltransferases. Families, Modules, and Implications for Genomics. *Plant Physiol* 124:1515-1519. doi: 10.1104/pp.124.4.1515
- Herrera Moro Chao, D., Kallemeijn, W.W., Marques, A.R.A., et al. (2015). Visualization of Active Glucocerebrosidase in Rodent Brain with High Spatial Resolution following In Situ Labeling with Fluorescent Activity Based Probes. *PLoS One* 10:e0138107 doi: 10.1371/journal.pone.0138107.
- Hertog, M.G.L., Hollman, P.C.H., Katan, M.B., Kromhout, D. (1993). Intake of potentially anticarcinogenic flavonoids and their determinants in adults in the Netherlands. *Nutr Cancer* 20:21–29. doi: 10.1080/01635589309514267
- Hidalgo, D., Sanchez, R., Lalaleo, L., et al. (2018). Biotechnological Production of Pharmaceuticals and Biopharmaceuticals in Plant Cell and Organ Cultures. *Curr. Med. Chem.* 25:3577–3596. doi: 10.2174/0929867325666180309124317.
- Hirota, S., Nishioka, T., Shimoda, T., et al. (2001). Quercetin Glucosides are Hydrolyzed to Quercetin in Human Oral Cavity to Participate in Peroxidase-Dependent Scavenging of Hydrogen Peroxide. *Food Sci Technol Res* 7:239–245. doi: 10.3136/fstr.7.239
- Hollman, P., Devries, J., Vanleeuwen, S.D., et al. (1995). Absorption of dietary quercetin glycosides and quercetin in healthy ileostomy volunteers. *Am J Clin Nutr* 62:1276–1282. doi: 10.1093/ajcn/62.6.1276
- Holst, O. (2008). Glycolipids: Occurrence, Significance, and Properties. In: Fraser-Reid, B.O., Tatsuta, K., Thiem, J. (eds). Springer Berlin Heidelberg, Berlin, Heidelberg, pp 1603–1627.
- Hölzl, G., Dörmann, P. (2019). Chloroplast Lipids and Their Biosynthesis. *Annu Rev Plant Biol* 70:51–81. doi: 10.1146/annurev-arplant-050718-100202
- Hostetler, G., Riedl, K., Cardenas, H., et al. (2012). Flavone deglycosylation increases their anti-inflammatory activity and absorption. *Mol Nutr Food Res* 56:558–569. doi: 10.1002/mnfr.201100596
- Huang, W-Y., Liu, Y-M., Wang, J., et al. (2014). Anti-Inflammatory Effect of the Blueberry Anthocyanins Malvidin-3-Glucoside and Malvidin-3-Galactoside in Endothelial Cells. *Molecules* 19:12827–12841. doi: 10.3390/molecules190812827
- Huby, E., Napier, J.A., Baillieul, F., et al. (2019). Sphingolipids: towards an integrated view of metabolism during the plant stress response. *New Phytol* 225:659–670. doi: 10.1111/nph.15997
- Hughes, M.A., Brown, K., Pancoro, A., et al. (1992). A molecular and biochemical analysis of the structure of the cyanogenic  $\beta$ -glucosidase (linamarase) from cassava (*Manihot esculenta* Cranz). *Arch Biochem Biophys* 295:273–279. doi:

[https://doi.org/10.1016/0003-9861\(92\)90518-2](https://doi.org/10.1016/0003-9861(92)90518-2)

- Husaini, A.M., Morimoto, K., Chandrasekar, B., et al. (2018). Multiplex Fluorescent, Activity-Based Protein Profiling Identifies Active  $\alpha$ -Glycosidases and Other Hydrolases in Plants. *Plant Physiol* 177:24-37. doi: 10.1104/pp.18.00250.
- Jansen, P.J., Lütjohann, D., Abildayeva, K., et al. (2006). Dietary plant sterols accumulate in the brain. *Biochim Biophys Acta - Mol Cell Biol Lipids* 1761:445–453. doi: <https://doi.org/10.1016/j.bbalip.2006.03.015>
- Jansing, J., Sack, M., Augustine, S.M., et al. (2019). CRISPR/Cas9-mediated knockout of six glycosyltransferase genes in *Nicotiana benthamiana* for the production of recombinant proteins lacking  $\beta$ -1,2-xylose and core  $\alpha$ -1,3-fucose. *Plant Biotechnol J* 17:350–361. doi: 10.1111/pbi.12981
- Jariwala, P.B., Pellock, S.J., Goldfarb, D., et al. (2020) Discovering the Microbial Enzymes Driving Drug Toxicity with Activity-Based Protein Profiling. *ACS Chem Biol*, 15: 217–225. doi: 10.1021/acscchembio.9b00788
- Jiang, J., Kallemeijn, W.W., Wright, D.W., et al. (2015). In vitro and in vivo comparative and competitive activity-based protein profiling of GH29  $\alpha$ -l-fucosidases. *Chem Sci* 6:2782–2789. doi: 10.1039/C4SC03739A
- Jiang, J., Kuo, C-L., Wu, L., et al. (2016). Detection of Active Mammalian GH31  $\alpha$ -Glucosidases in Health and Disease Using In-Class, Broad-Spectrum Activity-Based Probes. *ACS Cent Sci* 2:351–358. doi: 10.1021/acscentsci.6b00057
- Jones, P., Vogt, T. (2001). Glycosyltransferases in secondary plant metabolism: tranquilizers and stimulant controllers. *Planta* 213:164–174. doi: 10.1007/s004250000492
- Jones, P.J.H. (2015). Inter-individual Variability in Response to Plant Sterol and Stanol Consumption. *J AOAC Int* 98:724–728. doi: 10.5740/jaoacint.SGEJones
- Jung, J-W., Choi, H-Y., Huy, N-X., et al. (2019). Production of recombinant human acid  $\beta$ -glucosidase with high mannose-type N-glycans in rice *gnt1* mutant for potential treatment of Gaucher disease. *Protein Expr Purif* 158:81–88. doi: <https://doi.org/10.1016/j.pep.2019.02.014>
- Kallemeijn, W.W., Li, K-Y., Witte, M.D, et al. (2012). Novel Activity-Based Probes for Broad-Spectrum Profiling of Retaining  $\beta$ -Exoglycosidases In Situ and In Vivo. *Angew Chemie Int Ed* 51:12529–12533. doi: 10.1002/anie.201207771
- Kallemeijn, W.W., Witte, M.D., Wennekes, T., Aerts, J.M. (2014). Mechanism-based inhibitors of glycosidases: design and applications. *Adv Carbohydr Chem Biochem.* 71:297-338. doi: 10.1016/B978-0-12-800128-8.00004-2.
- Kamalu, B.P. (1993). Pathological changes in growing dogs fed on a balanced cassava (*Manihot esculenta* Crantz) diet. *Br J Nutr* 69:921–934. doi: 10.1079/BJN19930092
- Kamalu, BP. (1991). Digestibility of a nutritionally-balanced cassava (*Manihot esculenta* Crantz) diet and its effect on growth in young male dogs. *Br J Nutr* 66:199–208. doi: 10.1079/BJN19910025



- Kampen, J., Baranowski, D., Robertson, H., et al. (2015). The Progressive BSSG Rat Model of Parkinson's: Recapitulating Multiple Key Features of the Human Disease. *PLoS One*. 10:e0139694. doi: 10.1371/journal.pone.0139694.
- Kaschani, F., Gu, C., Niessen, S., et al. (2009). Diversity of Serine hydrolase activities of unchallenged and Botrytis-infected Arabidopsis thaliana. *Mol Cell Proteomics* 8:1082-1093. doi: 10.1074/mcp.M800494-MCP200
- Kelly, R.A. (1990). Cardiac glycosides and congestive heart failure. *Am J Cardiol* 65:E10–E16. doi: [https://doi.org/10.1016/0002-9149\(90\)90245-V](https://doi.org/10.1016/0002-9149(90)90245-V)
- Kepp, O., Menger, L., Vacchelli, E., et al. (2012). Anticancer activity of cardiac glycosides. *Oncoimmunology* 1:1640–1642. doi: 10.4161/onci.21684
- Ketudat Cairns, J.R., Esen, A. (2010).  $\beta$ -Glucosidases. *Cell Mol Life Sci* 67:3389–3405. doi: 10.1007/s00018-010-0399-2
- Kizhner T., Azulay, Y., Hainrichson, M., et al. (2015). Characterization of a chemically modified plant cell culture expressed human  $\alpha$ -Galactosidase-A enzyme for treatment of Fabry disease. *Mol Genet Metab* 114:259–267. doi: 10.1016/j.ymgme.2014.08.002
- Komvongsa, J., Mahong, B., Phasai, K., et al. (2015). Identification of Fatty Acid Glucose Esters as Os9BGlu31 Transglucosidase Substrates in Rice Flag Leaves. *J Agric Food Chem* 63:9764–9769. doi: 10.1021/acs.jafc.5b04105
- Kopertekh, L., Schiemann, (2019). Transient Production of Recombinant Pharmaceutical Proteins in Plants: Evolution and Perspectives. *Curr Med Chem*.26:365-380. doi: 10.2174/0929867324666170718114724.
- Koshland, D.E. (1953). Stereochemistry and the mechanism of enzymatic reactions. *Biol Rev* 28:416–436. doi: 10.1111/j.1469-185X.1953.tb01386.x
- Kren, V., Martinkova, L. (2001). Glycosides in Medicine: “The Role of Glycosidic Residue in Biological Activity.” *Curr. Med. Chem.* 8:1303–1328. doi: 10.2174/0929867013372193.
- Kristoffersen, P., Brzobohaty, B., Höhfeld, I., et al. (2000). Developmental regulation of the maize Zm-p60.1 gene encoding a  $\beta$ -glucosidase located to plastids. *Planta* 210:407–415. doi: 10.1007/PL00008149
- Kroos, M., Hoogeveen-Westerveld M., van der Ploeg, A., Reuser, A.J.J. (2012). The genotype–phenotype correlation in Pompe disease. *Am J Med Genet Part C Semin Med Genet* 160C:59–68. doi: 10.1002/ajmg.c.31318
- Kuo, C-L., Kallemeijn, W.W., Lelieveld, L.T., et al. (2019). In vivo inactivation of glycosidases by conduritol B epoxide and cyclophellitol as revealed by activity-based protein profiling. *FEBS J* 286:584–600. doi: 10.1111/febs.14744
- Kuo, C-L., van Meel, E., Kytidou, K., et al. (2018). Activity-Based Probes for Glycosidases: Profiling and Other Applications. *Methods Enzymol.* 598:217-235. doi: 10.1016/bs.mie.2017.06.039.
- Kytidou, K., Beekwilder, J., Artola, M., et al. (2018). Nicotiana benthamiana  $\alpha$ -galactosidase A1.1 can functionally complement human  $\alpha$ -galactosidase A

- deficiency associated with Fabry disease. *J Biol Chem* 293:10042–10058. doi: 10.1074/jbc.RA118.001774
- Kytidou, K., Beenakker, T.J.M., Westerhof, L.B., et al. (2017). Human Alpha Galactosidases Transiently Produced in *Nicotiana benthamiana* Leaves: New Insights in Substrate Specificities with Relevance for Fabry Disease. *Front Plant Sci* 8:1026. doi: 10.3389/fpls.2017.01026
- Lahav, D., Liu, B., van den Berg, R.J.B.H.N., et al. (2017). A Fluorescence Polarization Activity-Based Protein Profiling Assay in the Discovery of Potent, Selective Inhibitors for Human Nonlysosomal Glucosylceramidase. *J Am Chem Soc* 139:14192–14197. doi: 10.1021/jacs.7b07352
- Leah, R., Kigel, J., Svendsen, I., Mundy, J. (1995). Biochemical and Molecular Characterization of a Barley Seed  $\beta$ -Glucosidase. *J Biol Chem* 270:15789–15797. doi: 10.1074/jbc.270.26.15789
- Lee, K.H., Piao, H.L., Kim, H-Y., et al. (2006). Activation of Glucosidase via Stress-Induced Polymerization Rapidly Increases Active Pools of Abscisic Acid. *Cell* 126:1109–1120. doi: <https://doi.org/10.1016/j.cell.2006.07.034>
- Lelieveld, L.T., Mirzaian, M., Kuo, C.L., et al. (2019). Role of  $\beta$ -glucosidase 2 in aberrant glycosphingolipid metabolism: model of glucocerebrosidase deficiency in zebrafish. *J Lipid Res.* 60:1851-1867. doi: 10.1194/jlr.RA119000154.
- Lin, L-Z., Harnly, J.M. (2007). A Screening Method for the Identification of Glycosylated Flavonoids and Other Phenolic Compounds Using a Standard Analytical Approach for All Plant Materials. *J Agric Food Chem* 55:1084–1096. doi: 10.1021/jf062431s
- Lin, X., Ma, L., Moreau, R.A., Ostlund, R.E. (2011). Glycosidic Bond Cleavage is Not Required for Phytosteryl Glycoside-Induced Reduction of Cholesterol Absorption in Mice. *Lipids* 46:701–708. doi: 10.1007/s11745-011-3560-2
- Lin, X., Ma, L., Racette, SB, et al. (2009). Phytosterol glycosides reduce cholesterol absorption in humans. *Am J Physiol Liver Physiol* 296:G931–G935. doi: 10.1152/ajpgi.00001.2009
- Lin, Y., Shi, R., Wang, X., Shen, H-M. (2008). Luteolin, a Flavonoid with Potential for Cancer Prevention and Therapy. *Curr. Cancer Drug Targets* 8:634–646. doi: 10.2174/156800908786241050
- Loos, A, Van Droogenbroeck, B., Hillmer, S., et al. (2011) Expression of Antibody Fragments with a Controlled N-Glycosylation Pattern and Induction of Endoplasmic Reticulum-Derived Vesicles in Seeds of Arabidopsis. *Plant Physiol* 155:2036-2048. doi: 10.1104/pp.110.171330
- Lopez-Lazaro, M. (2009). Distribution and Biological Activities of the Flavonoid Luteolin. *Mini-Reviews Med. Chem.* 9:31–59. doi: 10.2174/138955709787001712
- Lu, H., Chandrasekar, B., Oeljeklaus, J., et al. (2015). Subfamily-Specific Fluorescent Probes for Cysteine Proteases Display Dynamic Protease Activities during Seed Germination. *Plant Physiol* 168:1462-1475. doi: 10.1104/pp.114.254466
- Luang, S., Cho, J-I., Mahong, B., et al. (2013). Rice Os9BGlu31 is a transglucosidase

- with the capacity to equilibrate phenylpropanoid, flavonoid, and phytohormone glycoconjugates. *J Biol Chem* 288:10111–10123. doi: 10.1074/jbc.M112.423533
- Lynch, D.V., Dunn, T.M. (2004). An introduction to plant sphingolipids and a review of recent advances in understanding their metabolism and function. *New Phytologist* 161:677–702. doi: 10.1111/j.1469-8137.2004.00992.x
- Madunić, J., Madunić, I.V., Gajski, G., et al. (2018). Apigenin: A dietary flavonoid with diverse anticancer properties. *Cancer Lett* 413:11–22. doi: 10.1016/j.canlet.2017.10.041
- Mamode Cassim, A., Gouguet, P., Gronnier, J., et al. (2019). Plant lipids: Key players of plasma membrane organization and function. *Prog Lipid Res* 73:1–27. doi: <https://doi.org/10.1016/j.plipres.2018.11.002>
- Marques, A.R.A., Mirzaian, M., Akiyama, H., et al. (2016a). Glucosylated cholesterol in mammalian cells and tissues: formation and degradation by multiple cellular  $\beta$ -glucosidases. *J Lipid Res.* 57:451–463. doi: 10.1194/jlr.M064923
- Marques, A.R.A., Willems, L.I., Herrera Moro, D., et al. (2016b). A Specific Activity-Based Probe to Monitor Family GH59 Galactosylceramidase, the Enzyme Deficient in Krabbe Disease. *ChemBioChem* 18:402–412. doi: 10.1002/cbic.201600561
- McGregor, N., Artola, M., Nin-Hill, A., et al. (2020). Rational Design of Mechanism-Based Inhibitors and Activity-Based Probes for the Identification of Retaining  $\alpha$ -L-Arabinofuranosidases. *J Am Chem Soc.*, ahead of print. doi: 10.1021/jacs.9b11351.
- Milbury, P.E., Cao, G., Prior, R.L., Blumberg, J. (2002). Bioavailability of elderberry anthocyanins. *Mech Ageing Dev* 123:997–1006. doi: [https://doi.org/10.1016/S0047-6374\(01\)00383-9](https://doi.org/10.1016/S0047-6374(01)00383-9)
- Milbury, P.E., Kalt, W. (2010). Xenobiotic Metabolism and Berry Flavonoid Transport across the Blood–Brain Barrier. *J Agric Food Chem* 58:3950–3956. doi: 10.1021/jf903529m
- Miyazawa, T., Nakagawa, K., Kudo, M., et al. (1999). Direct intestinal absorption of red fruit anthocyanins, cyanidin-3-glucoside and cyanidin-3,5-diglucoside, into rats and humans. *J. Agric. Food Chem.* 47:1083–1091. doi: 10.1021/jf9809582
- Mohnen, D. (2008). Pectin structure and biosynthesis. *Curr Opin Plant Biol.* 11:266–77. doi: 10.1016/j.pbi.2008.03.006.
- Morant, A.V., Jørgensen, K., Jørgensen, C., et al. (2008).  $\beta$ -Glucosidases as detonators of plant chemical defense. *Phytochemistry* 69:1795–1813. doi: <https://doi.org/10.1016/j.phytochem.2008.03.006>
- Msanne, J., Chen, M., Luttgeharm, K.D., et al. (2015). Glucosylceramides are critical for cell-type differentiation and organogenesis, but not for cell viability in *Arabidopsis*. *Plant J* 84:188–201. doi: 10.1111/tjp.13000.
- Murota, K., Terao, J. (2003). Antioxidative flavonoid quercetin: implication of its intestinal absorption and metabolism. *Arch. Biochem. Biophys.* 417:12–17. doi:

- Nakano, T., Inoue, I., Murakoshi, T. (2019). A Newly Integrated Model for Intestinal Cholesterol Absorption and Efflux Reappraises How Plant Sterol Intake Reduces Circulating Cholesterol Levels. *Nutrients*. 2019 Feb 1;11(2). pii: E310. doi: 10.3390/nu11020310.
- Naphatsamon, U., Ohashi, T., Misaki, R., Fujiyama K. (2018). The Production of Human  $\beta$ -Glucocerebrosidase in *Nicotiana benthamiana* Root Culture. *Int. J. Mol. Sci.* 19:E1972. doi: 10.3390/ijms19071972.
- Nesher, M., Shpolansky, U., Rosen, H., Lichtstein, D. (2007). The digitalis-like steroid hormones: New mechanisms of action and biological significance. *Life Sci* 80:2093–2107. doi: 10.1016/j.lfs.2007.03.013
- Newman, R.A., Yang, P., Pawlus, A.D., Block, K.I. (2008). Cardiac glycosides as novel cancer therapeutic agents. *Mol Interv* 8:36. doi: 10.1124/mi.8.1.8
- Nho, J-H., Jung, H-K., Lee, M-J., et al. (2018). Beneficial Effects of Cynaroside on Cisplatin-Induced Kidney Injury In Vitro and In Vivo. *Toxicol Res* 34:133–141. doi: 10.5487/TR.2018.34.2.133
- Nilsson, A.K., Johansson, O.N., Fahlberg, P., et al. (2015). Acylated monogalactosyl diacylglycerol: prevalence in the plant kingdom and identification of an enzyme catalyzing galactolipid head group acylation in *Arabidopsis thaliana*. *Plant J* 84:1152–1166. doi: 10.1111/tpj.13072
- Nisius, A. (1988). The stromacentre in *Avena* plastids: an aggregation of  $\beta$ -glucosidase responsible for the activation of oat-leaf saponins. *Planta* 173:474–481. doi: 10.1007/BF00958960
- Nyström, L., Schär, A., Lampi, A-M. (2012) Steryl glycosides and acylated steryl glycosides in plant foods reflect unique sterol patterns. *Eur J Lipid Sci Technol* 114:656–669. doi: 10.1002/ejlt.201200033
- Ohgami, S., Ono, E., Horikawa, M., et al. (2015). Volatile Glycosylation in Tea Plants: Sequential Glycosylations for the Biosynthesis of Aroma  $\beta$ -Primeverosides Are Catalyzed by Two *Camellia sinensis* Glycosyltransferases. *Plant Physiol* 168:464–477. doi: 10.1104/pp.15.00403
- Ostlund, R.E. (2004). Phytosterols and cholesterol metabolism. *Curr Opin Lipidol* 15:37–41. doi: 10.1097/00041433-200402000-00008
- Ostrowski, K., Barnard, E.A. (1961). Application of isotopically-labelled specific inhibitors as a method in enzyme cytochemistry. *Exp Cell Res* 25:465–468. doi: [https://doi.org/10.1016/0014-4827\(61\)90298-1](https://doi.org/10.1016/0014-4827(61)90298-1)
- Oxtoby, E., Dunn, M.A., Pancoro, A., Hughes, M.A. (1991). Nucleotide and derived amino acid sequence of the cyanogenic  $\beta$ -glucosidase (linamarase) from white clover (*Trifolium repens* L.). *Plant Mol Biol* 17:209–219. doi: 10.1007/BF00039495
- Pan, M-H., Lai, C-S., Ho, C-T. (2010) Anti-inflammatory activity of natural dietary flavonoids. *Food Funct* 1:15–31. doi: 10.1039/C0FO00103A
- Pandey, K.B., Rizvi, S.I. (2009). Plant polyphenols as dietary antioxidants in human health and disease. *Oxid Med Cell Longev* 2:270–278. doi: 10.4161/oxim.2.5.9498

- Pandey, R.P., Parajuli, P., Koirala, N., et al. (2014). Glucosylation of isoflavonoids in engineered *Escherichia coli*. *Mol Cells* 37:172–177. doi: 10.14348/molcells.2014.2348
- Pang JL, Ricupero DA, Huang S, et al. (2006). Differential activity of kaempferol and quercetin in attenuating tumor necrosis factor receptor family signaling in bone cells. *Biochem Pharmacol.* 7:818-26. doi: 10.1016/j.bcp.2005.12.023
- Pata, M.O., Hannun, Y.A., Ng, CK-Y. (2010). Plant sphingolipids: decoding the enigma of the Sphinx. *New Phytol* 185:611–630. doi: 10.1111/j.1469-8137.2009.03123.x
- Patel., S. (2016) Plant-derived cardiac glycosides: Role in heart ailments and cancer management. *Biomed Pharmacother* 84:1036–1041. doi: <https://doi.org/10.1016/j.biopha.2016.10.030>
- Patel, S.B., Graf, G.A., Temel, R.E. (2018). ABCG5 and ABCG8: more than a defense against xenosterols. *J Lipid Res* 59:1103–1113. doi: 10.1194/jlr.R084244
- Pegel, K. (1997). The importance of sitosterol and sitosterolin in human and animal nutrition. *S. Afr. J. Sci.* 93:263–268.
- Peterson, D.W. (1951). Effect of Soybean Sterols in the Diet on Plasma and Liver Cholesterol in Chicks. *Proc Soc Exp Biol Med* 78:143–147. doi: 10.3181/00379727-78-19002
- Plat, J., Baumgartner, S., Vanmierlo, T., et al. (2019). Plant-based sterols and stanols in health & disease: “Consequences of human development in a plant-based environment?” *Prog Lipid Res* 74:87–102. doi: <https://doi.org/10.1016/j.plipres.2019.02.003>
- Plumb, G.W., De Pascual-Teresa, S., Santos-Buelga, C., et al. (1998). Antioxidant properties of catechins and proanthocyanidins: Effect of polymerisation, galloylation and glycosylation. *Free Radic Res* 29:351–358. doi: 10.1080/10715769800300391
- Posé D., Castanedo, I., Borsani, O., et al. (2009). Identification of the *Arabidopsis* *dry2/sqe1-5* mutant reveals a central role for sterols in drought tolerance and regulation of reactive oxygen species. *Plant J* 59:63–76. doi: 10.1111/j.1365-313X.2009.03849.x
- Poulton, J.E. (1990). Cyanogenesis in Plants. *Plant Physiol* 94:401-405. doi: 10.1104/pp.94.2.401
- Pruett, S.T., Bushnev, A., Hagedorn, K., et al. (2008). Biodiversity of sphingoid bases (“sphingosines”) and related amino alcohols. *J Lipid Res* 49:1621–1639. doi: 10.1194/jlr.R800012-JLR200
- Ramos, S. (2007). Effects of dietary flavonoids on apoptotic pathways related to cancer chemoprevention. *J Nutr Biochem* 18:427. doi: 10.1016/j.jnutbio.2006.11.004
- Raychaudhuri, A., Tipton, P.A. (2003). A Familiar Motif in a New Context: the Catalytic Mechanism of Hydroxyisourate Hydrolase. *Biochemistry* 42:6848–6852. doi: 10.1021/bi034137o
- Record, I.R., Jannes, M., Dreosti, I.E., King, R.A. (1995). Induction of micronucleus

- formation in mouse splenocytes by the soy isoflavone genistein in vitro but not in vivo. *Food Chem Toxicol* 33:919–922. doi: [https://doi.org/10.1016/0278-6915\(95\)00062-7](https://doi.org/10.1016/0278-6915(95)00062-7)
- Richau, K.H., Kaschani, F., Verdoes, M., et al (2012) Subclassification and Biochemical Analysis of Plant Papain-Like Cysteine Proteases Displays Subfamily-Specific Characteristics. *Plant Physiol* 158:1583-1599. doi: 10.1104/pp.112.194001
- Robiquet, P., Boutron-Charlard, C. (1830). Nouvelles expériences sur les amandes amères et sur l'huile volatile qu'elles fournissent. *Ann. Chim. Phys.*, 44: 352.
- Roghani, M., Baluchnejadmojarad, T. (2009). Chronic epigallocatechin-gallate improves aortic reactivity of diabetic rats: Underlying mechanisms. *Vascul Pharmacol* 51:84–89. doi: <https://doi.org/10.1016/j.vph.2009.04.003>
- Ross, J.A., Kasum, C.M. (2002). Dietary Flavonoids: Bioavailability, Metabolic Effects, and Safety. *Annu Rev Nutr* 22:19–34. doi: 10.1146/annurev.nutr.22.111401.144957
- Ruderfer, I., Shulman, A., Kizhner, T., et al. (2018). Development and Analytical Characterization of Pegunigalsidase Alfa, a Chemically Cross-Linked Plant Recombinant Human  $\alpha$ -Galactosidase-A for Treatment of Fabry Disease. *Bioconjug Chem* 29:1630–1639. doi: 10.1021/acs.bioconjchem.8b00133
- Saeed, A.A., Genové, G., Li, T., et al. (2015). Increased flux of the plant sterols campesterol and sitosterol across a disrupted blood brain barrier. *Steroids* 99:183–188. doi: <http://dx.doi.org/10.1016/j.steroids.2015.02.005>
- Sarry, J-E., Günata, Z. (2004). Plant and microbial glycoside hydrolases: Volatile release from glycosidic aroma precursors. *Food Chem* 87:509–521. doi: <https://doi.org/10.1016/j.foodchem.2004.01.003>
- Schähs, M., Strasser, R., Stadlmann, J., et al. (2007). Production of a monoclonal antibody in plants with a humanized N-glycosylation pattern. *Plant Biotechnol J* 5:657–663. doi: 10.1111/j.1467-7652.2007.00273.x
- Schiffmann, R., Goker-Alpan, O., Holida, M., et al. (2019). Pegunigalsidase alfa, a novel PEGylated enzyme replacement therapy for Fabry disease, provides sustained plasma concentrations and favorable pharmacodynamics: A 1-year Phase 1/2 clinical trial. *J Inherit Metab Dis* 42:534–544. doi: 10.1002/jimd.12080
- Schiffmann, R., Kopp, J.B., Austin, H.A., et al. (2001). Enzyme replacement therapy in Fabry disease: a randomized controlled trial. *JAMA* 285:2743–9. doi: 10.1001/jama.285.21.2743
- Serim, S., Haedke, U., Verhelst, S.H.L. (2012). Activity-Based Probes for the Study of Proteases: Recent Advances and Developments. *ChemMedChem* 7:1146–1159. doi: 10.1002/cmdc.201200057
- Shaaltiel, Y., Bartfeld, D., Hashmueli, S., et al. (2007). Production of glucocerebrosidase with terminal mannose glycans for enzyme replacement therapy of Gaucher's disease using a plant cell system. *Plant Biotechnol J* 5:579–590. doi: 10.1111/j.1467-7652.2007.00263.x
- Shen, J-S., Busch, A, Day, TS, et al. (2016). Mannose receptor-mediated delivery of

- moss-made  $\alpha$ -galactosidase A efficiently corrects enzyme deficiency in Fabry mice. *J Inherit Metab Dis* 39:293–303. doi: 10.1007/s10545-015-9886-9
- Shen, W-B., McDowell, K.A., Siebert, A.A., et al. (2010). Environmental neurotoxin-induced progressive model of parkinsonism in rats. *Ann Neurol* 68:70–80. doi: 10.1002/ana.22018
- Silbernagel, G., Genser, B., Neste, P., März, W. (2013). Plant sterols and atherosclerosis. *Curr Opin Lipidol* 24:12–17. doi: 10.1097/MOL.0b013e32835b6271
- Sinnott, M.L. (1990). Catalytic mechanism of enzymic glycosyl transfer. *Chem Rev* 90:1171–1202. doi: 10.1021/cr00105a006
- Spassieva, S., Hille, J. (2003). Plant Sphingolipids Today - Are They Still Enigmatic? *Plant Biol* 5:125–136. doi: 10.1055/s-2003-40726
- Strasser, R., Altmann, F., Mach, L., et al (2004) Generation of *Arabidopsis thaliana* plants with complex N-glycans lacking  $\beta$ 1,2-linked xylose and core  $\alpha$ 1,3-linked fucose. *FEBS Lett* 561:132–136. doi: 10.1016/S0014-5793(04)00150-4
- Stupp, G.S., von Reuss, S.H., Izrayelit, Y., et al. (2013). Chemical Detoxification of Small Molecules by *Caenorhabditis elegans*. *ACS Chem Biol* 8:309–313. doi: 10.1021/cb300520u
- Su, J, Sherman, A, Doerfler, PA, et al (2015) Oral delivery of Acid Alpha Glucosidase epitopes expressed in plant chloroplasts suppresses antibody formation in treatment of Pompe mice. *Plant Biotechnol J* 13:1023–1032. doi: 10.1111/pbi.12413
- Suzuki, H., Takahashi, S., Watanabe, R., et al. (2006). An Isoflavone Conjugate-hydrolyzing  $\beta$ -Glucosidase from the Roots of Soybean (*Glycine max*) Seedlings: Purification gene cloning phylogenetics and cellular localization. *J Biol Chem* 281:30251–30259. doi: 10.1074/jbc.M605726200
- Tabata, R.C., Wilson, J.M.B., Ly, P., et al. (2008). Chronic Exposure to Dietary Sterol Glucosides is Neurotoxic to Motor Neurons and Induces an ALS–PDC Phenotype. *NeuroMolecular Med* 10:24–39. doi: 10.1007/s12017-007-8020-z
- Tada, H., Nohara, A., Inazu, A., et al. (2018). Sitosterolemia, Hypercholesterolemia, and Coronary Artery Disease. *J Atheroscler Thromb* 25:783–789. doi: 10.5551/jat.RV17024
- Tajima, Y., Kawashima I., Tsukimura T., et al. (2009). Use of a modified alpha-N-acetylgalactosaminidase in the development of enzyme replacement therapy for Fabry disease. *Am J Hum Genet* 85:569–580. doi: 10.1016/j.ajhg.2009.09.016
- Takahashi, A., Sakaguchi H., Higuchi O., et al. (2019). Intestinal absorption of black chokeberry cyanidin 3-glycosides is promoted by capsaicin and capsiate in a rat ligated small intestinal loop model. *Food Chem.* 277:323–326. doi: 10.1128/mBio.01421-17
- Theilmann, M.C., Goh, Y.J., Nielsen, K.F., et al. (2017). *Lactobacillus acidophilus* metabolizes dietary plant glucosides and externalizes their bioactive phytochemicals. *MBio* 8:e01421-17. doi: 10.1128/mBio.01421-17

- Tian, W., Ye, Z., Wang, S., et al. (2019). The glycosylation design space for recombinant lysosomal replacement enzymes produced in CHO cells. *Nat Commun* 10:1785. doi: 10.1038/s41467-019-09809-3
- Tohge, T., de Souza, L.P., Fernie, A.R. (2017). Current understanding of the pathways of flavonoid biosynthesis in model and crop plants. *J Exp Bot* 68:4013–4028. doi: 10.1093/jxb/erx177
- Trautwein, A.E., Vermeer, A.M., Hiemstra, H., Ras, T.R. (2018). LDL-Cholesterol Lowering of Plant Sterols and Stanols—Which Factors Influence Their Efficacy? *Nutrients* 10:E1262. doi: 10.3390/nu10091262
- Tsuda, T., Horio, F., Osawa, T. (1999) Absorption and metabolism of cyanidin 3-O- $\beta$ -D-glucoside in rats. *FEBS Lett* 449:179–182. doi: 10.1016/S0014-5793(99)00407-X
- Van der Hoorn, R.A.L., Morimoto, K. (2016). The Increasing Impact of Activity-Based Protein Profiling in Plant Science. *Plant Cell Physiol* 57:446–461. doi: 10.1093/pcp/pcw003
- Steyn, P.S., Van Heerder F.R. (1998). Bufadienolides of plant and animal origin. *Nat. Prod. Rep.* 15:397-413. doi: 10.1039/a815397y
- Van Kampen, J.M., Baranowski, D.B., Shaw, C.A., Kay, DG (2014). Panax ginseng is neuroprotective in a novel progressive model of Parkinson's disease. *Exp Gerontol* 50:95–105. doi: 10.1016/j.exger.2013.11.012
- Van Meel, E., Bos, E., van der Lienden, M.J.C., et al. (2019). Localization of active endogenous and exogenous  $\beta$ -glucocerebrosidase by correlative light- electron microscopy in human fibroblasts. *Traffic*. 20:346–356. doi: 10.1111/tra.12641
- Vanderjagt, D.J., Fry, D.E., Glew, R.H. (1994). Human glucocerebrosidase catalyses transglucosylation between glucocerebroside and retinol. *Biochem J* 300:309-315. doi: 10.1042/bj3000309
- Vanmierlo, T., Bogie, J.F.J., Mailleux, J., et al. (2015). Plant sterols: Friend or foe in CNS disorders? *Prog Lipid Res* 58:26–39. doi: 10.1016/j.plipres.2015.01.003
- Vanmierlo, T., Weingärtner, O., van der Pol, S., et al. (2012). Dietary intake of plant sterols stably increases plant sterol levels in the murine brain. *J Lipid Res* 53:726–735. doi: 10.1194/jlr.M017244
- Vetter, J. (2000). Plant cyanogenic glycosides. *Toxicon* 38:11–36. doi: [https://doi.org/10.1016/S0041-0101\(99\)00128-2](https://doi.org/10.1016/S0041-0101(99)00128-2)
- Wagatsuma, T., Khan, M.S.H., Watanabe, T., et al (2014) Higher sterol content regulated by CYP51 with concomitant lower phospholipid content in membranes is a common strategy for aluminium tolerance in several plant species. *J Exp Bot* 66:907–918. doi: 10.1093/jxb/eru455
- Walgren, R.A., Karnaky, K.J., Lindenmayer, G.E., Walle T. (2000) Efflux of dietary flavonoid quercetin 4'- $\beta$ -glucoside across human intestinal Caco-2 cell monolayers by apical multidrug resistance-associated protein-2. *J. Pharmacol. Exp. Ther.* 294:830–836.
- Walgren, R.A., Walle, U.K., Walle T. (1998) Transport of Quercetin and Its Glucosides



- across Human Intestinal Epithelial Caco-2 Cells. *Biochem Pharmacol* 55:1721–1727. doi: [https://doi.org/10.1016/S0006-2952\(98\)00048-3](https://doi.org/10.1016/S0006-2952(98)00048-3)
- Walle, T. (2004) Absorption and metabolism of flavonoids. *Free Radic Biol Med* 36:829–837. doi: [10.1016/j.freeradbiomed.2004.01.002](https://doi.org/10.1016/j.freeradbiomed.2004.01.002)
- Walle, T., Walle, U.K. (2003). The  $\beta$ -D-glucoside and sodium-dependent glucose transporter 1 (SGLT1)-inhibitor phloridzin is transported by both SGLT1 and multidrug resistance-associated proteins 1/2. *Drug Metab Dispos* 31:1288-1291. doi: [10.1124/dmd.31.11.1288](https://doi.org/10.1124/dmd.31.11.1288)
- Wang, K., Senthil-Kumar, M., Ryu, C-M., et al. (2012). Phytosterols Play a Key Role in Plant Innate Immunity against Bacterial Pathogens by Regulating Nutrient Efflux into the Apoplast. *Plant Physiol* 158:1789–1802. doi: [10.1104/pp.111.189217](https://doi.org/10.1104/pp.111.189217)
- Westerhof, L.B., Wilbers, R.H.P., van Raaij, D.R., et al. (2014). Monomeric IgA can be produced in planta as efficient as IgG, yet receives different N-glycans. *Plant Biotechnol J* 12:1333–1342. doi: [10.1111/pbi.12251](https://doi.org/10.1111/pbi.12251)
- Wicki J., Rose D.R., Withers, S.G. (2002). Trapping covalent intermediates on beta-glycosidases. *Methods Enzymol* 354:84-105. doi: [10.1016/s0076-6879\(02\)54007-6](https://doi.org/10.1016/s0076-6879(02)54007-6).
- Wilbers, R.H.P., Westerhof, L.B., van Noort, K., et al. (2017). Production and glyco-engineering of immunomodulatory helminth glycoproteins in plants. *Sci Rep* 7:45910. doi: [10.1038/srep45910](https://doi.org/10.1038/srep45910)
- Willems, L.I., Beenakker, T.J.M., Murray, B., et al. (2014a). Potent and Selective Activity-Based Probes for GH27 Human Retaining  $\alpha$ -Galactosidases. *J Am Chem Soc* 136:11622–11625. doi: [10.1021/ja507040n](https://doi.org/10.1021/ja507040n)
- Willems, L.I., Jiang, J., Li, K.Y., et al. (2014b). From covalent glycosidase inhibitors to activity-based glycosidase probes. *Chemistry*. 20:10864–10872. doi: [10.1002/chem.201404014](https://doi.org/10.1002/chem.201404014)
- Wink, M. (2015). Modes of Action of Herbal Medicines and Plant Secondary Metabolites. *Med (Basel, Switzerland)* 2:251–286. doi: [10.3390/medicines2030251](https://doi.org/10.3390/medicines2030251)
- Wintermans, J.F.G.M. (1960). Concentrations of phosphatides and glycolipids in leaves and chloroplasts. *Biochim Biophys Acta* 44:49–54. doi: [https://doi.org/10.1016/0006-3002\(60\)91521-3](https://doi.org/10.1016/0006-3002(60)91521-3)
- Witte, M.D., Kallemeijn, W.W., Aten, J., et al. (2010). Ultrasensitive in situ visualization of active glucocerebrosidase molecules. *Nat Chem Biol* 6:907–913. doi: [10.1038/nchembio.466](https://doi.org/10.1038/nchembio.466)
- Witte, M.D., van der Marel G.A., Aerts J.M.F.G, Overkleeft H.S. (2011) Irreversible inhibitors and activity-based probes as research tools in chemical glycobiology. *Org Biomol Chem* 9:5908–5926. doi: [10.1039/C1OB05531C](https://doi.org/10.1039/C1OB05531C)
- Wu L., Jiang J., Jin Y., et al. (2017). Activity-based probes for functional interrogation of retaining  $\beta$ -glucuronidases. *Nat Chem Biol* 13:867–873. doi: [10.1038/nchembio.2395](https://doi.org/10.1038/nchembio.2395)
- Wu, L., Armstrong, Z., Schröder, S.P., de Boer, C., Artola, M., Aerts, J.M., Overkleeft,

- H.S. Davies, G.J. (2019). An overview of activity-based probes for glycosidases. *Curr Opin Chem Biol.* 53:25-36. doi: 10.1016/j.cbpa.2019.05.030.
- Xiao, J., Capanoglu, E., Jassbi, A.R., Miron, A. (2016) Advance on the Flavonoid C-glycosides and Health Benefits. *Crit Rev Food Sci Nutr* 56:S29–S45. doi: 10.1080/10408398.2015.1067595
- Xiao, J., Muzashvili, T.S., Georgiev, M.I. (2014). Advances in the biotechnological glycosylation of valuable flavonoids. *Biotechnol Adv* 32:1145–1156. doi: 10.1016/j.biotechadv.2014.04.006
- Xifró, X., Vidal-Sancho, L., Boadas-Vaello, P., et al. (2015). Novel Epigallocatechin-3-Gallate (EGCG) Derivative as a New Therapeutic Strategy for Reducing Neuropathic Pain after Chronic Constriction Nerve Injury in Mice. *PLoS One* 10:e0123122. doi: 10.1371/journal.pone.0123122
- Xu, D., Hu, M.J., Wang, Y.Q. et al. (2019). Antioxidant Activities of Quercetin and Its Complexes for Medicinal Application. *Molecules* 24:E1123. doi: 10.3390/molecules24061123
- Yamamoto, N., Moon, J-H., Tsushida, T., et al. (1999). Inhibitory Effect of Quercetin Metabolites and Their Related Derivatives on Copper Ion-Induced Lipid Peroxidation in Human Low-Density Lipoprotein. *Arch Biochem Biophys* 372:347–354. doi: <https://doi.org/10.1006/abbi.1999.1516>
- Yao, J., Weng, Y., Dickey, A., Wang, Y.K. (2015). Plants as Factories for Human Pharmaceuticals: Applications and Challenges. *Int. J. Mol. Sci.* 16:28549–28565. doi: 10.3390/ijms161226122
- Zhang, J., Wu, J., Liu, F., et al. (2019). Neuroprotective effects of anthocyanins and its major component cyanidin-3-O-glucoside (C3G) in the central nervous system: An outlined review. *Eur J Pharmacol* 858:172500. doi: 10.1016/j.ejphar.2019.172500

# Chapter 3

---

Human alpha galactosidases  
transiently produced in *Nicotiana  
benthamiana* leaves: new insights in  
substrate specificities with relevance  
for Fabry disease

---

*Kassiani Kytidou, Thomas J. M. Beenakker, Lotte B. Westerhof, Cornelis H. Hokke, Geri F. Moolenaar, Nora Goosen, Mina Mirzaian, Maria J. Ferraz, Mark de Geus, Wouter W. Kallemeijn, Herman S. Overkleeft, Rolf G. Boot, Arjen Schots, Dirk Bosch, and Johannes M. F. G. Aerts*

*This work has been published in: **Frontiers in Plant Science**, (2017); 8: 1026  
doi:10.3389/fpls.2017.01026*



## Abstract

Deficiency of  $\alpha$ -galactosidase A ( $\alpha$ -GAL) causes Fabry disease (FD), an X-linked storage disease of the glycosphingolipid globotriaosylceramide (Gb3) in lysosomes of various cells and elevated plasma globotriaosylsphingosine (Lyso-Gb3) toxic for podocytes and nociceptive neurons. Enzyme replacement therapy is used to treat the disease, but clinical efficacy is limited in many male FD patients due to development of neutralizing antibodies (Ab). Therapeutic use of modified lysosomal  $\alpha$ -N-acetyl-galactosaminidase ( $\alpha$ -NAGAL) with increased  $\alpha$ -galactosidase activity ( $\alpha$ -NAGAL<sup>EL</sup>) has therefore been suggested. We transiently produced in *Nicotiana benthamiana* leaves functional  $\alpha$ -GAL,  $\alpha$ -NAGAL and  $\alpha$ -NAGAL<sup>EL</sup> enzymes for research purposes. All enzymes could be visualized with activity-based probes covalently binding in their catalytic pocket. Characterization of purified proteins indicated that  $\alpha$ -NAGAL<sup>EL</sup> is improved in activity towards artificial 4MU- $\alpha$ -galactopyranoside. Recombinant  $\alpha$ -NAGAL<sup>EL</sup> and  $\alpha$ -NAGAL are not neutralized by Ab-positive FD serum tested and are more stable in human plasma than  $\alpha$ -GAL. Both enzymes hydrolyze the lipid substrates Gb3 and Lyso-Gb3 accumulating in Fabry patients. The addition to FD sera of  $\alpha$ -NAGAL<sup>EL</sup>, and to a lesser extent that of  $\alpha$ -NAGAL, results in a reduction of the toxic Lyso-Gb3.

In conclusion, our study suggests that modified  $\alpha$ -NAGAL<sup>EL</sup> might reduce excessive Lyso-Gb3 in FD serum. This neo-enzyme can be produced in *Nicotiana benthamiana* and might be further developed for the treatment of Fabry disease aiming at reduction of circulating Lyso-Gb3.

## Introduction

Deficiencies in lysosomal enzymes are the cause of various inherited lysosomal storage disorders in humans (Futerman and van Meer, 2004). Examples are Gaucher disease (GD), Pompe disease and Fabry disease (FD) with deficiencies of acid beta-glucosidase (glucocerebrosidase, GBA), acid alpha-glucosidase and acid alpha-galactosidase ( $\alpha$ -GAL) respectively. For each of these diseases, enzyme replacement therapy (ERT) approaches have been designed and are applied with variable success. Highly efficient is ERT for Gaucher disease resulting in reversal and /or prevention of organomegaly and haematological abnormalities in non-neuropathic type 1 patients (Barton et al., 1990). ERT of Pompe disease has been shown to increase the life expectancy in patients suffering from the infantile form of the disorder (Van den Hout et al., 2000). Two similar approaches were also developed for Fabry disease using human  $\alpha$ -GAL produced in Chinese hamster ovary cells, (agalsidase beta; Fabrazyme™; Sanofi-Genzyme) or human fibroblasts (agalsidase alfa; Replagal™; Shire) (Eng et al., 2001; Schiffmann et al., 2001). Both enzyme preparations were registered in August 2001 as orphan drug in Europe, but only Fabrazyme was approved by the FDA in the U.S.A. (Desnick, 2004).

$\alpha$ -Galactosidase A ( $\alpha$ -GAL; E.C. 3.2.1.22) is encoded by the *GLA* (ID: 2717) gene at locus Xq22 (Desnick, 2001). The enzyme is synthesized as 429 amino acid precursor from which the signal peptide is removed to yield a 398 amino acid glycoprotein forming a homodimer (Brady 1967; Hamers, 1977; Bishop et al., 1988; Desnick, 2001). Formation of mannose-6-moieties (M6P) in the 3 N-linked glycans of  $\alpha$ -GAL allows transport to lysosomes by mannose-6-phosphate receptors (M6PR) (Sakuraba et al., 2005). The natural substrates of  $\alpha$ -GAL are glycosphingolipids with terminal  $\alpha$ -galactosyl moieties, including globotriaosylceramide (Gb3; ceramidetrihexoside: CTH), galabiosylceramide, and blood group B, B<sub>1</sub>, and P<sub>1</sub> antigens (Sweeley, 1963; Desnick, 2001). In various cell types of classic male FD patients Gb3 accumulates in intralysosomal lipid deposits. Both Fabrazyme and Replagal are aimed to be delivered to lysosomes of cells by M6PR mediated endocytosis (Sakuraba et al., 2005). Unfortunately, the evaluation of long-term ERT of FD patients indicates that clinical efficacy is relatively poor (Schuller et al., 2015). ERT treatments result in the case of some FD patients in stabilization of disease, but progression of symptoms has also been observed (Blom et al., 2003; Lin et al., 2009). The poor response to ERT of classic FD males, usually completely lacking  $\alpha$ -GAL protein, is partially explained by the common induction in these

individuals of neutralizing antibodies (Ab) against the therapeutic enzyme (Linthorst et al., 2004).

A recent important insight on pathogenesis of FD stems from the notion that the storage lipid Gb3 is partly actively converted to its sphingoid base globotriaosylsphingosine (Lyso-Gb3) in lysosomes (Aerts et al., 2008; Ferraz et al., 2016a). In symptomatic FD males plasma Lyso-Gb3 is chronically several hundred fold increased, and symptomatic female FD patients also show increased levels of the sphingoid base (Gold et al., 2013; Ferraz et al., 2016a). Excessive circulating Lyso-Gb3 seems a culprit, contributing to renal complications and neuropathic pain in FD patients as the results of toxicity for podocytes and nociceptive neurons respectively (Choi et al., 2015; Sanchez-Niño et al., 2015). In line with this, FD patients with Abs show a relapse of plasma Lyso-Gb3 to pre-treatment values (Ohashi et al., 2007; van Breemen et al., 2011; Rombach et al., 2012). In view of the toxicity of Lyso-Gb3 a treatment based on enzyme supplementation aiming to specifically reduce this lipid might be considered. Ideally, such therapeutic enzyme should not induce neutralizing antibodies in FD males as occurs with Fabrazyme and Replagal.

Plants, among others *Nicotiana benthamiana* (*N. benthamiana*), have been shown to be excellent production platforms of therapeutic enzymes (Fischer et al., 2004; Gomord and Faye, 2004). Besides the amply reviewed advantages such as associated low costs, feasibility of large-scale production and reduced risk for contaminating animal viruses and prions, plants may be engineered to process recombinant proteins with all post-translational modifications required for desired bioactivity and pharmacokinetics. Shaaltiel and colleagues were among the first to develop the production of a lysosomal hydrolase in plant cells for therapeutic use in humans (Shaaltiel et al., 2007). They generated recombinant glucocerebrosidase in carrot cells for the treatment of type 1 GD. Clinical investigations with GD patients demonstrated that the therapeutic efficacy of the plant-produced enzyme preparation is on a *par* with recombinant enzyme conventionally produced in mammalian cells. Moreover, no significant immune responses to the plant-produced glycoprotein as such were noted. These findings promoted swift registration of taliglucerase (Uplyso™; Protalix) as drug for type 1 GD in Europe, Israel and the U.S.A. (van Dussen et al., 2013). Another recent example forms the production in tobacco of acid alpha glucosidase for treatment of Pompe disease (Su et al., 2015). Furthermore, in *Nicotiana tabacum* cells a PEGylated human  $\alpha$ -Galactosidase A enzyme has been produced for treatment of FD (Kizhner et al., 2014). Human  $\alpha$ -Galactosidase A was also recombinantly produced in an engineered moss cell line by Jin-Song Shen and colleagues and shown to undergo mannose receptor mediated uptake (Shen et al., 2016).

The unfortunate detrimental immune response to infused human  $\alpha$ -GAL's in most FD males, leading to neutralizing antibodies, inspired Sakubara and colleagues to propose the use of a modified enzyme (Tajima et al., 2009). Their alternative approach elegantly exploits the existence of a homologous lysosomal enzyme named  $\alpha$ -galactosidase B or  $\alpha$ -*N*-acetyl-galactosaminidase ( $\alpha$ -NAGAL). It is encoded by the *NAGA* gene (ID: 4668) (22q13.2) arisen by gene duplication of the *GLA* gene. Until the late 70's both enzymes were actually considered as different isoforms of the same protein (Schram et al., 1977). Mature  $\alpha$ -NAGAL, a 411 amino acid glycoprotein with 4 N-linked glycans still shows considerably structural similarity to  $\alpha$ -GAL. The enzyme  $\alpha$ -NAGAL exerts  $\alpha$ -*N*-acetyl-galactosaminidase activity, but also hydrolyses at low rate artificial  $\alpha$ -galactosides like 4-methylumbelliferyl- $\alpha$ -galactopyranoside (4MU- $\alpha$ -GAL) or p-nitrophenyl- $\alpha$ -galactopyranoside (pNP- $\alpha$ -GAL). The similarity of  $\alpha$ -GAL and  $\alpha$ -NAGAL is also revealed by recently developed activity-based probes (ABP) that bind covalently to the catalytic nucleophile of both retaining glycosidases (Willems et al., 2014). In the present study we used a similar alpha-galactosyl configured cyclophellitol-aziridine ABP equipped with a Cy5 fluorophore, again labeling both  $\alpha$ -GAL and  $\alpha$ -NAGAL. X-ray crystallography of  $\alpha$ -GAL and  $\alpha$ -NAGAL provided a structural basis for the specificity of both proteins for substrates (Tomasic et al., 2010). The introduction of two amino acid substitutions in the catalytic pocket of  $\alpha$ -NAGAL, Ser188Glu and Ala191Leu, suffices to increase about 40 times the ability of the neo-enzyme ( $\alpha$ -NAGAL<sup>EL</sup>) to hydrolyse 4MU- $\alpha$ -GAL (Tajima et al., 2009). Furthermore, it was described that  $\alpha$ -NAGAL<sup>EL</sup> reduces Gb3 in cultured fibroblasts from a FD patient. Intravenous administration of  $\alpha$ -NAGAL<sup>EL</sup> in FD mice partially reduced Gb3 storage in liver, kidney, and heart (Tajima et al., 2009). Garman recapitulated some of the findings by demonstration of about 4.5 fold increased activity of  $\alpha$ -NAGAL<sup>EL</sup> towards pNP- $\alpha$ -GAL (Tomasic et al., 2010). The enzymes  $\alpha$ -GAL and  $\alpha$ -NAGAL differ not only in affinity for the sugar-moiety of natural substrates, but also their aglycon moieties (Clark and Garman, 2009;Guce et al., 2010). Whereas  $\alpha$ -GAL degrades glycosphingolipids,  $\alpha$ -NAGAL degrades glycopeptides and oligosaccharides as indicated by storage materials in Schindler disease (inherited  $\alpha$ -NAGAL deficiency).

In our present study we investigated whether it is feasible to produce in *N. benthamiana* leaves  $\alpha$ -GAL,  $\alpha$ -NAGAL and  $\alpha$ -NAGAL<sup>EL</sup>. All plant-produced enzymes were active and could be labelled by the Cy5 equipped ABP. The glycosidases were purified to homogeneity and characterized regarding enzymatic activity towards artificial alpha-galactoside and alpha-*N*-acetylgalactosiminide substrates, and their N-glycan composition. In addition, we produced the same enzymes in HEK293 cells, showing no difference in



specific activities to the ones produced in the *N. benthamiana* leaves. Moreover, we established whether the enzymes cross react with antibodies in serum of an FD patient with neutralizing activity (Linthorst et al., 2004). Next, we studied the activity of the various enzymes towards lipid substrates, in particular Gb3 and Lyso-Gb3. Finally, we examined the stability of various enzymes in plasma and their ability to degrade excessive Lyso-Gb3 in FD sera using LC-MS/MS and isotope-encoded internal standards (Gold et al., 2013; Ferraz et al., 2016a). From the results obtained we conclude that it seems feasible to produce a modified  $\alpha$ -NAGAL<sup>EL</sup> that is more stable in human plasma than  $\alpha$ -GAL and is better able to degrade excessive Lyso-Gb3 in FD serum. Further tailoring of an enzyme to optimally degrade circulating Lyso-Gb3 in the blood of FD patients is a therapeutic avenue to be considered, and plants might be used as a protein production platform for this purpose.

## Results

### **Transient production of human $\alpha$ -galactosidases in *N. benthamiana* leaves**

We first established the optimal conditions for production of  $\alpha$ -galactosidases  $\alpha$ -GAL,  $\alpha$ -NAGAL and  $\alpha$ -NAGAL<sup>EL</sup> in a transient expression system in *N. benthamiana*. In the constructs the sequences of mature  $\alpha$ -galactosidases were preceded by that of the *Arabidopsis thaliana* chitinase signal peptide. *Agrobacterium tumefaciens* infiltrated leaves of 5-6 weeks old *N. benthamiana* plants were collected at 1, 3 and 5 days post-infiltration (dpi), lysates were prepared and enzymatic activities of  $\alpha$ -galactosidases were measured using the respective 4MU substrate (Figure 1A). For each enzyme an optimal yield was observed at 5 dpi, while co-expressing the p19 silencing suppressor of tomato bushy stunt virus. This time point was used throughout all later experiments for harvesting. The amounts of active recombinant  $\alpha$ -GAL,  $\alpha$ -NAGAL and  $\alpha$ -NAGAL<sup>EL</sup> at 5 dpi was 71, 5 and 7 nmol/h/ $\mu$ g total protein, respectively, as measured with 4MU- $\alpha$ -GAL substrate. No 4MU- $\alpha$ -NAGAL activity was detected for the  $\alpha$ -NAGAL<sup>EL</sup> enzyme, whereas the wild type reached 33 nmol/h/ $\mu$ g at 5 dpi (Figure 1A). The amount of enzyme activity was proportional to the amount of active enzyme molecules detected with the fluorescent activity-based probe (Figure 1B) and that detected with western blotting using anti- $\alpha$ -GAL and  $\alpha$ -NAGAL antibodies (Figure 1C). The molecular weight of  $\alpha$ -GAL was about 44 kDa. Those of the two  $\alpha$ -NAGALs were about 49 kDa, the higher mass being due to the known presence of one extra N-glycan (Clark and Garman, 2009).

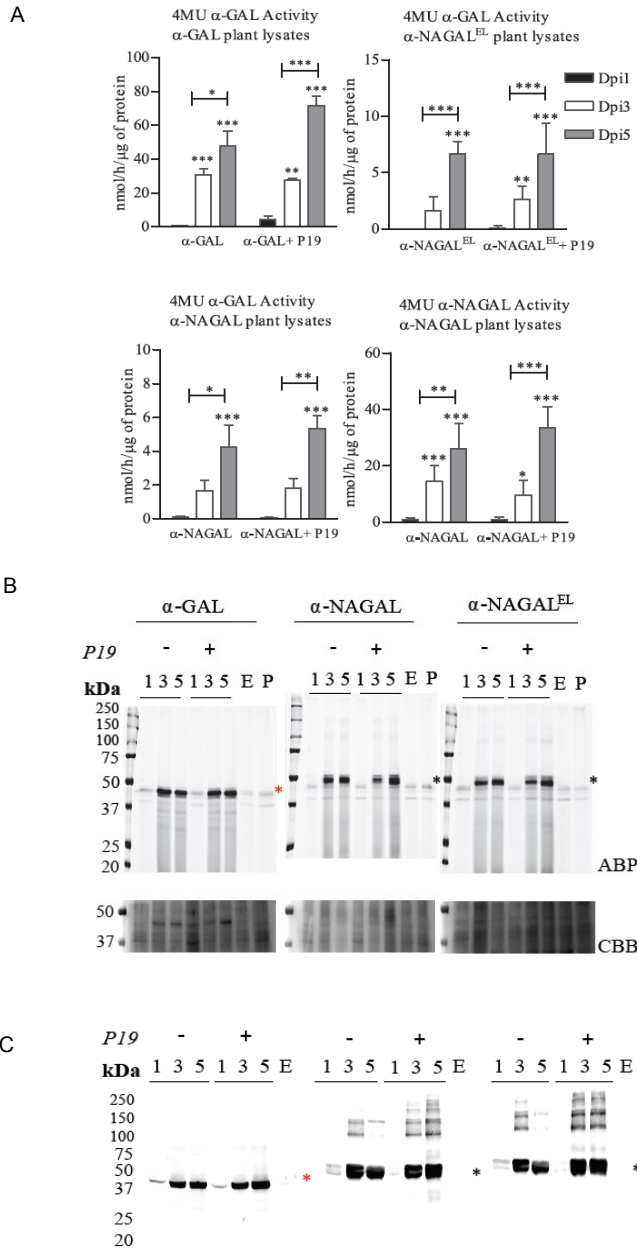
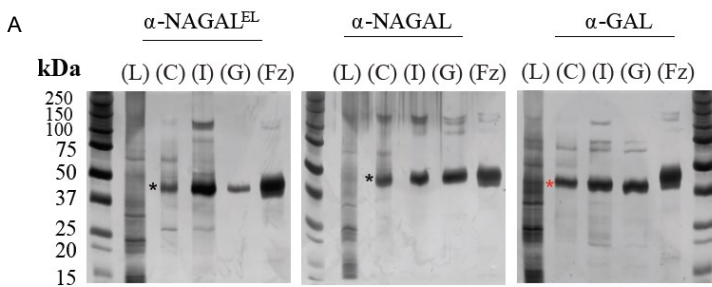


**Figure 1. Production of  $\alpha$ -galactosidases  $\alpha$ -GAL,  $\alpha$ -NAGAL and  $\alpha$ -NAGAL<sup>EL</sup> in transiently transformed *N. benthamiana* leaves.** Samples were harvested 1, 3 and 5 days post infiltration (dpi) either or not co-expressed with P19 silencing inhibitor. **(A)** Enzymatic activity was measured with corresponding 4MU-substrate. (Represented in black the 4MU activity of lysates harvested in 1st Dpi, light grey 3rd Dpi, dark grey 5th Dpi) (n=4, error bars indicate mean  $\pm$  standard deviation). Asterisk(s) indicate significant differences as measured by a two-way ANOVA corrected using Bonferroni post-hoc tests, \* =P<0.05, \*\* =P<0.01, \*\*\* =P<0.001). **(B)** ABP detection of active enzyme molecules present in

plant lysates. As controls an empty vector sample (E.V) and an untreated plant leaf (P.L). The gels were stained with Coomassie Brilliant Blue staining (CBB) as a loading control. **(C)** Western blot analysis of the plant produced  $\alpha$ -galactosidases using anti- $\alpha$ -GAL and anti-NAGA polyclonal rabbit antibodies raised against the human homologue. As control an empty vector sample (E). Black asterisk indicating the  $\alpha$ -NAGALs and red asterisk the  $\alpha$ -GAL.

### Purification and biochemical characterization of plant produced $\alpha$ -galactosidases

Recombinant  $\alpha$ -galactosidases were purified from lysates of *N. benthamiana* leaves by sequential chromatography during which the presence of enzymes was monitored by measurement of enzymatic activities with 4MU-substrates. As generic first step we used Concanavalin A-Sepharose chromatography exploiting the presence of mannose-containing N- glycans in the recombinant  $\alpha$ -galactosidases ensuring high affinity binding to the immobilized lectin (Yasuda et al., 2004). The recovery in this step was high (> 40 %) for each enzyme and led to > 50-fold purification (Table 1). The next step in purification was ion exchange chromatography performed at pH 5.0 for  $\alpha$ -GAL and at pH 6.3 for  $\alpha$ -NAGAL and  $\alpha$ -NAGAL<sup>EL</sup> as described in experimental procedures. This led for each enzyme to considerable further purification with acceptable recovery (Table 1). The final purification step for all enzymes was gel filtration, resulting in an apparently pure protein as judged by silver staining of protein resolved by SDS-PAGE (Figure 2A). About 1  $\mu$ g  $\alpha$ -GAL,  $\alpha$ -NAGAL and  $\alpha$ -NAGAL<sup>EL</sup> was purified from 1 mg of soluble lysate protein.



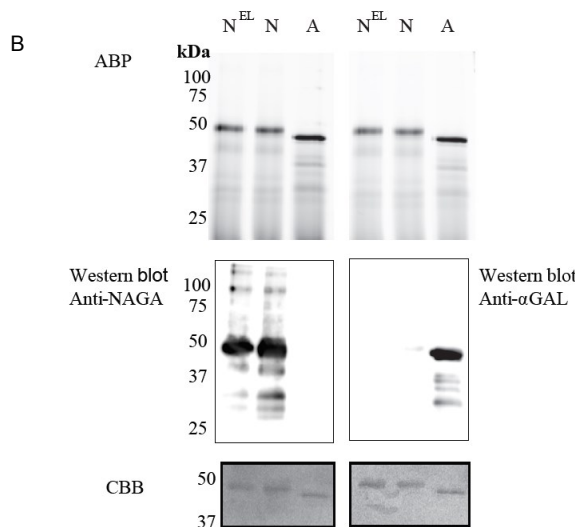


**Figure 2. Overview of enzyme purifications: activity based probe detection, Immunoblotting and Coomassie Brilliant Blue, staining of the plant produced pure enzymes. (A)** SDS-PAGE and silver staining of fractions obtained during purification. Four  $\mu\text{g}$  of total protein per lane was loaded for all unpurified samples and 1-2  $\mu\text{g}$  for all pure protein fractions ( $\alpha$ -NAGAL,  $\alpha$ -NAGAL<sup>EL</sup> and  $\alpha$ -GAL). Shown are: starting material/ Lysate (L), bound protein to Concanavalin A (C), pooled collected eluate of ion exchange (I), and the final pooled gel filtration fraction (GL) with highest enzyme specific activity. For comparison is shown recombinant  $\alpha$ -galactosidase A, Fabrazyme (Fz). Black asterisk indicating the  $\alpha$ -NAGALs and red asterisk the  $\alpha$ -GAL. **(B)** Before electrophoresis, 1 $\mu\text{g}$  of each pure enzyme was treated with 0.25 $\mu\text{M}$  of Cy5  $\alpha$ -galactosidase activity-based probe, ABP. N<sup>EL</sup> =  $\alpha$ -NAGAL<sup>EL</sup>, N =  $\alpha$ -NAGAL, A =  $\alpha$ -GAL. The gels were scanned  $\lambda_{\text{exc}}=635\text{nm}$ , then immunoblotted with anti- $\alpha$ -GAL or anti-NAGAL rabbit polyclonal antibodies, following Coomassie Brilliant blue, CBB, staining of the blots. The same gel had to be repeated since anti- $\alpha$ -GAL and anti-NAGA antibodies were both polyclonal anti-rabbit.

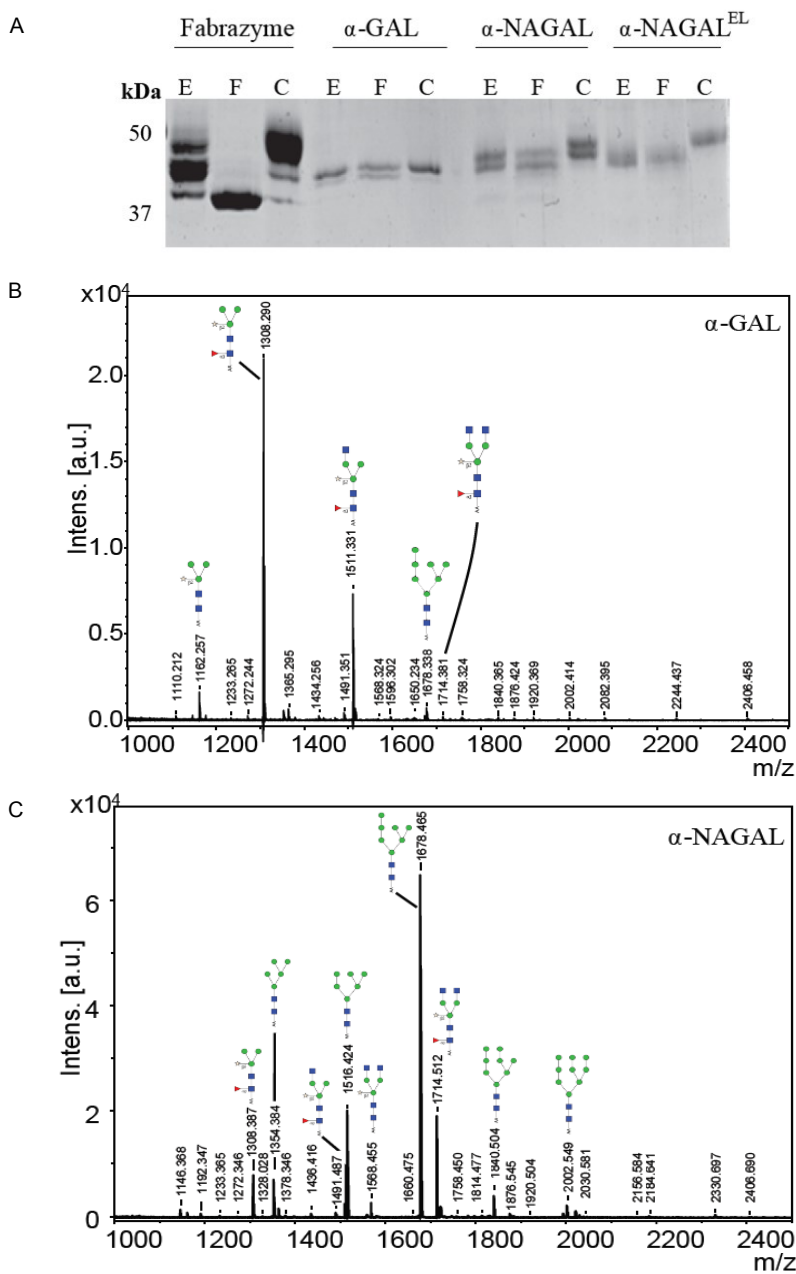
The apparent molecular weights of all three  $\alpha$ -galactosidases as determined by gel filtration coincided with dimers (113 kDa for  $\alpha$ -GAL, 134 kDa for  $\alpha$ -NAGAL, and 132kDa for  $\alpha$ -NAGAL<sup>EL</sup>) (Figure S2A and B). Of note, the specific activity of plant-produced  $\alpha$ -GAL (2.35 mmol/h/mg) was quite comparable to that of Fabrazyme (2.18 mmol/h/mg) (Table 2) (Tajima et al., 2009). After purification, further enzyme characterization was performed. Equal  $\mu\text{g}$  amounts of pure enzymes were incubated with fluorescent ABP followed by SDS-PAGE and fluorescence scanning analysis (Figure 2B). The intensity of the fluorescently labeled bands was the same for the three enzymes, revealing similar amounts of active enzyme molecules in each purified protein preparation. Western blotting using anti- $\alpha$ -GAL and anti- $\alpha$ -NAGAL antibodies showed that  $\alpha$ -NAGAL<sup>EL</sup> was not recognized by anti- $\alpha$ -GAL antibody (Figure 2B).

### N-glycan profile of the plant produced enzymes

Next, the N-glycan composition of the purified  $\alpha$ -galactosidases was examined using deglycosylation with Endo H and PNGase F endoglycosidases following SDS-PAGE analysis. Fabrazyme, produced in CHO cells, was used as a control. Consistent with literature reports, PNGase F led to conversion of Fabrazyme to a molecular mass of 39 kDa (Figure 3A). In the case of plant produced enzymes the reductions in molecular mass with EndoH or PNGase F were less pronounced (Figure 3A). This difference can be attributed to the presence of  $\alpha$ 1-3 core fucose residues, attached to most of the N-acetyl-glucosamine backbones (GlcNAc), inhibiting digestion by the endoglycosidases. The higher molecular weight of Fabrazyme compared to the plant produced enzymes could be due to the different N-glycan composition of this enzyme, mainly consisting of complex N-glycan structures, with additional mannose 6 phosphate residues (Sakuraba et al., 2005). To get more insight in the N-glycan composition of the plant produced enzymes, all N-linked glycans were released with PNGase A (not inhibited by the presence of  $\alpha$ 1-3 fucose) and subjected to MALDI-TOF MS (Figure 3B, C, D). The most prominent N-glycan type of  $\alpha$ -GAL recombinant protein was paucimannose structure ( $\text{Man}_3\text{GlcNAc}_2$ ) with  $\alpha$ 1-3 fucose attached on the core GlcNAc and  $\beta$ 1-2 xylose on the first mannose. Conceivably, the enzyme was secreted to the apoplastic fluid and hexosaminidases cleave the GlcNAc molecules yielding the paucimannosidic structure. On the other hand, both  $\alpha$ -NAGALs have oligo-mannose type N-glycans ( $\text{Man}_7\text{GlcNAc}_2$ ) as the most abundant N-glycan type, suggesting their retention in Golgi and /or ER compartments.

Table 1. Overview of enzyme purifications

| Enzymes                       | Purification steps | Volume (ml) | Total protein (mg) | Total activity ( $\mu\text{mol/h}$ ) | Total specific activity ( $\mu\text{mol/h/mg}$ ) | Purification fold | % Yield = recovery of activity |
|-------------------------------|--------------------|-------------|--------------------|--------------------------------------|--|-------------------|--------------------------------|
| $\alpha$ -GAL                 | Plant extract      | 49          | 136                | 3412                                 | 25   | 0                 | 100                            |
|                               | Con-A              | 3           | 1.3                | 1928                                 | 1444   | 57                | 57                             |
|                               | Cation exchange    | 2           | 0.4                | 860                                  | 2151   | 86                | 25                             |
|                               | Gel filtration     | 1.4         | 0.12               | 308                                  | 2585   | 103               | 9                              |
| $\alpha$ -NAGAL               | Plant extract      | 38          | 135                | 319                                  | 2.3  | 0                 | 100                            |
|                               | Con-A              | 3           | 1                  | 112                                  | 107  | 45                | 35                             |
|                               | Anion exchange     | 4           | 0.7                | 94                                   | 132  | 56                | 30                             |
|                               | Gel filtration     | 2           | 0.14               | 29.5                                 | 211  | 89                | 9                              |
| $\alpha$ -NAGAL <sup>EL</sup> | Plant extract      | 25          | 64                 | 314                                  | 5  | 0                 | 100                            |
|                               | Con-A              | 2           | 0.45               | 122                                  | 270  | 55                | 49                             |
|                               | Anion exchange     | 4           | 0.2                | 55                                   | 273  | 56                | 17                             |
|                               | Gel filtration     | 1.2         | 0.056              | 28                                   | 501  | 102               | 9                              |



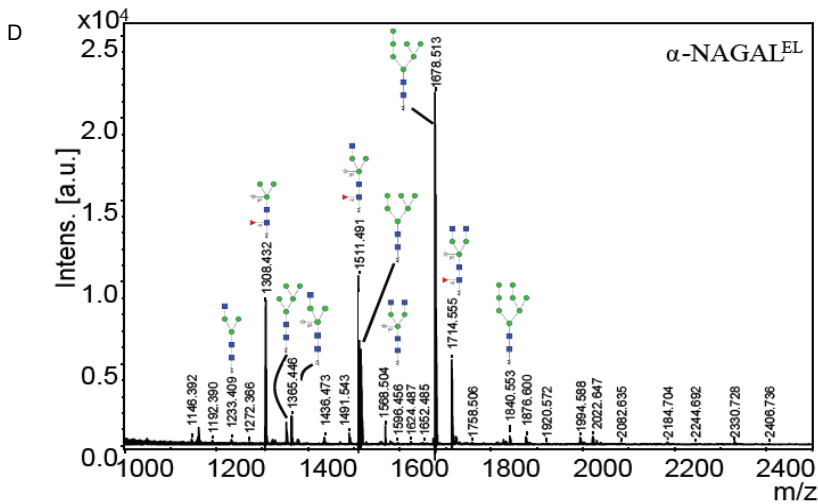


**Figure 3. N-glycans of  $\alpha$ -galactosidases.** (A) SDS-PAGE analysis followed by Coomassie Brilliant Blue staining of 1  $\mu$ g pure plant produced proteins and 3  $\mu$ g of Fabrazyme. E = protein treated with Endo H, F = protein treated with PNGase F, C = untreated protein. (B, C, D) N-glycosylation profiles were determined by MALDI-TOF MS analysis of 2-aminobenzoic acid derivatised PNGase-A released N-glycans of plant produced galactosidases. Glycan structures depicted were deduced from the measured m/z values. Blue square, N-acetylglucosamine; red triangle, fucose; open star, xylose; green circle, mannose. Presented N-glycan profiles of the following proteins: (B)  $\alpha$ -GAL, (C)  $\alpha$ -NAGAL, (D)  $\alpha$ -NAGAL<sup>EL</sup>.

### Cross reactivity with antibodies (Ab) in Fabry serum and stability tests

We next examined the cross reactivity of recombinant  $\alpha$ -galactosidases towards neutralizing antibodies in the serum of an Ab-positive male FD patient receiving ERT for six years (T=1). As a control, serum was used of the same patient before ERT (T=0) and still lacking antibodies against therapeutic  $\alpha$ -GAL. Inhibition of enzymatic activity by presence of Ab-positive serum was determined (Figure 4A). Activity of plant produced  $\alpha$ -GAL and Fabrazyme was clearly inhibited, but activities of  $\alpha$ -NAGALs, as determined with 4MU- $\alpha$ -GAL and/or 4MU- $\alpha$ -NAGAL substrates were not significantly influenced. The stability of the plant-produced galactosidases and Fabrazyme in human plasma was next studied by incubating enzymes at 37 °C for different time periods and detection of residual enzymatic 4MU- $\alpha$ -GAL activity (Figure 4B). Alpha-NAGAL<sup>EL</sup>, like  $\alpha$ -NAGAL, was more stable than both  $\alpha$ -GALs (Figure 4B).



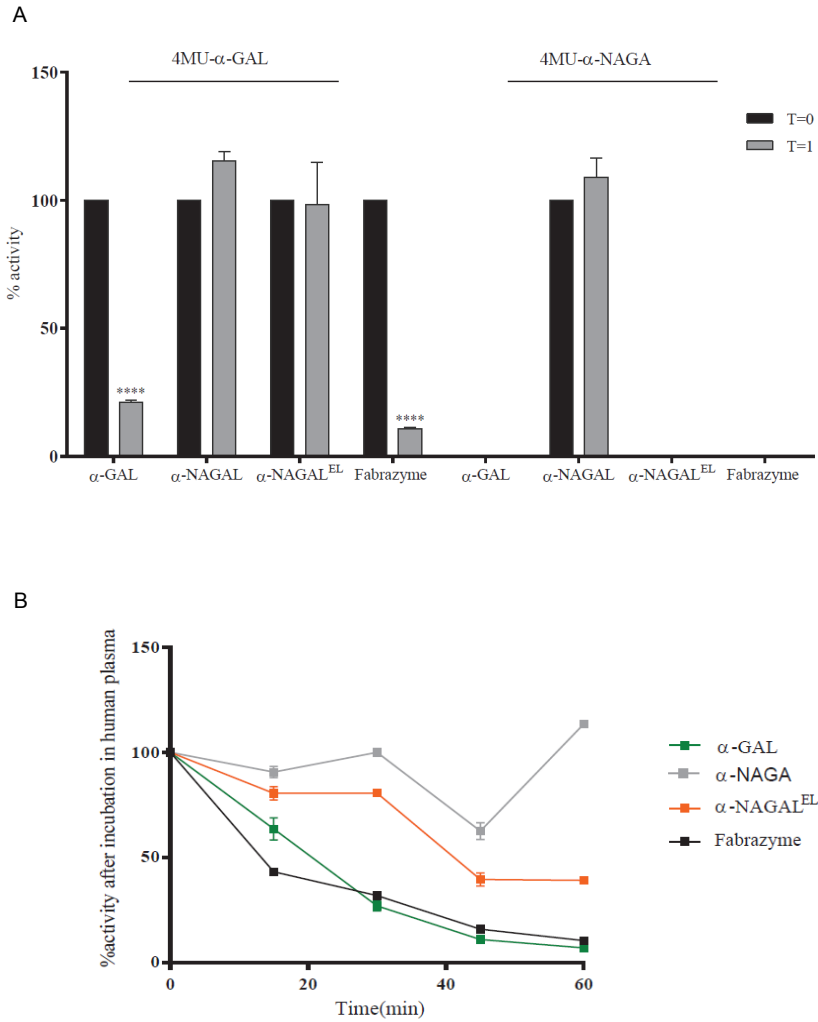


**Figure 4. Inhibition of activity of  $\alpha$ -galactosidases by Ab-positive Fabry serum. (A)** Percentage inhibition by FD serum, obtained after six years ERT (T=1), of enzymatic activity measured with 4MU- $\alpha$ -GAL and 4MU- $\alpha$ -NAGA. As negative control, serum of FD patient pre-ERT (T=0), was used. Asterisk(s) indicate significant difference as measured by a two-way ANOVA, \*\*\*\* = $P < 0.0001$ . **(B)** Percentage activity after incubation of 1  $\mu$ g/ml pure enzyme in human plasma for 15, 30, 45 and 60 min.

### Enzymatic activities of plant produced $\alpha$ -GAL, $\alpha$ -NAGAL and $\alpha$ -NAGAL<sup>EL</sup> towards artificial substrate(s) and their comparison with the same enzymes produced in HEK293 cells

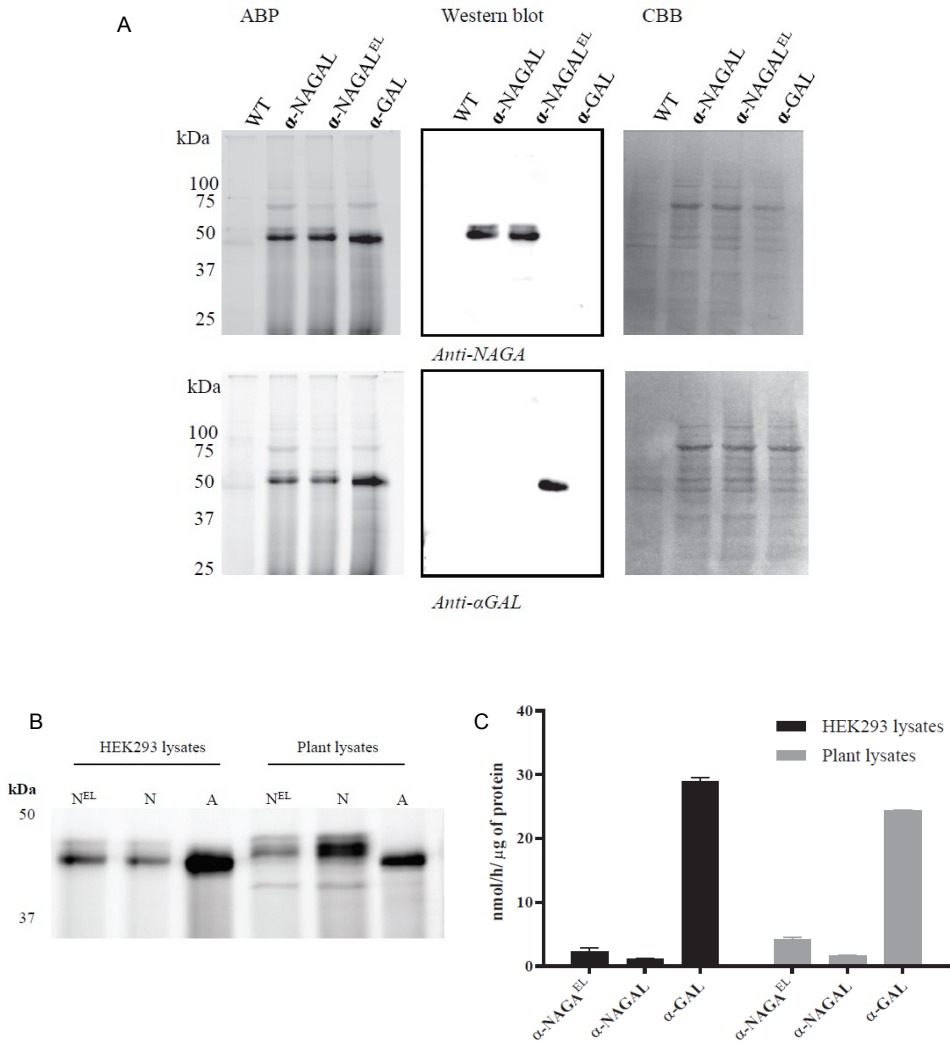
We next studied the substrate specificity of the various recombinant  $\alpha$ -galactosidases. First, activity was measured towards artificial 4MU- $\alpha$ -GAL and 4MU- $\alpha$ -NAGAL substrates. The amino acid substitutions Ser188Glu and Ala191Leu in the catalytic pocket of  $\alpha$ -NAGAL ( $\alpha$ -NAGAL<sup>EL</sup>) abolished activity towards 4MU- $\alpha$ -NAGAL as earlier reported (Tajima et al., 2009; Tomasic et al., 2010) (Table 2). The noted increase in hydrolytic specific activity towards 4MU- $\alpha$ -GAL (about a doubling) was less prominent as earlier reported by Tajima et al. The kinetic parameters  $k_{cat}$  and  $K_m$  determined with 4MU- $\alpha$ -GAL as substrate were improved by the amino acid substitutions in  $\alpha$ -NAGAL<sup>EL</sup> (Table 3). The plant produced  $\alpha$ -GAL showed comparable kinetic parameters to Fabrazyme (Table 3) (Hopkin et al., 2003; Lee et al., 2003). To determine whether production in *N. benthamiana* leaves influences kinetic features, the various recombinant enzymes were also generated in human HEK293 cells as described in experimental procedures (Figure 5A). ABP-labeling showed that similar proteins were produced in *N. benthamiana* and HEK293 cells (Figure 5B). The specific activity towards 4MU- $\alpha$ -GAL was also comparable, being relatively low for  $\alpha$ -NAGAL and increased (3-fold) by the amino substitutions in  $\alpha$ -NAGAL<sup>EL</sup> (Figure 5C).

Table 2. Specific activities as determined by 4MU substrates.

|                               | 4MU- $\alpha$ -GAL<br>specific activity<br>(mmol/h/mg) | 4MU- $\alpha$ -NAGAL<br>specific activity<br>(mmol/h/mg) |
|-------------------------------|--|--|
| $\alpha$ -GAL                 | 2.352  | <0.05  |
| $\alpha$ -NAGAL               | 0.192  | 1.33   |
| $\alpha$ -NAGAL <sup>EL</sup> | 0.547  | <0.05  |
| Fabrazyme                     | 2.184  | <0.05  |

Table 3. Michaelis-Menten kinetics as determined by 4MU substrates.

|                               | 4MU- $\alpha$ -GAL |                          |                        |                                  | 4MU- $\alpha$ -NAGAL |                          |                        |                                  |
|-------------------------------|--------------------|--------------------------|------------------------|----------------------------------|----------------------|--------------------------|------------------------|----------------------------------|
|                               | $K_m$ (mM)         | $V_{max}$<br>(mmol/h/mg) | $k_{cat}$ ( $s^{-1}$ ) | $k_{cat}/K_m$<br>( $mM/s^{-1}$ ) | $K_m$ (mM)           | $V_{max}$<br>(mmol/h/mg) | $k_{cat}$ ( $s^{-1}$ ) | $k_{cat}/K_m$<br>( $mM/s^{-1}$ ) |
| $\alpha$ -GAL                 | 2.478              | 4.219                    | 55.96                  | 22.58                            | No activity detected |                          |                        |                                  |
| $\alpha$ -NAGAL               | 6.02               | 0.527                    | 6.89                   | 1.14                             | 0.7                  | 3.9                      | 25.51                  | 36.13                            |
| $\alpha$ -NAGAL <sup>EL</sup> | 3.18               | 0.71                     | 14.52                  | 4.79                             | No activity detected |                          |                        |                                  |
| Fabrazyme                     | 2.431              | 3.954                    | 52.11                  | 21.43                            | No activity detected |                          |                        |                                  |



**Figure 5. Comparison of the biochemical properties of recombinant galactosidases produced in plants and HEK293 cells. (A)** Overexpression of human galactosidases in HEK293 cells was estimated via SDS-PAGE analysis. 20 $\mu$ g of total soluble protein were incubated with 0.5 $\mu$ M of Cy5 ABP, following Western blot analysis and Coomassie Brilliant Blue, CBB, staining of the blot. **(B)** ABP labelling of active enzyme molecules present in HEK293 and plant lysates overexpressing the proteins  $\alpha$ -NAGAL<sup>EL</sup>,  $\alpha$ -NAGAL and  $\alpha$ -GAL. Different total protein content was loaded in each lane. **(C)** The 4MU- $\alpha$ -GAL specific activities of HEK293 and plant lysates overexpressing the human galactosidases.

**Activity of recombinant enzymes towards (semi) natural substrates**

The activity of plant produced galactosidases towards lipid substrates was next determined. NBD-Gb3 was found to be degraded by Fabrazyme and plant-produced  $\alpha$ -GAL on a par (Figure 6A). Of note, significant degradation of NBD-Gb3 to NBD-Lac Cer by  $\alpha$ -NAGAL and  $\alpha$ -NAGAL<sup>EL</sup> was detected (Figure 6A). To further substantiate the findings, we incubated wild type and mutant  $\alpha$ -NAGALs with NBD-Gb3 in the absence or presence of 2.5mM N-acetylgalactosamine, a potent inhibitor of  $\alpha$ -NAGAL activity (Figure 6B). The wild type  $\alpha$ -NAGAL was inhibited, resulting in loss of NDB-Lac Cer formation, whereas  $\alpha$ -NAGAL<sup>EL</sup> was not. Next, activity towards 5  $\mu$ M of natural Gb3 and its deacetylated form Lyso-Gb3, was determined using detection of metabolites with LC-MS/MS. The analysis revealed a 2-5-fold increased activity of  $\alpha$ -NAGAL<sup>EL</sup> compared to  $\alpha$ -NAGAL with both substrates (Figure 6C). The pH optimum was pH 4.2 for  $\alpha$ -GALs and pH 5.2 for both  $\alpha$ -NAGALs (Figure S3).

Finally, serum of male FD patients, containing high amount of Lyso-Gb3, was incubated overnight with recombinant galactosidases (at a concentration of 8  $\mu$ mol/h/ml activity mimicking levels reached during ERT). Of note, the rate of degradation of Lyso-Gb3 in the serum sample was highest with  $\alpha$ -NAGAL<sup>EL</sup> (Figure 6D). Likely this reflects the greater stability and ongoing activity of  $\alpha$ -NAGAL<sup>EL</sup> at neutral pH as compared to that of  $\alpha$ -GALs.

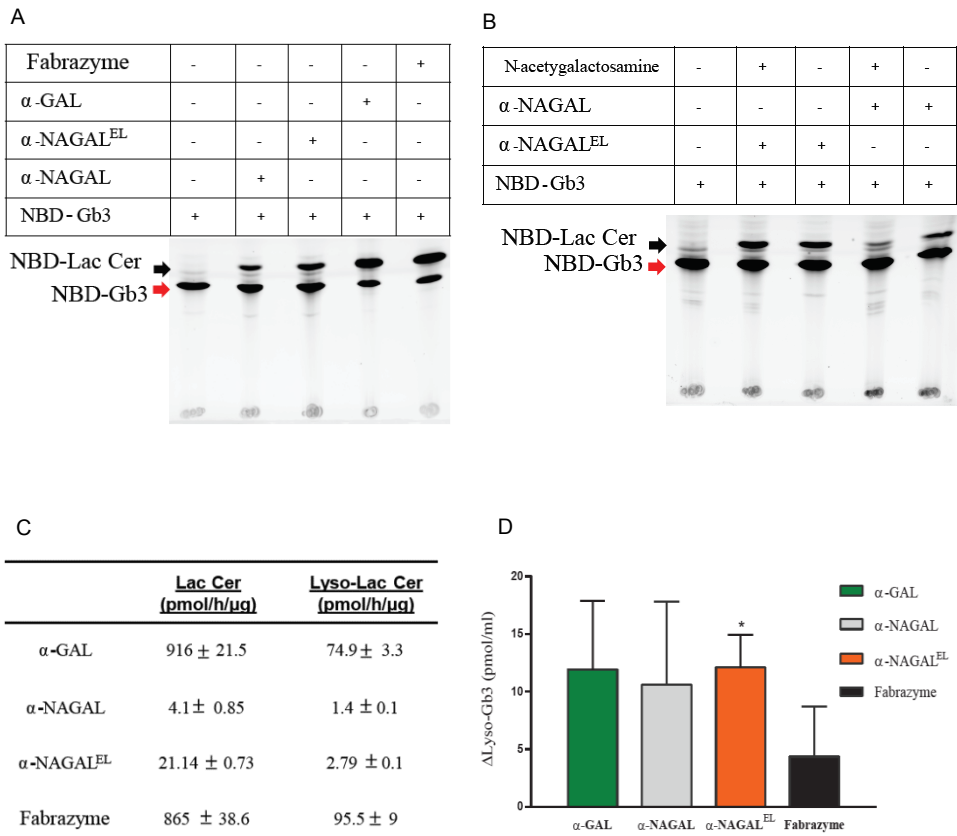


**Figure 6. Activity of  $\alpha$ -galactosidases towards semi-natural and natural lipid substrates. (A)** Pure recombinant proteins were incubated with 5  $\mu$ M of NBD-C12-Gb3. detection of formation of NBD-C12Lactosylceramide, Lac Cer detected by HPTLC. **(B)** Pure  $\alpha$ -NAGALs (wild type and modified) were incubated with 5 $\mu$ M of NBD-C12-Gb3 in presence/absence of 2.5 mM N-acetyl-galactosamine. Formation of NBD-C12-Lactosylceramide detected by HPLC. **(C)** Pure plant produced galactosidases and Fabrazyme were incubated with 5  $\mu$ M of C18-Gb3, and Lyso-Gb3. Formation of Lac Cer and Lyso-Lac Cer (pmol/h/ $\mu$ g) detected by LC-MS/MS. Data represent the mean  $\pm$  S.D, n=2. **(D)** Correction of Lyso-Gb3 in FD serum of 2 different Fabry patients pre-ERT after incubation with pure plant produced enzymes (each 8  $\mu$ mol artificial 4MU-substrate hydrolysis/h) overnight at 37°C. Lyso-Gb3 levels measured by LC-MS/MS. Data represent as mean  $\pm$  S.D, n=2. Asterisk(s) indicate significant difference as measured by a standard student t-test, \* =P<0.05.

## Discussion

The combined challenges of high costs, immunogenicity and poor efficacy posed by present Fabry ERT's prompted us to consider an examination of wildtype and mutant recombinant human  $\alpha$ -galactosidases. We used *N. benthamiana* leaves as production system for this purpose. All enzymes could be expressed at substantial amounts, 0.1-0.2 % of total soluble protein, in *N. benthamiana*. The expressed  $\alpha$ -GAL in *N. benthamiana* seems most likely to be secreted or transported to the vacuole as based on its N-glycan composition consisting largely of Man<sub>3</sub>GlcNAc<sub>2</sub> with  $\alpha$ 1-3 fucose attached to the core GlcNAc and  $\beta$ 1-2 xylose to the first mannose (Castilho and Steinkellner, 2012). In contrast, the transiently expressed  $\alpha$ -NAGALs show prominent Man<sub>7</sub>GlcNAc<sub>2</sub> N-glycans, more consistent with retention in the cis Golgi or ER (Castilho and Steinkellner, 2012).

Purification of all enzymes to homogeneity could be achieved by three relatively simple chromatographic steps. The observed specific activities of the purified enzymes were in the range of single digit nanomole substrate hydrolysis/ $\mu$ g pure protein per hour, being comparable to that of Fabrazyme. Recombinant, plant produced galactosidases were all labeled by fluorescent  $\alpha$ -galactosyl cyclophellitol-aziridine ABP. The intensity of ABP labeling per protein amount was identical for all galactosidases, substantiating further that in all cases the majority of purified protein is enzymatically active.

The observed specific activities of the produced  $\alpha$ -galactosidases warrant discussion. The specific activity of pure  $\alpha$ -NAGAL<sup>EL</sup> (0.55 mmol/h/mg) as measured with 4MU- $\alpha$ -GAL was 2-3-fold increased to that of wild type  $\alpha$ -NAGAL (0.19 mmol/h/mg). The  $K_m$  of  $\alpha$ -NAGAL<sup>EL</sup> (3 mM) was lower compared to that of  $\alpha$ -NAGAL (6 mM). Almost the same specific activity for  $\alpha$ -NAGAL<sup>EL</sup> (0.5 mmol hydrolysis/h/mg) was reported by Sakuraba and co-workers (Tajima et al., 2009). They related this to that of wild type  $\alpha$ -NAGAL from a different source, resulting in an apparent 43 fold improved  $\alpha$ -galactosidase activity imposed by the introduction of the S188E and A191L in  $\alpha$ -NAGAL (Tajima et al., 2009). Our results are in closer alignment with those of Garman and co-workers (Tomasic et al., 2010). Using p-nitrophenyl- $\alpha$ -Gal as substrate the  $k_{cat}/K_m$  value of  $\alpha$ -NAGAL<sup>EL</sup> was found to be 4.6-fold higher than that of  $\alpha$ -NAGAL, similar to the 4-fold increase of  $k_{cat}/K_m$  value with 4MU- $\alpha$ -GAL substrate observed by us (Tomasic et al., 2010). Comparison of plant produced  $\alpha$ -GAL with Fabrazyme revealed that their specific activities towards 4MU- $\alpha$ -GAL, as well as Gb<sub>3</sub>, are almost identical. We also produced the various recombinant  $\alpha$ -galactosidases in mammalian HEK293 cells showing similar

kinetic parameters as the plant-produced enzymes, indicating that these are not influenced by the production platforms.

Fabrazyme produced in CHO cell line contains the sialic acid N-glycolylneuraminic which does not occur in humans and therefore is potentially immunogenic (Bekri, 2006;Castilho and Steinkellner, 2012;Kizhner et al., 2014). The plant-produced recombinant enzymes of the current study do not contain N-glycolylneuraminic acid in their N-glycans. The N-glycan profiles of all plant-produced recombinant enzymes were relatively homogenous, but differences were seen in N-glycans among the various enzymes. Most importantly, the majority of N-glycans of all recombinant enzymes were found to be core  $\alpha$ 1-3 fucosylated and  $\beta$ 1-2 xylosylated. The same modifications occur in N-glycans of carrot-produced taliglucerase (human glucocerebrosidase) (Shaaltiel et al., 2007). Of note, there is no evidence that these modifications induce immune responses in Gaucher disease patients (Shaaltiel et al., 2007). *A priori* this does not exclude immunogenicity in FD patients however.

The recombinant enzymes produced in *N. benthamiana* lack M6P residues. In theory, the glycans may be swapped for other structures through the chemoenzymatic methodology developed by Fairbanks and colleagues (Priyanka et al., 2016). However, given the limited success of existing Fabry ERT aiming at M6P receptor mediated delivery of therapeutic enzyme to lysosomes it might be considered to refrain from this type of enzyme targeting. We earlier demonstrated that deacylated Gb3, Lyso-Gb3, is extremely elevated in FD patients and  $\alpha$ -galactosidase A deficient mice (Aerts et al., 2008;Ferraz et al., 2016b). Excessive Lyso-Gb3 has been shown to be toxic for nociceptive peripheral neurons and podocytes in FD patients (Choi et al., 2015;Sanchez-Niño et al., 2015). Reduction of Lyso-Gb3 in FD patients therefore seems therefore a valid therapeutic goal. In view of this consideration above, our finding that not only  $\alpha$ -GAL but also  $\alpha$ -NAGALs are able to degrade Gb3 and Lyso-Gb3 is of interest. The amino acid substitutions in  $\alpha$ -NAGAL<sup>EL</sup> improve ~ 2-fold the capacity of the enzyme to degrade Lyso-Gb3 and ~5 fold that for Gb3. The relative efficacy of  $\alpha$ -NAGAL<sup>EL</sup> compared to  $\alpha$ -GAL in ability to degrade Lyso-Gb3 in FD serum is even better. The greatest reduction of Lyso-Gb3 is detected with  $\alpha$ -NAGAL<sup>EL</sup> added to FD serum at 37 °C. The superior action of  $\alpha$ -NAGAL<sup>EL</sup> is likely due to its stability at neutral pH. This remarkable finding suggests that the use of non-antigenic, (modified)  $\alpha$ -NAGAL might be a way to reach desired reductions in circulating Lyso-Gb3. The use of (modified)  $\alpha$ -NAGALs benefits from the higher stability and activity of the enzyme at neutral pH as compared to  $\alpha$ -GAL. PEGylation could be employed to increase the presence of (modified)  $\alpha$ -NAGAL in the blood. Of note, endogenous  $\alpha$ -NAGAL in the circulation of normal individuals and FD patients is relatively

low (Aerts, unpublished observations) and therefore likely does not contribute significantly to metabolism of the glycosphingoid base in the blood.

In conclusion, we here demonstrate that production of substantial amounts of wild-type human  $\alpha$ -GAL,  $\alpha$ -NAGAL and modified  $\alpha$ -NAGAL<sup>EL</sup> is feasible in *N. benthamiana*, resulting in enzymes with comparable kinetic properties to those produced in mammalian cell production systems. The introduction of two amino acid substitutions in  $\alpha$ -NAGAL improves its  $\alpha$ -galactosidase activity as measured with artificial fluorogenic substrate and natural lipids. A significant difference between  $\alpha$ -GAL and  $\alpha$ -NAGAL is the greater stability and activity at neutral pH of the latter enzyme. Furthermore  $\alpha$ -NAGAL is not inhibited by existing Ab in male FD patients by present ERTs. Modifications in the catalytic pocket of  $\alpha$ -NAGAL can improve its capacity to degrade Gb3 and Lyso-Gb3. The kinetic properties of modified  $\alpha$ -NAGAL and its greater stability at neutral pH could be further exploited for treatment of FD. In particular, use of modified  $\alpha$ -NAGAL to reduce circulating Lyso-Gb3 in FD patients warrants further examination.



## Materials and Methods

**Plants.** *Nicotiana benthamiana* plants were grown at 21 °C and 60-70 % humidity in the Unifarm greenhouses of Wageningen University (Westerhof et al., 2014).

**Chemicals.** All chemicals were obtained from Sigma (Germany) if not indicated otherwise. Fluorescent NBD-lipids and pure lipids were purchased from Avanti (Alabama, USA). Antibodies purchased from Abcam (Cambridge, MA, USA).

**Activity based probes.** The fluorescent ABP directed against  $\alpha$ -galactosidases was produced based on previously described synthesis (Willems et al., 2014). Alpha-Galactopyranose configured cyclophellitol-aziridine was grafted with Cy5 as fluorophore as described in detail in the supplementary material (Scheme 1). The newly synthesized probe was examined on reactivity with human recombinant  $\alpha$ -GAL (Fabrazyme, Sanofi-Genzyme, Cambridge, USA) (Figure S1A and B).

**Preparation of human  $\alpha$ -GAL,  $\alpha$ -NAGAL and  $\alpha$ -NAGAL<sup>EL</sup> (S188E; A191L) plant expression vectors.** Both *GLA* (ID: 2717) and *NAGA* (ID: 4668) were amplified from MegaMan Human Transcriptome cDNA library (Stratagene). The coding region of genes was amplified by Phusion ® HighFidelity PCR MasterMix (BioLabs) using the following primers: *GLA* sense: 5'-CTCATGAGTGCCAAGACCAACCTCTTCCTCTTCCTCATCTTCTCCCTCTGCTCTCCCTC TCCTCCGCCCTGGACAATGGATTGGCAAG-3', *GLA* antisense: 5'- CCCGTACGTAAAG TAAGTCT-3', *NAGA* sense: 5'-CTCATGAGTGCCAAGACCAACCTCTTCCTCTTCCTCATC TTCTCCCTCTGCTCTCCCTCTCCTCCGCC-3', *NAGA* antisense: 5'-CCGTACGTCACTGCT GGGACA-3'. The genes were amplified between BspHI and BsiWI restriction sites, lacking the sequence encoding for their native signal peptide. Instead, the native signal peptide of *Arabidopsis thaliana* chitinase was added at primer sequences. Insertion of mutations S188E and A191L in *NAGA* gene was achieved via overlap extension PCR. PCR reactions were performed using the following primers: *NAGA* mutant antisense: 5'-CCTTCATAGAGTGGCCACTCGCAGGAG AAGGC-3', *NAGA* mutant sense: 5'-GCCTTCTCCTGCGAGTGGCCACTCTATGAAGG-3'. The elements were cloned into pGEM ®-T Easy Vector System (Promega), following electroporation of DH5 $\alpha$  *E. coli* cells. After clone selection and confirmation of sequences by sequencing (Macrogen), the complete open reading frames (ORFs) of *GLA*, *NAGA* and *NAGA*<sup>EL</sup> were inserted in plant expression vectors. A modified version of pMDC32 expression vector, named pHYG, (Westerhof et al.,

2012), was used as the main plant expression vector during all experiments. The vector was digested with Acc65I and NcoI, leaving compatible overhangs for ligation of the elements flanked between BspHI and BsiWI restriction sites. All constructs were under the control of cauliflower mosaic virus 35S constitutive promoter, with duplicate enhancer (d35S) and the nopaline synthase terminator (Tnos) derived from *Agrobacterium tumefaciens* (*A.tum*). The PHYG vectors harboring the genes were used for transformation of *A.tum* strain MOG101, following *N. benthamiana* plant leaf infiltrations.

***Agrobacterium tumefaciens* transient transformation assay.** *A.tum* cultures were grown as previously described (Westerhof et al., 2012; Westerhof et al., 2014). The constructs were co-expressed or not with the tomato bushy stunt virus silencing inhibitor p19 (Voinnet et al., 2003), by mixing *A.tum* cultures 1:1 following 1-2 hours incubation at room temperature.

**Infiltration of plants, harvesting and lysate preparation.** The inoculated bacterial cultures were used for infiltration of the two youngest leaves of 5-6 weeks old *N. benthamiana* plants. Whole leaves and leaf disks (50 mm) were harvested at different days post-infiltration (dpi), snap-frozen and homogenized in liquid nitrogen. Homogenization was performed with a tissue lyser (AKA Qiagen TissueLyser II) at 30 rounds/sec for 1 min. Extraction of total soluble proteins of samples was achieved using 2-3 ml per leaf gram of extraction buffer (30 mM citric acid /sodium phosphate buffer, pH 6.3, containing 2% (w/v) polyvinylpyrrolidone, 0.1% (v/v) Tween20, 0.5 M NaCl, and protease inhibitor by Roche, EDTA free) following homogenization at same tissue lyser program. When whole leaves were used, homogenization was performed by grounding with a mortar and pestle. Samples were next centrifuged for 15 min at 15000 g, (F13S 14x50 cy, Sorvall rotor), at 4 °C. The supernatant was collected and used for further analysis or it was stored at -80 °C upon desalting at G25-Sephadex column.

**Enzyme purification.** As first step in the purification of all enzymes, a 5 ml column of Concanavalin-A-Sepharose (GE healthcare Bio-Sciences) was used. The column was equilibrated with 40 ml washing buffer (0.1 M sodium acetate, 0.1 M NaCl, 1 mM MgCl<sub>2</sub>, 1 mM CaCl<sub>2</sub>, 1 mM MnCl<sub>2</sub>, pH 6.0). Then, protein sample (lysate) was applied to the column, 1:1 diluted in washing buffer (0.5 ml/min loading conditions). For α-GAL 49ml of protein lysate was applied on the column, for α-NAGAL 38 ml and α-NAGAL<sup>EL</sup> 25 ml. Proteins were eluted with 30 ml elution buffer (washing buffer supplemented with 0.9 M methyl-α-mannoside and 0.9 M methyl-α-glucoside). Ten fractions of 1 ml showing highest levels of enzymatic activity were pooled (post-ConA). Next, for α-GAL

purification, 10 ml of post-ConA was loaded on an ultrafiltration device (Centricon Plus-20, 15 ml with 10 kDa molecular cutoff, Millipore, Bedford, MA) to remove methyl-monosaccharides and buffer exchanged to 20 mM sodium acetate, pH 5.0, until obtaining a volume of 3 ml. Dialysis of the sample was continued in 20 mM sodium acetate buffer, pH 5.0, 4 °C, overnight. A HiTrap SP HP column (1 ml; GE healthcare Bio-Sciences) was equilibrated with 15 ml binding buffer: 20 mM sodium acetate buffer, pH 5.0. The sample, 3 ml, was applied on the column which was extensively washed with 10 ml binding buffer afterwards. Then, protein was eluted using a gradient of 0 to 300 mM NaCl, 15 ml. Enzyme eluted in 0.5 ml fractions 2-4, which were pooled. For wild type  $\alpha$ -NAGAL and modified  $\alpha$ -NAGAL<sup>EL</sup>, post-ConA, 2-3 ml, was buffer exchanged via ultrafiltration to 10 mM potassium phosphate buffer, KPi (pH 6.3) with 10 mM NaCl. Next, sample was dialyzed in the same buffer to further remove any methyl-monosaccharides. After this, sample was applied on a HiTrap Q HP column (1ml; GE healthcare Bio-Sciences). Anion exchange chromatography was performed using a gradient of 10 to 600 mM NaCl in 10 mM Kpi (pH 6.3). Enzymes eluted in 0.5 ml fractions 2-4, which were pooled. As final purification step for all enzymes gel filtration was used. A Superdex™ 200 Increase 10/300 GL (GE healthcare Bio-Sciences) column was prior equilibrated with 50 ml of 20 mM sodium acetate buffer with 150mM NaCl, pH 5.0. Samples were applied and chromatography performed at a flow 0.75 ml/min. 0.2 ml fractions were collected and analyzed on enzymatic activity. The final material was snap frozen in liquid nitrogen and stored at -80 °C until further use.

**Overproduction of  $\alpha$ -GAL,  $\alpha$ -NAGAL and  $\alpha$ -NAGAL<sup>EL</sup> in HEK293 cells.** Vectors for human cell line HEK293 were produced as follows: The complete open reading frames of human  $\alpha$ -GAL,  $\alpha$ -NAGAL and  $\alpha$ -NAGAL<sup>EL</sup> were amplified from previous pGEMt easy vectors harboring the genes with their native signal peptide, via PFX50 high fidelity DNA polymerase (Invitrogen), using the primers below.

*GLA* sense: 5'-GGGGACAAGTTTGTACAAAAAAGCAGGCTACCACCATGCA GCTGAGGAA CCCAGA-3', *GLA* antisense: 5'-GGGGACCACTTTGTACAAGAAAGCTGGGTC TTAAAGTAAGTCTTTTAATGACATC-3', *NAGA* sense: 5'-GGGGACAAGT TTGTACA AAAA AGCAGGCTACCACCATGCTGCTGAAGACAGTGCTC-3', *NAGA* antisense: 5'-GGGGACCA CTTTGTACAAGAAAGCTGGGTCTCACTGCTGGGACATCTCCAG-3'.

The elements were cloned via Gateway cloning into the donor vector pDONR221 (BP reaction), following transformation of DH5 $\alpha$  *E. coli* strain. Clones were collected upon kanamycin selection and their sequences were confirmed. Next, they were cloned into the destination vector, pcdna-DEST40-zeo (LP reaction),

forming the final construct to transfect HEK293 cells. The HEK293 cells were cultured in 6 well plates in 2.5 ml Dulbecco's Modified Eagles Medium (DMEM, Sigma) supplemented with 10% fetal calf serum, 1% penicillin/streptomycin and glutamax at 37 °C, at 7% CO<sub>2</sub>. Three µgram of pcdna-DEST40-zeo DNA was transfected into cultured HEK293 cells using polyethylenimine, primarily mixed with serum free DMEM medium. After 2 days of cell culture, 200 µg/µl of zeocin was added to the culture media for selection of clones harboring the gene of interest. The cells grew for 3 weeks at 37 °C, at 7% CO<sub>2</sub> in the presence of antibiotics and lysed in 20 mM potassium phosphate buffer (pH 6.5), 0.1% Triton with additional protease inhibitor by Roche. The cells were stored at -150 °C in DMEM, 20% fetal calf serum, 10% DMSO until further use.

**Enzymatic activity measurements.** Both  $\alpha$ -galactosidase A and  $\alpha$ -*N*-acetyl-galactosaminidase activities of samples were examined with corresponding 4-methylumbelliferyl (4MU) substrates. For  $\alpha$ -galactosidase activity measurement samples were incubated for 1hr at 37 °C with a final concentration of 1.2 mg/ml 4MU- $\alpha$ -D-galactosylpyranoside (4MU- $\alpha$ -GAL) in 150 mM McIlvaine pH 4.6, supplemented with 0.1% (w/v) BSA and released 4MU was quantified as described earlier (Blom et al., 2003).

Activity of plant produced recombinant enzymes and Fabrazyme towards 5 µM of NBD-C12-Gb3 substrate was measured for 3 hrs at 37 °C in 150 mM McIlvaine buffer (pH 4.6) containing 0.05% (v/v) Triton X-100 and 0.2% (w/v) sodium taurocholate, pH 4.6. Lipids were extracted with the Bligh and Dyer procedure, applied to HPTLC. The plate was scanned for fluorescent lipids with a Typhoon FLA 9500. Protein concentrations in assay were for Fabrazyme 3.8 µg/ml,  $\alpha$ -GAL 3.2 µg/ml,  $\alpha$ -NAGAL 40 µg/ml, and  $\alpha$ -NAGAL<sup>EL</sup> 16 µg/ml. Activity of recombinant enzymes towards natural C18: Gb3 was measured using 500 pmol of lipid in (100 µl total volume) 150 mM McIlvaine buffer with 0.05% (v/v) Triton X-100 and 0.2% (w/v) sodium taurocholate for 3 hrs at 37 °C. The pH was 4.2 for  $\alpha$ -GALs and 5.2 for  $\alpha$ -NAGALs. After incubation, neutral lipids were extracted by the Folch method. Deacetylation of lipids was performed as described earlier (Ferraz et al., 2016b). After deacetylation, samples were dried and further cleaned by adding 1:1 butanol: water. The butanol phase was collected, dried and lipids were dissolved in 200 µl methanol, ready for LC-MS/MS injection. The conversion of Gb3 to lactosylceramide (Lac Cer) was measured in LC-MS/MS using C17-Gb3 and C17-Lac Cer as controls and C17-Sphinganine as internal standard. The same assay conditions were used when applying natural Lyso-Gb3 as substrate. Lipids were extracted according to Bligh and Dyer and subjected to LC-MS/MS injection as above. Isotope <sup>13</sup>C-Lyso-Gb3 was used as an internal standard for monitoring the conversion of

Lyso-Gb3 into Lyso-Lac Cer. Protein concentrations in assays were for Fabrazyme 1.9  $\mu\text{g/ml}$ ,  $\alpha$ -GAL 1.6  $\mu\text{g/ml}$ ,  $\alpha$ -NAGAL 20  $\mu\text{g/ml}$  and  $\alpha$ -NAGAL<sup>EL</sup> 8  $\mu\text{g/ml}$ .

**Determination of kinetic parameters.**  $K_m$ ,  $V_{max}$  and  $k_{cat}$  values were determined using 4MU substrates. Reactions were performed for 1hr or 30min at 37 °C at 10 different 4MU- $\alpha$ -GAL and 4MU- $\alpha$ -NAGAL concentrations in 150 mM McIlvaine pH 4.6 supplemented with 0.1% (w/v) BSA. The 4MU- $\alpha$ -GAL concentrations in the assays ranged from 0.074 to 4.72 mM; for 4MU- $\alpha$ -NAGAL from 0.022 to 0.91 mM. Protein concentrations in the assays were: for  $\alpha$ -GAL 7 ng/ml, Fabrazyme 2 ng/ml,  $\alpha$ -NAGAL 16 ng/ml, when using 4MU- $\alpha$ -NAGAL substrate and 100 ng/ml, when using 4MU- $\alpha$ -GAL substrate, and for  $\alpha$ -NAGAL<sup>EL</sup> 16 ng/ml. Parameters were calculated using GraphPad Prism6.

**N-glycan analysis of plant produced  $\alpha$ -galactosidases.** Proteins were deglycosylated with EndoH and PNGase F (Wilbers et al., 2016). MALDI-TOF analysis performed as previously described (Wilbers et al., 2016).

**SDS-PAGE and Western blotting.** To examine purity and molecular mass of recombinant  $\alpha$ -galactosidases, sodium dodecyl sulphate-polyacrylamide gel electrophoresis (SDS- PAGE) (10 % polyacrylamide) was used (Witte et al., 2010). Samples were run under reduced conditions. After SDS-PAGE analysis, gels were stained with Coomassie Brilliant Blue staining or silver stain using the PhastSystem system (GE Healthcare). Western blotting and fluorescence scanning for ABP-labeled protein was performed exactly as described earlier (Willems et al., 2014).

**Protein determination.** Protein concentrations were determined with a Micro BCA Protein Assay Reagent Kit (PIERCE), and bovine serum albumin was used as a standard according to the supplier's protocol. In addition, pure protein concentrations were measured in NanoDrop 2000c (Thermo Scientific) via adjusting the molecular weight and extinction coefficient parameters.

**Detection of cross reactivity with Antibody (Ab) -positive FD serum.** Samples were incubated for 1hr 4 °C while rolling, with 2  $\mu\text{l}$  Ab<sup>+</sup> FD serum or normal serum of an FD patient and  $\alpha$ -galactosidase activity was measured with 4MU- $\alpha$ -GAL and 4MU- $\alpha$ -NAGAL substrate (Linthorst et al., 2004).

**Degradation of Lyso-Gb3 in FD serum.** To serum from 2 different FD patients pre-ERT, recombinant enzymes (8  $\mu\text{mol}$  artificial substrate hydrolysis/h/ml) were added and incubated overnight at 37 °C. Then, lipids were extracted as described before and applied to LC-MS/MS.

## References

- Aerts, J.M.F.G., Groener, J.E., Kuiper, S., et al (2008). Elevated globotriaosylsphingosine is a hallmark of Fabry disease. *Proceedings of the National Academy of Sciences* 105:2812-2817. doi: <https://doi.org/10.1073/pnas.0712309105>
- Barton, N.W., Furbish, F.S., Murray, G.J., et al (1990). Therapeutic response to intravenous infusions of glucocerebrosidase in a patient with Gaucher disease. *Proceedings of the National Academy of Sciences of the United States of America* 87: 1913-1916.
- Bekri, S. (2006). *Fabry Disease: Perspectives from 5 Years of FOS*. Oxford: Oxford PharmaGenesis. Chapter 6.
- Bishop, D.F., Kornreich, R., and Desnick, R.J. (1988). Structural organization of the human alpha-galactosidase A gene: further evidence for the absence of a 3' untranslated region. *Proceedings of the National Academy of Sciences* 85: 3903-3907. doi: <https://doi.org/10.1073/pnas.85.11.3903>
- Blom, D., Speijer, D., Linthorst, G.E., et al (2003). Recombinant Enzyme Therapy for Fabry Disease: Absence of Editing of Human  $\alpha$ -Galactosidase A mRNA. *The American Journal of Human Genetics* 72: 23-31. doi: 10.1086/345309
- Brady, R.O.G., Andrew E. Bradley, Roy M. Martensson, et al (1967). Enzymatic Defect in Fabry's Disease. *New England Journal of Medicine* 276: 1163-1167. doi: 10.1056/NEJM196705252762101
- Castilho, A., and Steinkellner, H. (2012). Glyco-engineering in plants to produce human-like N-glycan structures. *Biotechnology Journal* 7: 1088-1098. doi: <https://doi.org/10.1002/biot.201200032>
- Choi, L., Vernon, J., Kopach, O., et al (2015). The Fabry disease-associated lipid Lyso-Gb3 enhances voltage-gated calcium currents in sensory neurons and causes pain. *Neuroscience Letters* 594: 163-168. doi: 10.1016/j.neulet.2015.01.084
- Clark, N.E., and Garman, S.C. (2009). The 1.9 Å Structure of Human  $\alpha$ -N-Acetylgalactosaminidase: The Molecular Basis of Schindler and Kanzaki Diseases. *Journal of Molecular Biology* 393: 435-447. doi: <https://doi.org/10.1016/j.jmb.2009.08.021>
- Desnick, R.J. (2004). Enzyme replacement therapy for Fabry disease: lessons from two  $\alpha$ -galactosidase A orphan products and one FDA approval. *Expert Opinion on Biological Therapy* 4: 1167-1176. doi: <https://doi.org/10.1517/14712598.4.7.1167>
- Desnick, R.J., Ioannou Y.A. (2001).  $\alpha$ -Galactosidase a deficiency. Fabry disease, in Scriver C.R., Beaudet A.L., Sly W.S., Valle D. (Eds) *The Metabolic and Molecular Bases of Inherited Disease*, 8<sup>th</sup> ed. McGraw-Hill, New York, 3733-3774.

- Eng, C.M., Guffon, N., Wilcox, W.R., et al (2001). Safety and Efficacy of Recombinant Human  $\alpha$ -Galactosidase A Replacement Therapy in Fabry's Disease. *New England Journal of Medicine* 345: 9-16.
- Ferraz, M.J., Marques, A.R.A., Appelman, M.D., Aerts, J.M, et al (2016a). Lysosomal glycosphingolipid catabolism by acid ceramidase: formation of glycosphingoid bases during deficiency of glycosidases. *FEBS Letters* 590: 716-725. doi: <https://doi.org/10.1002/1873-3468.12104>
- Ferraz, M.J., Marques, A.R.A., Gaspar, P., Aerts, J.M, et al (2016b). Lyso-glycosphingolipid abnormalities in different murine models of lysosomal storage disorders. *Molecular Genetics and Metabolism* 117: 186-193. doi: <https://doi.org/10.1016/j.ymgme.2015.12.006>
- Fischer, R., Stoger, E., Schillberg, S., Christou, P., and Twyman, R.M. (2004). Plant-based production of biopharmaceuticals. *Current opinion in plant biology* 7: 152-158. doi: <https://doi.org/10.1016/j.pbi.2004.01.007>
- Futerman, A.H., and Van Meer, G. (2004). The cell biology of lysosomal storage disorders. *Nat Rev Mol Cell Biol* 5:554-565. doi: <https://doi.org/10.1038/nrm1423>
- Gold, H., Mirzaian, M., Dekker, N., et al (2013). Quantification of Globotriaosylsphingosine in Plasma and Urine of Fabry Patients by Stable Isotope Ultrapformance Liquid Chromatography–Tandem Mass Spectrometry. *Clinical Chemistry* 59:547-556. doi: <https://doi.org/10.1373/clinchem.2012.192138>
- Gomord, V., and Faye, L. (2004). Posttranslational modification of therapeutic proteins in plants. *Current opinion in plant biology* 7:171-181. doi: <https://doi.org/10.1016/j.pbi.2004.01.015>
- Guce, A.I., Clark, N.E., Salgado, E.N., et al (2010). Catalytic Mechanism of Human  $\alpha$ -Galactosidase. *The Journal of Biological Chemistry* 285: 3625-3632. doi: 10.1074/jbc.M109.060145
- Hopkin, R.J., Bissler, J., and Grabowski, G.A. (2003). Comparative evaluation of alpha-galactosidase A infusions for treatment of Fabry disease. *Genet Med* 5: 144-153. doi: 10.1097/01.gim.0000069509.57929.cd
- Kizhner, T., Azulay, Y., Hainrichson, M., et al (2014). Characterization of a chemically modified plant cell culture expressed human  $\alpha$ -Galactosidase-A enzyme for treatment of Fabry disease. *Molecular Genetics and Metabolism* 114: 259-267. doi: 10.1016/j.ymgme.2014.08.002
- Lee, K., Jin, X., Zhang, K., et al (2003). A biochemical and pharmacological comparison of enzyme replacement therapies for the glycolipid storage disorder Fabry disease. *Glycobiology* 13:305-313. doi: <https://doi.org/10.1093/glycob/cwg034>
- Lin, H.-Y., Chong, K.-W., Hsu, J.-H., et al (2009). High Incidence of the Cardiac Variant of Fabry Disease Revealed by Newborn Screening in the Taiwan Chinese Population. *Circulation: Cardiovascular Genetics* 2: 450-456. doi: <https://doi.org/10.1161/CIRCGENETICS.109.862920>

- Linthorst, G.E., Hollak, C.E.M., Donker-Koopman, W.E., et al (2004). Enzyme therapy for Fabry disease: Neutralizing antibodies toward agalsidase alpha and beta. *Kidney Int* 66: 1589-1595. doi: 10.1111/j.1523-1755.2004.00924.x
- Hamers M.N., Westerveld A., Khan M., Tager J.M. (1977). Characterization of alpha-galactosidase isoenzymes in normal and Fabry human-Chinese Hamster somatic cell hybrids. *Hum. Genet.* 36:289–297. doi: <https://doi.org/10.1007/BF00446279>
- Ohashi, T., Sakuma, M., Kitagawa, T., et al (2007). Influence of antibody formation on reduction of globotriaosylceramide (GL-3) in urine from Fabry patients during agalsidase beta therapy. *Molecular Genetics and Metabolism* 92: 271-273. doi: <https://doi.org/10.1016/j.ymgme.2007.06.013>
- Priyanka, P., Parsons, T.B., Miller, A., Platt, F.M., and Fairbanks, A.J. (2016). Chemoenzymatic Synthesis of a Phosphorylated Glycoprotein. *Angewandte Chemie International Edition* 55:5058-5061. doi: <https://doi.org/10.1002/ange.201600817>
- Rombach, S.M., Aerts, J.M.F.G., Poorthuis, B.J.H.M., et al (2012). Long-Term Effect of Antibodies against Infused Alpha-Galactosidase A in Fabry Disease on Plasma and Urinary (lyso)Gb3 Reduction and Treatment Outcome. *PLoS ONE* 7: e47805. doi: 10.1371/journal.pone.0047805
- Sakuraba, H., Murata-Ohsawa, M., Kawashima, I., et al (2005). Comparison of the effects of agalsidase alfa and agalsidase beta on cultured human Fabry fibroblasts and Fabry mice. *J Hum Genet* 51: 180-188. doi: 10.1007/s10038-005-0342-9
- Sanchez-Niño, M.D., Carpio, D., Sanz, A.B., et al (2015). Lyso-Gb3 activates Notch1 in human podocytes. *Human Molecular Genetics* 24: 5720-5732. doi: <https://doi.org/10.1093/hmg/ddv291>
- Schiffmann, R., Kopp, J.B., Austin, I.H., and Et Al. (2001). Enzyme replacement therapy in fabry disease: A randomized controlled trial. *JAMA* 285: 2743-2749. doi:10.1001/jama.285.21.2743
- Schram, A.W., Hamers, M.N., Brouwer-Kelder, B., et al (1977). Enzymological properties and immunological characterization of  $\alpha$ -galactosidase isoenzymes from normal and Fabry human liver. *Biochimica et Biophysica Acta (BBA) - Enzymology* 482: 125-137. doi: [https://doi.org/10.1016/0005-2744\(77\)90360-6](https://doi.org/10.1016/0005-2744(77)90360-6)
- Schuller, Y., Hollak, C.E.M., and Biegstraaten, M. (2015). The quality of economic evaluations of ultra-orphan drugs in Europe – a systematic review. *Orphanet Journal of Rare Diseases* 10: 1-12. doi: 10.1186/s13023-015-0305-y
- Shaaltiel, Y., Bartfeld, D., Hashmueli, S., et al (2007). Production of glucocerebrosidase with terminal mannose glycans for enzyme replacement therapy of Gaucher's disease using a plant cell system. *Plant Biotechnology Journal* 5: 579-590. doi: <https://doi.org/10.1111/j.1467-7652.2007.00263.x>
- Shen, J.-S., Busch, A., Day, T.S., et al (2016). Mannose receptor-mediated delivery of moss-made  $\alpha$ -galactosidase A efficiently corrects enzyme deficiency in Fabry mice. *Journal of Inherited Metabolic Disease* 39: 293-303. doi: <https://doi.org/10.1007/s10545-015-9886-9>



- Su, J., Sherman, A., Doerfler, P.A., et al (2015). Oral delivery of Acid Alpha Glucosidase epitopes expressed in plant chloroplasts suppresses antibody formation in treatment of Pompe mice. *Plant Biotechnology Journal* 13: 1023-1032. doi: <https://doi.org/10.1111/pbi.12413>
- Sweeley, C.C., B.K. (1963). Fabry's disease: classification as a sphingolipidosis and partial characterization of a novel glycolipid. *J. Biol. Chem.* 238: 3148-3150.
- Tajima, Y., Kawashima, I., Tsukimura, T., et al (2009). Use of a Modified  $\alpha$ -N-Acetylgalactosaminidase in the Development of Enzyme Replacement Therapy for Fabry Disease. *The American Journal of Human Genetics* 85, 569-580.
- Tomasic, I.B., Metcalf, M.C., Guce, A.I., et al (2010). Interconversion of the Specificities of Human Lysosomal Enzymes Associated with Fabry and Schindler Diseases. *The Journal of Biological Chemistry* 285: 21560-21566. doi: 10.1074/jbc.M110.118588
- Van Breemen, M.J., Rombach, S.M., Dekker, N., Poorthuis, B.J., Linthorst, et al (2011). Reduction of elevated plasma globotriaosylsphingosine in patients with classic Fabry disease following enzyme replacement therapy. *Biochimica et Biophysica Acta (BBA) - Molecular Basis of Disease* 1812: 70-76. doi: 10.1016/j.bbadis.2010.09.007
- Van Den Hout, H., Reuser, A.J.J., Vulto, A.G., et al (2000). Recombinant human  $\alpha$ -glucosidase from rabbit milk in Pompe patients. *The Lancet* 356: 397-398. doi: [https://doi.org/10.1016/S0140-6736\(00\)02533-2](https://doi.org/10.1016/S0140-6736(00)02533-2)
- Van Dussen, L., Zimran, A., Akkerman, E.M., Aerts, J.M.F.G., et al (2013). Taliglucerase alfa leads to favorable bone marrow responses in patients with type I Gaucher disease. *Blood Cells, Molecules, and Diseases* 50: 206-211. doi: <https://doi.org/10.1016/j.bcmd.2012.11.001>
- Voinnet, O., Rivas, S., Mesttre, P., and Baulcombe, D. (2003). An enhanced transient expression system in plants based on suppression of gene silencing by the p19 protein of tomato bushy stunt virus. *Plant J* 33: 949 - 956. doi: <https://doi.org/10.1046/j.1365-313X.2003.01676.x>
- Westerhof, L.B., Wilbers, R.H., Roosien, J., et al (2012). 3D domain swapping causes extensive multimerisation of human interleukin-10 when expressed in planta. *PLoS one* 7: e46460. doi: 10.1371/journal.pone.0046460
- Westerhof, L.B., Wilbers, R.H.P., Van Raaij, D.R., et al (2014). Monomeric IgA can be produced in planta as efficient as IgG, yet receives different N-glycans. *Plant Biotechnology Journal* 12:1333-1342. doi: <https://doi.org/10.1111/pbi.12251>
- Wilbers, R.H.P., Westerhof, L.B., Reuter, L.J., et al (2016). The N-glycan on Asn54 affects the atypical N-glycan composition of plant-produced interleukin-22, but does not influence its activity. *Plant Biotechnology Journal* 14: 670-681. doi: <https://doi.org/10.1111/pbi.12414>
- Willems, L.I., Beenakker, T.J.M., Murray, B., et al (2014). Potent and Selective Activity-Based Probes for GH27 Human Retaining  $\alpha$ -Galactosidases. *Journal of the*

American Chemical Society 136:11622-11625. doi:  
<https://doi.org/10.1021/ja507040n>

Witte, M.D., Kallemeijn, W.W., Aten, J., et al (2010). Ultrasensitive in situ visualization of active glucocerebrosidase molecules. *Nat Chem Biol* 6: 907-913. doi: <https://doi.org/10.1038/nchembio.466>

Yasuda, K., Chang, H.-H., Wu, H.-L., Ishii, S., and Fan, J.-Q. (2004). Efficient and rapid purification of recombinant human  $\alpha$ -galactosidase A by affinity column chromatography. *Protein Expression and Purification* 37: 499-506. <https://doi.org/10.1016/j.pep.2004.07.005>

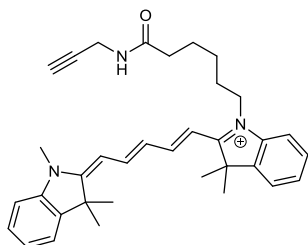
## Supplementary material

### Synthesis and characterization of activity-based probe $\alpha$ -galactopyranose-configured cyclophellitol aziridine tagged with fluorescent Cy-5.

#### Synthesis

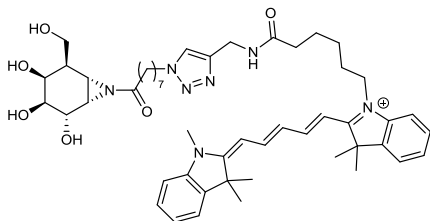
All chemicals were purchased from Acros, Sigma Aldrich, Biosolve, VWR, Fluka, Merck and Fisher Scientific and used as received unless stated otherwise. Dichloromethane (DCM), *N,N*-dimethylformamide (DMF) and toluene were stored over flame-dried 4 Å molecular sieves before use. Traces of water from reagents were removed by co-evaporation with toluene in reactions that require anhydrous conditions. All reactions were performed under an argon atmosphere unless stated otherwise. TLC analysis was conducted using Merck aluminium sheets (Silica gel 60 F<sub>254</sub>) with detection by UV absorption (254 nm), by spraying with a solution of (NH<sub>4</sub>)<sub>6</sub>Mo<sub>7</sub>O<sub>24</sub>·4H<sub>2</sub>O (25 g/L) and (NH<sub>4</sub>)<sub>4</sub>Ce(SO<sub>4</sub>)<sub>4</sub>·2H<sub>2</sub>O (10 g/L) in 10% sulfuric acid, a solution of KMnO<sub>4</sub> (20 g/L) and K<sub>2</sub>CO<sub>3</sub> (10 g/L) in water or ninhydrin (0.75 g/L), followed by charring at ~150 °C. Column chromatography was performed using Screening Device b.v. Silica Gel (particle size of 40 – 63 µm, pore diameter of 60 Å) in the indicated solvents. For reversed-phase HPLC purifications an Agilent Technologies 1200 series instrument equipped with a semiprep column (Gemini C18, 250x10 mm, 5 µm particle size, Phenomenex) was used. LC/MS analysis was performed on a Surveyor HPLC system (Thermo Finnigan) equipped with a C<sub>18</sub> column (Gemini, 4.6 mm x 50 mm, 5 µm particle size, Phenomenex), coupled to a LCQ Advantage Max (Thermo Finnigan) ion-trap spectrometer (ESI+). The applied buffers were H<sub>2</sub>O, MeCN and 1% aqueous TFA. <sup>1</sup>H NMR and <sup>13</sup>C NMR spectra were recorded on a Brüker AV-400 (400 and 101 MHz respectively) or a Bruker AV-850 (850 and 214 MHz respectively) spectrometer in the given solvent. Chemical shifts are given in ppm ( $\delta$ ) relative to the residual solvent peak as internal standard. Coupling constants are given in Hz. High-resolution mass spectrometry (HRMS) analysis was performed with a LTQ Orbitrap mass spectrometer (Thermo Finnigan), equipped with an electrospray ion source in positive mode (source voltage 3.5 kV, sheath gas flow 10 mL/min, capillary temperature 250 °C) with resolution  $R = 60000$  at  $m/z$  400 (mass range  $m/z = 150$ – $2000$ ) and dioctyl phthalate ( $m/z = 391.28428$ ) as a “lock mass”. The high-resolution mass spectrometer was calibrated prior to measurements with a calibration mixture (Thermo Finnigan).

**2-[5-(1,3,3-Trimethyl-2,3-dihydro-1H-indol-2-ylidene)-1,3-pentadi-enyl]-3,3-dimethyl-1-(6-oxo-6-(prop-2-yn-1-ylamino)hexy)-3H-indolium (1)**



Cy5 OSu ester **1** (Kvach et al., 2008) (3.10 g, 5.0 mmol) and propargylamine (0.35 mL, 5.5 mmol) were dissolved in CH<sub>2</sub>Cl<sub>2</sub> (25 mL). After addition of Et<sub>3</sub>N (6.0 mmol, 0.84 mL), the reaction mixture was stirred for 2.5 h at room temperature. The reaction mixture was concentrated *in vacuo* and purification by column chromatography (1% MeOH in CH<sub>2</sub>Cl<sub>2</sub> → 4% MeOH in CH<sub>2</sub>Cl<sub>2</sub>) gave Cy5-alkyne **2** (690 mg, 1.24 mmol, 25%) as a dark-blue foam. <sup>1</sup>H NMR (400 MHz, MeOD): δ 8.26 (t, *J* = 13.1 Hz, 2H), 7.48 (d, *J* = 7.4 Hz, 2H), 7.44 – 7.35 (m, 2H), 7.29 (d, *J* = 7.9 Hz, 2H), 7.24 (t, *J* = 7.4 Hz, 2H), 6.71 (t, *J* = 12.4 Hz, 1H), 6.31 (t, *J* = 13.5 Hz, 2H), 4.12 (t, *J* = 7.4 Hz, 2H), 3.92 (d, *J* = 2.5 Hz, 2H), 3.63 (s, 3H), 2.57 (t, *J* = 2.6 Hz, 1H), 2.23 (t, *J* = 7.3 Hz, 2H), 1.84 (dt, *J* = 14.9, 6.3 Hz, 2H), 1.75 – 1.66 (m, 14H), 1.51 – 1.46 (m, 2H). <sup>13</sup>C NMR (101 MHz, MeOD): δ 175.4, 175.2, 174.5, 155.4, 144.2, 143.5, 142.6, 142.5, 129.7, 129.6, 126.8, 126.1, 123.4, 123.3, 112.0, 111.8, 104.4, 55.9, 50.5, 44.8, 36.4, 31.8, 29.4, 28.2, 28.0, 27.9, 27.3, 26.4, 26.3. HRMS: Calculated for [C<sub>35</sub>H<sub>42</sub>N<sub>3</sub>O]<sup>+</sup> 520.33224, found 520.33172.

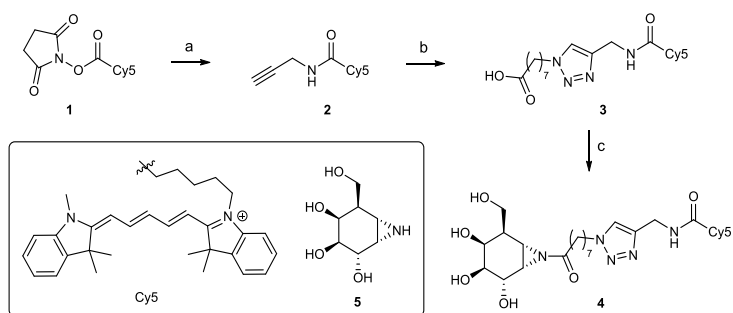
**Cy5-α-aziridine (4)**



To a solution of 8-azidooctanoic acid (David et al., 2003) (94 mg, 0.50 mmol) in DMF (4 mL) was added Cy5-alkyne **2** (282 mg, 0.50 mmol) at room temperature. After addition of copper (II)sulfate pentahydrate (500 μL, 1 M in H<sub>2</sub>O) and sodium ascorbate (700 μL, 1 M in H<sub>2</sub>O) the reaction mixture was heated up to 80 °C and stirred overnight. The reaction mixture was concentrated *in vacuo*, redissolved in CH<sub>2</sub>Cl<sub>2</sub> and washed with HCl (0.1 M, 3 x) and brine (1 x). The

organic layer was dried over  $\text{MgSO}_4$  and concentrated *in vacuo* to obtain Cy5 acid **3** (0.43 mmol, 0.32 g, 86%) which was used without further purification. LC/MS analysis:  $R_t$  7.27 min linear gradient 10%  $\rightarrow$  90% B in 12.5 min,  $m/z$  705.33  $[\text{M}]^+$ . HRMS: calculated for  $[\text{C}_{43}\text{H}_{57}\text{N}_6\text{O}_3]^+$  705.44867, found 705.44892. To a solution of crude Cy5 acid **3** (111 mg, 0.12 mmol) in DMF (0.8 mL) was added EEDQ (30 mg, 0.12 mmol) and stirred for 2 h at room temperature to obtain a pre-activated mixed anhydride solution. Aziridine **5** (17.4 mg, 0.1 mmol) was dissolved in DMF (0.4 mL) and pre-activated mixed anhydride solution (0.5 eq.) was added at 0 °C. After stirring for 30 min additional pre-activated mixed anhydride solution (0.5 eq.) was added. The reaction mixture was stirred for 30 min after which additional EEDQ (25 mg, 0.10 mmol) was added. After stirring overnight at 4 °C, the reaction mixture was quenched with MeOH at 0 °C and concentrated *in vacuo*. Purification by semi preparative reversed phase HPLC at neutral conditions (A: 50 mM  $\text{NH}_4\text{HCO}_3$  in  $\text{H}_2\text{O}$ , B: MeCN; linear gradient: 44%  $\rightarrow$  50% B in 12 min) gave compound **4** (4.39 mg, 4.88  $\mu\text{mol}$ , 5%) as a blue powder. LC/MS analysis:  $R_t$  6.13 min and 6.37 min, linear gradient 10%  $\rightarrow$  90% B in 12.5 min,  $m/z$  862.40  $[\text{M}]^+$ .  $^1\text{H}$  NMR (850 MHz, MeOD):  $\delta$  8.24 (td,  $J = 13.2, 3.5$  Hz, 2H), 7.84 (d,  $J = 4.7$  Hz, 1H), 7.49 (d,  $J = 7.3$  Hz, 2H), 7.44 – 7.39 (m, 2H), 7.32 – 7.24 (m, 4H), 6.62 (t,  $J = 12.3$  Hz, 1H), 6.30 – 6.25 (m, 2H), 4.41 (d,  $J = 7.2$  Hz, 2H), 4.38 – 4.34 (m, 2H), 4.11 – 4.06 (m, 3H), 3.87 – 3.84 (m, 1H), 3.63 (s, 3H), 3.59 – 3.55 (m, 2H), 3.53 (dd,  $J = 10.7, 6.3$  Hz, 1H), 3.44 (dd,  $J = 10.7, 6.0$  Hz, 1H), 3.36 (dd,  $J = 8.9, 1.9$  Hz, 1H), 2.95 (dd,  $J = 6.0, 4.0$  Hz, 1H), 2.60 (d,  $J = 6.0$  Hz, 1H), 2.25 (t,  $J = 7.3$  Hz, 2H), 2.01 (td,  $J = 7.4, 3.8$  Hz, 1H), 1.88 – 1.86 (m, 2H), 1.84 – 1.79 (m, 2H), 1.74 – 1.71 (m, 13H), 1.62 – 1.55 (m, 2H), 1.48 – 1.45 (m, 2H), 1.36 – 1.27 (m, 6H).  $^{13}\text{C}$  NMR (214 MHz, MeOD):  $\delta$  187.2, 174.3, 174.0, 173.2, 154.1, 154.0, 144.7, 142.8, 142.1, 141.2, 141.1, 128.3, 128.3, 125.2, 124.9, 124.8, 122.7, 122.0, 121.8, 110.6, 110.4, 103.0, 102.8, 72.9, 71.7, 68.1, 64.2, 61.4, 61.4, 49.7, 43.3, 43.1, 41.8, 38.0, 35.0, 34.2, 29.7, 28.7, 28.5, 28.2, 26.7, 26.5, 26.4, 25.9, 25.8, 24.9. HRMS: calculated for  $[\text{C}_{50}\text{H}_{68}\text{N}_7\text{O}_6]^+$  863.53038, found 863.52566.

The synthetic strategy towards  $\alpha$ -galactopyranose-configured cyclophellitol aziridine ABP **4** is depicted in Scheme 1. It was envisioned that coupling of Cy5-functionalized spacer **3** with reported aziridine **5** (Willems et al., 2014) using 2-ethoxy-1-ethoxycarbonyl-1,2-dihydroquinoline (EEDQ) as the coupling reagent, would result in ABP **4**. Hence, Cy5-functionalized spacer **3** was synthesized in 2 steps from Cy5-OSu ester **1** (Kvach et al., 2008). Propargylamine was reacted with Cy5-OSu ester **1** to obtain compound **2** with an alkyne moiety. Copper(I)-catalyzed click reaction of **2** with 8-azidooctanoic acid gave Cy5-functionalized spacer **3**, which in turn was coupled to aziridine **5** to obtain ABP **4**.



**Scheme 1. Overview of synthesis.** Reagent and conditions: a) propargylamine,  $\text{Et}_3\text{N}$ ,  $\text{CH}_2\text{Cl}_2$ , 2.5 h, room temperature, 25%; b) 8-azido-octanoic acid,  $\text{CuSO}_4 \cdot 5\text{H}_2\text{O}$ , sodium ascorbate, DMF, 80 °C, overnight; c) **5** (Willems et al., 2014), EEDQ, 0 °C to 4 °C, overnight, DMF, 5% over 2 steps.

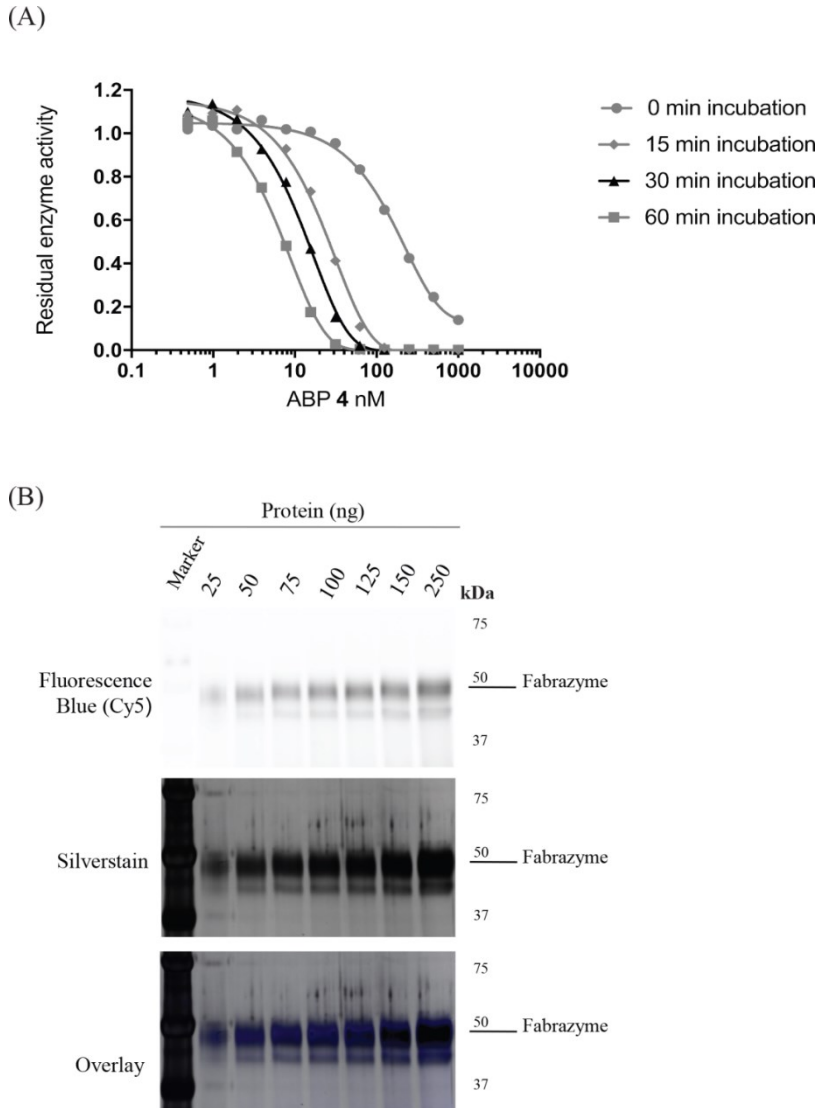


**Figure S1. Characterization of ABP.** (A) Inhibition of 4MU- $\alpha$ -GAL activity of Fabrazyme, after incubation with different ABP concentrations for different time periods. (B) In vitro labeling of human recombinant  $\alpha$ -GAL, Fabrazyme.

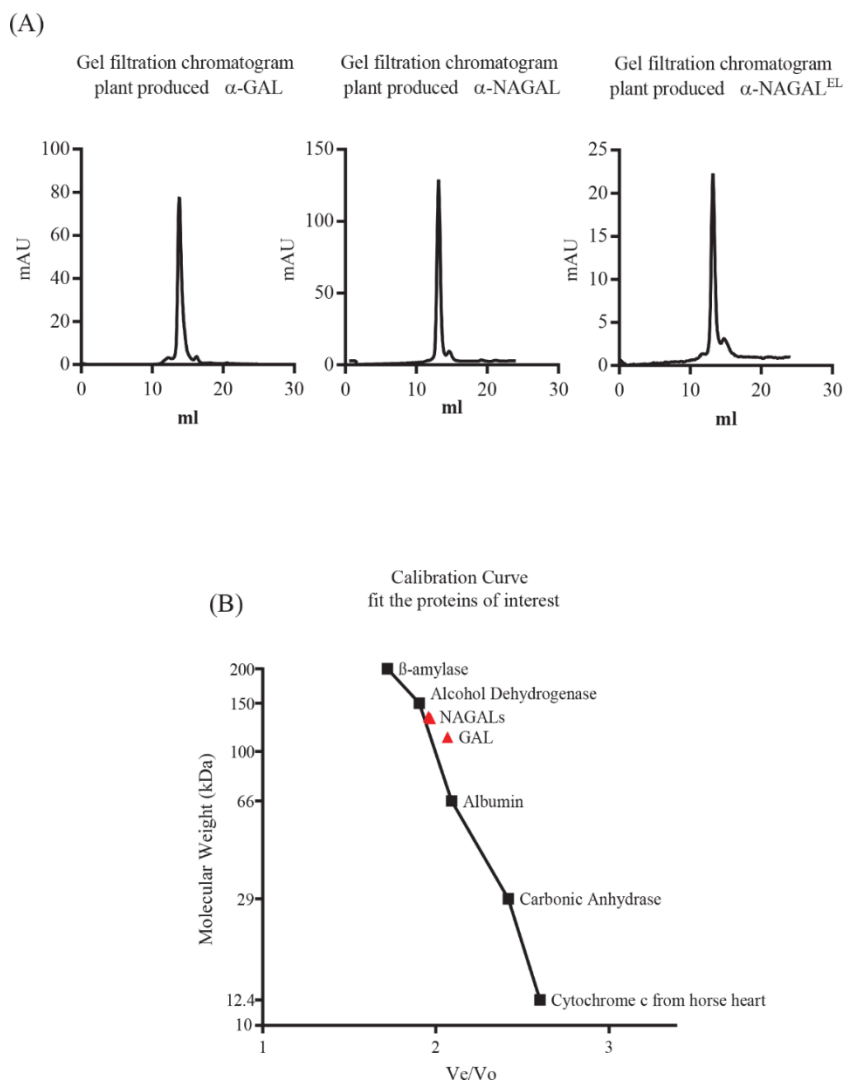


**Figure S2. Gel filtration chromatograms of plant produced enzymes and calibration curve. (A)** Chromatograms of all recombinant  $\alpha$ -galactosidases after their application in Superdex™ 200 Increase 10/300 GL. **(B)** Gel filtration chromatography calibration curve of proteins with known molecular weight, fitting the results of the plant produced enzymes. Proteins used for the calibration curve were  $\beta$ -amylase, alcohol dehydrogenase, albumin, carbonic anhydrase, cytochrome c from horse heart and Dextran.



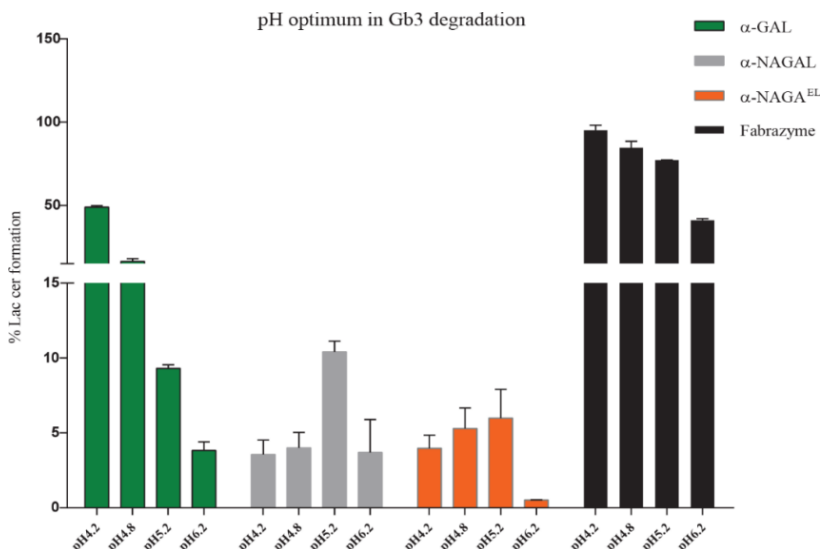


**Figure S3. pH optimum of recombinant galactosidases towards Gb3.** Different amounts of recombinant proteins,  $\alpha$ -NAGAL<sup>EL</sup>,  $\alpha$ -NAGAL,  $\alpha$ -GAL and Fabrazyme were incubated with 100pmol of C18:Gb3 overnight at 37 °C. For detection of Lac Cer formation, lipids extracted and subjected to LC-MS/MS.

## References

- David, O., Meester, W.J., Bieräugel, H., Schoemaker, H.E., Hiemstra, H. and van Maarseveen, J.H. (2003) Intramolecular Staudinger Ligation: A Powerful Ring- Closure Method To Form Medium- Sized Lactams. *Angewandte Chemie International Edition* 42, 4373-4375. doi: <https://doi.org/10.1002/anie.200351930>
- Kvach, M.V., Ustinov, A.V., Stepanova, I.A., Malakhov, A.D., Skorobogatyi, M.V., Shmanai, V.V. and Korshun, V.A. (2008) A Convenient Synthesis of Cyanine Dyes: Reagents for the Labeling of Biomolecules. *European Journal of Organic Chemistry* 2008, 2107-2117. doi: <https://doi.org/10.1002/ejoc.200701190>
- Willems, L.I., Beenakker, T.J.M., Murray, B., Gagestein, B., van den Elst, H., van Rijssel, E.R., Codée, J.D.C., Kallemeijn, W.W., Aerts, J.M.F.G., van der Marel, G.A. and Overkleeft, H.S. (2014) Synthesis of  $\alpha$ - and  $\beta$ -Galactopyranose-Configured Isomers of Cyclophellitol and Cyclophellitol Aziridine. *European Journal of Organic Chemistry* 2014, 6044-6056. doi: <https://doi.org/10.1002/ejoc.201402589>



# Chapter 4

---

*Nicotiana benthamiana*  
 $\alpha$ -galactosidase A1.1 can functionally  
complement human  
 $\alpha$ -galactosidase A deficiency associated  
with Fabry disease

---

*Kassiani Kytidou, Jules Beekwilder, Marta Artola, Eline van Meel, Ruud H.P. Wilbers, Geri F. Moolenaar, Nora Goosen, Patrick Voskamp, Bogdan I. Florea, Cornelis H. Hokke, Herman S. Overkleeft, Arjen Schots, Dirk Bosch, Navraj Pannu, Johannes M.F.G. Aerts.*

*This work has been published in: Journal of Biological Chemistry, (2018); 293 :10042-10058. doi: 10.1074/jbc.RA118.001774*



## Abstract

$\alpha$ -Galactosidases (EC 3.2.1.22) are retaining glycosidases that cleave terminal  $\alpha$ -linked galactose residues from glycoconjugate substrates.  $\alpha$ -Galactosidases take part in the turnover of cell wall-associated galactomannans in plants and in the lysosomal degradation of glycosphingolipids in animals. Deficiency of human  $\alpha$ -galactosidase A ( $\alpha$ -Gal A) causes Fabry disease (FD), a heritable, X-linked lysosomal storage disorder, characterized by accumulation of globotriaosylceramide (Gb3) and globotriaosylsphingosine (lyso-Gb3). Current management of FD involves enzyme-replacement therapy (ERT). An activity-based probe (ABP) covalently labeling the catalytic nucleophile of  $\alpha$ -Gal A has been previously designed to study  $\alpha$ -galactosidases for use in FD therapy. Here, we report that this ABP labels proteins in *Nicotiana benthamiana* leaf extracts, enabling the identification and biochemical characterization of an *N. benthamiana*  $\alpha$ -galactosidase we name here A1.1 (gene accession ID GJZM-1660). The transiently overexpressed and purified enzyme was a monomer lacking *N*-glycans and was active toward 4-methylumbelliferyl- $\alpha$ -D-galactopyranoside substrate ( $K_m = 0.17$  mM) over a broad pH range. A1.1 structural analysis by X-ray crystallography revealed marked similarities with human  $\alpha$ -Gal A, even including A1.1's ability to hydrolyze Gb3 and lyso-Gb3, which are not endogenous in plants. Of note, A1.1 uptake into FD fibroblasts reduced the elevated lyso-Gb3 levels in these cells, consistent with A1.1 delivery to lysosomes as revealed by confocal microscopy. The ease of production and the features of A1.1, such as stability over a broad pH range, combined with its capacity to degrade glycosphingolipid substrates, warrant further examination of its value as a potential therapeutic agent for ERT-based FD management.

## Introduction

$\alpha$ -Galactosidases (EC 3.2.1.22) occur widely in plants, animals, and microorganisms. Based on primary and secondary structures, they are classified into the three glycoside hydrolase families 4, 27, and 36. Family 27 contains mainly eukaryotic  $\alpha$ -galactosidases removing terminal  $\alpha$ -galactosyl moieties from glycoconjugates (Henrissat and Romeu 1995; Maranville and Zhu 2000; Carmi et al. 2003). Plant  $\alpha$ -galactosidases are so far known to participate in the catabolism of galactosyl-sucrose oligosaccharides, raffinose family of oligosaccharides, and cell wall galactomannans primarily during germination of seeds (Murali et al. 1994; Gao and Schaffer 1999; Kim et al. 2002; Carmi et al. 2003; Fujimoto et al. 2003). In man, a single  $\alpha$ -galactosidase occurs in lysosomes,  $\alpha$ -galactosidase A ( $\alpha$ -Gal A), and is primarily responsible for the metabolism of glycosphingolipids (Desnick 1995; Toumi et al. 2012).

A well-established classification of the plant enzymes is based on their pH optimum for enzymatic activity: acidic ones with broad pH optima from 4.5 to 6.5, and alkaline ones with pH optimum between 7.0 and 7.5 (Carchon and DeBruyne 1975; Carmi et al. 2003). These two classes of plant  $\alpha$ -galactosidases might differ in localization. The acidic  $\alpha$ -galactosidases most likely locate inside the vacuoles and apoplast, whereas alkaline  $\alpha$ -galactosidases act in the cytoplasm with a neutral pH, where they might catalyze removal of terminal galactose residues of substrates (Carchon and DeBruyne 1975; Carmi et al. 2003). One of the first plant  $\alpha$ -galactosidases to be cloned and biochemically characterized was an enzyme from coffee beans (Marraccini Pierre et al. 2005). It occurs as two different isoforms with molecular masses of 28 and 36.5 kDa showing slightly different pH optima (pH 5.3 and 6.3) and isoelectric points (Haibach et al. 1991; Ioannou et al. 2001). Similar heterogeneity of  $\alpha$ -galactosidases exists in other plant species, for example in rice (Kim et al. 2002). Interestingly, the acidic plant  $\alpha$ -galactosidases are most homologous to the human enzyme (Carmi et al. 2003). For example, rice  $\alpha$ -galactosidase shows 37% homology in amino acid sequence to human  $\alpha$ -Gal A (Fujimoto et al. 2003).

The human  $\alpha$ -Gal A enzyme is able to cleave  $\alpha$ -1,4-linked galactosyl moieties from glycosphingolipids such as globotriaosylceramide (Gb3; ceramide trihexoside) and galabiosylceramide and from blood groups B, B1, and P1 antigens. The hydrolase is encoded by the *GLA* gene (gene ID, 2717) at locus Xq22 (Ioannou et al. 2001). Its mature form lacking the signal sequence contains 398 amino acids with three *N*-glycans, naturally forming homodimers (Hamers et al. 1977; Bishop et al. 1988; Ioannou et al.

2001; Schiffmann et al. 2001). Mannose 6-phosphate moieties (Man-6-P) on the three *N*-linked glycans of  $\alpha$ -Gal A mediate the transport of newly formed enzyme to lysosomes by Man-6-P receptors (MPRs). Alternative sorting via the mannose receptor pathway was suggested by Sakuraba *et al.* (Sakuraba et al. 2005) and Shen *et al.* (Shen et al. 2016).

Dysfunction or absence of  $\alpha$ -Gal A leads to Fabry disease (FD), an X-linked lysosomal disorder characterized by accumulation of glycosphingolipids with terminal galactosyl moieties in tissues and body fluids of FD patients (Charles C. Sweeley and Bernard Klionsky 1963; Desnick 1995). The classic manifestation of FD in males involves development of acroparasthesias, corneal clouding, and neuropathic pain followed by later-onset renal and cardiac disease and strokes. Female carriers may develop an attenuated disease. In so-called atypical manifestations of FD, associated with missense mutations in  $\alpha$ -Gal A, pathology is to a single organ like heart or kidney and only develops late in life (Desnick 1995).

Enzyme-replacement therapy (ERT) with an MPR-targeted recombinant enzyme is used to treat FD (Schiffmann et al. 2001; Eng et al. 2007). Two therapeutic enzymes (agalsidase  $\alpha$ , Replagal®, and agalsidase  $\beta$ , Fabrazyme®) produced in mammalian cells are in use, and a plant-produced enzyme is being developed (Sakuraba et al. 2005; Kizhner et al. 2015). The efficacy of present ERT interventions is considered to be poor (Arends et al. 2017). Unfortunately, most male FD patients lack the  $\alpha$ -Gal A protein and consequently develop neutralizing antibodies against the therapeutic recombinant enzymes that might contribute to the noted poor responses to current treatments (Linthorst et al. 2004). Indeed, it was recently reported that compared with agalsidase inhibition-negative men, agalsidase inhibition-positive men showed greater left ventricular mass and substantially lower renal function (Lenders and Brand 2018). Additionally, these patients presented more often with symptoms such as diarrhea, fatigue, and neuropathic pain. Despite the lack of residual  $\alpha$ -Gal A, even in classic male FD patients, Gb3 accumulation is leveling with age. In Fabry patients, accumulating Gb3 is alternatively metabolized in lysosomes by acid ceramidase to globotriaosylsphingosine (lyso-Gb3) (Ferraz et al. 2016). In plasma of male FD patients and mice, lyso-Gb3 is several hundred-fold elevated, an abnormality that can be exploited for diagnosis and monitoring of disease progression and therapeutic correction (Aerts et al. 2008; Gold et al. 2013; Mirzaian et al. 2016, 2017). Excessive lyso-Gb3 is toxic for nociceptive neurons and podocytes, which might explain the development of neuropathic pain and renal failure in FD patients (Choi et al. 2015;

Sanchez-Niño et al. 2015). Again, the formation of neutralizing antibodies in male FD patients receiving ERT is reported to impair reduction in plasma lyso-Gb3 (Linthorst et al. 2004).

Recently, novel chemical tools have been developed to study different retaining glycosidases, including  $\alpha$ -galactosidases (Witte et al. 2011; Willems et al. 2014a). These activity-based probes (ABPs) are mechanism-based irreversible inhibitors functionalized with a bio-orthogonal tag such as a fluorophore or biotin. The first of these, ABPs, was developed for retaining  $\beta$ -glucosidases such as the human lysosomal glucocerebrosidase (GBA). The natural glucosyl-configured suicide inhibitor cyclophellitol covalently binds the catalytic nucleophile residue, Glu-340, in the enzymatic pocket of GBA (Witte et al. 2010). Equipped with a fluorescent reporter, the C-6 functionalized cyclophellitol permits specific and sensitive visualization of active enzyme molecules. Their amphiphilic nature renders the fluorescent ABPs membrane-permeable and allows *in situ* detection of active glucocerebrosidase in cells and organisms. Subsequently, cyclophellitol aziridine-type probes were developed to label, again in a mechanism-based manner, a broad range of  $\beta$ -glucosidases (Kallemeijn et al. 2014, 2017). Next, the approach was extended to other retaining glycosidases by variation of the cyclophellitol configuration, yielding ABPs for  $\alpha$ -galactosidases,  $\beta$ -galactosidases,  $\alpha$ -fucosidases, and  $\beta$ -glucuronidases (Willems et al. 2014b, a; Jiang et al. 2015; Wu et al. 2017). Equipping the cyclophellitol scaffold with a biotin allows streptavidin-mediated enrichment and subsequent chemical proteomics experiments using LC-MS/MS. The successful application of biotin-tagged ABPs in proteomics profiling of  $\beta$ -glucosidases from different plant species was demonstrated (Chandrasekar et al. 2014). A potent fluorescent  $\alpha$ -galactosyl-configured cyclophellitol aziridine ABP was developed and shown to label human  $\alpha$ -Gal A as well as  $\alpha$ -Gal B, the homologous N-acetyl galactosaminidase arisen by a gene duplication (Willems et al. 2014a).

In this study, we used fluorescent  $\alpha$ -galactosyl-configured cyclophellitol-aziridine ABPs and synthesized a biotinylated cyclophellitol-aziridine ABP to search for  $\alpha$ -galactosidases in *Nicotiana benthamiana*. With these tools, we were able to identify an abundant apoplast  $\alpha$ -galactosidase. We successfully cloned the gene and transiently overexpressed the protein, which we named A1.1, in *N. benthamiana* leaves. The recombinant enzyme was purified, crystallized, and biochemically characterized. We here report on the outcome of the investigation, including a comparison of the plant  $\alpha$ -galactosidase with the human enzyme, which is deficient in FD patients.



## Results

### Screening for $\alpha$ -galactosidases in *N. benthamiana* leaf extracts and apoplast fractions.

*N. benthamiana* leaf extracts and apoplast samples thereof were prepared and examined for  $\alpha$ -galactosidase activity using 4-methylumbelliferyl- $\alpha$ -D-galactose (4MU- $\alpha$ -Gal) as substrate. Enzyme activity, with a broad pH optimum of 5.0 – 6.7, was detected in both samples (Fig. 1A). Next, we incubated the leaf and apoplast samples with Cy5-functionalized TB474 ABP at different pH values. In the case of the leaf extract, Cy5-ABP-labeled proteins with apparent molecular mass of ~39 and 45 kDa were detected (Fig. 1B). The apoplast fraction contained mainly the ~39-kDa labeled protein (Fig. 1B). To assess whether the plant  $\alpha$ -galactosidases of interest are glycosylated, their binding to concanavalin A (ConA)-Sepharose beads was examined (Fig. 1, C and D). After incubation of samples with the lectin beads, ABP labeling and 4MU- $\alpha$ -Gal activities were performed. The ~39-kDa protein did not bind to the lectin beads, in contrast to the ~45 kDa protein (Fig. 1C). Approximately 50–55% of the 45-kDa protein is bound to the lectin beads, as judged by quantification of the band intensity of Fig. 1C. This band corresponds to 5–10% of the total 4-MU- $\alpha$ -Gal activity, suggesting that the 45-Da protein is not as active as the 39 kDa protein. More than 80% of the total 39-kDa labeled protein in both lysate and apoplast fractions was found in the unbound

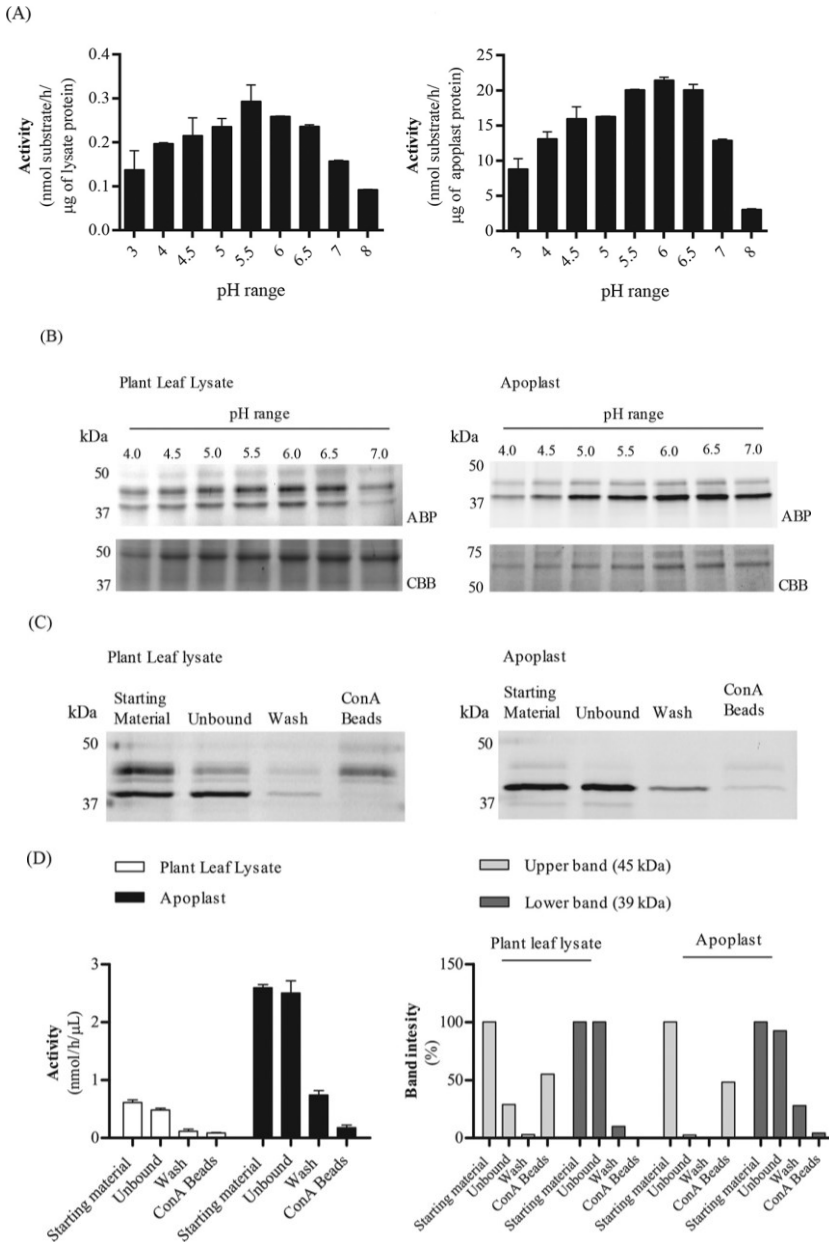


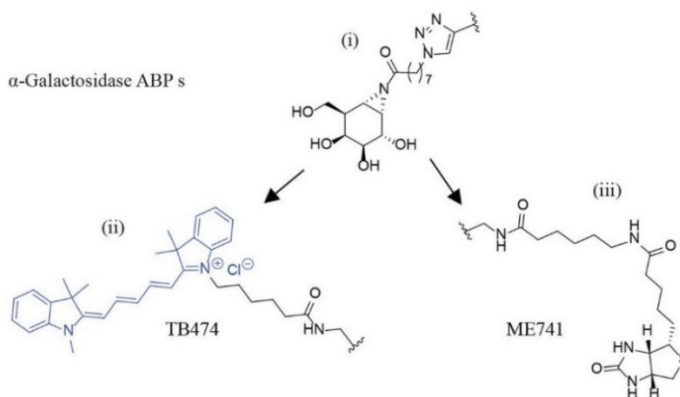
**Figure 1. Screening for  $\alpha$ -galactosidases in *N. benthamiana*.** Plant leaf lysates and apoplast samples were tested on their  $\alpha$ -galactosidase activity via 4MU-Gal assays and ABP *in vitro* labeling, following in-gel detection of the labeled proteins. A, 4MU- $\alpha$ -Gal activities present in plant leaf lysates and apoplast samples were first examined at different pH values of 3–8. ( $n=2$ , error bars indicate mean  $\pm$  S.D.) B, 45  $\mu$ g of plant leaf lysate and 12  $\mu$ g of apoplast sample were incubated with 0.25  $\mu$ M TB474 for 30 min at pH 4–7 at room temperature. Labeled proteins were detected via in-gel fluorescent scanning (ABP), and the gels were stained with Coomassie Brilliant Blue (CBB) to show equal total protein loading. C, plant leaf lysates and

apoplast samples were incubated with ConA- Sepharose beads for 2h at 4 °C. After incubation, the samples were centrifuged, and different fractions were tested for  $\alpha$ -galactosidase activity via ABP labeling and (*D, left panel*) 4MU- $\alpha$ -Gal assays. ( $n = 2$ , error bars indicate mean  $\pm$  S.D.) In addition, *D, right panel*, quantification of the band intensity of C is presented. Samples tested: *starting material* = sample prior to ConA-Sepharose bead incubation, containing all proteins. *Unbound* = supernatant after incubation with the beads and centrifugation. This sample contains all material not bound to the beads. *Wash* = wash of the beads. *Beads* = pellet after incubation with the beads and centrifugation, containing the proteins attached to the ConA-Sepharose beads.

### Identification of potential *N. benthamiana* $\alpha$ -galactosidases.

Newly designed biotinylated ABP ME741 (Fig. 2A) was found to completely compete labeling of plant  $\alpha$ -galactosidase in the apoplast fraction and leaf extracts by the Cy5-TB474 ABP (Fig. 2B). Conversely, labeling of plant  $\alpha$ -galactosidase by biotinylated ME741 (visualized by Western blotting with streptavidin- HRP) is blocked by prior incubation with TB474 ABP. Thus, both probes recognize the same  $\alpha$ -galactosidases. Next, we conducted large-scale pull downs of the  $\alpha$ -galactosidases present in leaf and apoplast samples using biotinylated ME741. After the pulldown, the target proteins were bound to streptavidin beads following bead tryptic digestion. Tryptic peptides were analyzed by nanoscale LC coupled to tandem MS (nano-LC-MS/MS) (Jiang et al. 2016). Peak lists were then searched against the Swiss-Prot (version June, 2017) database, and the identified peptides were manually curated. In this manner, peptides from known, well-annotated plant  $\alpha$ -galactosidases, similar in sequence to potential *N. benthamiana*  $\alpha$ -galactosidases, were identified (Table S1).

(A)



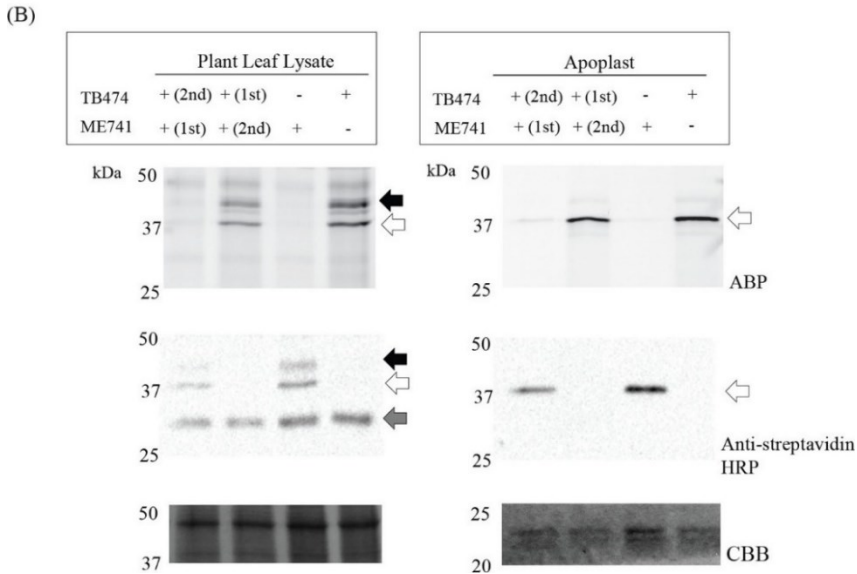


**Figure 2. Pulldown of plant  $\alpha$ -galactosidases using ME741 and their identification by proteomics.**

A, i,  $\alpha$ -galactosidase-configured aziridine scaffold; ii, Cy5 ABP, TB474; iii, biotin ABP, ME741. B, to prove that the same  $\alpha$ -galactosidases are recognized by both ABPs, ME741 and TB474, competition experiments were performed.  $\alpha$ -Galactosidases present in apoplast and plant leaf lysates were incubated with 0.25  $\mu$ M ME741, at pH 5.5, for 30 min at room temperature, with or without subsequent incubation with 0.25  $\mu$ M TB474, under the same conditions. Similarly, the samples were incubated first with TB474 and then with ME741. The labeled proteins were detected via in-gel fluorescent scanning and Western blot analysis using streptavidin-HRP (dilution 1:4000). The blot was then stained with CBB to show equal protein loading. The black arrow indicates the 45-kDa band; the open arrow indicates the 29-kDa protein, and the gray arrow indicates unspecific biotinylated plant proteins.

The identified peptides belonged to *Coffea arabica*  $\alpha$ -galactosidase (protein accession code Q42656) and *Arabidopsis thaliana*  $\alpha$ -galactosidase 1 and 2 (protein accession codes Q9FT97 and Q8RX86, respectively). Next, we conducted alignment analysis of the cDNA sequence encoding for *C. arabica*  $\alpha$ -galactosidase, as it is a well-characterized protein, known not to be *N*-glycosylated, toward the cDNA sequence of *N. benthamiana* (Sol Genomics Network). Based on the alignment, we designed specific primers to amplify the gene encoding for that most similar to Coffee, *N. benthamiana*  $\alpha$ -galactosidase, which we named A1.1. An additional peptide search was then conducted, after the insertion to the Swiss-Prot database of this new potential *N. benthamiana* enzyme, and the results were even more prominent (Table S2). We could identify more peptides, with better scores and higher protein coverage, indicating that this is the protein we were looking for and not the homologues from the other organisms.

### ***N. benthamiana* A1.1 purification and characterization**

To verify that A1.1 is truly an active  $\alpha$ -galactosidase, we transiently overexpressed the enzyme via the *Agrobacterium tumefaciens* infiltration of *N. benthamiana* leaves. The p19 RNAi silencing inhibitor was used to ensure optimum protein expression levels (Wilbers et al. 2017). Leaves were harvested at different days post-infiltration (dpi), and A1.1 expression in the total leaf as well as in apoplast fluid was detected by 4MU- $\alpha$ -Gal activities, TB474 ABP labeling, and Coomassie Brilliant Blue staining of SDS-polyacrylamide gels (Fig. 3, *A* and *B*). Optimal starting materials for purification were apoplast fractions, collected at 4 dpi, showing the highest 4MU- $\alpha$ -Gal activity. The  $\alpha$ -galactosidase activity per  $\mu$ g of protein in apoplast fractions was 20 – 40-fold higher in the case of leaves overexpressing A1.1, as compared with those treated with empty vector or nontreated plant leaves. A1.1  $\alpha$ -galactosidase was purified to homogeneity in three purification steps with high recovery (>30%) (Table 1). The presence of the enzyme in fractions was monitored by enzymatic assay with 4MU- $\alpha$ -Gal substrate. As the first purification step, we used ConA column chromatography, collecting the unbound material (flow-through fraction). In this step, other  $\alpha$ -galactosidases were removed by binding to the lectin column. Next, cation-exchange chromatography was applied, resulting in a further modest purification (recovery 40%). Finally, the sample was subjected to gel-filtration chromatography, revealing that A1.1 behaves as monomer of about 30 kDa (Fig. S1). The final preparation of A1.1 was apparently pure as judged by SDS-PAGE analysis following silver staining of the gel (see Fig. 3*B* for an overview of the entire purification).

A1.1 seems not to carry *N*-glycosyl groups as demonstrated by the lack of effect of PNGase and EndoH on its molecular weight (Fig. 3*C*). The molecular weight of A1.1, in contrast to that of Fabrazyme, is not influenced after the endoglycanase treatments (Fig. 3*C*). Consistently, following incubation of A1.1 with PNGase A, no released *N*-glycans were detected by MALDI-TOF MS analysis (Fig. S2).

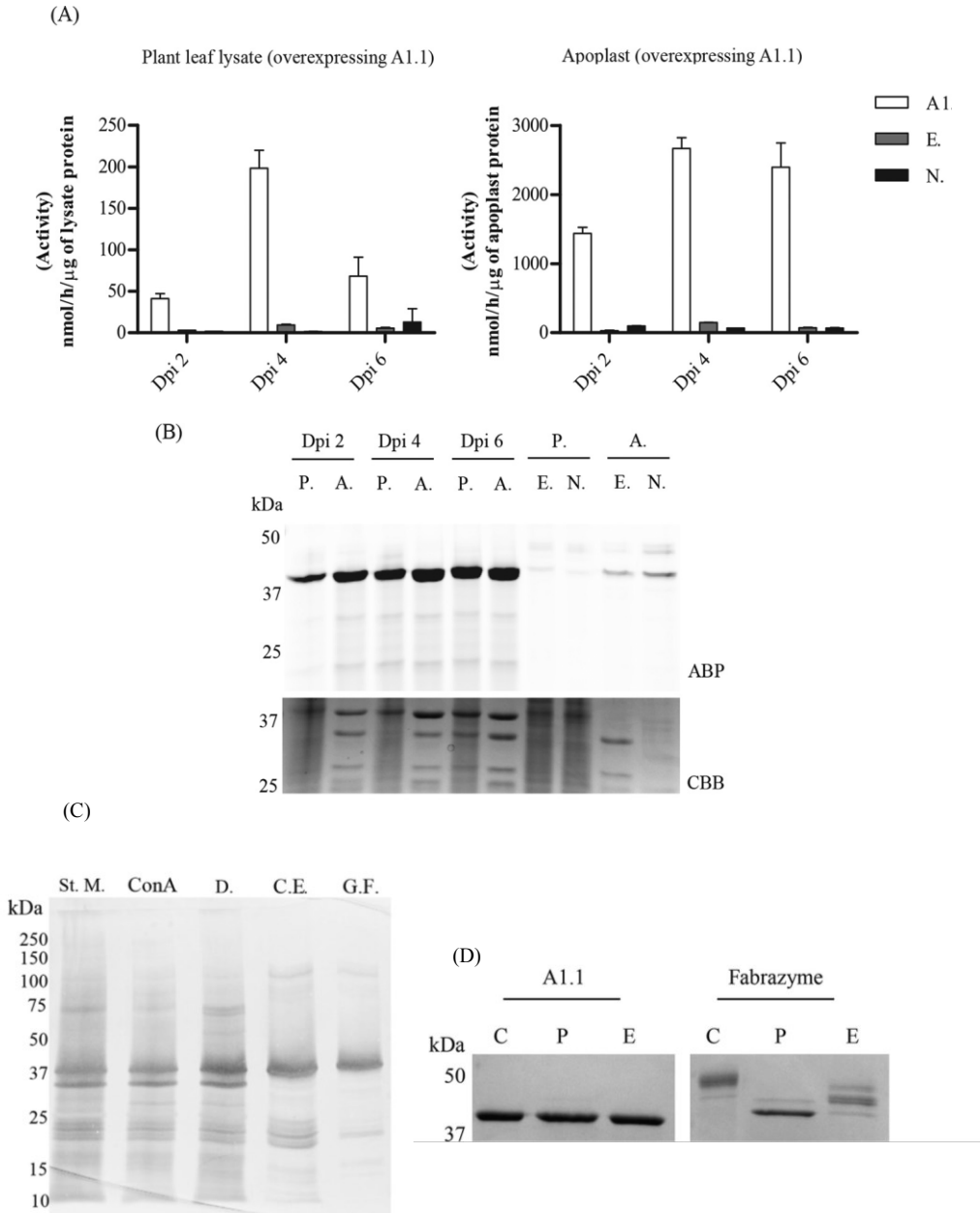


**Figure 3. Overexpression and biochemical characterization of the newly identified *N. benthamiana*  $\alpha$ -galactosidase, A1.1.** A, transient overexpression of A1.1 in *N. benthamiana* leaves via *A. tumefaciens* transformation assays. Infiltrated leaves and apoplast samples were harvested on different days post-infiltration (dpi): 2, 4, and 6. The expression levels of the enzyme were first tested via 4MU- $\alpha$ -Gal activities in lysates and apoplast fractions of different dpi. *n* = 2. (A1.1 = leaf overexpressing A1.1; E. = empty vector; N. = nontreated plant leaf.) B, next, the expression levels of active enzyme molecules were

tested via in-gel ABP labeling. CBB staining of the gels followed to ensure the presence of the overexpressed enzyme. (*P.* = plant lysate; *A.* = apoplast sample; *E.* = empty vector; *N.* = nontreated plant leaf.) C, purification overview. SDS-PAGE analysis following silver staining of fractions obtained during different purification steps. (*St. M.* = starting material; *ConA* = fraction not bound to concanavalin A column; *D.* = sample obtained after 48 h of dialysis; *C.E.* = pooled collected eluate from cation-exchange chromatography; *G.F.* = final pooled fraction obtained after gel filtration.) 2  $\mu$ g of total protein were loaded in each lane, except in *G.F.*, where 1  $\mu$ g was loaded. D, SDS-PAGE analysis following Coomassie Brilliant Blue staining of 1  $\mu$ g of pure A1.1 and Fabrazyme after treatment with PNGase F and EndoH (*C* = untreated pure enzyme; *P* = enzyme treated with PNGase F; *E* = enzyme treated with EndoH), shows that A1.1 is not likely *N*-glycosylated, whereas Fabrazyme is, due to the difference in molecular weight after treatment.

Table 1. Overview of A1.1 purification.

| Purification steps | Protein concentration (mg/mL) | Volume (mL) | Total protein (mg) | Total activity ( $\mu$ mol/h/mL) | Total specific activity ( $\mu$ mol/h/mg) | Purification fold | % Yield= Recovery activity |
|--------------------|-------------------------------|-------------|--------------------|----------------------------------|---|-------------------|----------------------------|
| Starting material  | 1.3                           | 20          | 26                 | 63338                            | 2436                                      | 1                 | 100                        |
| ConA               | 0.44                          | 45          | 20                 | 50171                            | 2534                                      | 1                 | 79                         |
| Dialysis           | 0.38                          | 45          | 17                 | 49550                            | 2905                                      | 1.2               | 78                         |
| Ion exchange       | 1.2                           | 4.5         | 5.4                | 25977                            | 4810                                      | 2                 | 41                         |
| Gel filtration     | 5                             | 0.6         | 3                  | 20879                            | 6959                                      | 2.9               | 33                         |

### Structural features of A1.1 $\alpha$ -galactosidase determined by crystallography

Pure *N. benthamiana* A1.1 was crystallized. The protein structure was determined at a resolution of 2.8 Å using the molecular replacement method with the rice  $\alpha$ -Gal A (PDB code 1UAS) as search model. The statistics data of the collection and refinement are listed in Table 2. The protein model is a monomer, consisting of 363 amino acids (not including the first 57 amino acid signal-peptide sequence) and being separated into two domains. The N-terminal domain or catalytic domain (1–278) contains a TIM ( $\beta/\alpha$ )<sub>8</sub>-barrel, a common motif among glycosidases (Fujimoto et al. 2003), and the C-terminal domain (279–363) contains eight  $\beta$ -strands forming a “Greek key” motif (Fig. 4A).

The active site of the enzyme is found by prediction as the final model obtained without a bound ligand, at the C-terminal end of the catalytic domain. Similar to other glycoside hydrolases of family 27, two aspartic acid residues (Asp-181 and Asp-236) were observed to serve as the catalytic amino acids, one acting as the nucleophile and the other as the acid/base, taking part in the double displacement reaction mechanism of  $\alpha$ -galactosidases (Guce et al. 2010). A1.1 is negatively charged at the site of its

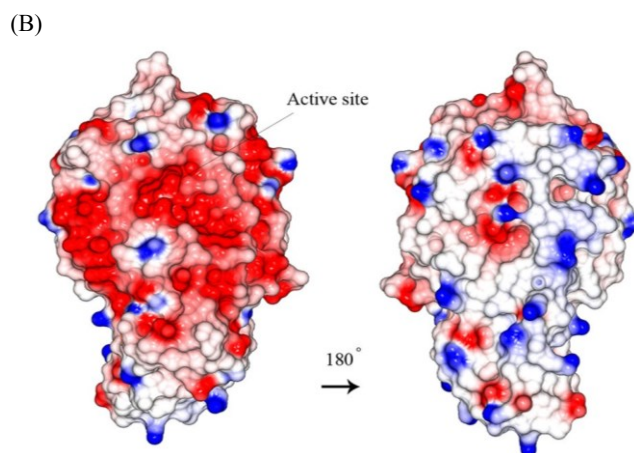
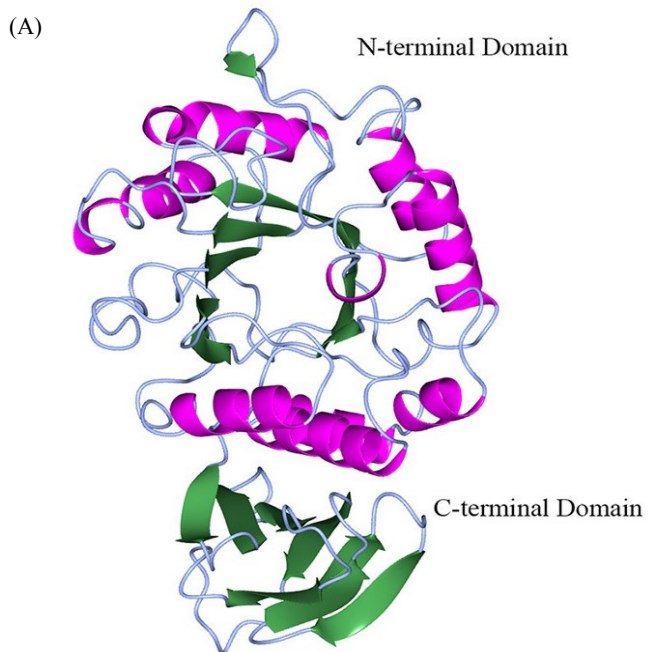
active site and more neutral at the opposite site (Fig. 4B). The pI of the enzyme is at around 5.32. Amino acid sequence alignment of A1.1, human (protein accession code P06280), rice (protein accession code Q9FXT4), and coffee (protein accession code Q42656)  $\alpha$ -Gals reveals great secondary structure identity of all enzymes (Fig. 4C). A1.1 share 42% amino acid identity with the human enzyme, showing overall highly conserved secondary structures at the catalytic domain and not as much at the C-terminal domain. No Asn-Xaa-(Ser/Thr/Cys) motifs are present in amino acid sequences of A1.1, revealing that the protein is most likely not *N*-glycosylated. In contrast, four potential *N*-glycosylation sites are present in human enzyme. A common amino acid sequence pattern (CEW, at positions 212–214 in Fig. 4C) occurs in all aligned galactosidases, as described previously by Motabar *et al.* (Motabar *et al.* 2010).

The overall structure of A1.1 is very similar to that of human (PDB code 3HG2)  $\alpha$ -Gal A, as visualized by the superimposed models, consistent with their 42% sequence identity (Fig. 4D, *left panel*). In addition, a closer look at the active site of both enzymes shows great conservation of the majority of the amino acids (Fig. 4D, *right panel*).

Table 2. Data collection and refinement statistics. PBD: 6F4C.

| Data collection and refinement statistics                      |  |
|--|--|
| Space group  | P 41 21 2                                      |
| Unit-cell parameters<br>a, b, c, $\alpha$ , $\beta$ , $\gamma$ | 74.04Å, 74.04Å, 133.31Å<br>90.00, 90.00, 90.00 |
| Resolution (Å)   | 25.00 2.80<br>24.77 2.80                       |
| % Data completeness<br>(in resolution range)                   | 98.4 (25.00-2.80)<br>99.9 (24.77-2.80)         |
| < I= $\sigma$ (I) >  | 2.53 (at 2.80Å)                                |
| Refinement program REFMAC 5.8.0158                             |  |
| R, Rfree   | 0.216, 0.287<br>0.225, 0.282                   |
| Rfree test set   | 486 reflections (5.30%)                        |
| F <sub>o</sub> ,F <sub>c</sub> correlation                     | 0.88   |
| Total number of atoms  | 2861   |
| Average B, all atoms (Å <sup>2</sup> )                         | 4.0  |
| Ramachandran plot (%)  |  |
| Preferred regions  | 96   |
| Allowed regions  | 3  |
| Outlayers  | 1  |





(C)

Nicotiana  
 1 10 20 30 40 50  
 Nicotiana .....MPPPIKLLMCCCLCGVTITTYARPPPNLIADSNSSSSSNAYIRRSLLSN  
 Rice MARASSSSPPSPRLLLLLLVAVAAATLPEAA..ALGNFTAESRGARWRSSRRARRAFEN  
 Coffee .....MVKSPGTEDYTRRSLLAN  
 Human .....MQLRNPELHLGCAALRFL.....VSWDIPGARALDN

Nicotiana  
 β1 α1 α2 η1 β2  
 60 70 80 90 100  
 Nicotiana GLGRFPQMGWSSWNHFAENIE.....EKMIREFADAMVITGLASITGYEYINIDDD  
 Rice GLGRFPQMGWSSWNHFPYGIN.....EQIIRRETADALVNTGLAKLGYVYVNEDDC  
 Coffee GLGRFPQMGWSSWNHFRNLD.....EKLIREFADAMVITGLAALGYKVINIDDD  
 Human GLARFPQMGWLHWRERFMCNLDQEQEPDSCISEKLFMRMELMVSEGWKDAEYELCIDDC

Nicotiana  
 TT α3 β3 TT  
 110 120 130 140 150 160  
 Nicotiana WAELNRDSQGNMVPKGSTFPSSGIKALAVYVHAKGLKGIYS DAGSQTCSNKMTGSLGHEE  
 Rice WAELNRDSQGNFVFNRTQTFPSGIKALADYVHAKGLKGIYS DAGSQTCSNKMPGSLDHEE  
 Coffee WAELNRDSQGNLVPKGSTFPSSGIKALADYVHAKGLKGIYS DAGTQCSKTMPSGLGHEE  
 Human WMAPQRDSQGRLOADPQRFPFGRQLANVYVHAKGLKGIYADVGNKTCAGFPFGSFGYYD

Nicotiana  
 α4 β4 α5 β5  
 170 180 190 200 210  
 Nicotiana QDAKTFASWGVYLYKYDNCNNEINR.SPKERYPIMSKALQNSGRALFYSICEWGD....D  
 Rice QDVKTFASWGVYLYKYDNCNDAGR.SVMERYTRMSNAMKTYGKNIFFSLCWEWGK....E  
 Coffee QDAKTFASWGVYLYKYDNCNNNNI.SPKERYPIMSKALQNSGRALFYSICEWGE....E  
 Human IDAQTFAWGVYLYKYDNCYCDSEINLADGYKHMSLALNRTGRSIVYS.CEWP LYMWFPQ

\*

Nicotiana  
 η2 β6 α6 η3 β7 TT  
 220 230 240 250 260 270  
 Nicotiana DPATFAWSSVGNWRITGDISDNWD SMTSRADM...NDKWA SYAGPGGWNDPDMLEVGN  
 Rice NPATFAWGRMGNSWRITGDIADNWG SMTSRAD E...NDQWAA SYAGPGGWNDPDMLEVGN  
 Coffee DPATFAWKEVGNWRITGDISDSSW SMTSRADM...NDKWA SYAGPGGWNDPDMLEVGN  
 Human KPNYFEIRQYCNHWRNFADIDSSW SIKSILD WTSFNQERIVD SYAGPGGWNDPDMLEVGN

\*

Nicotiana  
 α7 β8 η4 α8 α9 TT β9  
 280 290 300 310 320 330  
 Nicotiana GGMTTAEYRSHFSTWALAKAPLIIGCDIRSMDO TAEHTLSNKEVIAYNODKLGVOGKVKV  
 Rice GGMSEAEYRSHFSTWALAKAPLLIGCDVRSMSQTKNITLSNSEVIAYNODSLGVQGRKVKQ  
 Coffee GGMTTAEYRSHFSTWALAKAPLLIGCDIRSMGATFQLSNSEVIAYNODKLGVOGKVKV  
 Human EGLTWNQQTQMAIWAIAAPLFMSNDTRHISPAKALLQDKDVIAINODPLKQCGVQLR

Nicotiana  
 β10 β11 β12 β13 β14  
 340 350 360 370 380 390  
 Nicotiana QNGDLVWVAGPLSKRVAVLVLWNRSSSKADITAYWSDIGLDSSTVVDARDLWAHSTKGSV  
 Rice SDNGLVWVAGPLSNRNKAVLWNRSSSYQAITITAHWSNIGAGSVAVTARDLWAHSSFAA  
 Coffee TYGDLVWVAGPLSKRVAVLWNRSSSTAITITAYWSDVGLPSTAVVNRARDLWAHSTKESV  
 Human QGDNEVWVERPLSLAVAVAMINRQETGGPRSYTIAVASHGKGVYAC.....

Nicotiana  
 β15 β16  
 400 410  
 Nicotiana KGQISASTDSHDCRMVYITPKK.....  
 Rice QGQISASVAPHDCKMYVITPK.....  
 Coffee KGQISAAVDAHDSKMYVITPK.....  
 Human .....LNPACFITQLPKVRRKLGFEWTSRLRSHINPTGTVLLQLENTMQMSLKDLL

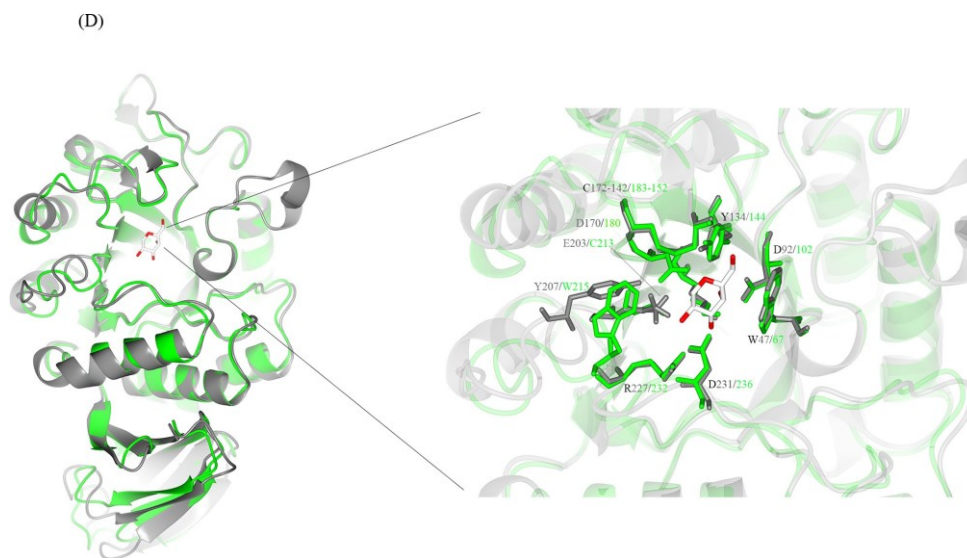


**Figure 4. Structural similarities of  $\alpha$ -galactosidases from different species.** *A*, stereo view of the ribbon model of A1.1 (PDB code 6F4C). Catalytic domain contains a  $(\beta/\alpha)_8$ -barrel. C-terminal domain forms a Greek key.  $\beta$ -Strands are represented in *green*;  $\alpha$ -helices are represented in *pink*; and loops are represented in *light blue*. *B*, electrostatic map of A1.1: *red* indicates the  $-$  charges; *blue* indicates the  $+$  charges. *C*, multiple amino acid sequence alignment of A1.1: human, rice, and coffee galactosidases. The sequence alignment showing structural details of A1.1 was achieved using ESPript3.0.  $\alpha$ -Helices are shown as *coils* labeled *a*;  $\beta$ -strands are shown as *arrows* labeled  $\beta$ , and  $\beta$ -turns are labeled *TT*. Identical residues are shown on a *red background*; conserved residues are shown in *red*, and conserved regions are shown as *blue boxes*. The catalytic residues are indicated with an *asterisk*. *D*, *right panel*, stereo view of the superimposed models of A1.1 with the human  $\alpha$ -galactosidase. 348 residues were aligned, having a root-mean-square deviation of 1.3358 Å of their C- $\alpha$  atoms. The A1.1 model (PDB code 6F4C) is shown in *green*; the human  $\alpha$ -Gal model (PDB code 3HG2) is shown in *gray*. The backbone of a modeled galactose molecule is shown in *white*, and its oxygen atoms are shown in *red*. *Left panel*, a closer look at the amino acids around the active site of both enzymes, presented as *fat bonds*.

### Catalytic features of A1.1

We first examined substrate specificity of pure A1.1 using artificial 4-MU- glycoside substrates (Table 3). The enzyme hydrolyzes with considerable affinity 4MU- $\alpha$ -Gal substrate but is inactive toward  $\beta$ -D-glucopyranoside,  $\beta$ -D-galactopyranoside,  $\alpha$ -D-mannopyranoside,  $\alpha$ -L-fucopyranoside, *N*-acetyl- $\alpha$ -D-galactosaminide, and *N*-acetyl- $\beta$ -D-glucosaminide. The pH optimum of A1.1 with 4MU- $\alpha$ -Gal substrate is broad, ranging from pH 5.0 to 6.5 (Fig. 5A). The apparent  $K_m$  with 4-MU- $\alpha$ -Gal is 0.17 mM and  $k_{cat}$  81 s<sup>-1</sup> (Fig. 5B). Comparable kinetic values are also obtained with Fabrazyme, although its pH optimum toward 4MU- $\alpha$ -Gal substrate is rather acidic at pH 4.5 (Fig. 5, A and B).

The structural resemblance of A1.1 with human  $\alpha$ -Gal A prompted us to examine its activity toward glycosphingolipid substrates. First, we tested the activity of A1.1 toward artificial NBD-labeled Gb3. A1.1 was found to convert NBD-Gb3 to NBD-lactosylceramide by removal of the terminal  $\alpha$ -linked galactose. The activity of A1.1 toward NBD-Gb3 is in several aspects comparable with that of Fabrazyme (recombinant human  $\alpha$ -Gal A). The pH optimum is similarly acidic at pH 4.5 (Fig. 5C). The affinity of A1.1 for NBD-Gb3 is high with an apparent  $K_m$  of 32  $\mu$ M, similar again to that of Fabrazyme. However, the  $k_{cat}$  value is  $\sim$ 4-fold lower than that of human  $\alpha$ -galactosidase (Fig. 5B).

Table 3. Activity of A1.1 towards different 4MU substrates.

| 4MU substrates                          | Activity (nmol/h/ $\mu$ g) |
|---|----------------------------|
| $\beta$ -D-glucopyranoside<br>pH 5.2    | 0                          |
| $\beta$ -D-glucopyranoside<br>pH 5.8    | 8                          |
| $\beta$ -D-glucopyranoside<br>pH 7      | 0                          |
| $\alpha$ -D-galactopyranoside<br>pH 4.6 | 905                        |
| $\alpha$ -D-galactopyranoside<br>pH 6   | 1645                       |
| $\beta$ -D-galactopyranoside            | 8                          |

Next, we tested natural glycosphingolipids as substrates. A1.1 degrades natural C18-Gb3 by converting it to C18-LacCer as measured by HPLC analysis (47). Its activity is again comparable with that of human enzyme: 96.3% of C18-Gb3 is converted to LacCer upon overnight incubation with 3  $\mu$ g of A1.1 at pH 4.5 *versus* 98.3% conversion with the same amount of Fabrazyme at the same condition. In addition, A1.1 hydrolases best this lipid substrate (C18-Gb3) again at acidic conditions, pH 4.6, the same as for the human enzyme (Fig. S3, A and B).

Finally, we determined by LC-MS/MS the ability of A1.1 to degrade lyso-Gb3, the toxic base of Gb3, to lactosylsphingosine (Mirzaian et al. 2017). A1.1 degrades lyso-Gb3, showing a  $K_m$  of 37  $\mu$ M, quite comparable with that of Fabrazyme. Its  $k_{cat}$  value, however, is  $\sim$ 2-fold lower than that of the human enzyme (Fig. 5B). The noted activity of A1.1 toward

glycosphingolipid substrates *in vitro* resembles the earlier observed ability of rice  $\alpha$ -galactosidase to hydrolyze Gb3 *in vitro* (Chien et al. 2008).

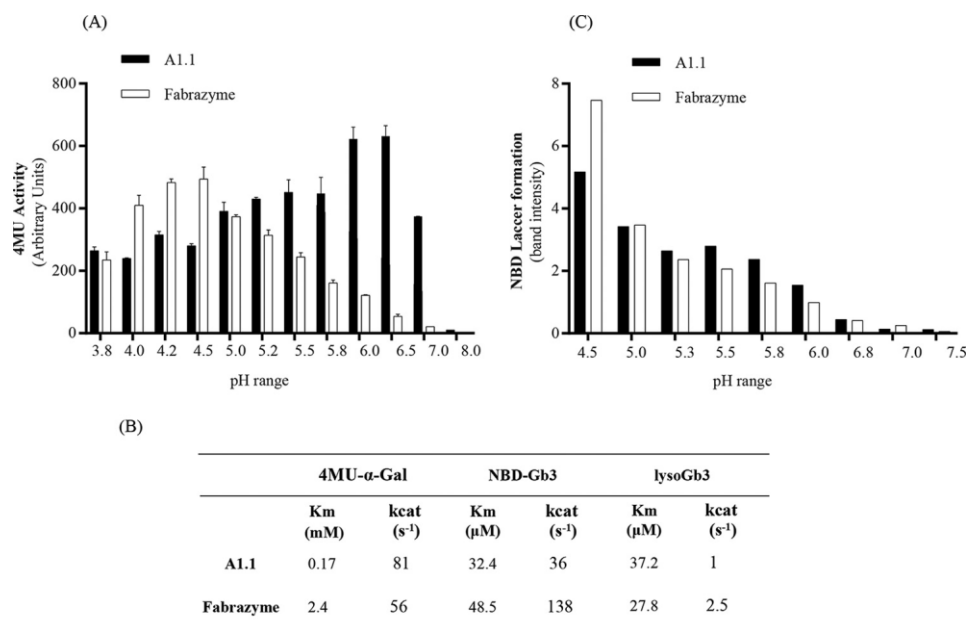


**Figure 5. Activity of *N. benthamiana* A1.1 and Fabrazyme toward 4MU- $\alpha$ -GAL and human glycosphingolipids.** A, 4MU- $\alpha$ -Gal activities of pure A1.1 and Fabrazyme at different pH values (3.8–8). B, Michaelis-Menten kinetic values of both enzymes toward 4MU- $\alpha$ -Gal, NBD-Gb3, and lyso-Gb3 substrates. Data represent mean values,  $n > 2$ . C, degradation of 5  $\mu$ M NBD-Gb3 to NBD-Lac Cer by 50 ng of A1.1 or Fabrazyme at varying pH values (4.5–7.5). Quantification of HPTLC plates were conducted more than once, showing one gel quantification.

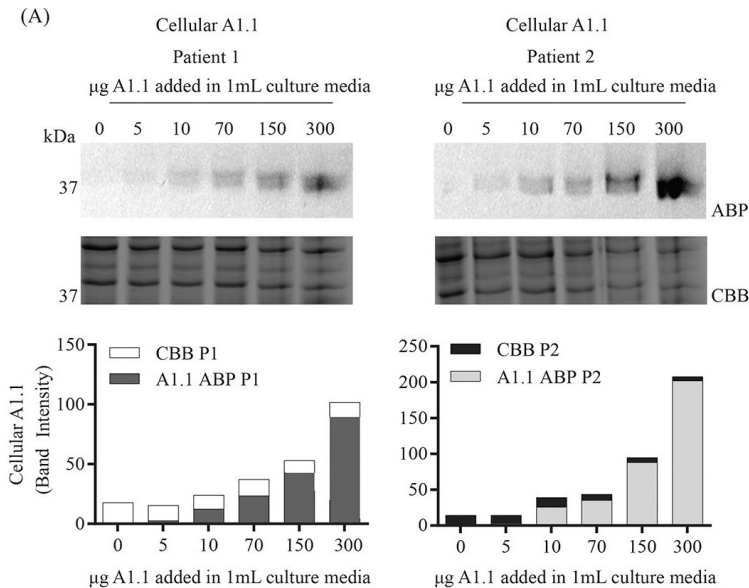
### A1.1 reduces lyso-Gb3 in intact FD fibroblasts

At first the uptake of A1.1 from lysosomes of two different FD patients' fibroblasts was evaluated. Different amounts of pre-labeled enzyme with TB474 A1.1 were applied overnight to the cells. After extensive washing (Fig. S4), the cells were lysed, and the uptake of A1.1 was studied via SDS-PAGE analysis (Fig. 6A). The cells from both FD patients were able to uptake A1.1. An increase in the uptake depending on the concentration of the pre-labeled protein added to the culture media was observed. To estimate the amount of the internalized enzyme, 1% of the input using 150 and 300  $\mu$ g/ml were loaded on gel, together with 13–17% of the total lysates after treatment with the pre-labeled enzyme (Fig. 6B). The quantification of the gels revealed that 0.3–

0.6% of the 150  $\mu\text{g/ml}$  entered the cells, and 0.5–1% of the 300  $\mu\text{g/ml}$  (Fig. 6C).

In addition, the uptake of the enzyme was studied by confocal microscopy. For this, A1.1 was again labeled with TB474 and subsequently applied to the FD fibroblasts. After a 16-h uptake, punctate fluorescence was observed in some cells, which was reminiscent of a lysosomal pattern, possibly through fluid-phase endocytosis. Immunofluorescent staining of the late endosomal/lysosomal marker LAMP-1 occasionally showed co-localization with TB474-A1.1, indicating lysosomal delivery of the enzyme (Fig. 6D).

To examine whether A1.1 is also able to degrade glycosphingolipid *in vivo*, we incubated the same cultured FD fibroblasts the exposure to A1.1 (Fig. 7A) with 300  $\mu\text{g/ml}$  A1.1. After overnight incubation, the cells were first washed and lysed, and the levels of both lyso-Gb3 and Gb3 were determined by LC-MS/MS. In addition, the 4MU- $\alpha$ GAL cellular activity was measured. The elevated lyso-Gb3 and Gb3 in both FD fibroblasts were found to be significantly reduced by the exposure to A1.1 (Fig. 7A). In addition, the 4MU- $\alpha$ Gal cellular activity was significantly increased after exposure to the recombinant protein (Fig. 7B). Activities were also measured at washing steps 1 and 5 to ensure that no protein remained outside of the cells prior to lysis (Fig. S5).



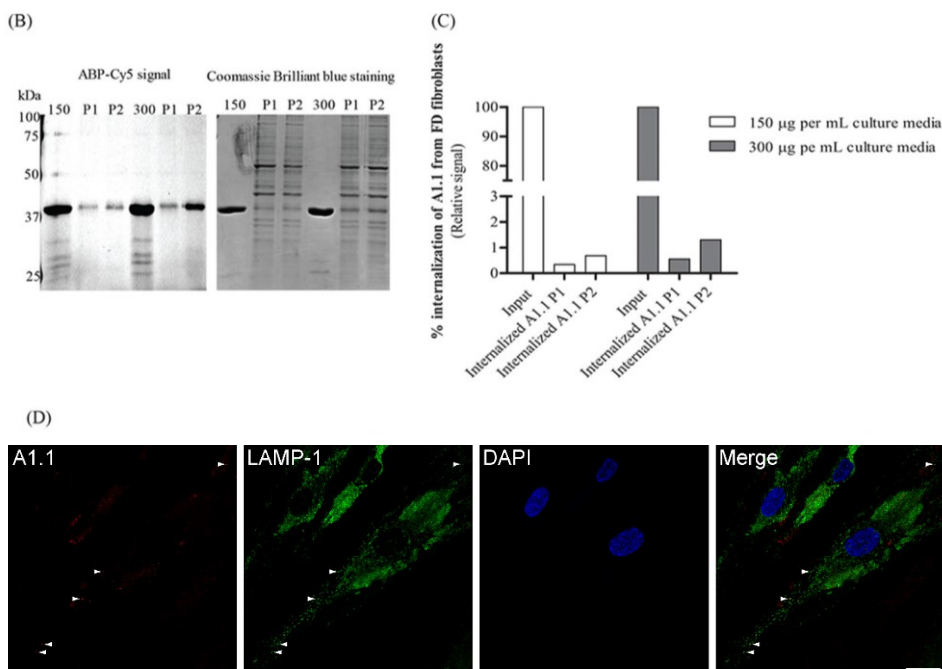


**Figure 6. Internalization of TB474-labeled A1.1 from Fabry fibroblasts.** *A*, Fabry fibroblasts from two different patients were grown in 12-well plates. The cells were incubated with different amounts pre-labeled with TB474, A1.1 (0, 5, 10, 70, 150, and 300  $\mu$ g per 1 ml of culture media). Lysis of the cells took place, and samples were measured for Cy5 signal, through SDS-PAGE. *Left top panel*, results were obtained when using patient 1 cell line, SDS-polyacrylamide gel image, following fluorescent scanning and quantification of signal, *left bottom panel*, results obtained from patient 2 cell line. The gels were conducted more than once. The uptake is gradually increased while increasing the amount of pre-labeled protein in both cell lines. 10  $\mu$ g of total fibroblast protein was added in each well. Coomassie staining of the cells took place to show equal loading. *ABP* = activity-based probe signal; *CBB* = Coomassie Brilliant Blue signal; *P1* = patient 1; *P2* = patient 2. *B*, estimation of the % of the internalization of pre-labeled A1.1 (150 and 300  $\mu$ g per ml of culture media) from the same FD fibroblasts. Loaded on gel, 1% of the pre-labeled A1.1 input, together with 10  $\mu$ g of total fibroblast protein, accounted for 13–17% of the total cell lysate. *C*, quantification of signal obtained in *B*. The uptake of 150  $\mu$ g of A1.1 accounted for 0.3–0.5% of the total input and 0.5–1% when using 300  $\mu$ g. *ABP* = activity-based probe signal; *P1* = patient 1; *P2* = patient 2. *D*, overnight uptake of A1.1, pre-labeled with TB474, by FD fibroblasts monitored by confocal microscopy. Cells were grown overnight on glass coverslips and incubated with 150  $\mu$ g of pre-labeled A1.1 per ml of culture medium (here shown cells from patient 1). *Panel in red*, visualization of the internalized TB474-labeled A1.1. *Panel in green*, lysosomal labeling using anti-LAMP-1 antibody. *Panel in blue*, cellular nuclei stained with DAPI. *D*, overlay image. The *white arrowheads* indicate examples of co-localization of internalized TB474-labeled A1.1 with the late endosomal/lysosomal marker LAMP-1. Scale bar 25  $\mu$ m.

## Discussion

We earlier used *N. benthamiana* for expression of WT and mutagenized human  $\alpha$ -galactosidase and  $\alpha$ -galactosaminidase (Chapter 3, Kytidou et al. 2017). The *N. benthamiana* plant is a convenient production platform for recombinant proteins given the ease of cultivation and transfection with *A. tumefaciens* (Kytidou et al. 2017). In chapter 3, we employed a cyclophellitol-type activity-based probe (TB474) to visualize the recombinant human  $\alpha$ -galactosidases. In the course of the experiments, we noted the presence of two endogenous enzymes (39 and 45 kDa) labeled by TB474. We focused attention to the 39-kDa enzyme (named A1.1) that is present in relatively high concentrations in the apoplast. Using biotin-containing ABP (ME741) and streptavidin pulldown, the identity of the 39 kDa protein in apoplast fluid was determined by proteomics. The corresponding gene (accession ID: GJZM- 1660) was cloned from a *N. benthamiana* cDNA library and transiently overexpressed in *N. benthamiana* leaves using infiltrations with *A. tumefaciens* harboring the appropriate expression vectors. A high yield of A1.1 in the apoplast fluid was protein and it was purified with 33% recovery to homogeneity by sequential ConA chromatography, cation-exchange chromatography, and gel filtration. The molecular mass of 39 kDa of the purified enzyme is similar to that reported for rice and coffee  $\alpha$ -galactosidases (Maranville and Zhu 2000; Fujimoto et al. 2003; Chien et al. 2008).

We characterized A1.1 regarding structural features. The mature form of the enzyme consists of 363 amino acids and has a molecular mass of 39 kDa. The purified enzyme is an active monomer, based on gel filtration behavior. This feature is common to rice  $\alpha$ -galactosidase, but the human enzyme occurs as a homodimer (Kytidou et al. 2017). As predicted by the absence of appropriate Asn-Xaa-(Ser/Thr/Cys) motifs, A1.1 is not *N*-glycosylated, and endoglycanase digestion points to no *N*-linked glycans. Similarly, rice and coffee  $\alpha$ -galactosidases lack *N*-glycans (Zhu et al. 1995; Fujimoto et al. 2003). Based on amino acid sequence alignments, the enzyme has 82% identity with coffee  $\alpha$ -galactosidase, 68% identity with rice  $\alpha$ -galactosidase, and 42% identity with human  $\alpha$ -galactosidase A, also revealing great secondary structural conservation.

Crystals of pure A1.1 were obtained, and the structure was resolved by X-ray diffraction at a resolution of 2.8 Å. The enzyme contains a C-terminal domain with Greek key motif and N-terminal domain with a ( $\beta/\alpha$ )<sub>8</sub>-barrel, the common catalytic domain among the hydrolases of family 27 (Fujimoto et al. 2003). The active site of retaining  $\alpha$ -galactosidases



contains a catalytic nucleophile and acid/base residue mediating double-displacement as a catalytic mechanism (Mathew and Balasubramaniam 1987; Garman et al. 2002). In the active site of A1.1, other amino acids appear involved in substrate recognition, such as Trp-67, Asp-102, Tyr-144, and Lys-179. Two disulfide bonds occur close to the catalytic pocket, Cys-72/104 and Cys-152/183, as also present in human  $\alpha$ -galactosidase A (Bishop et al. 1988; Garman et al. 2002). Notably, the existence of a second ligand-binding site in human  $\alpha$ -galactosidase A, centered on Tyr-329, was postulated by Guce *et al.* (Guce et al. 2010). This putative site, speculated to bind  $\beta$ -galactose, is located between the two domains of the human monomer enzyme, being exposed at the surface. However, in A1.1, instead of the Tyr-329, a Lys-330 is present, and the overall second binding-site region is different from the human enzyme. The C-terminal domain of A1.1 contains eight  $\beta$ -strands forming a Greek key motif. The C-terminal amino acid sequences of human and A1.1  $\alpha$ -galactosidases are different. Coffee  $\alpha$ -galactosidase, however, contains a C-terminal domain that is similar to A1.1 and is thought to essentially contribute to the overall structure of the enzyme, as its deletion results in loss of enzymatic activity (Maranville and Zhu 2000).

A1.1 shows strong specificity regarding the substrate sugar. It hydrolyzes 4MU- $\alpha$ -galactopyranoside liberating fluorescent methylumbelliferone, but it does not correspond to  $\beta$ -D-glucopyranoside,  $\beta$ -D-galactopyranoside,  $\alpha$ -D-mannopyranoside,  $\alpha$ -L-fucopyranoside, *N*-acetyl- $\alpha$ -D-galactosaminide, or *N*-acetyl- $\beta$ -D-glucosaminide. The broad pH optimum of A1.1, pH 5.0–6.5, is also reported for coffee and rice enzymes (Marraccini Pierre et al. 2005; Chien et al. 2008). The activity of A1.1 toward 4MU- $\alpha$ -galactopyranoside ( $K_m$  of 0.17 mM) is quite comparable with that of human  $\alpha$ -galactosidase A ( $K_m$  of 2.4 mM). For the rice enzyme, a high affinity toward pNP- $\alpha$ -Gal substrate was earlier reported by Chien *et al.* (Chien et al. 2008) ( $K_m$  of 0.47 mM). For coffee  $\alpha$ -galactosidase, a pH optimum of 6.5 with a  $K_m$  of 0.29 mM toward 4MU- $\alpha$ -Gal substrate was observed by Maranville and Zhu (Maranville and Zhu 2000).

$\alpha$ -Galactosidases from rice and coffee have been shown to remove terminal  $\alpha$ 1–3-linked galactose residues from type B glycolipid antigens on red blood cells, converting them to type O structures (Mathew and Balasubramaniam 1987; Chien et al. 2008). The ability of A1.1 to hydrolyze terminal  $\alpha$ -galactoses from artificial and natural glycosphingolipid substrates was therefore studied. A1.1 was found to be well able to hydrolyze NBD-Gb3, C18-Gb3, and lyso-Gb3 *in vitro*. Of note, the presence of Gb3 in *N. benthamiana* leaves has not been reported. We could not detect Gb3 with a regular sphingolipid base (data not shown). A similar observation was

earlier made for rice  $\alpha$ -galactosidase; Gb3 was shown to be converted to LacCer, but kinetic parameters were not determined (Chien et al. 2008). We observed a considerable affinity of pure A1.1 for lipids as substrates ( $K_m$  values of 32  $\mu$ M for NBD-Gb3 and 38  $\mu$ M for lyso-Gb3), almost equal to those observed for human  $\alpha$ -galactosidase A.

Presently, two different recombinant human  $\alpha$ -galactosidase A preparations are used to treat FD, an X-linked disorder with lysosomal Gb3 accumulation in various cell types and affecting heart and kidney (Ferraz et al. 2014). The therapeutic enzymes use Man-6-P containing *N*-linked glycans that are aimed to correct the lysosomal enzyme deficiency in all cell types following uptake and delivery to lysosomes by the ubiquitous MPR at the surface of cells (Ferraz et al. 2014). Exposure of cultured fibroblasts to recombinant human  $\alpha$ -galactosidase A (Fabrazyme) results in a reduction of excessive Gb3 and is deacylated metabolite lyso-Gb3 (Ferraz et al. 2014). We investigated whether recombinant A1.1 also manages to degrade the toxic lyso-Gb3 accumulating in cells of FD patients. Indeed, an overnight incubation of patient fibroblasts with 300  $\mu$ g/ml A1.1 resulted in significant reduction of both lyso-Gb3 and Gb3 accumulating glycosphingolipids, reaching levels found in normal fibroblasts ( $\sim$ 4 pmol/mg and  $\sim$ 15 nmol/mg for lyso-Gb3 and Gb3, respectively). It should be kept in mind that because A1.1 lacks glycans, no lectin-mediated uptake of the enzyme by cells occurs, in contrast to that of Man-6-P-rich Fabrazyme. The ability of the latter enzyme to correct lyso-Gb3 in cultured fibroblasts is therefore far superior than that of A1.1. A same reduction in cellular lyso-Gb3 of FD fibroblasts was obtained, reaching levels found in normal fibroblasts, with 60-fold less Fabrazyme than A1.1 (Fig. S6).

Unfortunately, the present enzyme replacement therapies meet limited clinical success. Although storage lipid is cleared from endothelial cells, complications in heart and kidney may nevertheless develop in FD patients, possibly due to the use of insufficient therapeutic enzyme to penetrate these organs. High costs of the present  $\alpha$ -galactosidase A preparations hamper the use of significantly higher doses. The elevated circulating lyso-Gb3, considered to be toxic for podocytes and nociceptive neurons, is not completely corrected by present ERT (Choi et al. 2015; Mirzaian et al. 2017). Finally, a complicating factor with the present ERT of FD proves to be the antigenicity of recombinant human  $\alpha$ -galactosidase A in the majority of male FD patients that lack any endogenous enzyme (Lenders et al. 2016). In these individuals, neutralizing antibodies against therapeutic enzyme develop quickly, resulting in a relapse in the reduction of circulating toxic lyso-Gb3 (Linthorst et al. 2004). The clinical outcome of

ERT in antibody-positive FD patients is reported to be poorer (Linthorst et al. 2004). In view of all this, the use of a plant  $\alpha$ -galactosidase to treat male FD patients deserves consideration. First, plant  $\alpha$ -galactosidase could be produced in *N. benthamiana* or other plant production platforms at considerably lower costs than the present human recombinant enzymes, allowing use of higher doses. Second, A1.1 is able to degrade toxic lyso-Gb3. The enzyme can in principle be further engineered to increase stability and desired enzymatic activity. The lack of *N*-glycans on a plant-derived  $\alpha$ -galactosidase might even be beneficial, preventing a lectin receptor-mediated sink in the endothelium and liver as observed with present therapeutic human glycoprotein enzymes. Finally, we observed that *N. benthamiana* A1.1 does not cross-react with neutralizing antibodies directed against human  $\alpha$ -galactosidase A that are present in serum of male FD patients treated with therapeutic enzyme (Fig. S7). Antigenicity of a plant protein might be a concern, but it should be kept in mind that this also exists with the human enzyme preparations in most male FD patients. The considerable progress made in induction of tolerance against foreign proteins may be exploited (Rezende and Weiner 2017). It is presently unclear how antigenic a plant  $\alpha$ -galactosidase will be: the absence of glycans might reduce C-type lectin receptor-mediated presentation by dendritic cells.

In conclusion, further research on the optimization of plant  $\alpha$ -galactosidases such as A1.1 to reduce toxic lyso-Gb3 in FD should be considered to meet the need for an affordable treatment of this devastating disorder.

## Material and Methods

**Chemicals.** All chemicals were obtained from Sigma (Germany) if not indicated otherwise. Fluorescent NBD-lipids and pure lipids were purchased from Avanti Polar Lipids (Alabaster, AL). Anti- bodies purchased from Abcam (Cambridge, MA).

**Plants.** *N. benthamiana* plants were grown at 21 °C and 60–70% humidity in the Unifarm greenhouses of Wageningen University (Westerhof et al. 2014).

**Patient materials.** Fibroblast cell lines from classical FD individuals were obtained from the Lysosomal Outpatient Clinic of the Academic Medical Center in Amsterdam (AMC). The cells were cultured in Dulbecco's modified Eagle's medium/Nutrient Mixture F-12 (DMEM/F-12, Sigma) media, supplemented with 10% fetal calf serum and 1% penicillin/streptomycin, at 37 °C with 5% CO<sub>2</sub> in a humidified incubator. Plasma specimens from FD individuals were obtained from the Lysosomal Outpatient Clinic of the Academic Medical Center in Amsterdam (see supplementary material). All patient materials were obtained after approval of the Academic Medical Center's review board and abide by the Declaration of Helsinki principles.

**ABP ME741, synthesis.** The  $\alpha$ -galactopyranose-configured cyclophellitol aziridine grafted with Cy5 as fluorophore ABP (TB474) was synthesized as described previously (Kytidou et al. 2017). The biotinylated  $\alpha$ -galactopyranoside cyclophellitol aziridine (ME741) was synthesized by copper-catalyzed click chemistry of azido cyclophellitol aziridine intermediate with biotin alkyne (Scheme S1). The  $\alpha$ -galactose- configured azido cyclophellitol aziridine (Willems et al. 2014a) (14.6 mg, 0.043 mmol) synthesized in 15 steps from D-xylose, and the desired biotin-alkynes (18.5 mg, 0.047 mmol) were dissolved in N,N- dimethylformamide (2 ml). CuSO<sub>4</sub> (0.043 ml, 1 M in H<sub>2</sub>O) and sodium ascorbate (0.043 ml, 1 M in H<sub>2</sub>O) were added, and the reaction mixture was stirred at room temperature under argon atmosphere for 18 h. Then the solution was diluted with CH<sub>2</sub>Cl<sub>2</sub>, washed with H<sub>2</sub>O, dried over MgSO<sub>4</sub>, and concentrated under reduced pressure. The crude was purified by semi- preparative reversed-phase HPLC (linear gradient: 15–24% B in A, 12 min, solutions used A, 50 mM NH<sub>4</sub>HCO<sub>3</sub> in H<sub>2</sub>O, and B, MeCN) and lyophilized to yield biotinylated ABP ME741 as a white powder (8.0 mg, 11  $\mu$ ,mol, 26%). <sup>1</sup>H NMR (600 MHz, CD<sub>3</sub>OD) contained the following: 3 7.85 (d, J = 3.7 Hz, 1H, CH); 4.90 (s, 1H,

NH); 4.49 (dd,  $J = 7.9, 4.9$  Hz, 1H, CH); 4.42 (d,  $J = 2.3$  Hz, 2H, CH<sub>2</sub>); 4.38 (td,  $J = 7.1, 2.5$  Hz, 2H, CH<sub>2</sub>); 4.30 (dd,  $J = 7.9, 4.5$  Hz, 1H, CH); 4.08 (dd,  $J = 8.6, 3.9$  Hz, 1H, CH); 3.85–3.87 (m, 1H, CH); 3.81–3.68 (m, 2H, CH<sub>2</sub>); 3.36 (dd,  $J = 8.6, 1.7$  Hz, 1H, CH); 3.24–3.17 (m, 1H, CH); 3.16 (td,  $J = 7.0, 2.5$  Hz, 2H, CH<sub>2</sub>); 2.92 (dd,  $J = 12.7, 5.0$  Hz, 1H, 1/2CH<sub>2</sub>); 2.70 (d,  $J = 12.7$  Hz, 1H, 1/2CH<sub>2</sub>); 2.61 (d,  $J = 6.1$  Hz, 1H, CH); 1.91–1.86 (m, 4H, 2CH<sub>2</sub>); 1.75–1.56 (m, 4H, 2CH<sub>2</sub>); 1.51 (p,  $J = 7.2$  Hz, 2H, CH<sub>2</sub>); 1.43 (p,  $J = 8.8, 8.2$  Hz, 2H, CH<sub>2</sub>); 1.39–1.26 (m, 4H, 2CH<sub>2</sub>). <sup>13</sup>C NMR (151 MHz, CD<sub>3</sub>OD) contained the following: 3 188.7, 176.0, 176.0, 166.1, 146.2, 146.2, 74.3, 74.2, 73.2, 73.1, 70.5, 69.5, 63.4, 62.8, 61.6, 57.0, 51.4, 51.3, 44.8, 43.3, 41.1, 40.2, 39.4, 37.1, 36.8, 36.8, 35.6, 31.3, 31.2, 30.4, 30.1, 30.0, 29.9, 29.8, 29.7, 29.5, 27.5, 27.4, 27.3, 27.2, 26.9, 26.5, 25.8 ppm; HRMS was calculated for C<sub>34</sub>H<sub>56</sub>N<sub>8</sub>O<sub>8</sub>S [M + H]<sup>+</sup> 737.40201 and found was 737.40146.

***N. benthamiana* leaf extracts.** Leaves of 5– 6-week-old *N. benthamiana* plants were collected, snap-frozen in liquid nitrogen, and homogenized by grinding with a mortar and a pestle. To 1 g of leaf, 4 ml of ice-cold extraction buffer (30 mM citrate/phosphate buffer, pH 6, containing 2% w/v polyvinylpyrrolidone, 0.1% v/v Tween 20, 0.15 M NaCl, and protease inhibitor by Roche Applied Science, EDTA-free) was added, and the material was again homogenized. The homogenates were centrifuged at 16,000 rcf, at 4 °C, for 10 min, and the supernatant containing soluble proteins was collected.

**Isolation of apoplast proteins.** For the isolation of apoplast proteins, *N. benthamiana* leaves were gently submerged in ice-cold extraction buffer (50 mM PBS, pH 6, 0.1 M NaCl, and 0.1% v/v Tween 20) and exposed to vacuum for 10 min. Then the vacuum was released very slowly to ensure infiltration of the apoplast. The leaves were then collected and carefully placed in 10-ml syringes plugged in 50-ml tubes. The samples were centrifuged for 10 min at 2000 rcf, and apoplast fluid was collected (Wilbers et al. 2017).

**Small-scale ABP labeling of  $\alpha$ -galactosidases in *N. benthamiana* plant leaf extracts and apoplast fluid.** 10  $\mu$ l of *N. benthamiana* plant leaf extracts (4.5 mg of total soluble protein/ml) and 20  $\mu$ l of apoplast sample (0.21 mg of total soluble protein/ml) were incubated with 0.25  $\mu$ M fluorescent TB474 in 150 mM citrate/phosphate buffer at different pH values, for 30 min at room temperature. Gel loading buffer (with additional  $\beta$ -mercaptoethanol) was added to samples, followed by incubation for 5 min at 95 °C. The proteins in the samples were separated by 10% polyacrylamide gels. Labeled proteins were visualized by fluorescence scanning as described earlier (Willems et al. 2014c).

**Analysis of N-glycosylation by concanavalin A lectin binding.** Concanavalin A-Sepharose 4B beads (ConA beads) were first washed three times in 0.1 M sodium acetate, 0.1 M NaCl, 1 mM MgCl<sub>2</sub>, 1 mM CaCl<sub>2</sub>, 1 mM MnCl<sub>2</sub>, pH 6.0, washing buffer using brief centrifugation at 2000 rcf for 2 min. Next, 150 µl of beads were mixed with 300 µl of plant leaf extracts or 150 µl of apoplast sample and incubated for 2h at 4 °C while rotating. After this incubation, the mixture was centrifuged at 16,000 rcf at 4 °C for 10 min. The supernatant was collected, and the beads were washed three times with washing buffer. The samples were stored for a short period at 4 °C until further use.

**Competitive ABPP using ME741 ABP.** The ability of biotinylated ME741 to label  $\alpha$ -galactosidases was first established by performing competition experiments. Homogenates were first labeled with Cy5 functionalized TB474 at 0.25 µM for 30 min at room temperature, followed by labeling the homogenate with biotinylated ME741 ABP at 0.25 µM and the other way around. Subsequently, SDS-PAGE and Western blot analysis with HRP-streptavidin was performed as described previously (Jiang et al. 2016; Wu et al. 2017).

***In vitro* biotin pulldown of bound targets, followed by on-bead tryptic digestion and LC-MS/MS identification.** Plant leaf extracts (4.5 mg of total soluble protein/ml) and apoplast samples (0.21 mg of total soluble protein/ml (no. 1) and 0.6 mg of total soluble protein/ml (no. 2)) were pre-incubated or not with 5 µM TB474 for 2 h at room temperature, following overnight incubation with 5 µM ME741, room temperature at a final volume of 500 µl. Then the reaction was stopped by the addition of 120 µl of 10% (w/v) SDS and subsequent incubation of the sample at 95 °C for 5 min. Preparation of proteins for on-bead and tryptic digestion following LC-MS/MS identification was performed exactly as described previously (Jiang et al. 2016). Prior to LC-MS analysis, peptides were desalted by StageTips as described by Rappsilber et al. (Rappsilber et al. 2007) Empore<sup>TM</sup> C18 47-mm extraction discs were used to fabricate the StageTips. Typically, two discs were placed on top of each other to make StageTips with two layers of column material inserted in a yellow pipette tip.

**MS acquisition.** The Synapt G2Si mass spectrometer (Waters) operating with Masslynx for acquisition and ProteinLynx Global Server (PLGS) for peptide identification was used for analysis. The following settings in positive resolution mode were used: source temperature of 80 °C; capillary

voltage 3.0 kV; nano flow gas of 0.25 bar; purge gas 250 liters/h; trap gas flow 2.0 ml/min; cone gas 100 liters/h; sampling cone 25 V; source offset 25; lock mass acquisition was done with a mixture of Leu-enkephalin (556.2771) and Glu-fibrinogen (785.84265) and lockspray volt- age 3.5 kV; and Glu-fibrinogen fragmentation was used as calibrant. An UDMSe data-independent acquisition method was used for analysis. Briefly, the mass range is set from 50 to 2000 Da with a scan time of 0.6 s in positive resolution mode. The collision energy is set to 4V in the trap cell for low-energy MS mode. For the elevated energy scan, the transfer cell collision energy is ramped to higher collision energies, and data are recorded. The lock mass is sampled every 30 s and used for accurate determination of parent ions mass after peak picking. Peak lists containing parent and daughter ions were compiled in .mgf format and searched against the Swiss-Prot (version June 2017) database. The identified peptides were manually curated.

**Plant expression vector for overexpression of A1.1.** The *N. benthamiana*  $\alpha$ -galactosidase A1.1 (gene accession ID: GJZM-1660), was amplified from an *N. benthamiana* cDNA library made by our laboratory using the Invitrogen™ CloneMiner™ II cDNA library construction kit (Thermo Fisher Scientific). The gene was amplified with its native signal peptide, using Phusion® High Fidelity PCR Master Mix (Bio- Labs), with the following primers: sense, 5'-CCCATGGGTTT-GCCACCAATTTTAAAGCTGCTACTAT-3', and antisense, 5'-GGGTACCTTATTTTTTAGGAGTCAGAACATACATCCTGCA-3'. The gene was flanked between NcoI and Acc65I restriction sites, and it was cloned into a pGEM®-T Easy Vector System (Promega). Confirmation of sequences was done by sequencing (Macrogen, the Netherlands), and the complete ORF of the gene was inserted into the pHYG plant expression vector, as described previously (Westerhof et al. 2012). The construct was under the control of cauliflower mosaic virus 35S constitutive promoter, with duplicate enhancer and the nopaline synthase terminator (Kytidou et al. 2017). The pHYG vectors harboring the genes were used for transformation of *A. tumefaciens* strain MOG101, following *N. benthamiana* plant leaf infiltrations.

***A. tumefaciens* transient transformation assay and plant infiltrations.**

*A. tumefaciens* cultures were grown as described previously (Westerhof et al. 2012, 2014). The constructs were co-expressed with the tomato bushy stunt virus silencing inhibitor p19 to ensure optimum expression levels (Kytidou et al. 2017; Wilbers et al. 2017).

The inoculated bacterial cultures were used for infiltration of 5– 6-week-old *N. benthamiana* plants, as described previously (Westerhof et al. 2014).

**Isolation of apoplast overexpressing A1.1.** The isolation of apoplast fluid was performed as described previously (Wilbers et al. 2017), using as extraction buffer 30 mM citrate/phosphate, pH 6, 0.5 M NaCl, and 0.1% (v/v) Tween 20. The sample was passed through a G-25 Sephadex column for desalting and snap-frozen in liquid nitrogen. The sample was stored at –80 °C until further use.

**Enzyme purification.** Chromatography with 5 ml of concanavalin A-Sepharose column (GE Healthcare) was used as a first step for purification. The column was equilibrated with 40 ml of washing buffer (0.1 M sodium acetate, 0.1 M NaCl, 1 mM MgCl<sub>2</sub>, 1 mM CaCl<sub>2</sub>, 1 mM MnCl<sub>2</sub>, pH 6.0). Then, 40 ml of apoplast fluid overexpressing A1.1 was applied to the column, 1:1, diluted in washing buffer (1 ml/min loading conditions). The enzyme was present in the (unbound) flow-through fractions, ensuring separation from bound plant glycoproteins. About 40 ml of sample was collected and tested for enzymatic activity. Next, the sample was extensively dialyzed in 20 mM sodium acetate buffer, pH 5.5, 4 °C, for 2 days. Subsequently, the dialyzed fraction was subjected to chromatography on two HiTrap SP HP columns, 1 ml each, plugged on top of each other (GE Healthcare), and equilibrated with 30 ml of binding buffer: 20 mM sodium acetate buffer, pH 5.0. The sample, 40 ml, was applied on the columns, which were extensively washed with 30 ml of binding buffer afterward. Then, protein was eluted using a 15-ml gradient of 0 – 400 mM NaCl. Fractions containing the highest protein activity and purity were pooled. Next, the pooled sample (4.5 ml) was applied to a HiLoad™ 16/600 Superdex™ 200 preparation grade column (GE Healthcare). The column was first equilibrated with 500 ml of 20 mM sodium acetate buffer with 150 mM NaCl, pH 5.5, and the sample was applied to the column at a flow rate of 1 ml/min. Four samples of 2 ml each, with the highest purity and activity, were collected and concentrated using Centricon Plus-20, 15 ml with 10-kDa molecular cutoff (Millipore, Bedford, MA) until 0.8 ml. The final material was snap-frozen in liquid nitrogen and stored at –80 °C until further use.

**Protein determination.** Total soluble protein content from cell lysates was measured using the Pierce BCA protein assay kit (Thermo Fisher Scientific), using BSA as a standard, according to the manufacturer's protocol. Pure protein concentrations were measured in Nano-Drop 2000c



(Thermo Fisher Scientific).

**Enzymatic assays and determination of kinetic parameters.** Different 4-MU substrates were used to test the specificity of A1.1. Tested substrates were the following glycosides linked to 4-MU:  $\beta$ -D-glucopyranoside,  $\alpha$ -D-galactopyranoside,  $\beta$ -D-galactopyranoside,  $\alpha$ -D-mannopyranoside,  $\alpha$ -L-fucopyranoside, N-acetyl- $\alpha$ -D-galactosaminide, and N-acetyl- $\beta$ -D-glucosaminide at the following assay concentrations and pH conditions: 1.36 mg/ml, pH 5.2, 5.8, and 7; 1.25 mg/ml, pH 4.6 and 6; 0.144 mg/ml, pH 4.3; 2.7 mg/ml, pH 4; 0.26 mg/ml, pH 5.5; 0.4 mg/ml, pH 4.6; 1.52 mg/ml, pH 4.4, respectively. All substrates were dissolved in 150 mM citrate/phosphate (McIlvaine) buffer, at the appropriate pH for each enzyme, supplemented with 0.1% (w/v) BSA. Released 4-MU was fluorometrically quantified as described earlier (Aerts et al. 1986; Blom et al. 2003).  $K_m$  and  $k_{cat}$  values were determined using 4-MU- $\alpha$ -GAL substrate. Reactions were performed for 25 min at 37 °C at 10 different 4-MU- $\alpha$ -GAL concentrations in 150 mM citrate/phosphate buffer, pH 6, for A1.1 or pH 4.6 for Fabrazyme supplemented with 0.1% (w/v) BSA. The 4-MU- $\alpha$ -GAL concentrations in the assays ranged from 0.074 to 4.72 mM. Protein concentrations in the assays were as follows: A1.1, 1.6 and 4 ng/ml; Fabrazyme, 2 and 5 ng/ml. GraphPad Prism7 was used for all calculations.

**Activity toward lipid substrates.** For activity measurement, 50 ng of A1.1 or Fabrazyme were incubated with 5  $\mu$ M NBD-C12- globotriaosylceramide, (NBD- Gb3) for 1 h at 37 °C in 150 mM citrate/phosphate buffers at different pH values (4.5–7.5), containing 0.05% (v/v) Triton X-100 and 0.2% (w/v) sodium taurocholate. The lipids were next extracted by the Bligh and Dyer protocol and subjected to HPTLC as described earlier (Marques et al. 2016). The plate was scanned for fluorescent lipids with a Typhoon FLA 9500. Kinetics parameters  $K_m$  and  $k_{cat}$  were determined using NBD-Gb3 substrate, at pH 4.5.

Alternatively, HPLC analysis and LC-MS/MS were used to study hydrolysis of C18-Gb3 (Matreya, State College, PA) and C18 -lyso-Gb3 (Avanti, Alabaster, AL) by A1.1, respectively. For the degradation of C18-Gb3, 5  $\mu$ M natural lipid were incubated with 3  $\mu$ g of pure A1.1 or Fabrazyme overnight at 37 °C. Following extraction (Bligh and Dyer protocol), neutral glycosphingolipids were analyzed by HPLC using C17-sphinganine as internal standard (Gold et al. 2013). For lyso-Gb3, eight different concentrations of the lipid, ranging from 2 to 200  $\mu$ M, were incubated with 2.5  $\mu$ g/ml of A1.1 and Fabrazyme for 45 min at 37 °C. LC-MC/MS was used to measure glycosphingoid bases (lyso- glycosphingolipids), as described previously (Kytidou et al. 2017; Mirzaian et al. 2017). As internal standard

[<sup>13</sup>C]lyso-Gb3 was used (Mirzaian et al. 2017). Kinetics parameters  $K_m$  and  $k_{cat}$  were determined at pH 4.5, using GraphPad Prism7 for calculations. The mature form of A1.1, having a mass of 39 kDa, and the mature monomer human  $\alpha$ -galactosidase (Fabrazyme), 51 kDa, adjusted to the carbohydrate mass, were used to calculate  $k_{cat}$  values.

**Uptake of TB474-labeled A1.1 by FD fibroblasts and confocal microscopy.**

Fabry fibroblasts from two different patients were grown in 12-well plates. Different amounts of pre-labeled TB474 with A1.1 were added to 500  $\mu$ l of the culture media. The amounts were 0, 2.5, 5, 35, 75, and 150  $\mu$ g. After overnight incubation, the cells were extensively washed with PBS and lysed in 100  $\mu$ l of ice-cold 50 mM phosphate buffer, pH 6.5, supplemented with 0.1% Triton X-100. The total protein content of the cells was measured. Then 10  $\mu$ g of total protein of the lysates, accounting to 15–20% of total cell lysate, were analyzed in SDS-PAGE. Quantification of the gels took place using ImageJ program.

The pre-labeling of the enzyme was done for 4 h, at room temperature, in 150 mM citrate/phosphate buffer, pH 5.5, at a final TB474 concentration of 0.25  $\mu$ M, 100- $\mu$ l volume, followed by removal of unbound TB474 by passing the sample over a 0.7-ml Pierce™ polyacrylamide spin desalting column 7000 MWCO (Thermo Fisher Scientific), according to the manufacturer's protocol.

For the confocal microscopy experiments, the same Fabry fibroblasts were grown in 12-well plates containing coverslips, until they reached 70 – 80% confluency. On the day of the uptake, the culture medium was removed, and 500  $\mu$ l of fresh culture medium was placed in each well. 75  $\mu$ g of A1.1 pre-labeled with TB474 was applied to the fibroblasts overnight.

After the incubation, the fibroblasts were washed extensively with PBS and subsequently were fixed with 4% (w/v) formaldehyde/PBS for 25 min at room temperature. After the fixation, the cells were washed three times quickly with PBS and incubated for 10 min with 2% (w/v) BSA and 0.1% (w/v) saponin in PBS (“permeabilization buffer”). To stain for LAMP-1, the cells were incubated for 1 h at room temperature with rabbit anti- LAMP-1 antibody (Abcam) at a dilution of 1:400 in permeabilization buffer. The cells were washed three times in permeabilization buffer and incubated for 1h at room temperature with Alexa Fluor 488-coupled donkey anti-rabbit IgG (Invitrogen), 1:500 in permeabilization buffer. After the incubation, the cells were further washed in permeabilization buffer and quickly with distilled water. The coverslips were mounted on a micro- scope slide (VWR) with ProLong Diamond antifade reagent containing DAPI (Molecular Probes).

Imaging of the cells was performed with a Leica SP8 confocal microscope with a X63/1.40 NA HC Plan Apo CS2 oil immersion objective and equipped with a hybrid detector. TB474-labeled A1.1 was imaged with excitation at 638 nm and emission at 650–700 nm; LAMP-1 with excitation at 488 nm and emission at 500–540 nm; and DAPI at 405 nm excitation and emission at 420–480 nm.

**A1.1 treatment of FD fibroblasts.** FD fibroblasts were grown in 12-well plates in a humidified incubator at 37 °C with 5% CO<sub>2</sub>. To 500  $\mu$ l of the culture medium, 150  $\mu$ g of A1.1 were added, followed by overnight incubation. Next, cells were extensively washed in PBS, collected, and lysed in 100  $\mu$ l of ice-cold 50 mM phosphate buffer, pH 6.5, supplemented with 0.1% Triton X-100. Protein determination of lysates took place, and the lysates were used for lipid extractions, following LC-MS/MS analysis and 4MU- $\alpha$  GAL activity assays.

**Crystallization conditions and data collection.** Purified A1.1 was concentrated to 5 mg/ml and incubated with 10  $\mu$ M TB474 for 30 min at room temperature. After incubation, crystallization conditions were screened by sitting-drop vapor diffusion using the JCSG+ kit Premier (Molecular Dimensions). The screenings were performed by the NT8 robot (Formulatrix) at 20 °C, using 200 nl drops, with a well volume of 70  $\mu$ l. After 12 h the crystals were formed at the H9 condition of the JCSG+ screening. The condition consisted of 0.1 M BisTris buffer, pH 5.5, 0.2 M LiSO<sub>4</sub>, 25% w/v PEG 3350. The crystal had a rhombus shape with 30.7/37- $\mu$ m size. The crystal was flash-frozen in liquid nitrogen using 20% glycerol as a cryoprotectant. X-ray data collection was performed at the ESRF (Grenoble, France) on beamline ID30A-3, using a PIXEL, Eiger\_4M (DECTRIS), X-ray detector. A total of 1900 images were collected, with an oscillation of 0.05° and exposure time of 0.01 s (total of 19 s). Then the data were processed by XDS and scaled by AIMLESS. The structure was solved using the molecular replacement method (MOLREP), having 1UAS as search model, through the CCP4 suite and further refined using REFMAC. Manual model building was done using Coot. Images of structures were obtained using CCP4mg, and amino acid alignments were performed using ClustalOmega and ESPript3.0.

The superposition of A1.1 and human proteins was performed by secondary structure-matching (Krissinel and Henrick 2004), using the A monomer of human  $\alpha$ -galactosidase (PDB 3HG2) and our structure. Secondary structure matching aligned 348 residues with a root-mean-square deviation of 1.3358 Å of the C- $\alpha$  atoms of the aligned residues.

## Acknowledgments

We thank Mina Mirzaian, Kimberley Zwiers, and Rafaella Tassoni for their technical support and discussion. We also thank Thomas J. M. Beenakker for the synthesis of TB474 ABP.

## References

- Aerts JMFG, Groener JE, Kuiper S, et al (2008) Elevated globotriaosylsphingosine is a hallmark of Fabry disease. *Proc Natl Acad Sci U S A* 105:2812–2817. doi: 10.1073/pnas.0712309105
- Aerts JMFG, Donker-Koopman WE, Koot M, et al (1986) Deficient activity of glucocerebrosidase in urine from patients with type 1 Gaucher disease. *Clin Chim Acta* 158:155–163. doi: [http://dx.doi.org/10.1016/0009-8981\(86\)90231-7](http://dx.doi.org/10.1016/0009-8981(86)90231-7)
- Arends M, Biegstraaten M, Hughes DA, et al (2017) Retrospective study of long-term outcomes of enzyme replacement therapy in Fabry disease: Analysis of prognostic factors. *PLoS One* 12:1–17. doi: 10.1371/journal.pone.0182379
- Bishop DF, Kornreich R, Desnick RJ (1988) Structural organization of the human alpha-galactosidase A gene: further evidence for the absence of a 3' untranslated region. *Proc Natl Acad Sci U S A* 85:3903–3907. doi: 10.1073/pnas.85.11.3903
- Blom D, Speijer D, Linthorst GE, et al (2003) Recombinant Enzyme Therapy for Fabry Disease: Absence of Editing of Human  $\alpha$ -Galactosidase A mRNA. *Am J Hum Genet* 72:23–31. doi: <https://doi.org/10.1086/345309>
- Carchon H, DeBruyne CK (1975) Purification and properties of coffee-bean alpha-D-galactosidase. *Carbohydr Res* 41:175–189. doi: 10.1016/s0008-6215(00)87017-2
- Carmi N, Zhang G, Petreikov M, et al (2003) Cloning and functional expression of alkaline  $\alpha$ -galactosidase from melon fruit: Similarity to plant SIP proteins uncovers a novel family of plant glycosyl hydrolases. *Plant J.* 33:97–106.
- Chandrasekar B, Colby T, Emran Khan Emon A, et al (2014) Broad-range Glycosidase Activity Profiling. *Mol Cell Proteomics* 13:2787–2800. doi: 10.1074/mcp.O114.041616
- Charles C. Sweeley and Bernard Klionsky (1963) Fabry's Disease: Classification as a Sphingolipidosis and Partial Characterization of a Novel Glycolipid. *J Biol Chem* 238:3148–3150.
- Chien S-F, Chen S-H, Chien M-Y (2008) Cloning, Expression, and Characterization of Rice  $\alpha$ -Galactosidase. *Plant Mol Biol Report* 26:213–224. doi: 10.1007/s11105-008-0035-6
- Choi L, Vernon J, Kopach O, et al (2015) The Fabry disease-associated lipid Lyso-Gb3 enhances voltage-gated calcium currents in sensory neurons and causes pain. *Neurosci Lett* 594:163–168. doi: 10.1016/j.neulet.2015.01.084
- Desnick, R.J., Ioannou Y.A. (2001).  $\alpha$ -Galactosidase a deficiency. Fabry disease, in Scriver C.R., Beaudet A.L., Sly W.S., Valle D. (Eds) *The Metabolic and Molecular Bases of Inherited Disease*, 8th ed. McGraw-Hill, New York, 3733-3774.
- Eng C, Muenzer J, Wraith E, et al (2007) 39 Formation of a Lysosomal Disease Testing

- Network to enhance the delivery of diagnostic services to patients with lysosomal storage disorders. *Mol Genet Metab* 92:20. doi: <https://doi.org/10.1016/j.ymgme.2007.08.044>
- Ferraz MJ, Kallemeijn WW, Mirzaian M, et al (2014) Gaucher disease and Fabry disease: New markers and insights in pathophysiology for two distinct glycosphingolipidoses. *Biochim Biophys Acta - Mol Cell Biol Lipids* 1841:811–825. doi: <https://doi.org/10.1016/j.bbalip.2013.11.004>
- Ferraz MJ, Marques ARA, Appelman MD, et al (2016) Lysosomal glycosphingolipid catabolism by acid ceramidase: formation of glycosphingoid bases during deficiency of glycosidases. *FEBS Lett* 590:716–725. doi: [10.1002/1873-3468.12104](https://doi.org/10.1002/1873-3468.12104)
- Fujimoto Z, Kaneko S, Momma M, et al (2003) Crystal structure of rice  $\alpha$ -galactosidase complexed with D-galactose. *J Biol Chem* 278:20313–20318. doi: [10.1074/jbc.M302292200](https://doi.org/10.1074/jbc.M302292200)
- Gao Z, Schaffer AA (1999) A Novel Alkaline  $\alpha$ -Galactosidase from Melon Fruit with a Substrate Preference for Raffinose. *Plant Physiol* 119:979–988.
- Garman SC, Hannick L, Zhu A, Garboczi DN (2002) The 1.9 Å Structure of  $\alpha$ -N-Acetylgalactosaminidase. *Structure* 10:425–434. doi: [10.1016/S0969-2126\(02\)00726-8](https://doi.org/10.1016/S0969-2126(02)00726-8)
- Gold H, Mirzaian M, Dekker N, et al (2013) Quantification of Globotriaosylsphingosine in Plasma and Urine of Fabry Patients by Stable Isotope Ultrapformance Liquid Chromatography Tandem Mass Spectrometry. *Clin Chem* 59:547–556. doi: [10.1373/clinchem.2012.192138](https://doi.org/10.1373/clinchem.2012.192138)
- Guce AI, Clark NE, Salgado EN, et al (2010) Catalytic Mechanism of Human  $\alpha$ -Galactosidase. *J Biol Chem* 285:3625–3632. doi: [10.1074/jbc.M109.060145](https://doi.org/10.1074/jbc.M109.060145)
- Haibach F, Hata J, Mitra M, et al (1991) Purification and characterization of a *Coffea canephora*  $\alpha$ -D-galactosidase isozyme. *Biochem Biophys Res Commun* 181:1564–1571. doi: [10.1016/0006-291X\(91\)92117-3](https://doi.org/10.1016/0006-291X(91)92117-3)
- Hamers MN, Westerveld A, Khan M, Tager JM (1977) Characterization of  $\alpha$ -galactosidase isoenzymes in normal and fabry human-Chinese hamster somatic cell hybrids. *Hum Genet* 36:289–297. doi: [10.1007/BF00446279](https://doi.org/10.1007/BF00446279)
- Henrissat B, Romeu A (1995) Families, superfamilies and subfamilies of glycosyl hydrolases. *Biochem J* 311:350 LP – 351.
- Ioannou YA, Zeidner KM, Gordon RE, Desnick RJ (2001) Fabry Disease: Preclinical Studies Demonstrate the Effectiveness of  $\alpha$ -Galactosidase A Replacement in Enzyme-Deficient Mice. *Am J Hum Genet* 68:14–25.
- Jiang J, Kallemeijn WW, Wright DW, et al (2015) In vitro and in vivo comparative and competitive activity-based protein profiling of GH29  $\alpha$ -l-fucosidases. *Chem Sci* 6:2782–2789. doi: [10.1039/C4SC03739A](https://doi.org/10.1039/C4SC03739A)

- Jiang J, Kuo C-L, Wu L, et al (2016) Detection of Active Mammalian GH31  $\alpha$ -Glucosidases in Health and Disease Using In-Class, Broad-Spectrum Activity-Based Probes. *ACS Cent Sci* 2:351–358. doi: 10.1021/acscentsci.6b00057
- Kallemeijn WW, Scheij S, Hoogendoorn S, et al (2017) Investigations on therapeutic glucocerebrosidases through paired detection with fluorescent activity-based probes. *PLoS One* 12:1–23. doi: 10.1371/journal.pone.0170268
- Kallemeijn WW, Witte MD, Voorn-Brouwer TM, et al (2014) A Sensitive Gel-based Method Combining Distinct Cyclophellitol-based Probes for the Identification of Acid/Base Residues in Human Retaining  $\beta$ -Glucosidases. *J Biol Chem* 289:35351–35362.
- Kim W-D, Kobayashi O, Kaneko S, et al (2002)  $\alpha$ -Galactosidase from cultured rice (*Oryza sativa* L. var. Nipponbare) cells. *Phytochemistry* 61:621–630. doi: 10.1016/S0031-9422(02)00368-0
- Kizhner T, Azulay Y, Hainrichson M, et al (2015) Characterization of a chemically modified plant cell culture expressed human  $\alpha$ -Galactosidase-A enzyme for treatment of Fabry disease. *Mol Genet Metab* 114:259–267. doi: <https://doi.org/10.1016/j.ymgme.2014.08.002>
- Krissinel E, Henrick K (2004) Secondary-structure matching (SSM), a new tool for fast protein structure alignment in three dimensions. *Acta Crystallogr Sect D* 60:2256–2268. doi: 10.1107/S0907444904026460
- Kytidou K, Beenakker TJM, Westerhof LB, et al (2017) Human Alpha Galactosidases Transiently Produced in *Nicotiana benthamiana* Leaves: New Insights in Substrate Specificities with Relevance for Fabry Disease. *Front Plant Sci* 8:1026. doi: 10.3389/fpls.2017.01026
- Lenders M, Brand E (2018) Effects of Enzyme Replacement Therapy and Antidrug Antibodies in Patients with Fabry Disease. *J Am Soc Nephrol* 29:2265 LP – 2278. doi: 10.1681/ASN.2018030329
- Lenders M, Stypmann J, Duning T, et al (2016) Serum-Mediated Inhibition of Enzyme Replacement Therapy in Fabry Disease. *J Am Soc Nephrol* 27:256–264. doi: 10.1681/ASN.2014121226
- Linthorst GE, Hollak CEM, Donker-Koopman WE, et al (2004) Enzyme therapy for Fabry disease: Neutralizing antibodies toward agalsidase alpha and beta. *Kidney Int* 66:1589–1595. doi: <http://dx.doi.org/10.1111/j.1523-1755.2004.00924.x>
- Maranville E, Zhu A (2000) The Carboxyl Terminus of Coffee Bean  $\alpha$ -Galactosidase Is Critical for Enzyme Activity pressing C-terminal deletion mutants in the methyl-. *Arch Biochem Biophys* 373:225–230. doi: 10.1006/abbi.1999.1532
- Marques ARA, Mirzaian M, Akiyama H, et al (2016) Glucosylated cholesterol in mammalian cells and tissues: formation and degradation by multiple cellular  $\beta$ -glucosidases. *J Lipid Res*. 57:451–63. doi: 10.1194/jlr.M064923

- Marraccini Pierre, Rogers W John, Caillet Victoria, et al (2005) Biochemical and molecular characterization of alpha-D-galactosidase from coffee beans. *Plant Physiol Biochem* 43:909–920.
- Mathew CD, Balasubramaniam K (1987) Mechanism of action of  $\alpha$ -galactosidase. *Phytochemistry* 26:1299–1300. doi: 10.1016/S0031-9422(00)81798-7
- Mirzaian M, Wisse P, Ferraz MJ, et al (2017) Simultaneous quantitation of sphingoid bases by UPLC-ESI-MS/MS with identical  $^{13}\text{C}$ -encoded internal standards. *Clin Chim Acta* 466:178–184. doi: 10.1016/J.CCA.2017.01.014
- Mirzaian M, Wisse P, Ferraz MJ, et al (2016) Accurate quantification of sphingosine-1-phosphate in normal and Fabry disease plasma, cells and tissues by LC-MS / MS with  $^{13}\text{C}$ -encoded natural S1P as internal standard. *Clin Chim Acta* 459:36–44. doi: 10.1016/j.cca.2016.05.017
- Motabar O, Liu K, Southall N, et al (2010) High throughput screening for inhibitors of alpha-galactosidase. *Curr Chem Genomics* 4:67–73. doi: 10.2174/1875397301004010067
- Murali R, Ioannou YA, Desnick RJ, Burnett RM (1994) Crystallization and Preliminary X-ray Analysis of Human  $\alpha$ -Galactosidase A Complex. *J Mol Biol* 239:578–580. doi: 10.1006/jmbi.1994.1397
- Rappsilber J, Mann M, Ishihama Y (2007) Protocol for micro purification, enrichment, pre fractionation and storage of peptides for proteomics using StageTips. *Nat Protoc* 2:1896–1906. <https://doi.org/10.1038/nprot.2007.261>
- Rezende RM, Weiner HL (2017) History and mechanisms of oral tolerance. *Semin Immunol*. 30: 3-11. doi: <https://doi.org/10.1016/j.smim.2017.07.004>
- Sakuraba H, Murata-Ohsawa M, Kawashima I, et al (2005) Comparison of the effects of agalsidase alfa and agalsidase beta on cultured human Fabry fibroblasts and Fabry mice. *J Hum Genet* 51:180–188. doi: 10.1007/s10038-005-0342-9
- Sanchez-Niño MD, Carpio D, Sanz AB, et al (2015) Lyso-Gb3 activates Notch1 in human podocytes. *Hum Mol Genet* 24:5720–5732. doi: <https://doi.org/10.1093/hmg/ddv291>
- Schiffmann R, Kopp JB, Austin III HA, et al (2001) Enzyme Replacement Therapy in Fabry Disease A Randomized Controlled Trial. *JAMA* 285:2743–2749. doi: 10.1001/jama.285.21.2743
- Shen J-S, Busch A, Day TS, et al (2016) Mannose receptor-mediated delivery of moss-made  $\alpha$ -galactosidase A efficiently corrects enzyme deficiency in Fabry mice. *J Inherit Metab Dis* 39:293–303. doi: 10.1007/s10545-015-9886-9
- Toumi DS, Reustle I, Krczal GM, et al (2012) Molecular cloning and characterisation of a cDNA encoding a putative alkaline alpha-galactosidase from grapevine (*Vitis vinifera* L.) that is differentially expressed under osmotic stress. *Acta Physiol Plant* v. 34:891-903–2012 v.34 no.3. doi: 10.1007/s11738-011-0887-5

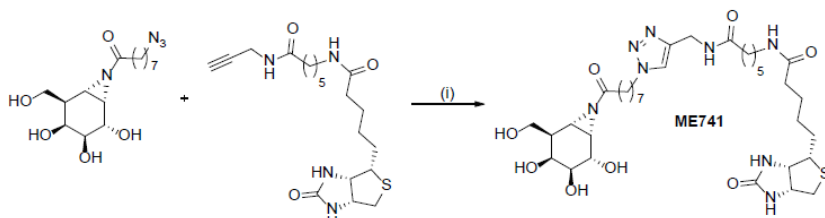


- Westerhof LB, Wilbers RHP, Roosien J, et al (2012) 3D Domain Swapping Causes Extensive Multimerisation of Human Interleukin-10 When Expressed In Planta. *PLoS One* 7:1–10. doi: 10.1371/journal.pone.0046460
- Westerhof LB, Wilbers RHP, van Raaij DR, et al (2014) Monomeric IgA can be produced in planta as efficient as IgG, yet receives different N-glycans. *Plant Biotechnol J* 12:1333–1342. doi: 10.1111/pbi.12251
- Wilbers RHP, Westerhof LB, van Noort K, et al (2017) Production and glyco-engineering of immunomodulatory helminth glycoproteins in plants. *Sci Rep* 7:45910. doi: 10.1038/srep45910
- Willems LI, Beenakker TJM, Murray B, et al (2014a) Potent and Selective Activity-Based Probes for GH27 Human Retaining  $\alpha$ -Galactosidases. *J Am Chem Soc* 136:11622–11625. doi: 10.1021/ja507040n
- Willems LI, Beenakker TJM, Murray B, et al (2014b) Synthesis of  $\alpha$ - and  $\beta$ -Galactopyranose-Configured Isomers of Cyclophellitol and Cyclophellitol Aziridine. *European J Org Chem* 2014:6044–6056. doi: 10.1002/ejoc.201402589
- Willems LI, Jiang J, Li KY, et al (2014c) From covalent glycosidase inhibitors to activity-based glycosidase probes. *Chem - A Eur J* 20:10864–10872. doi: 10.1002/chem.201404014
- Witte MD, Kallemeijn WW, Aten J, et al (2010) Ultrasensitive in situ visualization of active glucocerebrosidase molecules. *Nat Chem Biol* 6:907–913. doi: <https://doi.org/10.1038/nchembio.466>
- Witte MD, Van der Marel GA, Aerts JMFG, Overkleeft HS (2011) Irreversible inhibitors and activity-based probes as research tools in chemical glycobiology. *Org Biomol Chem* 9:5908–5926. doi: 10.1039/C1OB05531C
- Wu L, Jiang J, Jin Y, et al (2017) Activity-based probes for functional interrogation of retaining  $\beta$ -glucuronidases. *Nat Chem Biol* 13:867–873. doi: 10.1038/nchembio.2395
- Zhu A, Wang Z-K, Goldstein J (1995) Identification of tyrosine 108 in coffee bean  $\alpha$ -galactosidase as an essential residue for the enzyme activity. *Biochim Biophys Acta - Protein Struct Mol Enzymol* 1247:260–264. doi: 10.1016/0167-4838(94)00228-9

## Supplementary Material

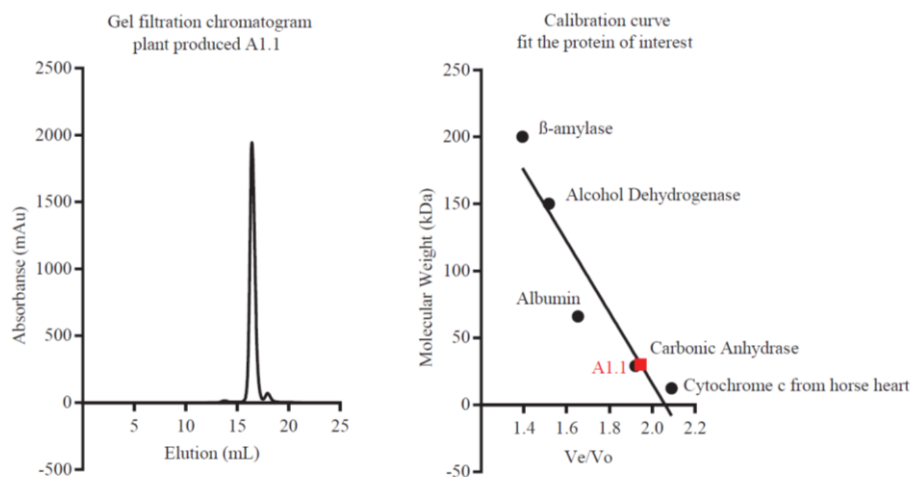
### Scheme S1. Synthesis of ME741 (Biotinylated $\alpha$ -Galactosidase ABP)

$\alpha$ -Galactose configured biotinylated cyclophellitol aziridine ME741 was synthesized by copper-catalyzed click chemistry of azido cyclophellitol aziridine intermediate with biotin alkyne (Figure S1).

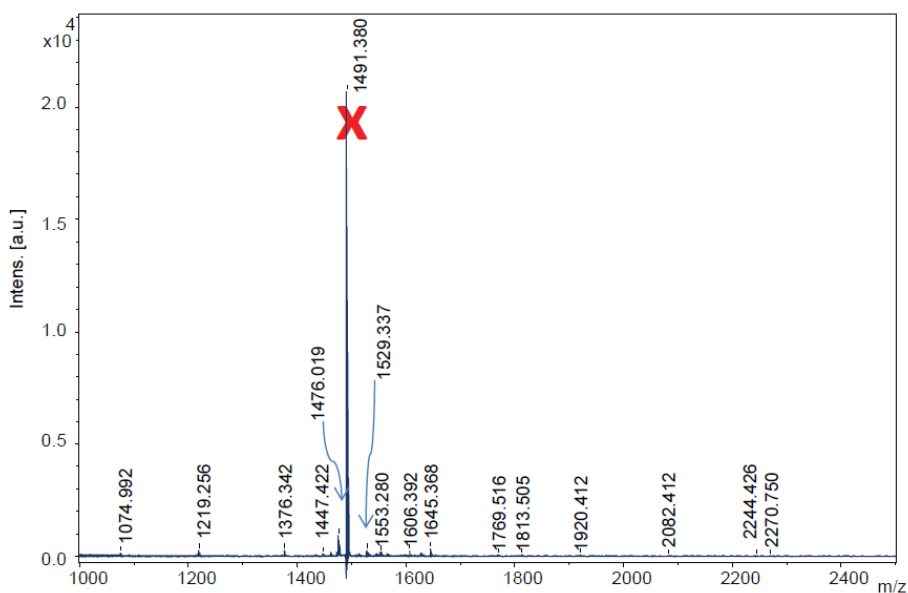


**Scheme S1. Synthesis of biotinylated  $\alpha$ -Galactosidase ABP ME741.** Reagents and conditions:

- (i)  $\text{CuSO}_4 \cdot \text{H}_2\text{O}$ , sodium ascorbate, DMF, rt, 18 h, 26%.

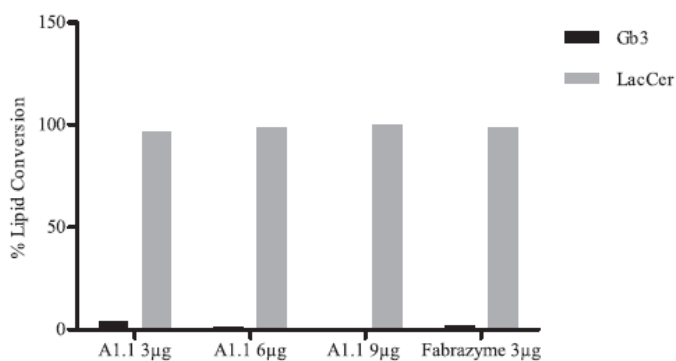


**Figure S1. Analytical gel filtration chromatography analysis of A1.1.** Left panel. Gel filtration chromatogram of the *N. benthamiana* produced A1.1, after its application in Superdex™ 200 Increase 10/300 GL. Right panel. Gel filtration chromatography calibration curve of proteins with known molecular weight, fitting the results of the plant produced A1.1. In black circle,  $\beta$ -amylase, alcohol dehydrogenase, albumin, carbonic anhydrase, cytochrome c from horse heart and Dextran. In red box A1.1.



**Figure S2. Determination of A1.1 N-glycosylation profile.** MALDI-TOF MS analysis of 2-aminobenzoic acid derivatised PNGase-A possibly released N-glycans of plant produced A1.1. No N-linked glycans were detected.

(A)



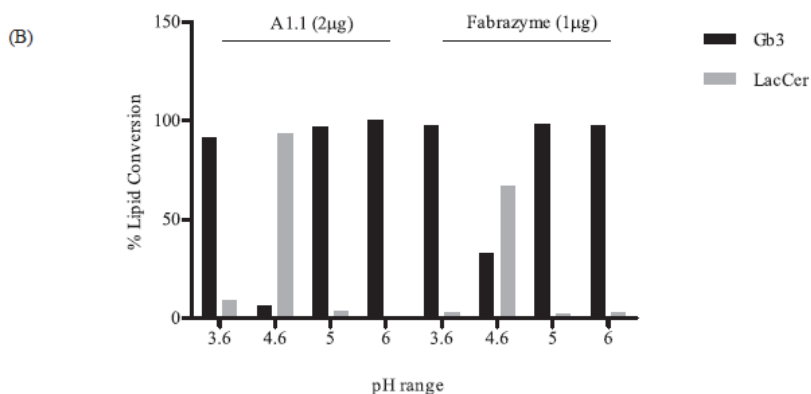


**Figure S3. Activity of A1.1 and Fabrazyme towards lipid substrates, as measured by HPLC analysis.** (A) HPLC analysis of degradation of C18-Gb3 to LacCer by different µg amounts of A1.1 or Fabrazyme. (B) Degradation of C18-Gb3 to LacCer by A1.1 or Fabrazyme in different pHs (3.6-6).

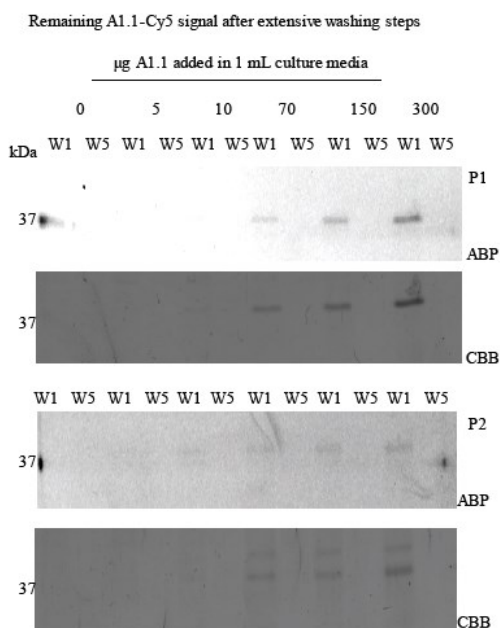


**Figure S4. Detection of remaining Cy5 signal after exposure of FD fibroblasts to prelabelled A1.1, from Figure 6.** After incubation of the 2 different FD fibroblasts, with prelabelled A1.1, extensive washing steps (x5) of the cells performed. To ensure that all of the not internalized to the cells prelabelled protein is washed out prior to lysate making, samples from both wash 1 and wash 5 (W1 and W5) were

analysed in SDS-PAGE, following the fluorescent signal. 10 % of the total wash volume was loaded on the gels. ABP= activity-based probe, CBB= Coomassie brilliant blue, P1= patient 1, P2= patient 2.

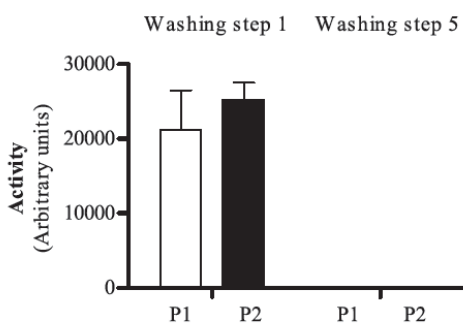


**Figure S5. 4MU- $\alpha$ -GAL activities found in washing steps of Figure 7.** After treatment with 300  $\mu$ g/mL of A1.1, the FD cells were extensively washed with PBS (x5 times). Activities in washing steps 1 and 5 were performed to ensure that no remaining activity is found to the cells prior to lysate making. P1= patient 1, P2= patient 2.

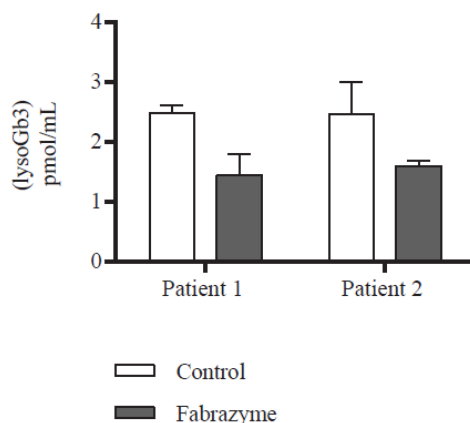


**Figure S6. LC-MS/MS analysis of lysoGb3 found in FD fibroblasts after incubation with Fabrazyme.** Fibroblasts from FD patients were grown in 12 well plates. Overnight incubation with 5  $\mu$ g/mL of Fabrazyme took place, followed by lipid extraction and LC-MS/MS analysis.  $^{13}\text{C}$ lysoGb3 was used as internal standard. (n=2, error bars indicate mean  $\pm$  standard deviation).

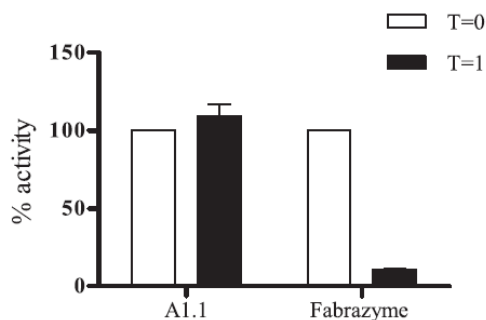


**Figure S7. 4MU- $\alpha$ -Gal activity of recombinant galactosidases after incubation in FD serum, before and after ERT.** A1.1 and Fabrazyme were incubated in Fabry serum at a concentration of 1 mg/mL each, before and after ERT (T=0, T=1, respectively). (n=2, error bars indicate mean  $\pm$  standard deviation).

**Table S1. Proteomics analysis using Swissprot (version June 2017)**

|             | Sample      | Protein Accession code | Protein Name              | Organism                    | Coverage % AA | ppm                  | Score                | Sequence                                       |
|-------------|-------------|------------------------|---------------------------|-----------------------------|---------------|----------------------|----------------------|--|
| Apoplast #1 | DMSO        |                        |                           |                             |               |                      |                      |  |
|             | Competition | Q8RX86                 | $\alpha$ -galactosidase 2 | <i>Arabidopsis thaliana</i> | 2             | -4                   | 28                   | EVIAVNQDK                                      |
|             | Pull down   | Q8RX86                 | $\alpha$ -galactosidase 2 | <i>Arabidopsis thaliana</i> | 2             | -7                   | 56                   | EVIAVNQDK                                      |
|             |             | Q42656                 | $\alpha$ -galactosidase   | <i>Coffea arabica</i>       | 4             | -5<br>-4             | 29<br>13             | GSTFPSGIK<br>ALADYVHSK                         |
|             |             | Q9FT97                 | $\alpha$ -galactosidase 1 | <i>Arabidopsis thaliana</i> | 3             | -4<br>-12            | 23<br>35             | STFPSGIK<br>YPVMTR                             |
| Apoplast #2 | DMSO        |                        |                           |                             |               |                      |                      |  |
|             | Competition | Q8RX86                 | $\alpha$ -galactosidase 2 | <i>Arabidopsis thaliana</i> | 2             | -8                   | 54                   | EVIAVNQDK                                      |
|             | Pull down   | Q42656                 | $\alpha$ -galactosidase   | <i>Coffea arabica</i>       | 8             | -6<br>-8<br>-8<br>-7 | 38<br>22<br>30<br>52 | GSTFPSGIK<br>ALADYVHSK<br>YPLMSK<br>APLLIGCDIR |
|             |             | Q8RX86                 | $\alpha$ -galactosidase 2 | <i>Arabidopsis thaliana</i> | 2             | 8                    | 56                   | EVIAVNQDK                                      |
|             |             | Q9FT97                 | $\alpha$ -galactosidase 1 | <i>Arabidopsis thaliana</i> | 7             | -7<br>5<br>-8        | 10<br>31<br>29       | STFPSGIK<br>LGIYSDAGYFTCSK<br>YPVMTR           |

**Table S2. Proteomics analysis using Swissprot (version June 2017, including *N. benthamiana*  $\alpha$ -galactosidase sequence).**

|                      | Sample      | Coverage<br>(% of AA) | Start-End | ppm       | Score           | Sequence        | AA identified |
|----------------------|-------------|-----------------------|-----------|-----------|-----------------|-----------------|---------------|
| Plant leaf lysate #1 | DMSO        | 0                     |           |           |                 |                 |               |
|                      | Competition | 0                     | 139-152   | 4         | 39              | LGIYSDAGSQTCSK  | 29            |
|                      | Pull down   | 7                     | 213-245   | 6         | 17              | TTGDISDNWDSMTSR |               |
| Apoplast #1          | DMSO        | 0                     |           |           |                 |                 |               |
|                      | Competition | 0                     |           |           |                 |                 |               |
|                      | Pull down   | 17                    | 118-126   | -5        | 29              | GSTFPSGIK       | 70            |
|                      |             |                       | 127-135   | -4        | 13              | ALADYVHSK       |               |
|                      |             |                       | 139-152   | 1         | 82              | LGIYSDAGSQTCSK  |               |
|                      |             |                       | 153-166   | -7        | 42              | QMTGSLGHEEQDAK  |               |
|                      |             | 231-245               | 8         | 22        | TTGDISDNWDSMTSR |                 |               |
|                      | 314-322     | -7                    | 56        | EVIAVNQDK |                 |                 |               |
| Apoplast #2          | DMSO        | 0                     |           |           |                 |                 |               |
|                      | Competition | 11                    | 118-126   | -8        | 20              | GSTFPSGIK       | 46            |
|                      |             |                       | 139-152   | 2         | 45              | LGIYSDAGSQTCSK  |               |
|                      |             |                       | 153-166   | -6        | 57              | QMTGSLGHEEQDAK  |               |
|                      |             |                       | 314-322   | -8        | 54              | EVIAVNQDK       |               |
|                      | Pull down   | 33                    | 118-126   | -6        | 38              | GSTFPSGIK       | 135           |
|                      |             |                       | 127-135   | -8        | 22              | ALADYVHSK       |               |
|                      |             |                       | 139-152   | 1         | 48              | LGIYSDAGSQTCSK  |               |
|                      |             |                       | 153-166   | 2         | 34              | QMTGSLGHEEQDAK  |               |
|                      |             |                       | 192-197   | -8        | 30              | YPIMSK          |               |
|                      |             |                       | 231-245   | 4         | 80              | TTGDISDNWDSMTSR |               |
|                      |             |                       | 291-300   | -7        | 52              | APLIIGCDLR      |               |
|                      |             |                       | 301-313   | -12       | 40              | SMDQTAHELNSK    |               |
|                      |             |                       | 314-322   | 8         | 56              | EVIAVNQDK       |               |
|                      |             |                       | 348-355   | -9        | 10              | VALVLWNR        |               |
|                      |             |                       | 381-388   | -5        | 34              | DLWAHSTK        |               |
|                      |             |                       | 393-405   | -9        | 12              | GQISASIDSHDCR   |               |
|                      |             | 406-412               | -13       | 33        | MYVLTPK         |                 |               |





# Chapter 5

---

$\alpha$ -D-Gal-cyclophellitol cyclosulfamidate  
and Gal-DNJ stabilize therapeutic  
lysosomal  
 $\alpha$ -galactosidase A and *Nicotiana*  
*benthamiana*, A1.1

---

*Kassiani Kytidou, Maria Joao Ferraz, Herman S. Overkleeft, Johannes M. F. G. Aerts, Marta Artola*

*Part of this work has been published in: Chemical Science, (2019); 10: 9233-9243. doi: 10.1039/c9sc03342d*



## Abstract

Deficiency in lysosomal  $\alpha$ -D-galactosidase leads to an X-linked inherited lysosomal storage disorder (LSD) known as Fabry disease. Current treatment of the disease involves the enzyme replacement therapy (ERT) agalsidase beta (Fabrazyme®) and the recently approved pharmacological chaperone 1-deoxygalactonojirimycin (Gal-DNJ, Migalastat®). Co-treatment of ERT with enzyme active-site stabilizers has shown to improve the outcome of the treatment of LSDs. Herein we describe the use of a newly synthesized  $\alpha$ -D-gal-cyclophellitol cyclosulfamidate as a new class of neutral, competitive glycosidase inhibitor, and the already available chaperone 1-deoxygalactonojirimycin as potential stabilizers of both human agalsidase beta and plant derived *Nicotiana benthamiana*, A1.1,  $\alpha$ -D-galactosidases. Our results suggest that both  $\alpha$ -D-gal-cyclophellitol cyclosulfamidate and Gal-DNJ are able to stabilize both enzymes *in vitro* and *in situ*, sharing a potential use as pharmaceutical chaperones.

## Introduction

Lysosomal  $\alpha$ -galactosidase A ( $\alpha$ -gal A, EC 3.2.1.22, GH27), is a retaining glycosidase which catalyses the hydrolysis of  $\alpha$ -1,4-linked galactosyl moieties from glycoconjugates, such as globotriaosylceramide (Gb3) and its sphingoid base, globotriaosylsphingosine (Lyso-Gb3).  $\alpha$ -gal A is encoded by the GLA (ID: 2717) gene at locus Xq22 (Desnick et al. 2003). Any mutation in the GLA gene might lead to a deficiency or complete loss of enzymatic activity, resulting in a lysosomal storage disorder (LSD) called Fabry disease (FD, OMIM #301500). This X-linked inherited LSD is characterized by toxic accumulation of Gb3 in lysosomes and Lyso-Gb3 in plasma and tissues (Aerts et al. 2008; Gold et al. 2013). The accumulation of glycosphingolipid metabolites is thought to cause progressive renal and cardiac insufficiency and CNS pathology in Fabry patients (Desnick et al. 2001). Due to the vast number of different mutations occurring in GLA gene, there is a broad range of FD phenotypes. In classic male FD patients, there is absence of  $\alpha$ -gal A, thus complete lack of enzymatic activity, whereas usually female carriers develop atypical disease manifestations, caused by missense mutations, having residual enzyme activity levels.

A well-established treatment of FD involves replacement of the defective enzyme via enzyme replacement therapy (ERT), through the intravenous treatment with recombinant human  $\alpha$ -gal A (agalsidase beta, Fabrazyme® or agalsidase alpha, Replagal®). Even though this treatment is currently available, its clinical efficacy is limited (Alegra et al. 2012; Arends et al. 2017b, a).

Recently, we have identified a novel plant  $\alpha$ -D-galactosidase, A1.1, derived from *Nicotiana benthamiana* (*N. benthamiana*), which shows great structural and biological similarities to the lysosomal enzyme ((Kytidou et al. 2018) Chapter 4). Crystal structure of A1.1 revealed that both human and plant enzymes share a highly conserved active site (Kytidou et al. 2018). In addition, A1.1 presents comparable pharmacokinetic abilities to human enzyme. In particular, *in situ* experiments with cultured Fabry fibroblasts treated with A1.1 showed correction of abnormal lipid levels, suggesting that A1.1 could be considered as a promising candidate for treatment of Fabry disease.

Another available treatment approach is the use of pharmacological chaperones (PC), to improve enzyme's folding, thus its activity. 1-Deoxygalactonojirimycin (Gal-DNJ **8**, Migalastat®, Figure 1) has recently been approved as pharmacological chaperone (PC) for the treatment of Fabry disease in patients with amenable mutations (Markham 2016). Gal-DNJ, after binding to mutant  $\alpha$ -gal A, it stabilizes its protein fold, allowing the mutant enzyme to

be trafficked to lysosomes. This treatment only targets individuals with specific mutations and its efficacy is greatly debated (Fan and Ishii 2007; Hughes et al. 2017; Sunder-Plassmann et al. 2018).

An alternative therapeutic intervention strategy has recently been proposed, which comprises jointly-administering recombinant enzyme and a pharmacological chaperone or enzyme stabilizer (Porto et al. 2009; Benjamin et al. 2012). This strategy aims to stabilize the recombinant enzyme in circulation such that larger proportions may reach the disease affected tissues; permitting the use of extended intervals between injections and lower enzyme dosages which should diminish side effects, improve patient's life-style and reduce treatment costs (Castelli et al. 2012; Warnock et al. 2015). The design and availability of inhibitors with good selectivity and pharmacokinetic/pharmacodynamic properties are highly required in order to drive this strategy into clinic (Castelli et al. 2012; Porto et al. 2012; Pisani et al. 2014).

We here report the biological evaluation of a newly synthesized enzyme stabilizer,  $\alpha$ -gal-cyclosulfamidate (**4**), as a new class of neutral, conformationally-constrained competitive  $\alpha$ -galactosidase inhibitor that acts by mimicry of the Michaelis complex conformation (Figure 1) (Artola et al. 2019). Together with this new inhibitor, the already available pharmacological chaperone, Gal-DNJ (**8**) is also tested for their ability to stabilize human and plant derived *N. benthamiana*  $\alpha$ -D-galactosidases. Our results reveal that both inhibitors are promising candidates in co-administration therapeutic strategy for Fabry disease.

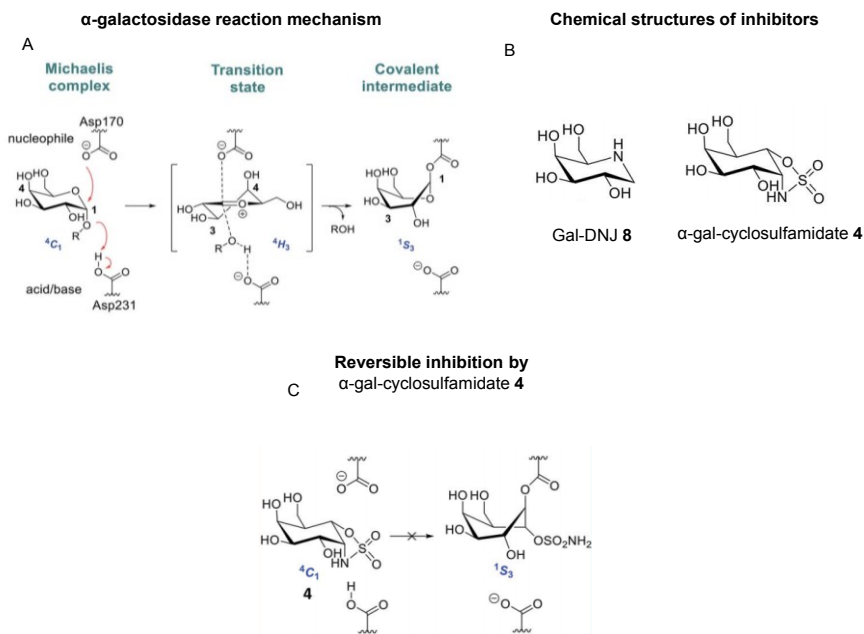


**Figure 1. Reaction coordinates of  $\alpha$ -galactosidases and inhibitors.** A. Reaction itinerary of retaining  $\alpha$ -galactosidase, showing conformations of the  ${}^4C_1$  Michaelis complex,  ${}^4H_3$  transition state, and  ${}^1S_3$  covalent intermediate. B. Chemical structures of 1-deoxygalactonojirimycin **8** and cyclosulfamidate **4**, C. Reversible inhibition by  $\alpha$ -gal cyclosulfamidate **4**.

## Results

The rational design and synthesis of  $\alpha$ -D-galactose configured cyclosulfamidate **4** together with crystallographic studies in complex with human  $\alpha$ -D-galactosidase is described in Artola et al. 2019.

### **Stabilization of human $\alpha$ -galactosidase by Gal-DNJ **8** and $\alpha$ -cyclosulfamidate **4** in cell culture medium.**

The lysosomal  $\alpha$ -gal A shows poor stability in plasma at pH of 7.3 - 7.4, with only ~25 % of the hydrolytic activity being retained after incubation of enzyme at 1  $\mu$ g/mL in human plasma for 30 minutes (Kytidou et al. 2017; Kizhner et al. 2017). At first, we investigated the ability of Gal-DNJ **8** and  $\alpha$ -cyclosulfamidate **4** to stabilize human  $\alpha$ -gal A in cell culture medium, pH 7.2, mirroring plasma conditions. Incubation of  $\alpha$ -gal A (25  $\mu$ L of 2.5  $\mu$ g/ $\mu$ L) in cell culture medium (Dulbecco's Modified Eagles Medium/Nutrient Mixture F-12 (DMEM/F12), supplemented with 10 % fetal calf serum and 1 % penicillin/streptomycin) led to 80 % loss of activity within 15 min, in line with the poor stability of this enzyme in blood plasma. To assess the stabilizing effects of Gal-DNJ **8** and  $\alpha$ -cyclosulfamidate **4** in cell culture media,  $\alpha$ -gal A was incubated with increasing concentrations of these compounds, followed by capture of the enzyme on concanavalin A (ConA) sepharose beads, washing to remove unbound inhibitor. Then, residual  $\alpha$ -galactosidase activity with fluorogenic 4-methylumbelliferyl (4MU)- $\alpha$ -D-galactopyranose substrate was quantified (Figure 2A). Gal-DNJ **8** and  $\alpha$ -cyclosulfamidate **4** both prevented inactivation of agalsidase beta in cell culture media (pH 7.2) - ~75 % residual  $\alpha$ -gal-A activity was retained after incubation with Gal-DNJ **8** (at 50  $\mu$ M) or **4** (at 500  $\mu$ M) (Figure 2B).

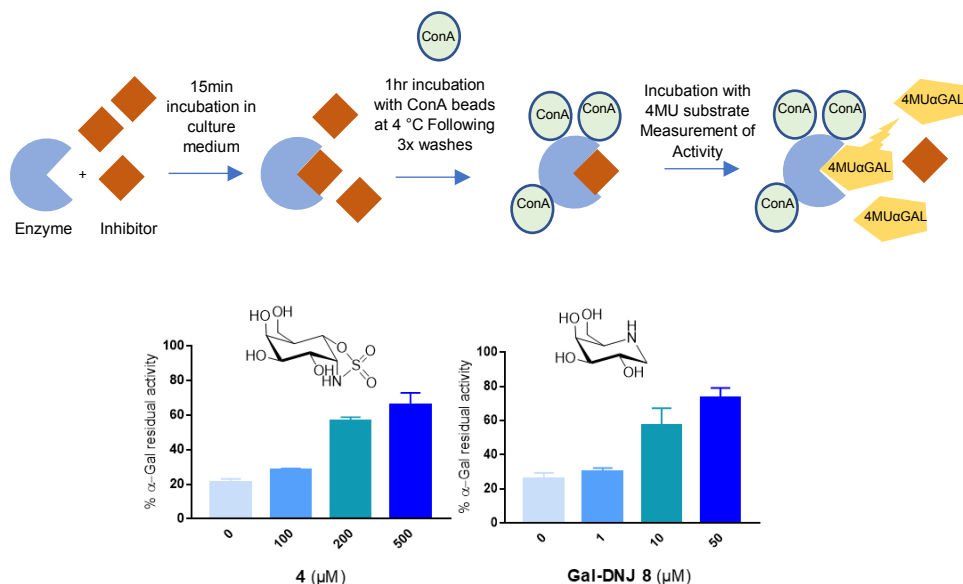


**Figure 2. Human  $\alpha$ -gal A stabilization by Gal-DNJ 8 and  $\alpha$ -cyclosulfamidate 4 in culture medium.** Upper part. Schematic representation of stabilization assay. Recombinant human  $\alpha$ -gal A (Fabrazyme) was incubated with inhibitor for 15 min in DMEM/F-12 medium and subsequently incubated with ConA sepharose beads for 1 h at 4 °C and washed to remove unbound inhibitor. Residual  $\alpha$ -Gal activity was quantified with 4-MU- $\alpha$ -gal substrate. Lower part. Percentage of  $\alpha$ -gal A residual activity measured after 15 min incubation in DMEM/F-12 medium in the presence of inhibitor  $\alpha$ -gal-cyclosulfamidate 4 (at 0, 100, 200, 500  $\mu$ M) and Gal-DNJ 8 (0, 1, 10 and 50  $\mu$ M), followed by post final ConA purification. Percentages are calculated considering the 100 % activity of  $\alpha$ -gal A obtained at 0 min incubation time (n=2, error bars indicate mean  $\pm$  standard deviation).

### Stabilization of plant alpha galactosidase A1.1 by Gal-DNJ 8 and $\alpha$ -cyclosulfamidate 4 in human plasma.

Similar to agalsidase beta, the plant alpha galactosidase A1.1 (chapter 4) presents poor stability in human plasma. A combination of  $\alpha$ -galactosidase A1.1 with an enzyme stabilizer could be a potential therapeutic alternative for Fabry disease. Therefore, the ability of Gal-DNJ 8 and  $\alpha$ -cyclosulfamidate 4 to stabilize an enzyme other than the human origin was also tested. Thus, A1.1 (400 ng) was first pre-incubated with and without 250  $\mu$ M of 25  $\mu$ M of Gal-DNJ 8 or  $\alpha$ -cyclosulfamidate 4 for 20 min at 37 °C in 20  $\mu$ L of 150 mM Mcllvaine buffer pH 5.3. The enzyme-inhibitor mixture was then passed over a 0.7-ml Pierce™ polyacrylamide spin desalting column (see materials and methods), in order to remove the excess of inhibitor. Afterwards, samples were incubated in 400  $\mu$ L of human plasma (AB) for different time periods (0, 15, 30, 45 and 60 min). Alpha galactosidase activity was then measured revealing that A1.1 was



successfully stabilized by both Gal-DNJ **8** and  $\alpha$ -cyclosulfamidate (Figure 3). Interestingly, A1.1 maintained over 90 % of its activity after 60 min incubation with Gal-DNJ **8** (25  $\mu$ M) or  $\alpha$ -cyclosulfamidate **4** (250  $\mu$ M) in human plasma, whereas the absence of inhibitor resulted in loss of enzymatic activity with just ~20 % remaining. These results suggest that competitive cyclosulfamidate inhibitors are also enzyme stabilizers of plant derived A1.1, an enzyme that holds promises on its use as an alternative recombinant enzyme for Fabry disease.

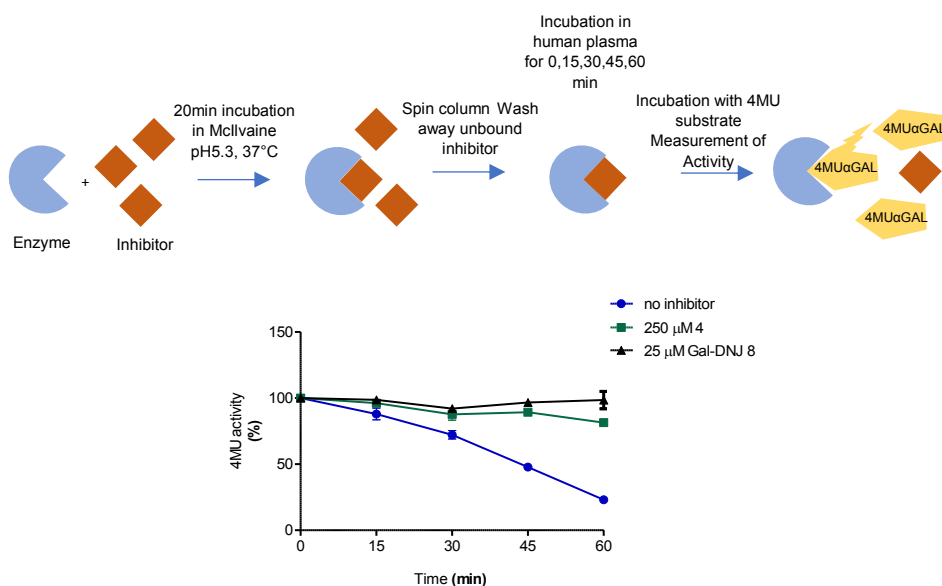


**Figure 3. Stabilization of A1.1 by Gal-DNJ **8** and  $\alpha$ -cyclosulfamidate **4** in human plasma over time.** A. Schematic representation of stabilization assay. A1.1 (400 ng) was incubated with and without 25  $\mu$ M of Gal-DNJ **8** or 250  $\mu$ M of **4** for 20 min at 37  $^{\circ}$ C in 20  $\mu$ L of 150 mM Mcllvaine buffer pH 5.3. The enzyme plus inhibitor mixtures were passed through a desalting column to remove the excess of inhibitors follow by incubations in 400  $\mu$ L of human plasma (AB) (protein concentration in plasma 1  $\mu$ g/mL). B. Samples were taken at different time intervals (0, 15, 30, 45, 60 min) and  $\alpha$ -galactosidase activity was measured using fluorogenic 4-methylumbelliferyl (4MU)- $\alpha$ -D-galactopyranose substrate. Only 20 % of A1.1 activity remained after 60 min incubation in human plasma, whereas higher than 90 % enzyme activity was observed under the same conditions in the presence of both Gal-DNJ **8** or **4**. Error bars indicate standard deviations, n=2.

**Competitive activity-based protein profile (ABPP) on recombinant  $\alpha$ -galactosidases.**

Next, we investigated the binding efficiency of both enzyme stabilizers Gal-DNJ **8** and  $\alpha$ -cyclosulfamidate **4**, towards human commercial agalsidase beta (Fabrazyme®) and agalsidase alpha (Replagal®), and the plant produced  $\alpha$ -galactosidase B (*N*-acetylgalactosaminidase, NAGA) (Chapter 3 (Kytidou et al. 2017)) via competitive activity-based protein profiling (ABPP, Figure 4). NAGA enzyme is reported to have residual  $\alpha$ -galactosidase activity (Kytidou et al. 2017) and mutant form of NAGA, NAGAEL, with further improved  $\alpha$ -gal activity, has been recently proposed as a promising alternative recombinant enzyme for the treatment of Fabry (Tajima et al. 2009; Kytidou et al. 2017). All enzymes were first incubated with increasing concentrations of Gal-DNJ **8** and  $\alpha$ -cyclosulfamidate **4** for 30 min at 37 °C, followed by incubation with 0.2  $\mu$ M of an  $\alpha$ -galactosidase Cy5 activity-based probe (ABP 10) for 30 min at 37 °C. Afterwards, the samples were analysed by sodium dodecyl sulfate-polyacrylamide gels (SDS- PAGE) and scanned as previously described (Willems et al. 2014; Kytidou et al. 2017). Competitive ABPP revealed that Gal-DNJ **8** (1-10  $\mu$ M) and  $\alpha$ -cyclosulfamidate **4** (100-500  $\mu$ M) inhibit both recombinant human agalsidase alpha and agalsidase beta, and plant produced *N*-acetylgalactosaminidase NAGA and its mutant form NAGAEL (data not shown).

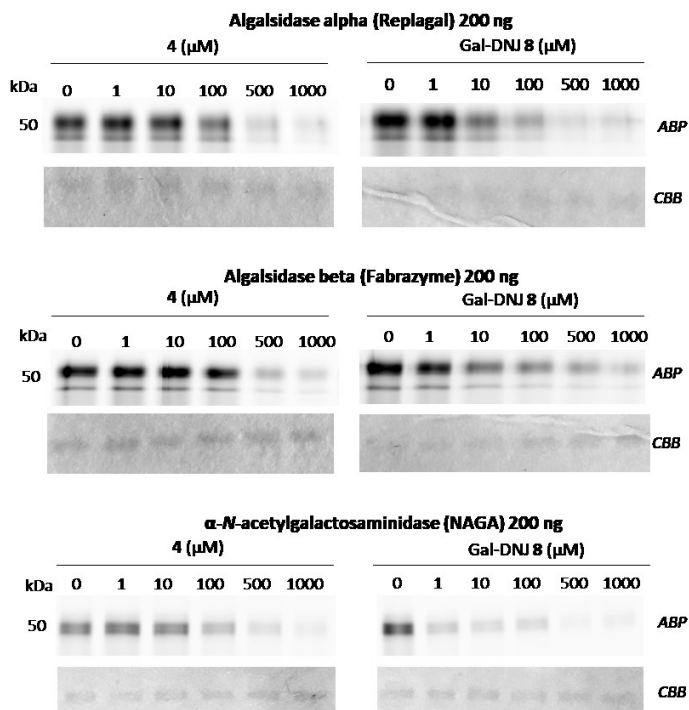


**Figure 4. Competitive ABPP in  $\alpha$ -galactosidases.** Agalsidase alpha (Replagal, 200 ng), agalsidase beta (Fabrazyme, 200 ng),  $\alpha$ -N-acetylgalactosaminidase (NAGA, 200 ng) and its mutant form NAGAEL (200 ng) were pre-incubated with Gal-DNJ **8** (0-1000  $\mu$ M) or  $\alpha$ -cyclosulfamidate **4** (0-1000  $\mu$ M) for 30 min at 37  $^{\circ}$ C, followed by fluorescent labelling with Cy5  $\alpha$ -galactosidase ABP (TB474) for 30 min at 37  $^{\circ}$ C. ABP: activity-based probe, CBB: coomassie brilliant blue staining.

### ***In situ* treatment of cultured fibroblasts from patients with Fabry disease.**

To further prove the stabilizing effect of both competitive inhibitors, we investigated their abilities *in situ*. First, 5 different primary cell lines from adult male Fabry patients were treated with either **8** (20  $\mu$ M) or **4** (200  $\mu$ M) (in blue), or with a combination of both enzyme agalsidase beta (100 ng) and stabilizing agent (in green) (Figure 5A). Treatment with 0.5 % DMSO was also performed, as a control. The cell lines used in this study were: wild-type (WT, Control) representing normal  $\alpha$ -gal A activity, 2 classic Fabry mutant fibroblasts (R301X and D136Y) with no  $\alpha$ -gal A activity and 2 atypical variant Fabry mutants (A143T and R112H) with substantially lowered residual  $\alpha$ -gal A activity. After 24h treatment, the cells were harvested and lysed in ice cold lysis buffer and the intracellular  $\alpha$ -gal A activity of the corresponding cell lysates was measured. WT cell line presented normal  $\alpha$ -gal A activity whereas untreated classic Fabry patients (R301X and D136Y) and variant mutation

samples (A143T and R112H) showed reduced enzymatic activity. None of the cell lines, not even classical Fabry fibroblasts R301X and D136Y, showed significant increase in  $\alpha$ -gal A activity when incubated with **8** (20  $\mu$ M) or **4** (200  $\mu$ M) alone for 24 h. Of note, Gal-DNJ **8** is known to enhance  $\alpha$ -gal A activity in R301Q lymphoblasts after *in situ* 4-day treatment of a 100  $\mu$ M daily dose (Asano et al. 2000). Treatment with Fabrazyme showed a considerable increase in  $\alpha$ -gal A activity in all the studied cell lines.

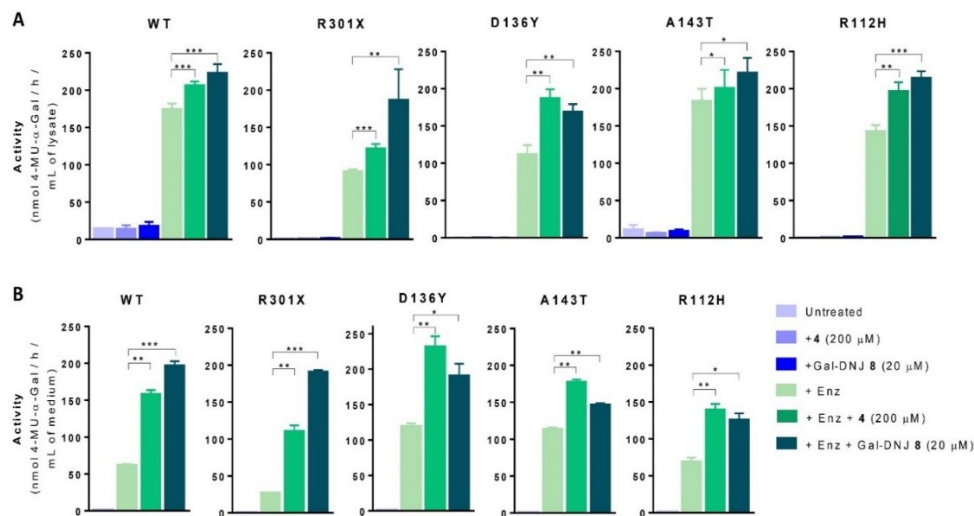


**Figure 5. Effect on  $\alpha$ -gal A activity in fibroblasts culture and medium following treatment with Gal-DNJ **8** and  $\alpha$ -cyclosulfamidate **4**.** A. Fibroblasts of WT, classic Fabry (R301X and D136Y) and variant Fabry (A143T and R112H) were treated with 0.5% DMSO or incubated with Gal-DNJ **8** (20  $\mu$ M),  $\alpha$ -cyclosulfamidate **4** (200  $\mu$ M), agalsidase beta (200 ng/mL) or a combination of enzyme and stabilizing agent for 24 h. Then, the medium was collected, cells were harvested, and  $\alpha$ -gal A activity was measured in the cell homogenates by 4-MU- $\alpha$ -gal assay. In all cell lines co-administration of Gal-DNJ **8** or  $\alpha$ -cyclosulfamidate **4** with agalsidase beta increased intracellular  $\alpha$ -gal A activity when compared to cells treated with only agalsidase beta. B.  $\alpha$ -Gal A activity in cell culture medium samples was measured after ConA purification.  $\alpha$ -Gal A activity is at least two times higher in all the cell lines treated with Gal-DNJ **8** (20  $\mu$ M) or  $\alpha$ -cyclosulfamidate **4** (200  $\mu$ M). Reported activities are mean  $\pm$  standard deviation from two biological replicates, each with two technical replicates, \*  $p < 0.5$ ; \*\*,  $p < 0.01$ ; \*\*\*,  $p < 0.001$ .

This effect was improved in most cases with the combinatorial treatment of Fabrazyme and **8** or **4** after 24 h incubation. In addition, we also measured  $\alpha$ -gal A activity in media in order to confirm that the increase in  $\alpha$ -gal A activity in cell lysates is due to stabilization of the enzyme (Figure 5B). Thus, culture media were collected before harvesting the cells and  $\alpha$ -gal A activity was measured after ConA purification.  $\alpha$ -Gal A activity in media was at least double in all the cell lines treated with **8** (20  $\mu$ M) or **4** (200  $\mu$ M), in accordance with these compounds preventing  $\alpha$ -gal A degradation during cell culture.

**Correction of Gb3 and LysoGb3 by Gal-DNJ 8 and  $\alpha$ -cyclosulfamidate 4 in Fabry fibroblasts.**

Elevated Gb3 metabolite is present in Fabry patients, which is further metabolized by acid ceramidase into LysoGb3 in lysosomes (Ferraz et al. 2016). LysoGb3 is a well-established hallmark of Fabry disease which allows diagnostic monitoring of disease progression (Aerts et al. 2008; Gold et al. 2013; Mirzaian et al. 2017; Maruyama et al. 2019), and has been linked to neuropathic pain and renal failure through its effect on nociceptive neurons and podocytes (Choi et al. 2015; Sanchez-Niño et al. 2015; Colpart and Félix 2017). We here studied the co-administration of Fabrazyme together with Gal-DNJ 8 and  $\alpha$ -cyclosulfamidate 4, and its efficiency in correcting these toxic metabolites. Lipids (Gb3 and LysoGb3) were measured by LC-MS/MS, after *in situ* treatment of cells (Figures 6A, B). Levels of Gb3 and LysoGb3 in wild type fibroblasts ranged around 2000 pmol/ml and 2 pmol/ml, respectively. Cultured fibroblasts from classic Fabry patients (R301X and D136Y) treated with Fabrazyme, resulted in a reduction of Gb3 and lysoGb3, to levels close to the ones observed in wild type cells. This reduction was similar when fibroblasts were treated with the combination of Gal-DNJ 8 (20  $\mu$ M) or  $\alpha$ -cyclosulfamidate 4 (200  $\mu$ M) and Fabrazyme. Variant Fabry A143T cell line presents normal Gb3 and lysoGb3 basal levels, whereas in R112H fibroblasts, these metabolites are increased and not corrected by Fabrazyme itself or inhibitor-Fabrazyme combination treatment (Artola et al. 2019).

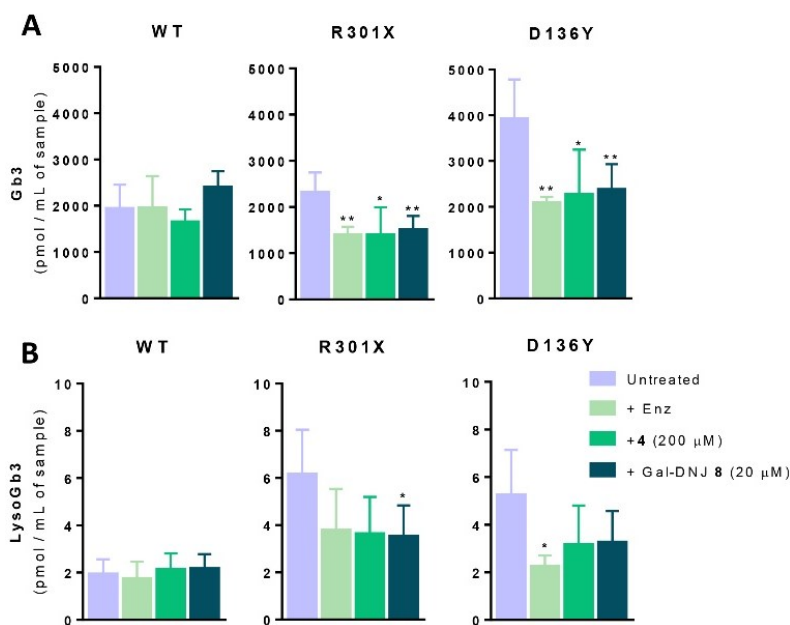


**Figure 6. Gb3 and Lyso-Gb3 quantification in cultured fibroblasts treated with Fabrazyme co-administrated with Gal-DNJ 8 and  $\alpha$ -cyclosulfamidate 4.** Gb3 (A) and lysoGb3 (B) levels (pmol/mL of sample) measured by LC-MS/MS in Fabry fibroblasts from WT and classic Fabry patients (R301X and D136Y) treated with Fabrazyme (200 ng/mL) with or without Gal-DNJ 8 (20  $\mu$ M) and  $\alpha$ -cyclosulfamidate 4 (200  $\mu$ M) for 24 h. Reported activities are mean  $\pm$  standard deviation from two biological replicates, each with two technical replicates, \*  $p < 0.5$ ; \*\*,  $p < 0.01$ .

#### 4-Day treatment of cultured fibroblasts with co-administration treatment increased $\alpha$ -gal A activity and Gb3 metabolites correction by $\alpha$ -cyclosulfamidate 4 and Gal-DNJ 8.

The potential beneficial effect of co-administration treatment *in situ* was further studied via extended incubation-time treatments. WT and classic Fabry (R301X) fibroblasts were treated with Fabrazyme (200 ng/mL) or with a combination of enzyme (200 ng/mL) and Gal-DNJ 8 (20  $\mu$ M) or  $\alpha$ -cyclosulfamidate 4 (200  $\mu$ M) for 4 days. Fibroblasts were treated every 24 h with new medium supplemented with enzyme with or without inhibitor, and medium samples were collected for  $\alpha$ -gal A activity measurements.  $\alpha$ -Gal A activity was 3-4 times higher in fibroblasts treated with the combination of recombinant  $\alpha$ -gal A and Gal-DNJ 8 (20  $\mu$ M) or  $\alpha$ -cyclosulfamidate 4 (200  $\mu$ M) than those treated with Fabrazyme alone (Figure 7A). This increase in  $\alpha$ -gal A activity correlates with the reduction of Lyso-Gb3 from  $\sim 14$  pmol/mL to  $\sim 4$  pmol/mL in the cell lysates of Fabry (classic R301X) fibroblasts (Figure 7B). We finally studied whether the amount of required ERT could be decreased when stabilized with 8 or 4 and still produce a similar effect. WT and Fabry (classic

R301X) fibroblasts were treated with Fabrazyme at 200 ng/mL and 100 ng/mL. This reduction in toxic metabolites can be achieved in 4 days with half the concentration of enzyme (100 ng/mL) when either Gal-DNJ **8** (20  $\mu$ M) or  $\alpha$ -cyclosulfamidate **4** (200  $\mu$ M) is added (Figure 7C, D), with a similar reduction of toxic LysoGb3 from  $\sim$ 10 pmol/mL to  $\sim$ 5-6 pmol/mL in the cell lysates of Fabry (classic R301X) fibroblasts (Figure 7E).

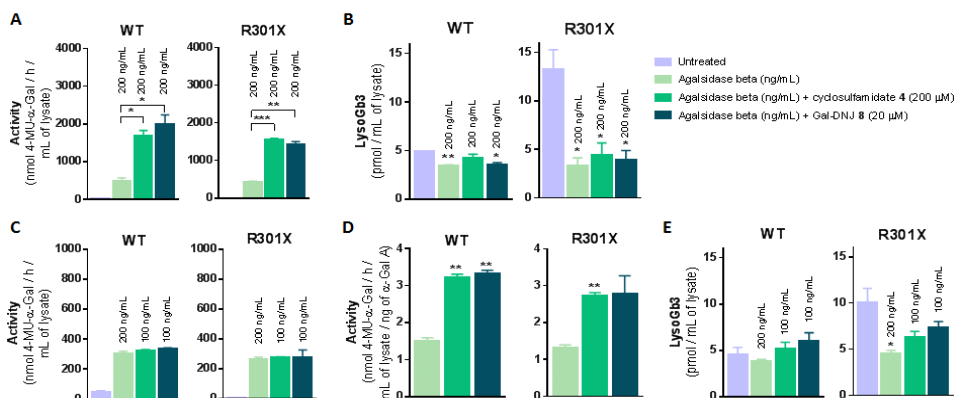


**Figure 7. Effect on  $\alpha$ -gal A activity and Lyso-Gb3 correction in cultured fibroblasts treated with Gal-DNJ **8** and  $\alpha$ -cyclosulfamidate **4**.** Fibroblasts of WT and classic Fabry (R301X) were incubated with agalsidase beta (200 ng/mL) or the combination of enzyme (200 ng/mL or 100 ng/mL) and stabilizing agent (**8** at 20  $\mu$ M or **4** at 200  $\mu$ M) for 4 days. Then, the medium was collected, cells were harvested, and  $\alpha$ -gal A activity was measured in the cell homogenates by 4-MU- $\alpha$ -gal assay. A. Intracellular  $\alpha$ -gal A activity in fibroblasts treated with agalsidase beta (200 ng/mL) or the combination of Gal-DNJ **8** (20  $\mu$ M) or  $\alpha$ -cyclosulfamidate **4** (200  $\mu$ M) with agalsidase beta (200 ng/mL) for 4 days. B. LysoGb3 levels measured by LC-MS/MS in Fabry fibroblasts from panel A. C. Intracellular  $\alpha$ -gal A activity is comparable in cell lines treated with the combination of Gal-DNJ **8** (20  $\mu$ M) or  $\alpha$ -cyclosulfamidate **4** (200  $\mu$ M) but this requires only half the concentration of agalsidase beta (100 ng/mL). D. Intracellular  $\alpha$ -gal A activity per ng of agalsidase beta in fibroblasts treated with agalsidase beta (100 ng/mL) or the combination of Gal-DNJ **8** (20  $\mu$ M) or  $\alpha$ -cyclosulfamidate **4** (200  $\mu$ M) with half concentration of agalsidase beta (100 ng/mL). E. LysoGb3 levels measured by LC-MS/MS in Fabry fibroblasts from panel C or D. Reported lipid levels are mean  $\pm$  standard deviation from two biological replicates, each with two technical replicates, \*  $p < 0.5$ ; \*\*,  $p < 0.01$ ; \*\*\*,  $p < 0.001$ .

## Discussion

Current ERT treatment for Fabry disease employs intravenous administration of recombinant human  $\alpha$ -galactosidase (agalsidase beta, Fabrazyme® or agalsidase alpha, Replagal®) and reduces the levels of Gb3 and lyso-Gb3 in some tissues of Fabry patients, but its clinical efficacy is still limited (Alegra et al. 2012; van Dussen et al. 2014; Arends et al. 2017b, a). One approach to overcome such limitations is to apply an alternative recombinant enzyme. Tajima and colleagues, first suggested the use of modified NAGA enzyme (NAGAEL), which has improved  $\alpha$ -gal activity and can eliminate possible immunoreactions raised by current ERT treatments (Tajima et al. 2009). Their findings were recapitulated in chapter 3 of this thesis (Kytidou et al. 2017). Another promising ERT candidate, is the *N. benthamiana*  $\alpha$ -galactosidase, A1.1, recently identified and biochemically characterized (chapter 4, (Kytidou et al. 2018)). This enzyme holds great promise as an improved ERT for Fabry due to its high  $\alpha$ -gal activity, great similarity with human enzyme and its easy production. In addition, a chemically cross-linked recombinant  $\alpha$ -galactosidase, with improved stability in human plasma has also been recently reported and studied (Ruderfer et al. 2018). This enzyme, Pegunigalsidase Alfa, is currently under clinical trials (Holida et al. 2019).

Since the limited enzyme stability in plasma is a major drawback, another therapeutic approach employs the use of enzyme active site binders that stabilize recombinant enzyme in circulation. Gal-DNJ **8** (Migalastat®) is currently in use in the clinic as the first pharmacological chaperone for Fabry disease. However it lacks selectivity versus the lysosomal  $\beta$ -glucosidase (GBA) (Artola et al. 2019). Here, we investigate the use of a new, first-in-class conformational  $\alpha$ -galactosidase inhibitor,  $\alpha$ -cyclosulfamidate **4**, as a potential stabilizer of both human (Fabrazyme) and plant (A1.1)  $\alpha$ -galactosidases.  $\alpha$ -Cyclosulfamidate **4** reversibly and selectively inhibits Fabrazyme with an  $IC_{50}$  value of 67  $\mu$ M and a  $K_i$  of 110  $\mu$ M (Artola et al. 2019). We demonstrate that  $\alpha$ -cyclosulfamidate **4** stabilizes recombinant human  $\alpha$ -D-galactosidase (agalsidase beta, Fabrazyme®) in cell culture medium. Interestingly, the same stabilization effect is observed with plant  $\alpha$ -galactosidase A1.1 in human plasma when incubated with 25  $\mu$ M of Gal-DNJ **8** or 250  $\mu$ M of  $\alpha$ -gal-cyclosulfamidate **4**.

To further study this stabilizing effect, we investigated whether Gal-DNJ **8** and  $\alpha$ -gal-cyclosulfamidate **4** would stabilize  $\alpha$ -gal A activity *in situ* conditions. Treatment of fibroblasts (WT, classic and variant Fabry cell lines) with only Gal-DNJ **8** (at 20  $\mu$ M) and  $\alpha$ -gal-cyclosulfamidate **4** (at 200  $\mu$ M) for 24 h showed no effect on  $\alpha$ -D-galactosidase activity. However, we observe an increased  $\alpha$ -D-



galactosidase activity in all cells treated with the combination of Fabrazyme and stabilizing agents (**8** at 20  $\mu$ M and **4** at 200  $\mu$ M) when compared to the cells treated only with Fabrazyme. This result also correlates with an increased  $\alpha$ -D-galactosidase activity in the cell medium of the cells treated with enzyme and **8** or **4**. The stabilizing effect is more pronounced when cells are treated for longer time (4 days), suggesting that the Fabrazyme complexed with Gal-DNJ **8** or  $\alpha$ -gal-cyclosulfamidate **4** is stabilized in the cell medium, internalized and dissociated from the reversible inhibitor in the lysosomes. Finally, co-administration of Gal-DNJ **8** or  $\alpha$ -gal-cyclosulfamidate **4** with Fabrazyme highlights a similar correction of toxic Gb3 and lyso-Gb3 metabolite levels as with the ERT alone. Importantly, similar  $\alpha$ -gal A activity and correction of toxic metabolites is achieved with half the concentration of Fabrazyme when this is stabilized by Gal-DNJ **8** or  $\alpha$ -gal-cyclosulfamidate **4**. The synergy between Gal-DNJ **8** and the human recombinant  $\alpha$ -gal A in cultured fibroblasts from Fabry patients has recently been demonstrated both in Fabrazyme and Replagal (Porto et al. 2012; Pisani et al. 2014). This synergism, together with our Fabrazyme stabilization results, supports the idea that the efficacy of a combination treatment may be superior to ERT or PC alone for several reasons. Co-administration of ERT and active site inhibitor may be effective in all Fabry patients, independent of mutations in their endogenous  $\alpha$ -gal A. Furthermore, stabilization of the recombinant human  $\alpha$ -gal A by a stabilizing agent may reduce the required enzyme dosages or extend IV injections intervals, and therefore improve patient's life-style and reduce side effects and treatment costs.

In conclusion, the combination treatment of recombinant enzyme together with chaperones or enzyme stabilizers prompts great expectations for Fabry treatment. The newly developed inhibitor cyclosulfamidate **4** although it is a 1000-fold weaker inhibitor of recombinant  $\alpha$ -gal A compared to Gal-DNJ **8** *in vitro*, it stabilizes  $\alpha$ -gal A *in situ* at only 10 fold higher concentration and proves that competitive glycosidase inhibitors are attractive starting points for clinical development as stabilizers of (recombinant) glycosidases in the context of lysosomal storage disorders. The improvement of recombinant enzyme stability in human plasma is of great demand and the use of such stabilizers holds great promises.

## Material and Methods.

**Tissue and cell samples.** Patients with Fabry disease were diagnosed on the basis of reduced  $\alpha$ -gal A activity and/or demonstration of an abnormal genotype. Wild-type male human fibroblasts (c104) were obtained from Cambrex-Lonza (CC-2511, lot nr 104564, East Rutherford, NJ, USA). Fibroblast cell lines from classical FD (R301X and D136Y) and variant FD (A143T and R112H) individuals were obtained from the Lysosomal Outpatient Clinic of the Academic Medical Center in Amsterdam (AMC). Informed consent was obtained from all patients for investigations in accordance with the Declaration of Helsinki. For lysis, cells were washed three times with PBS, subsequently lysed by scraping in potassium phosphate buffer ( $K_2HPO_4$ –  $KH_2PO_4$ , 25 mM, pH 6.5, supplemented with 0.1 % (v/v) Triton X-100 and protease inhibitor cocktail (Roche, Basel, Switzerland), aliquoted and stored at  $-20\text{ }^\circ\text{C}$  until use. Lysate protein concentrations were determined with a Bradford assay using BSA as a standard. Naga enzyme was produced in *Nicotiana benthamiana* plants and purified in house as described in chapter 3, (Kytidou et al. 2017).

***In vitro* stabilization of Fabrazyme in cell culture medium.** Inhibitors' stabilization effect was studied in Dulbecco's Modified Eagles Medium/Nutrient Mixture F-12 (DMEM/F12, Sigma-Aldrich) medium, supplemented with 10 % fetal calf serum and 1 % penicillin/streptomycin at pH 7.2, mimicking fibroblasts cell culture conditions. Agalsidase beta (25  $\mu\text{L}$ , 2.5 mg/mL) was incubated at  $37\text{ }^\circ\text{C}$  in cell culture medium at pH 7.2 for 5, 10, 15, 20, 30 and 60 min. After 15 min, 80 % degradation was observed, and this time point was used for further analysis. Thus, inhibitors (12.5  $\mu\text{L}$ ) at increasing concentrations (starting around the  $IC_{50}$  value of the corresponding inhibitor) were incubated with agalsidase beta (12.5  $\mu\text{L}$ , 5 mg/mL) in cell medium conditions at pH 7.2 for 15 min and 0 min (for 100 % hydrolytic activity reference). Then, in duplicates 25  $\mu\text{L}$  of sample (12.5  $\mu\text{L}$  enzyme plus 12.5  $\mu\text{L}$  inhibitor in cell culture medium and 1 % DMSO) were incubated in a shaker at  $4\text{ }^\circ\text{C}$  for 1 hour with 25  $\mu\text{L}$  of ConA beads. The samples were next centrifuged at 16000 rcf for 10 minutes at  $4\text{ }^\circ\text{C}$  and the supernatant was discarded. The ConA beads were likewise washed 3x with 500  $\mu\text{L}$  of washing buffer (sodium acetate buffer pH 6 supplemented with 0.1 M NaCl, 1 mM  $CaCl_2$  and 1 mM  $MnCl_2$ ). Afterwards, 100  $\mu\text{L}$  of 4-MU- $\alpha$ -D-galactopyranoside substrate (4.2 mM) in 150 mM McIlvaine buffer pH 4.6 supplemented with 0.1 % BSA (w/v) was added to the ConA beads and the mixture was incubated for 30 min at  $37\text{ }^\circ\text{C}$ . Finally, all enzyme reactions were quenched with 200  $\mu\text{L}$  1 M NaOH-Glycine (pH 10.3), and liberated 4MU fluorescence was measured with a LS55

fluorescence spectrophotometer (Perkin Elmer;  $\lambda_{EX}$  366 nm,  $\lambda_{EM}$  445 nm). Values plotted for [I] are those in the final reaction mixture, containing E + I + S and the percentage of  $\alpha$ -galactosidase activity was calculated considering incubation time 0 min as 100 % activity.

***In vitro* stabilization of A1.1 in human plasma.** The *N. benthamiana*  $\alpha$ -galactosidase A1.1 (400 ng), was first incubated with 25  $\mu$ M of Gal-DNJ or 250  $\mu$ M of  $\alpha$ -gal-cyclosulfamidate **2** or 0.5 % DMSO (assay total volume 20  $\mu$ L) for 20 min, at 37 °C (water bath) in 150 mM citric/phosphate (McIlvaine) buffer, pH 5.3. Then the samples were passed through 0.7-ml Pierce™ polyacrylamide spin desalting columns, pre-equilibrated with 150 mM citric/phosphate (McIlvaine) buffer, pH 5.3. Then, samples were incubated in 400  $\mu$ L human plasma (AB) (protein concentration, 1  $\mu$ g per mL of plasma) and samples were taken at different time points (0, 15, 30, 45, 60 min). Measurement of 4-MU- $\alpha$ -galactosidase activities of the different samples followed, exactly as described earlier (Blom et al. 2003; Kytidou et al. 2017).

**Competitive activity-based protein profile (ABPP) in recombinant  $\alpha$ -galactosidases.** Agalsidase beta or alpha (200 ng), or *N*-acetylgalactosaminidase (NAGA, 200 ng) were incubated with different concentrations of both inhibitor **2** and GalDNJ **1**, ranging from 1 to 1000  $\mu$ M, for 15 min. Then, enzymes were also incubated with 0.2  $\mu$ M of Cy5  $\alpha$ -Gal ABP TB474, for 30 min in a water bath at 37 °C. After ABP incubation, proteins were denatured by boiling the samples with Laemmli buffer (50 % (v/v) 1 M Tris-HCl, pH 6.8, 50 % (v/v) 100 % glycerol, 10 % (w/v) DTT, 10 % (w/v) SDS, 0.01 % (w/v) bromophenol blue) for 5 min at 98 °C, and separated by electrophoresis on sodium dodecyl sulphate-polyacrylamide gels, 10 % (SDS-PAGE), following fluorescent scanning of the gels as previously described (Willems et al. 2014; Kytidou et al. 2017). Coomassie brilliant blue staining of the gels was performed in order to show equal protein loading.

***In situ* treatment of cultured fibroblasts from patients with Fabry disease. 24 h Treatment.** Fibroblasts (5 cell lines (males): WT, Fabry variants R112H and A143T, and Fabry classic D136Y and R301X) were grown in 12 well plates (0.5 mL of medium) in a humidified incubator at 37 °C with 5 % CO<sub>2</sub>. Experiments were performed in triplicates. Fibroblasts were untreated as control (1  $\mu$ L DMSO), or treated with 1  $\mu$ L of 100  $\mu$ g/mL of agalsidase beta, with inhibitor **4** (1  $\mu$ L of 100 mM stock solution, final concentration 200  $\mu$ M) or Gal-DNJ **8** (1  $\mu$ L of 10 mM stock solution, final concentration 20  $\mu$ M), or with the combination of 1  $\mu$ L of 100  $\mu$ g/mL of agalsidase beta and inhibitor **4** or Gal-DNJ **8** at 200 or

20  $\mu\text{M}$ , respectively, followed by 24 h incubation. Next, the medium was collected for  $\alpha$ -galactosidase activity assays and cells were washed, collected (combine the triplicates) and lysed in ice-cold 25 mM phosphate buffer, pH 6.5, supplemented with 0.1 % Triton X-100 and protease inhibitor cocktail table (Roche). The lysates were stored at  $-20\text{ }^{\circ}\text{C}$  until further use.

**4-day Treatment.** Fibroblasts WT and classic Fabry (R301X) cell lines were grown in 12 well plates (0.5 mL of medium) in a humidified incubator at  $37\text{ }^{\circ}\text{C}$  with 5 %  $\text{CO}_2$ . Experiments were performed in triplicates. Fibroblasts were untreated as control (1  $\mu\text{L}$  DMSO), or treated with 1  $\mu\text{L}$  of 100 ng/ $\mu\text{L}$  of agalsidase beta, or with the combination of 1  $\mu\text{L}$  of 100 ng/ $\mu\text{L}$  agalsidase beta and inhibitor **4** (1  $\mu\text{L}$  of 100 mM stock solution, final concentration 200  $\mu\text{M}$ ) or Gal-DNJ **8** (1  $\mu\text{L}$  of 10 mM stock solution, final concentration 20  $\mu\text{M}$ ), followed by a 4-day incubation. The medium was collected for  $\alpha$ -galactosidase activity assays every 24 h and new medium supplemented with DMSO, agalsidase beta or the combination of enzyme and inhibitor was added. On the fifth day, cells were washed, collected (combine the triplicates) and lysed in ice-cold 25 mM phosphate buffer, pH 6.5, supplemented with 0.1 % Triton X-100 and protease inhibitor cocktail table (Roche). The lysates were stored at  $-20\text{ }^{\circ}\text{C}$  until further use. A second experiment was performed in treated fibroblast WT and classic Fabry (R301X) with 1  $\mu\text{L}$  of DMSO as control, or treated with 1  $\mu\text{L}$  of 100 ng/ $\mu\text{L}$  of agalsidase beta, or with the combination of half amount of enzyme (1  $\mu\text{L}$  of 50 ng/ $\mu\text{L}$  agalsidase beta) and inhibitor **4** (1  $\mu\text{L}$  of 100 mM stock solution, final concentration 200  $\mu\text{M}$ ) or Gal-DNJ **8** (1  $\mu\text{L}$  of 10 mM stock solution, final concentration 20  $\mu\text{M}$ ), followed by 4-day incubation. Released 4-MU was fluorometrically quantified in fibroblast lysates as described above (Blom et al. 2003). Reactions were performed in duplicates for 30 min at  $37\text{ }^{\circ}\text{C}$  at 4.2 mM of 4-methylumbeliferone(4-MU)- $\alpha$ -D-galactopyranoside in 150 mM citrate-phosphate buffer pH 4.6 supplemented with 0.1 % (w/v) BSA. Reaction were as follow: 15  $\mu\text{L}$  of Buffer with  $\alpha$ -GAL B inhibitor NAGA (100  $\mu\text{M}$ ) was incubated for 30 minutes at  $37\text{ }^{\circ}\text{C}$  with 10  $\mu\text{L}$  of fibroblast lysate, then 100  $\mu\text{L}$  of 4MU substrate (4.2 mM) was added and the mixture was incubated for 30 min. Finally, stop buffer was added (200  $\mu\text{L}$ ) and fluorescence was measured.  $\alpha$ -Galactosidase activity in the cell medium samples was measured with a ConA purification pre-step to wash away the competitive inhibitors. Thus, in duplicate 25  $\mu\text{L}$  of sample medium was incubated in a shaker at  $4\text{ }^{\circ}\text{C}$  for 1 hour with 25  $\mu\text{L}$  of ConA beads. Then, the samples were centrifuged at 16000 rcf for 5 minutes at  $4\text{ }^{\circ}\text{C}$  and the supernatant was discarded. The conA beads were likewise washed 3x with 200  $\mu\text{L}$  of washing buffer (sodium acetate buffer pH 6 supplemented with 0.1 M NaCl, 1 mM  $\text{CaCl}_2$  and 1 mM  $\text{MnCl}_2$ ). Afterwards,

100  $\mu$ L of 4-MU substrate (4.2 mM) was added to the ConA beads and the mixture was incubated for 30 min at 37 °C. Finally, stop buffer was added (200  $\mu$ L) and fluorescence was measured.

**Gb3 and LysoGb3 determination.** Gb3 and LysoGb3 were extracted as previously described by a modification of the Bligh and Dyer method using acidic buffer (100 mM ammonium formate buffer pH 3.1) (Mirzaian et al. 2017). Prior to extraction, 20  $\mu$ L of the internal standard C17-dh-Ceramide (20  $\mu$ M) and 20  $\mu$ L of  $^{13}\text{C}5$ -LysoGb3 (0.1  $\mu$ M) were added to 50  $\mu$ L of cell homogenate.10 Briefly, lipids were extracted by adding methanol, chloroform, and ammonium formate buffer (1:1:0.9; v/v/v) which resulted in 2 phases. The upper phase was dried under N<sub>2</sub> stream and further extracted with water/butanol (1:1; v/v) before being applied to the UPLC-MS. The lower phase was transferred to a Pyrex tube and de-acylated in a microwave for 1 h with 500  $\mu$ L of methanolic NaOH (0.1 M). De-acylated lipids were additionally extracted with water/butanol (1:1; v/v) before being applied to the UPLC-MS. Lipids were analysed by reverse-phase liquid Chromatography using a Waters UPLC-Xevo-TQS micro and a BEH C18 column, 2.1  $\times$  50 mm with 1.7  $\mu$ m particle size (Waters, USA). Data was processed with MassLynx 4.1 Software (Waters Corporation, USA).

## References

- Aerts JMFG, Groener JE, Kuiper S, et al (2008) Elevated globotriaosylsphingosine is a hallmark of Fabry disease. *Proc Natl Acad Sci U S A* 105:2812–2817. doi: 10.1073/pnas.0712309105
- Alegra T, Vairo F, de Souza M V, et al (2012) Enzyme replacement therapy for Fabry disease: A systematic review and meta-analysis. *Genet Mol Biol* 35:947–954. doi: <https://doi.org/10.1590/S1415-47572012000600009>
- Arends M, Biegstraaten M, Hughes DA, et al (2017a) Retrospective study of long-term outcomes of enzyme replacement therapy in Fabry disease: Analysis of prognostic factors. *PLoS One* 12:1–17. doi: 10.1371/journal.pone.0182379
- Arends M, Wijburg FA, Wanner C, et al (2017b) Favourable effect of early versus late start of enzyme replacement therapy on plasma globotriaosylsphingosine levels in men with classical Fabry disease. *Mol Genet Metab* 121:157–161. doi: 10.1016/j.ymgme.2017.05.001
- Artola M, Hedberg C, Rowland RJ, et al (2019)  $\alpha$ -D-Gal-cyclophellitol cyclosulfamidate is a Michaelis complex analog that stabilizes therapeutic lysosomal  $\alpha$ -galactosidase A in Fabry disease. *Chem Sci* 10:9233–9243. doi: 10.1039/C9SC03342D
- Asano N, Ishii S, Kizu H, et al (2000) *In vitro* inhibition and intracellular enhancement of lysosomal  $\alpha$ -galactosidase activity in Fabry lymphoblasts by 1-deoxygalactonojirimycin and its derivatives. *Eur J Biochem* 267:4179–4186. doi: 10.1046/j.1432-1327.2000.01457.x
- Benjamin ER, Khanna R, Schilling A, et al (2012) Co-administration with the pharmacological chaperone AT1001 increases recombinant human  $\alpha$ -galactosidase a tissue uptake and improves substrate reduction in Fabry mice. *Mol Ther* 20:717–726. doi: 10.1038/mt.2011.271
- Blom D, Speijer D, Linthorst GE, et al (2003) Recombinant Enzyme Therapy for Fabry Disease: Absence of Editing of Human  $\alpha$ -Galactosidase A mRNA. *Am J Hum Genet* 72:23–31. doi: <https://doi.org/10.1086/345309>
- Castelli J, Sitaraman S, Lockhart DJ, et al (2012) Safety and pharmacodynamic effects of a pharmacological chaperone on  $\alpha$ -galactosidase A activity and globotriaosylceramide clearance in Fabry disease: report from two phase 2 clinical studies. *Orphanet J Rare Dis* 7:91. doi: 10.1186/1750-1172-7-91
- Choi L, Vernon J, Kopach O, et al (2015) The Fabry disease-associated lipid Lyso-Gb3 enhances voltage-gated calcium currents in sensory neurons and causes pain. *Neurosci Lett* 594:163–168. doi: 10.1016/j.neulet.2015.01.084
- Colpart P, Félix S (2017) Fabry nephropathy. *Arch Pathol Lab Med* 141:1127–1131. doi: 10.5858/arpa.2016-0418-RS
- Desnick RJ, Brady R, Barranger J, et al (2003) Fabry Disease, an Under-Recognized Multisystemic Disorder: Expert Recommendations for Diagnosis, Management,

- and Enzyme Replacement Therapy. *Ann Intern Med* 138:338–346. doi: 10.7326/0003-4819-138-4-200302180-00014
- Desnick, R.J., Ioannou Y.A. (2001).  $\alpha$ -Galactosidase a deficiency. Fabry disease, in Scriver C.R., Beaudet A.L., Sly W.S., Valle D. (Eds) *The Metabolic and Molecular Bases of Inherited Disease*, 8th ed. McGraw-Hill, New York, 3733-3774.
- Fan J-Q, Ishii S (2007) Active-site-specific chaperone therapy for Fabry disease. *FEBS J* 274:4962–4971. doi: 10.1111/j.1742-4658.2007.06041.x
- Ferraz MJ, Marques ARA, Appelman MD, et al (2016) Lysosomal glycosphingolipid catabolism by acid ceramidase: formation of glycosphingoid bases during deficiency of glycosidases. *FEBS Lett* 590:716–725. doi: 10.1002/1873-3468.12104
- Gold H, Mirzaian M, Dekker N, et al (2013) Quantification of globotriaosylsphingosine in plasma and urine of fabry patients by stable isotope ultraperformance liquid chromatography-tandem mass spectrometry. *Clin Chem* 59:547–556. doi: 10.1373/clinchem.2012.192138
- Holida MD, Bernat J, Longo N, et al (2019) Once every 4 weeks - 2 mg/kg of pegunigalsidase alfa for treating Fabry disease Preliminary results of a phase 3 study. *Mol Genet Metab* 126:S73. doi: <https://doi.org/10.1016/j.ymgme.2018.12.176>
- Hughes DA, Nicholls K, Shankar SP, et al (2017) Oral pharmacological chaperone migalastat compared with enzyme replacement therapy in Fabry disease: 18-month results from the randomised phase III ATTRACT study. *J Med Genet* 54:288 LP – 296. doi: 10.1136/jmedgenet-2016-104178
- Kizhner T, Azulay Y, Hainrichson M, et al (2017) Characterization of a chemically modified plant cell culture expressed human  $\alpha$ -Galactosidase-A enzyme for treatment of Fabry disease. *Mol Genet Metab* 114:259–267. doi: 10.1016/j.ymgme.2014.08.002
- Kytidou K, Beekwilder J, Artola M, et al (2018) *Nicotiana benthamiana*  $\alpha$ -galactosidase A1.1 can functionally complement human  $\alpha$ -galactosidase A deficiency associated with Fabry disease. *J Biol Chem* 293:10042–10058. doi: 10.1074/jbc.RA118.001774
- Kytidou K, Beenakker TJM, Westerhof LB, et al (2017) Human Alpha Galactosidases Transiently Produced in *Nicotiana benthamiana* Leaves: New Insights in Substrate Specificities with Relevance for Fabry Disease. *Front Plant Sci* 8:1026. doi: 10.3389/fpls.2017.01026
- Markham A (2016) Migalastat: First Global Approval. *Drugs* 76:1147–1152. doi: 10.1007/s40265-016-0607-y
- Maruyama H, Miyata K, Mikame M, et al (2019) Effectiveness of plasma lyso-Gb3 as a biomarker for selecting high-risk patients with Fabry disease from multispecialty clinics for genetic analysis. *Genet Med* 21:44–52. doi: <https://doi.org/10.1038/gim.2018.31>
- Mirzaian M, Wisse P, Ferraz MJ, et al (2017b) Simultaneous quantitation of sphingoid bases by UPLC-ESI-MS/MS with identical <sup>13</sup>C-encoded internal standards. *Clin Chim Acta* 466:178–184. doi: 10.1016/J.CCA.2017.01.014
- Pisani A, Porto C, Andria G, Parenti G (2014) Synergy between the pharmacological

- chaperone 1-deoxygalactonojirimycin and agalsidase alpha in cultured fibroblasts from patients with Fabry disease. *J Inherit Metab Dis* 37:145–146. doi: 10.1007/s10545-013-9641-z
- Porto C, Cardone M, Fontana F, et al (2009) The pharmacological chaperone N-butyldeoxyojirimycin enhances enzyme replacement therapy in pompe disease fibroblasts. *Mol Ther* 17:964–971. doi: 10.1038/mt.2009.53
- Porto C, Pisani A, Rosa M, et al (2012) Synergy between the pharmacological chaperone 1-deoxygalactonojirimycin and the human recombinant alpha-galactosidase A in cultured fibroblasts from patients with Fabry disease. *J Inherit Metab Dis* 35:513–520. doi: 10.1007/s10545-011-9424-3
- Ruderfer I, Shulman A, Kizhner T, et al (2018) Development and Analytical Characterization of Pegunigalsidase Alfa, a Chemically Cross-Linked Plant Recombinant Human  $\alpha$ -Galactosidase-A for Treatment of Fabry Disease. *Bioconj Chem* 29:1630–1639. doi: 10.1021/acs.bioconjchem.8b00133
- Sanchez-Niño, M.D., Carpio, D., Sanz, A.B., et al (2015). Lyso-Gb3 activates Notch1 in human podocytes. *Human Molecular Genetics* 24, 5720-5732. doi: <https://doi.org/10.1093/hmg/ddv291>
- Sunder-Plassmann G, Schiffmann R, Nicholls K (2018) Migalstat for the treatment of Fabry disease. *Expert Opin Orphan Drugs* 6:301–309. doi: 10.1080/21678707.2018.1469978
- Tajima Y, Kawashima I, Tsukimura T, et al (2009) Use of a modified alpha-N-acetylgalactosaminidase in the development of enzyme replacement therapy for Fabry disease. *Am J Hum Genet* 85:569–580. doi: 10.1016/j.ajhg.2009.09.016
- van Dussen L, Biegstraaten M, Hollak CEM, Dijkgraaf MGW (2014) Cost-effectiveness of enzyme replacement therapy for type 1 Gaucher disease. *Orphanet J Rare Dis* 9:1–12. doi: 10.1186/1750-1172-9-51
- Warnock DG, Bichet DG, Holidia M, et al (2015) Oral migalstat HCl leads to greater systemic exposure and tissue levels of active  $\alpha$ -galactosidase A in fabry patients when co-administered with infused agalsidase. *PLoS One* 10:1–17. doi: 10.1371/journal.pone.0134341
- Willems LI, Beenakker TJM, Murray B, et al (2014) Potent and Selective Activity-Based Probes for GH27 Human Retaining  $\alpha$ -Galactosidases. *J Am Chem Soc* 136:11622–11625. doi: 10.1021/ja507040n



# Chapter 6

---

Cross species investigations with  
activity-based probes. Future  
prospects

---

*Kytidou Kassiani, Rebecca Katzy, Eline van Meel, Johannes M.F.G Aerts*

*To be submitted in revised form*



## Abstract

The potential use of ABPs cross species was investigated. Studied were lysates derived from Bright Yellow tobacco cell lines (BY2) and the food supplement Beano containing a fungal (*A. niger*)  $\alpha$ -galactosidase.

The investigations with BY2 cell lysates led to the discovery of a plant  $\beta$ -glucosidase that is potently labeled by the  $\beta$ -glucose configured epoxide cyclophellitol ABP and its identity was next established by proteomics. The enzyme, here named B56, is active towards NBD-GlcCer lipid, revealing its potential use in therapy of Gaucher disease.

ABPs could be also successfully applied to label the  $\alpha$ -galactosidase from *A. niger* present in the food supplement Beano. The enzyme was found to be active towards artificial 4-methylumbelliferyl- $\alpha$ -galactoside but not towards NBD-Gb3.

As Fabry patients suffer from intestinal complications, possibly induced by accumulating lysoGb3 in the intestine, future application of other  $\alpha$ GAL enzymes might be considered for diminishing such toxic agents.

## Introduction

Retaining glycosidases are remarkably conserved among species in their catalytic mechanism based on double displacement. This reaction is essentially governed by appropriately placed nucleophile and acid/base residues in the catalytic pocket (Davies and Henrissat 1995). Due to the conserved structural prerequisites for catalytic activity, glycosidases across species are found to be targeted by activity-based probes (ABPs) consisting of a correctly configured cyclophellitol with a reporter group linked to it (Witte et al. 2010).

Retaining glycosidases fulfil important functions in human physiology. For example, in the lysosomes of cells specialized glycosidases are essential in turnover of glycoconjugates. Examples are the acid  $\beta$ -glucosidase (glucocerebrosidase, GBA) hydrolyzing glucosylceramide (GlcCer) and  $\alpha$ -galactosidase A (GLA) hydrolyzing globotriaosylceramide (Gb3) (Ferraz et al. 2014). Inherited deficiencies in these enzymes of glycosphingolipid metabolism cause the lysosomal storage disorders Gaucher disease and Fabry disease, respectively (Beutler and Grabowski 2001; Desnick et al. 2003).

Cyclophellitol and cyclophellitol-aziridine are known suicide inhibitors of  $\beta$ -glucosidases (Kallemeijn et al. 2014b; Li et al. 2014; Kuo et al. 2018). Different sets of ABPs have been designed to label the retaining  $\beta$ -glucosidases present in human cells and tissues. One set consists of cyclophellitol (-epoxide) with linked to C6 (C8 cyclophellitol numbering) a spacer with attached reporter (fluorophore or biotin) (Witte et al. 2011). The other set consists of cyclophellitol-aziridine with linked to the nitrogen a spacer with attached reporter. The first set of ABPs specifically labels GBA, whilst the second set labels all human  $\beta$ -glucosidases (GBA, GBA2, GBA3 and LPH) (Kallemeijn et al. 2012, 2014a).

Differently configured cyclophellitol-aziridines have been subsequently designed to label various classes of retaining glycosidase (Witte et al. 2011; Kallemeijn et al. 2012; Willems et al. 2014a; Kallemeijn et al. 2014a; Jiang et al. 2015, 2016; Marques et al. 2017; Wu et al. 2017; Artola et al. 2018). For example, galactose-configured cyclophellitol-aziridine ABP labels the highly homologous  $\alpha$ -galactosidase enzymes GLA and  $\alpha$ -N-acetylgalactosaminidase (NAGA) (Kytidou et al. 2017). Earlier we labeled with the same ABP an ubiquitous retaining  $\alpha$ -galactosidase in *Nicotiana benthamiana* (*N. benthamiana*) (Kytidou et al. 2018). The protein, named A1.1, was identified, cloned and characterized. Crystallography revealed a high similarity in 3D-structure with the human counterparts GLA and NAGA (Kytidou et al. 2018). The A1.1 enzyme shows activity towards Gb3, albeit this lipid does not occur in

plants. The A1.1.  $\alpha$ -galactosidase differs from GLA and NAGA in complete lack of N-glycans and a broader pH optimum (Kytidou et al. 2018). Its potential value to treat patients suffering from Fabry disease with recombinant A1.1 is being investigated.

The metabolism of the glycosphingolipid GlcCer is of great interest in relation to various diseases. Impaired lysosomal degradation due to deficient GBA activity causes formation of lipid-laden macrophages (Gaucher cells) that are thought to contribute to the hepatomegaly, splenomegaly, and cytopenia in Gaucher patients (Ferraz et al. 2014). Accumulation of GlcCer is partly prevented by its conversion to glucosylsphingosine (GlcSph) by the lysosomal enzyme acid ceramidase (Dekker et al. 2011; Ferraz et al. 2016). Recent studies suggest that GlcSph is a toxic agent that promotes gammopathy in Gaucher patients and multiple myeloma as well as increases the risk for Parkinson disease in carriers of a mutant GBA allele (Siebert et al. 2014; Nair et al. 2016). GlcCer is also degraded by the cytosol-face GBA2, a membrane-bound  $\beta$ -glucosidase (Ferraz et al. 2014). GBA2 not only acts as hydrolase but also as transglucosidase transferring glucose from GlcCer to cholesterol to yield glucosylcholesterol (GlcChol) (Marques et al. 2016). For a number of decades type Gaucher patients are treated by enzyme replacement therapy (ERT) involving chronic intravenous infusion with recombinant GBA (Barton et al. 1991; Brady 2003). ERT allows correction of Gaucher cells, but does not prevent all complications in Gaucher patients, for example skeletal disease and neurological impairment (Ferraz et al. 2014).

Plants contain also the glycosphingolipid GlcCer and therefore very likely also possess a glucosyl-ceramidase fragmenting the lipid to ceramide and glucose, similar in function to GBA1 (chapter 2). Plants might also contain a transglucosylating  $\beta$ -glucosidase, similar in function to GBA2. Glucosylated sterols are also abundant plants and yet unidentified enzymes involved in their synthesis and degradation have to exist (Grille et al. 2010). In this investigation, cyclophellitol and cyclophellitol-aziridine ABPs (Figure 1) were used in *Nicotiana tabacum* Bright yellow-2 cells (BY-2) to study the retaining  $\beta$ -glucosidases in plants.

Another example of cross species use of glycosidase ABPs is provided by experiments performed with Beano<sup>®</sup>, a dietary supplement used to reduce flatulence after consumption of beans and cabbage. The supplement degrades complex carbohydrates present in such foods and thus prevents intestinal bacteria producing excessively intestinal gas (Prestige Brands Holdings, Inc., 2016a). A key component of Beano is an  $\alpha$ -galactosidase from the fungus *Aspergillus niger* (*A. niger*) according to the producer (Prestige Brands Holdings, Inc., 2016b).

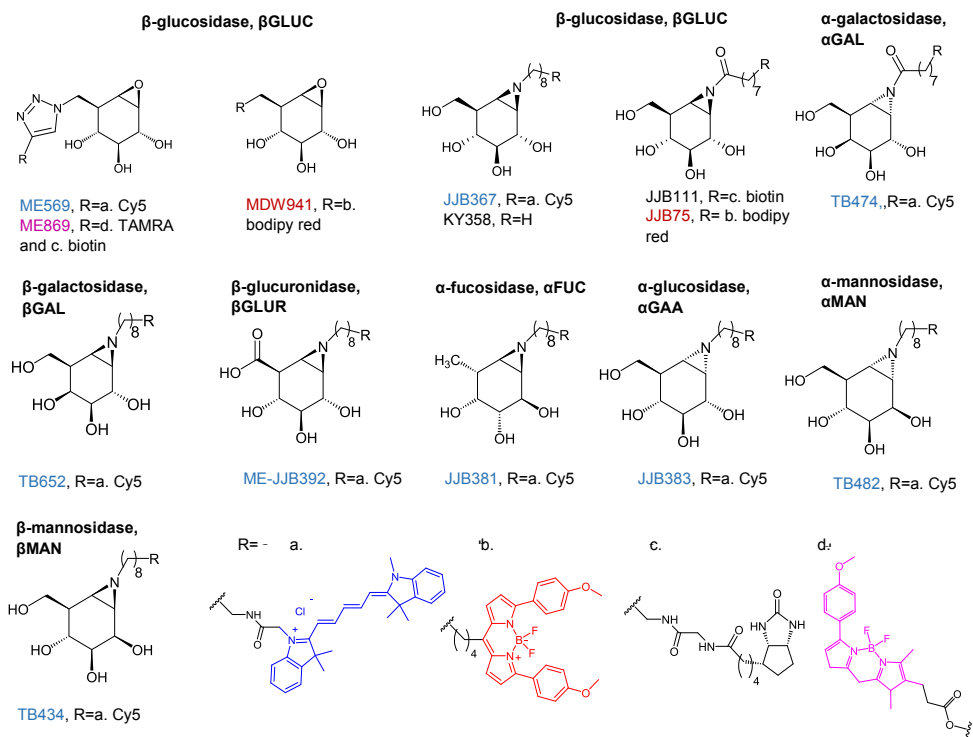


**Figure 1.** Chemical structures and codes of the ABPs used in this study and their targeting enzymes.

## Results

### Targeting *Nicotiana tabacum* BY-2 cells $\beta$ -glucosidases

An investigation regarding  $\beta$ -glucosidases involved in glycolipid metabolism in *N. tabacum* BY-2 cells was conducted. In this study use was made of the cyclophellitol ABP and cyclophellitol-aziridine ABP and lysates of cultured BY-2 cells as source of enzymes (Figure 2). Cells were cultured in Linsmaier and Skoog medium (Linsmaier and Skoog 1965) supplemented with 0,09 M sucrose and 0.2 mg/lit 2,4-dichlorophenoxyacetic acid and were harvested at day 7 of sub-culturing. Cell lysates were prepared in ice cold lysis buffer (10 mM  $\text{Na}_2\text{HPO}_4/\text{NaH}_2\text{PO}_4$  buffer, pH 6, with 0,15 M NaCl and 0,1 % Triton X-100), using the FastPrep-24 machine (MP Biomedicals). Then, lysates were used directly for experiments or were further fractionated into soluble or insoluble fractions after centrifugation for 10 min at 16,000 rpm, 4 °C.  $\beta$ -glucosidase activity present in all fractions was first measured using 1.25 mg/mL of the 4-methylumbelliferyl (4MU) - $\beta$ -D-glucoopyranoside substrate, at pH5 (Figure 2A). Activity present in soluble fraction was around 10 times lower than the one measured in full lysate. Insoluble fraction contained the highest activity, possibly due to high protein content of the preparation. Then, the fractions were incubated with 0.5  $\mu\text{M}$  ME569, JJB367 or TB474 at pH5 conditions, for 30min, 37 °C. Figure 2B shows that a single protein with apparent MW at 57 kDa was labeled by the epoxide ABP, ME569. The protein was more prominent in the soluble fraction. Multiple proteins were labelled using the epoxide ABP, JJB367 at apparent MWs of 79, 73, 70, 65 kDa. Some of them were present in the soluble and others in the insoluble fraction. Use was made of the  $\alpha$ -galactosidase configure ABP, TB474 to visualize  $\alpha$ -galactosidases in the various fractions. Proteins with MWs of 45 and 39 kDa were labeled, as earlier observed with *N. benthamiana* leaves (Kytidou et al. 2018) (Chapter 3).

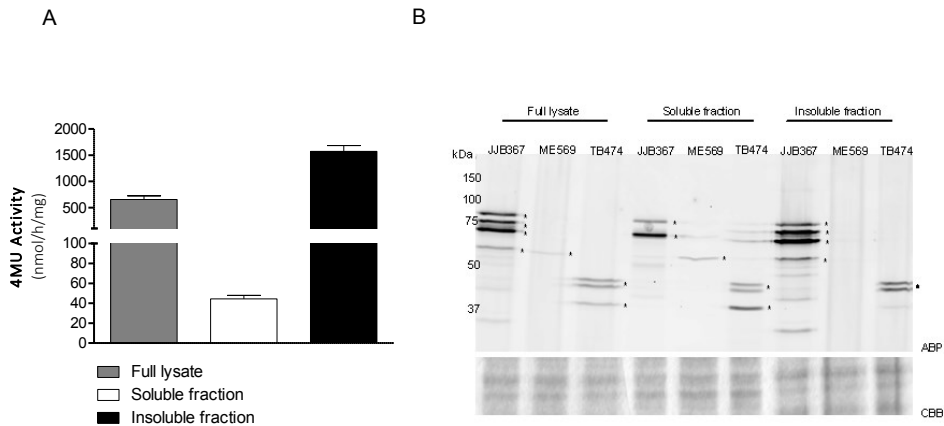


**Figure 2. Targeting retaining glycosidases in BY2 cells.** A. 4MU activities of BY2 lysates, as measured using the 4MU- $\beta$ -D-glucopyranoside substrate. error bars indicate standard deviations,  $n=4$  biological replicates. B. Full and fractionated BY2 cell lysates were incubated for 30min, 37°C, pH5 with 0.5 $\mu$ M JJB367, ME569 or TB474 ABPs. The samples were then applied to 10 % SDS-PAGE gels and fluorescent scanning of the gels followed. Interestingly, a specific protein was labeled using the epoxide ME569, at 57 kDa. Multiple proteins were identified using JJB367 and the already characterized  $\alpha$ -galactosidases using TB474.

### **N-glycosylation profile of the labeled BY2 $\beta$ -glucosidases as revealed by Concanavalin A binding.**

Lysates were incubated with Concanavalin A (Con A) beads to separate proteins into a lectin binding fraction and non-binding fraction. Enzymatic activity was first measured, using 4-MU- $\beta$ -glucoside, in all fractions (Figure 3A). Results revealed that most enzymatic activity was present in the supernatant (non-binding fraction) fractions. Then, samples were incubated with 0.5  $\mu$ M MDW941 at a pH of 5 or 0.5  $\mu$ M JJB367 at a pH of 5 (conditions determined to be optimal for labeling). According to figure 3B the ME569-ABP-identified protein (MW 57 kDa) was present in the non-binding fraction upon Con A separation, suggesting that the protein might not contain N-linked glycans. Some of the proteins labeled with JJB367 were in the Con A binding fraction and others in the non-binding fraction.



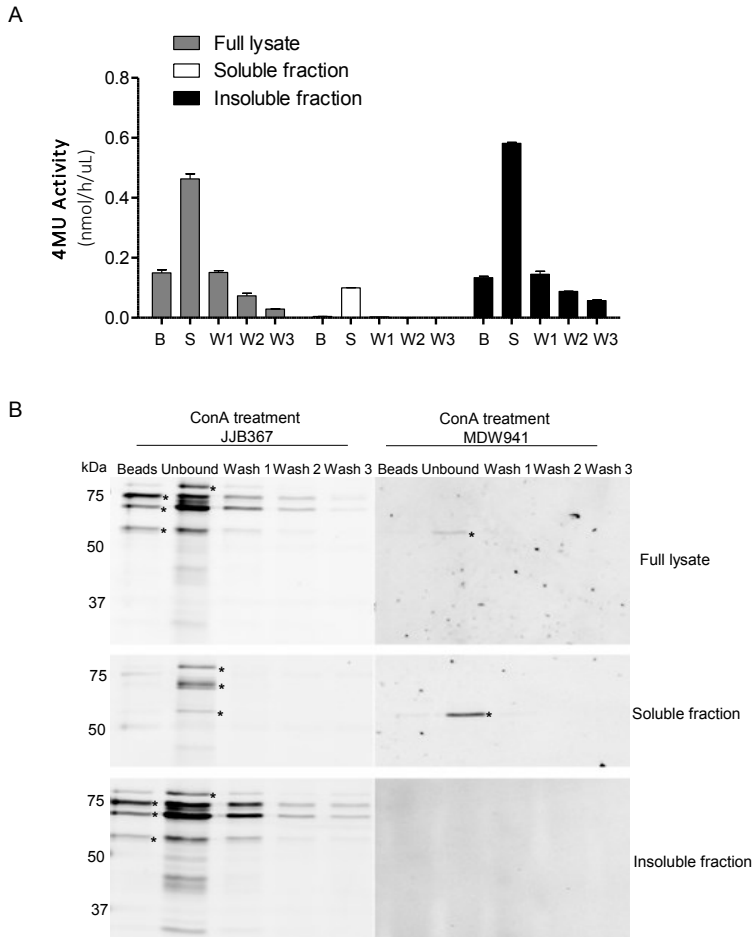


**Figure 3. Studying the N-glycosylation profile of BY2  $\beta$ -glucosidases.** Concanavalin A (Con A) treatment of BY2 cell lysates following 4MU activity measurements (A) and ABP labeling (B). BY2 cell lysates were first incubated for 1hr, 4°C while rolling with ConA beads. After incubation, centrifugation of the samples took place and the different fractions were obtained (beads (B), supernatant/ unbound (S), wash 1,2,3 (W1, W2, W3)). Then, the fractions were incubated for 30 min, 37 °C, with 0.5  $\mu$ M JJB367 or MDW941.

Next, biotinylated versions of the ABPs (JJB111 and ME869) (Figure 1) were used to target proteins followed by a pulldown with streptavidin-beads, as earlier described (Jiang et al. 2015, 2016). The nature of the enriched proteins was determined using LC-MS/MS based proteomics exactly as earlier described (Jiang et al. 2015, 2016). Measurement of the biotinylated targets was performed via on bead and in gel trypsin digestions, using the aziridine biotinylated ABP, JJB11 and also the newly synthesized cyclophellitol-epoxide-biotinylated ABP, ME869. Table 1 shows the outcome of on-bead digestions

using JJB111 in soluble fraction. The ME869, was found to label the protein A0A1S4CL56, named as B56, with predicted MW of 57 kDa, consistent with that observed for the labeled protein (Table 1). In the CAZy database, B56 is based on its amino acid composition classified as member of GH family 5. The GH5 family consists of glycoside hydrolases with various functions, including endo- $\beta$ -1,4-glucanase / cellulase, endo- $\beta$ -1,4-xylanase,  $\beta$ -glucosidase,  $\beta$ -mannosidase, glucan  $\beta$ -1,3-glucosidase, exo- $\beta$ -1,4-glucanase / cellodextrinase, glucan endo-1,6- $\beta$ -glucosidase, mannan endo- $\beta$ -1,4-mannosidase, cellulose  $\beta$ -1,4-cellobiosidase, chitosanase,  $\beta$ -primeverosidase, xyloglucan-specific endo- $\beta$ -1,4-glucanase, endo- $\beta$ -1,6-galactanase,  $\beta$ -1,3-mannanase, arabinoxylan-specific endo- $\beta$ -1,4-xylanase, mannan transglycosylase, lichenase / endo- $\beta$ -1,3-1,4-glucanase,  $\beta$ -glycosidase, endo- $\beta$ -1,3-glucanase / laminarinase,  $\beta$ -N-acetylhexosaminidase, chitosanase,  $\beta$ -D-galactofuranosidase,  $\beta$ -galactosylceramidase, endoglycoceramidase,  $\beta$ -glucosylceramidase and steryl  $\beta$ -glucosidase ([www.cazy.org](http://www.cazy.org)). More recently human GBA1 has been classified from GH5 to GH30 (Ben Bdira et al. 2018).

**Table 1. List of on-bead identified JJB111 protein targets.**

| UniProt code               | Protein name                                       | MW (Da) | Score | SeqCov (%) | GH Family |
|----------------------------|--|---------|-------|------------|-----------|
| <a href="#">A0A1S4CR57</a> | beta-glucosidase BoGH3B-like                       | 68860   | 685   | 30         | 3         |
| <a href="#">A0A1S3ZME1</a> | probable beta-D-xylosidase 6                       | 88005   | 418   | 23         | 3         |
| <a href="#">A0A1S4CL56</a> | probable glucan 1,3-beta-glucosidase A isoform X2  | 57212   | 269   | 44         | 5         |
| <a href="#">A0A1S4C677</a> | beta-galactosidase                                 | 98264   | 163   | 24         | 35        |
| <a href="#">A0A1S3XJ27</a> | beta-glucosidase BoGH3B-like isoform X1            | 69022   | 136   | 17         | 3         |
| <a href="#">A0A1S4AT57</a> | glucan endo-1,3-beta-glucosidase, basic vacuolar   | 40474   | 100   | 25         | 17        |
| <a href="#">A0A1S3ZEV9</a> | lysosomal beta glucosidase-like                    | 70183   | 81    | 6          | 3         |
| <a href="#">A0A1S3ZJ12</a> | beta-galactosidase 17-like                         | 36223   | 72    | 24         | 35        |
| <a href="#">A0A1S4C5S1</a> | probable beta-D-xylosidase 5                       | 89322   | 67    | 1          | 3         |
| <a href="#">A0A1S3YQ73</a> | beta-glucosidase 18-like                           | 61221   | 44    | 7          | 1         |
| <a href="#">A0A1S3XGA2</a> | beta-xylosidase/alpha-L-arabinofuranosidase 2-like | 86389   | 40    | 5          | 3         |

**Activity of BY2 glycosidases towards NBD-GlcCer substrate.**

It will be of great interest to study more closely A56 regarding various enzymatic and structural features. It has been observed that part of the enzymatic activity towards the fluorogenic substrate 4MU- $\beta$ -glucoside in the soluble fraction of BY2 lysate is inhibited by MDW941. Its pH optimum is about 5.0 and the activity seems not to be bound by Concanavalin A (Figure 3). Lysates of BY2 cell were found to degrade NBD-glucosylceramide to NBD-ceramide and this activity was inhibitable with ABP1 and ABP2 (Figure 4).

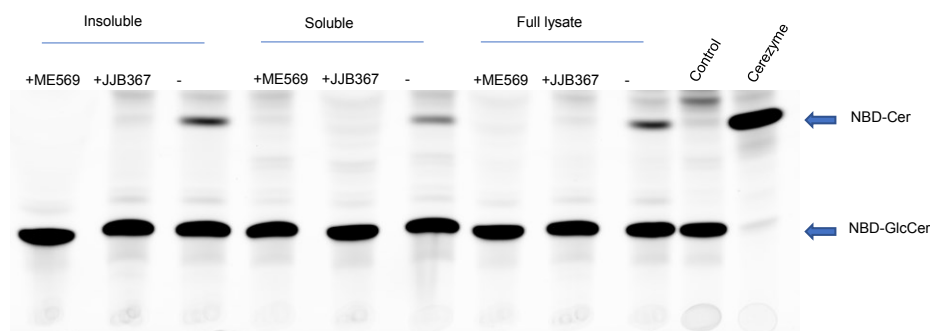


**Figure 4. NBD-GlcCer lipid hydrolysis via BY2 cell lysates.** Full and fractionated BY2 cell lysates were pre-incubated with or without 10 $\mu$ M ME569 or JJB367, for 2h, 37°C. Then, the samples were incubated with 2 $\mu$ M of C6: NBD-GlcCer, for 2h 37°C, pH5. Cerezyme was used as a positive control of the lipid hydrolysis reaction. BY2 cell lysates contain enzymes able to hydrolyse the human NBD-lipid, and they are inhibited by both epoxide and aziridine ABPs (ME569 and JJB367, respectively).

A straight-forward approach to characterize better B56 would be to overexpress the enzyme and purify it, along the same line as earlier performed for the A1.1.  $\alpha$ -galactosidase (Kytidou et al. 2018). It should be in particular established whether the B56 protein shows activity towards natural GlcCer and GlcChol (chapter 2). In addition, its ability to act as transglucosidase should be tested (Marques et al. 2016). Moreover, its subcellular localization will be of interest. Information on stability of the protein and resistance towards proteases is required to get an impression of its value to modulate glycolipid metabolism in humans. Presently available data suggest, but do not prove, that A56 lacks N-glycans given its poor binding to Concanavalin A.

Cyclophellitol-aziridine ABPs were found to label proteins A0A1S4CR57, A0A1S3ZME1 and A0A1S3ZJV9 with MWs of 69, 88 and 70 kDa, respectively. All three proteins are predicted to belong to GH3, a family of various  $\beta$ -glucosidases including cell wall degrading enzymes [ $\beta$ -glucosidase, xylan 1,4- $\beta$ -xylosidase,  $\beta$ -glucosylceramidase,  $\beta$ -N-acetylhexosaminidase,  $\alpha$ -L-

arabinofuranosidase, glucan 1,3- $\beta$ -glucosidase, glucan 1,4- $\beta$ -glucosidase, isoprimeverose-producing oligoxyloglucan hydrolase, coniferin  $\beta$ -glucosidase, exo-1,3-1,4-glucanase,  $\beta$ -N-acetylglucosaminide phosphorylases,  $\beta$ -1,2-glucosidase,  $\beta$ -1,3-glucosidase, xyloglucan-specific exo- $\beta$ -1,4-glucanase / exo-xyloglucanase (<http://www.cazy.org/GH3.html>).

Indeed, fluorescence microscopy revealed labeling of the cell wall by fluorescent cyclophellitol-aziridine ABP (Figure 5). The labeling was inhibited after overnight incubation with an ABP without the fluorophore (KY358), revealing that it was specific targeting enzyme molecules. Both JJB367 and JJB75 fluorescent ABPs were used for the same microscopy experiment, here presented only results using JJB75 (Figure 5). Since the BY2 cultures used during these experiments were harvested at day 3 of post culturing, the ABP-labelled proteins seem to be mainly the ones at MW of ~69 (Figure S1). Possibly targeting, the enzyme  $\beta$ -glucosidase BoGH3B (A0A1S4CR57) of GH3 family, as also measured during in-gel proteomics analysis. In addition, to further support the previous, *in situ* ABP labeling presented at figure S2, reveals that using 0.5  $\mu$ M concentration of JJB75 probe (concentration used during microscopy experiments) mainly targets enzyme(s) present at MW of 69 kDa. One can further exploit the localization of targeted proteins after ABP labeling also via fractionating the samples and isolating the vacuoles or extracellular area of BY2 cells.

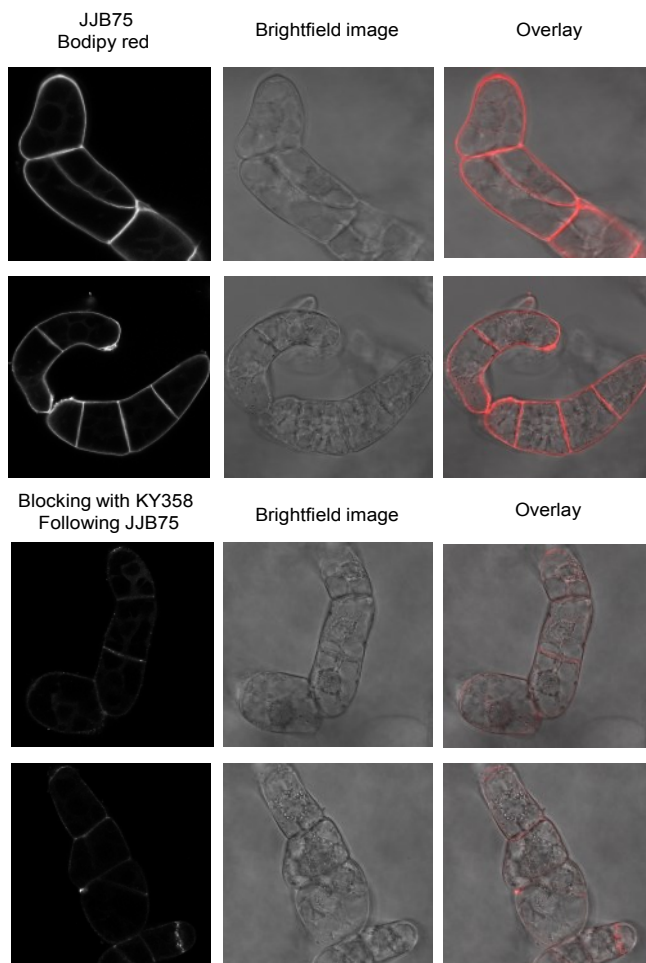


**Figure 5. Live confocal microscopy of BY2 cells using ABPs.** 3 days old BY2 cells (500  $\mu$ L) were incubated in a 12-well plate with 0.5  $\mu$ M of JJB75 for 2-3 h. To ensure that the labeling was specific, samples were also pre-incubated overnight with the non-fluorescent ABP, KY358 and then JJB75 labeling followed as before. The signal was lost after pre-incubation with the non-fluorescent ABP suggesting that the labeling was specific.

### ***In silico* model of B56 and its active site similarities with human GBA1 enzyme**

There are no striking amino acid sequence similarities of B56 with the human GBA1 enzyme, and its homologues in mice (*Mus musculus*) and zebrafish (*Danio rerio*). The protein shows amino acid sequence similarities with bacterial and yeast enzymes. A hypothetical structural model of the  $\beta$ -glucosidase B56 was made, in Swiss-model program, using as a structural model the Glucan 1,3- $\beta$ -glucosidase of the yeast *Candida albicans* (Figure 6).

The proteins have 36 % sequence similarity and both belong to GH family 5. The modeled 3D-structure was superimposed on the established 3D-structure of human GBA1 (PDB code: 2NT0). Overall the proteins were very different but their active site shared conserved moieties. Most importantly, two glutamic acid residues serving as the nucleophile and acid/base moieties of the retaining mechanism, were conserved among the two enzymes. In human GBA1 the catalytic residues are E235 and E340 and in B56 putatively E346 and E450. B56 is a predicted monomer, without N-linked glycans in contrast to the human enzyme which is a natural dimer, having 5 predicted N-linked glycosylation sites of which 4 are used (Ben Bdira et al. 2018).

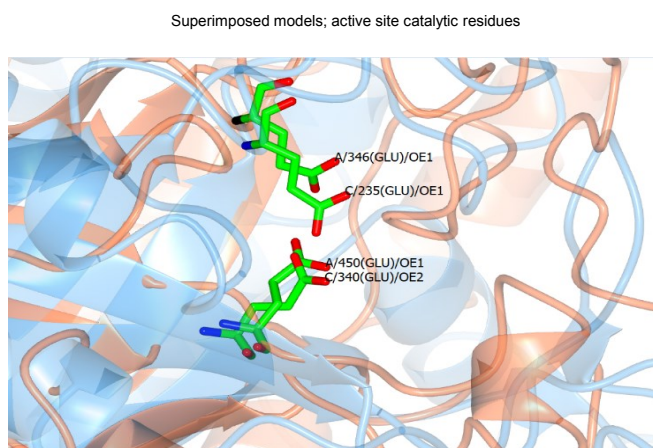


**Figure 6.** *In silico* structural models of B56 and the human GBA1 (PDB code: 2NT0). Superimposed active sites of human GBA1 (light blue) and B56 (light orange). The two catalytic residues (E235/E340 for human GBA1 and E346/E450 for B56) are conserved between the two proteins.

### Screening for different retaining glycosidases in BY-2 cells using different configured ABPs

In a pilot investigation lysate of BY-2 cells were labeled with ABPs directed against different classes of retaining glycosidases (see figure 1;  $\alpha$ -glucosidase,  $\alpha$ -galactosidase,  $\beta$ -mannosidase,  $\alpha$ -fucosidase,  $\beta$ -galactosidases,  $\beta$ -glucuronidase,  $\alpha$ -mannosidase). Discrete proteins were visualized with most probes (Figure 7), except for  $\alpha$ -fucosidase. Thus, the same approach could be used to identify retaining glycosidases for other research questions of interest.

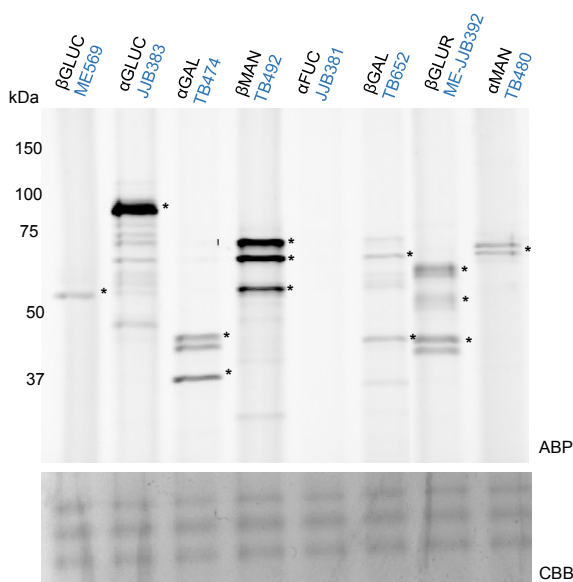


**Figure 7. Screening for different retaining glycosidases in BY2 cell lysates, using different ABPs.** 20ug of total protein were incubated with 0.5uM of different Cy5-labeled ABPs (ME569, JJB383, TB474, TB492, JJB381, TB652, ME-JJB392, TB480). Most of the ABP labeling revealed possible candidate enzymes, yet to be characterized and identified.

### Fungal $\alpha$ -galactosidase: investigations with ABP (ABP labeling Beano® $\alpha$ -galactosidase)

Alpha-galactose configured TB474 was used to study the content on  $\alpha$ -galactosidases of Beano® (Figure 1). For this purpose, Beano tablets were dissolved in water. The obtained solution was analyzed on protein content and incubated with TB474.  $\alpha$ -galactosidases belong to family GH27 and GH36. They hydrolyze on galactose oligosaccharides, galactomannans and galactolipids, whose terminal 1,6- $\alpha$ -D-galactosyl moieties are release (<https://www.brenda-enzymes.org/enzyme.php?ecno=3.2.1.22>). *A. niger* is

known to express 4  $\alpha$ -galactosidases ( $\alpha$ -Gal I-IV) (Ademark et al. 2001a). The enzymes  $\alpha$ -Gal II, III and IV are isoforms of AglB (GH27), whilst  $\alpha$ -Gal I (GH36) is entirely distinct (Ademark et al. 2001b).

Using TB474 directed against  $\alpha$ -galactosidases in the Beano solution, discrete proteins were labeled. Proteins with apparent MW of 60-65 kDa were labelled. Ademark and colleagues found that a protein closely related to *A. niger*  $\alpha$ -galactosidase B consisted of two subunits with a molecular weight of 64 kDa (Ademark et al. 2001a, b). Beano contains also an invertase with sucrose activity (Prestige Brands Holdings, Inc., 2016b). This protein of approximately 135 kDa is unlikely to be the labelled protein with apparent MW of about 100 kDa reflects.

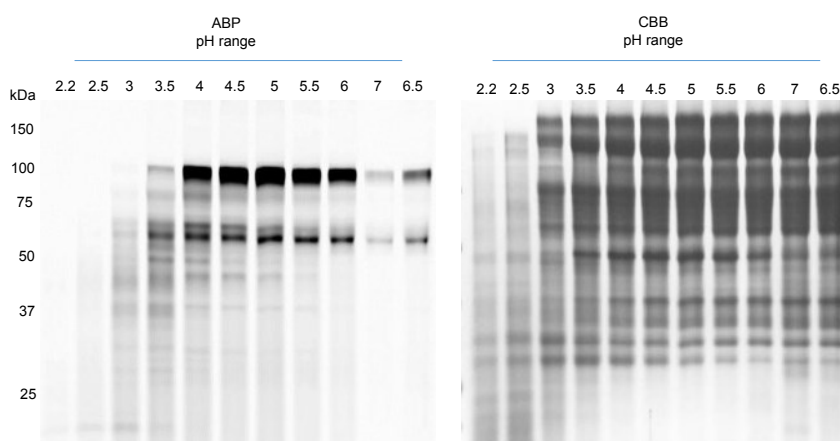


**Figure 8. ABP labeling of alpha galactosidases present in Beano<sup>®</sup> supplement.** The ABP labeling performed using 0.5 $\mu$ M of TB474 and the incubations performed in different pH buffer conditions (pH range 2.2- 6.5). The proteins are optimum labeled at pH 4.5-5. Coomassie staining of the gel followed to ensure equal loading and detect the general protein content of the supplement.

It was next examined whether incubation of Beano solution with TB474 led to inactivation of  $\alpha$ -galactosidase activity. Most activity was lost following incubation with ABP and enzyme assay for 1 hour.

Next, apparent IC<sub>50</sub> values of the potential natural substrate raffinose and D-galactose against human, fungal and plant  $\alpha$ -galactosidases were determined (table 2). Competition of ABP labeling by the same substrates and with the additional tetrasaccharide stachyose was also tested (Figure 8). In this experiment Beano  $\alpha$ -galactosidase, human  $\alpha$ -galactosidase GLA, and recombinant plant  $\alpha$ -galactosidase A1.1 were compared. It was noted that raffinose and stachyose strongly competed labeling of *A. niger* enzyme,



indicating that these are likely substrates. This was also the case for plant A 1.1., but not so for human GLA.

**Table 2. Apparent IC<sub>50</sub> values for *in vitro* inhibition of fungal, human and plant  $\alpha$ -galactosidases by raffinose and D-galactose.**

| IC <sub>50</sub> s (mM) | Beano | Fabrazyme | A1.1 |
|-------------------------|-------|-----------|------|
| Raffinose               | 317   | 1779      | 187  |
| D-galactose             | 327   | 83        | 10   |

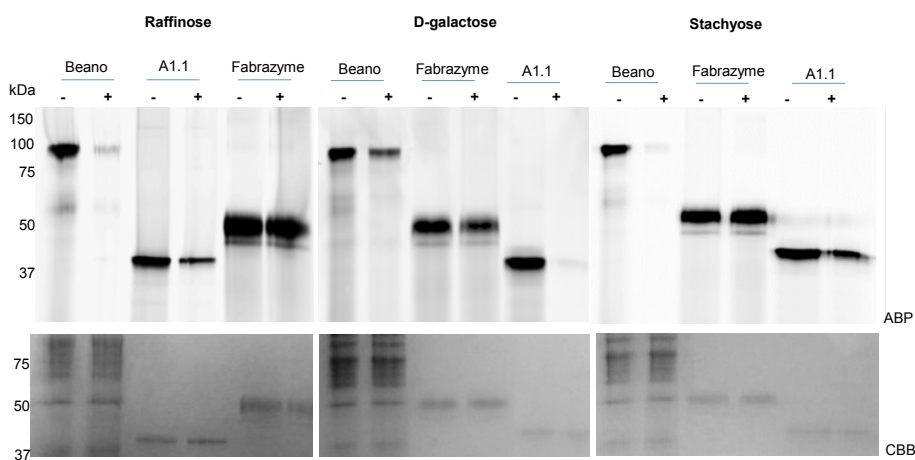


**Figure 9. ABP signal competition with raffinose, D-galactose and stachyose.** All enzymes, were pre-incubated for 1h, 37°C, with and without 500mM of the trisaccharide raffinose, monosaccharide D-galactose or the tetrasaccharide stachyose. Then ABP labeling followed using 0.5  $\mu$ M of TB474, for 30min, 37 °C. The samples were then run on 10% SDS-PAGE gels and competition of the ABP signal revealed that Beano and A1.1 enzymes were highly inhibited by all saccharides, whereas human enzyme (Fabrazyme) was inhibited by D-galactose.

Finally, it was tested whether Beano solution was able to degrade NBD-GB3 (Figure 9). The enzyme despite its high activity towards the artificial fluorogenic 4MU- $\alpha$ -galactoside, which was comparable to that of Fabrazyme (recombinant human  $\alpha$ -galactosidase A), it was not found active towards the NBD-GB3 lipid.

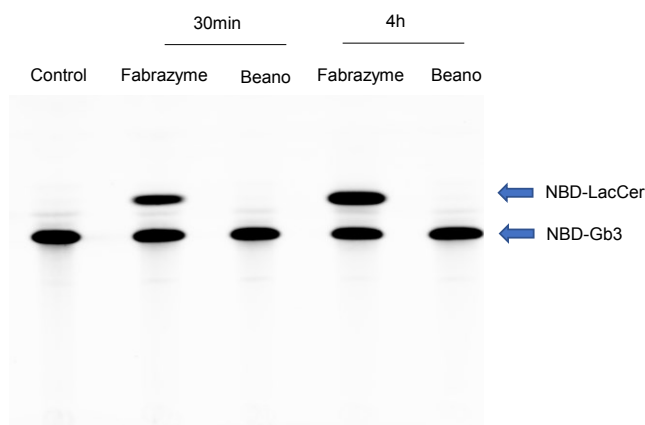


**Figure 10. Beano and Fabrazyme activity towards NBD-Gb3.** NBD-Gb3 lipid (2 $\mu$ M) was incubated with the same 4MU- $\alpha$ GAL activity input of Beano and Fabrazyme enzymes in different time points (30min and 4h). Beano enzyme cannot degrade the lipid substrate in contrast to Fabrazyme.

Investigations on intestinal  $\alpha$ -galactosidases may be of great interest in relation to Fabry disease (Ferraz et al. 2014). As the result of deficiency of the lysosomal enzyme  $\alpha$ -galactosidase A, Fabry disease patients accumulate Gb3 and the deacylated form of the lipid called globotriaosylsphingosine or lysoGb3 (Aerts et al. 2008). LysoGb3 is formed from Gb3 by lysosomal acid ceramidase and part of the water-soluble lipid may leave the body via urine and bile (Ferraz et al. 2016). It has recently been reported that lysoGb3 impacts on microbiota and decreases production of the beneficial short-chain fatty acid butyrate (Aguilera-Correa et al. 2019). The investigation indicates that intestinal lysoGb3 has harmful effects and may contribute to the commonly reported intestinal complaints of Fabry patients (Hoffmann et al. 2007). Our investigations suggest that the Beano  $\alpha$ -galactosidase may have no therapeutic potential regarding gastrointestinal complaints of Fabry patients since it seems unable to degrade (lyso)Gb3.

## Discussion

The studies described in this chapter further illustrate how ABPs can conveniently be used in fundamental research. Firstly, ABPs can be used to identify likely substrates by testing competition of ABP labeling by compounds (Figure 7). The same principle is applied in ABPP (activity-based profiling) screening of drug laboratories as was demonstrate by Lahav *et al.* in their search for potent inhibitors of the retaining human  $\beta$ -glucosidase GBA2 (Lahav *et al.* 2017). Secondly, ABPs can be used to identify the various classes of retaining glycosidase in different species. Examples for this are provided by the work of the van der Hoorn laboratory regarding plant glycosidase (Chandrasekar *et al.* 2014; Husaini *et al.* 2018). Along the same line, the panel of available ABPs labeling distinct glycosidases was used by Kuo *et al.* to determine target and off-target interactions of inhibitors such as conduritol B-epoxide and cyclophellitol, aiming to covalently inhibit the lysosomal  $\beta$ -glucosidase GBA1 (Kuo *et al.* 2019). The outcome of this investigation allowed design of a very specific GBA1 suicide inhibitor allowing generation of genuine Gaucher models (Artola *et al.* 2019).

## Materials and methods

**BY2 cell culturing and lysis.** BY-2 cells were cultured in Linsmaier and Skoog medium (Linsmaier and Skoog 1965) supplemented with 0,09 M sucrose and 2,4-dichlorophenoxyacetic acid (0.2 mg/l). The medium was autoclaved and kept at 4 °C until further use. Cells were sub-cultured every seven days (1-5 mL cells into 100 mL medium). BY2 cultures were kept in dark on a rotary shaker , 130 rpm at 27 °C (Nagata et al. 1992). Cell lysates were made using ice cold lysis buffer (10 mM Na<sub>2</sub>HPO<sub>4</sub>/NaH<sub>2</sub>PO<sub>4</sub>, pH 6, 0,15 M NaCl, 0,1 % Triton X-100 with additional protease inhibitor), using 500 µL of buffer per gram of cells. Then the cells were further lysed using the FastPrep-24 (MP Biomedicals). After lysis, part of the samples was collected (Full lysate) and the rest was fractionated, after centrifuge at 16,000rpm for 10 min, 4 °C. The obtained supernatant was collected (soluble fraction) and also the pellet (insoluble fraction). Protein concentration of the samples was measured using the Micro BCA Protein Assay Reagent Kit (PIERCE), according to manufacturer protocol. The samples were stored at -20 °C until further use.

**Beano<sup>®</sup> lysates.** 1 tablet of Beano<sup>®</sup> (Prestige Brands Holdings, Inc), was dissolved in 1 mL MQ. Protein content of the sample followed, using the Micro BCA Protein Assay Reagent Kit (PIERCE). The sample was aliquoted and stored at -20 °C until further use.

**Fluorescent ABP labeling and SDS-PAGE analysis.** *In vitro* ABP labeling assay was performed at 37 °C, for 30 min to 1h, using different ABPs (Figure 1) at final concentration 0.5 µM, volume 20 µL. The incubation was done in 150 mM Mcllvaine buffer, pH5, using 20 µg of total protein concentration. SDS-PAGE loading buffer was then added to the samples, following boiling at 95 °C, for 5min. Then samples were applied on 10 % SDS-PAGE gels and fluorescent scanning of the gels tool place as previously described (Willems et al. 2014b).

**Concanavalin A beads.** Cell lysates were incubated for 1h, 4°C while rolling with Concanavalin-A (ConA) Sepharose beads (GE healthcare Bio-Sciences) and the protocol was followed exactly as previously described (Kytidou et al. 2018).

**Proteomics analysis.** *On bead proteomics analysis:* 450 µL of BY2 cell lysates (Full lysate, soluble, insoluble fraction), having a protein content between 2-5 mg/mL, were incubated with 5 µM of the biotinylated aziridine ABP, JJB111 or with DMSO (control) overnight at room temperature. After incubations,

proteins were linearized with 2 % SDS, precipitated using chloroform/ methanol precipitation, cystine bridges were reduced and alkylated following the exact protocol described at Jiang et al. 2016 (Jiang et al. 2016). Pull downs with avidin agarose beads (Pierce) 50  $\mu$ L per sample were followed. The beads were washed with PBS and added to each sample in 1 mL PBS with beads per sample. The samples were incubated with the beads overnight at 4 °C while rolling. The beads were isolated through centrifugation (2500 g, 2 min) and a sample was taken of the supernatant: post-pulldown sample. This sample, together with the pre-pulldown sample, was used for SDS-PAGE analysis of the pulldown efficiency. The beads were washed with 0,5 % (w/v) SDS in PBS (1x) and PBS (3x). Then samples were prepared for proteomics analysis exactly as described at (Jiang et al. 2016; Kytidou et al. 2018).

*In gel proteomics analysis* 50 mL BY2 lysates were first incubated with 50 mL of diluted (x10) ConA beads overnight, 4 °C while rotating. Then, the sample was centrifuged max. speed, for 15min, 4 °C and supernatant was collected. The supernatant sample was then concentrated using the Amicon ultra-centrifugal tubes, according to the manufacture's protocol, up to 2 mL. Then, 200  $\mu$ L of the sample were incubated with or without 2  $\mu$ M of ME869 or JJB111 probes, overnight at room temperature. After ABP incubations the samples were treated exactly as described for the on-bead proteomics analysis, until the streptavidin bead incubations. In these experiments, the Dynabeads™ MyOne™ Streptavidin beads were used and the protocol was exactly as previously described (Kytidou et al. 2018). After binding to streptavidin beads, samples were applied on 10 % pre-cast SDS-PAGE gels (Bio rad). Excise of the bands followed, and the samples were further treated for proteomics analysis as previously described (Jiang et al. 2016; Wu et al. 2017). The Synapt G2Si mass spectrometer (Waters) operating with Masslynx for acquisition and ProteinLynx Global Server (PLGS) for peptide identification was used for analysis. Peak lists containing parent and daughter ions were compiled in .mgf format and searched against the Swiss-Prot (version 2017).

**Enzyme activity assays.** 4MU activity assays were performed exactly as previously described (Kallemeijn et al. 2012; Kytidou et al. 2017).

**Microscopy.** BY2 cultures at day 3 of sub-culturing were transferred in 12-well plates (500  $\mu$ L). 0.5  $\mu$ M of JJB75 (red bodipy) or JJB367 (Cy5) ABPs were applied directly to the cells and they were incubated for 2-3 h, at 130 rpm, 27 °C in the dark. Cells were also pre-incubated overnight with 60  $\mu$ M of KY358, non-fluorescent ABP and then fluorescent ABP labeling followed. Then, the cells were washed 5x times with PBS to ensure that there is no free probe

left and placed in chambers for fluorescent detection at EVOS microscope (Thermo Fisher Scientific). For Cy5,  $\lambda_{\text{ex}} = 638 \text{ nm}$ ,  $\lambda_{\text{em}} = 650\text{--}700 \text{ nm}$ . For red bodipy,  $\lambda_{\text{ex}} 594 \text{ nm}$ ,  $\lambda_{\text{em}} = 605\text{--}645 \text{ nm}$ .

## **Acknowledgments**

We are thankful to Jill van Haaster, Ivanna Denysiuk, Hanna Terpstra and Kate Bila, for their contribution to this study through practical work. We also thank Marta Artola for the design and production of ME869 probe, and Herman Overkleeft for supervision.

## References

- Ademark P, de Vries RP, Hägglund P, et al (2001a) Cloning and characterization of *Aspergillus niger* genes encoding an  $\alpha$ -galactosidase and a  $\beta$ -mannosidase involved in galactomannan degradation. *Eur J Biochem* 268:2982–2990. doi: 10.1046/j.1432-1327.2001.02188.x
- Ademark P, Larsson M, Tjerneld F, Ståhlbrand H (2001b) Multiple alpha-galactosidases from *Aspergillus niger*: Purification, characterization and substrate specificities. *Enzym Microb Technol* 29:441–448. doi: 10.1016/S0141-0229(01)00415-X
- Aerts JMFG, Groener JE, Kuiper S, et al (2008) Elevated globotriaosylsphingosine is a hallmark of Fabry disease. *Proc Natl Acad Sci U S A* 105:2812–2817. doi: 10.1073/pnas.0712309105
- Aguilera-Correa J-J, Madrazo-Clemente P, Martínez-Cuesta MDC, et al (2019) Lyso-Gb3 modulates the gut microbiota and decreases butyrate production. *Sci Rep* 9:12010. doi: 10.1038/s41598-019-48426-4
- Artola M, Kuo C-L, Lelieveld LT, et al (2019) Functionalized Cyclophellitols Are Selective Glucocerebrosidase Inhibitors and Induce a Bona Fide Neuropathic Gaucher Model in Zebrafish. *J Am Chem Soc* 141:4214–4218. doi: 10.1021/jacs.9b00056
- Artola M, Kuo C-L, McMahon SA, et al (2018) New Irreversible  $\alpha$ -l-Iduronidase Inhibitors and Activity-Based Probes. *Chemistry* 24:19081–19088. doi: 10.1002/chem.201804662
- Barton NW, Brady RO, Dambrosia JM, et al (1991) Replacement Therapy for Inherited Enzyme Deficiency — Macrophage-Targeted Glucocerebrosidase for Gaucher's Disease. *N Engl J Med* 324:1464–1470. doi: 10.1056/NEJM199105233242104
- Ben Bdira F, Artola M, Overkleeft HS, et al (2018) Distinguishing the differences in  $\beta$ -glycosylceramidase folds, dynamics, and actions informs therapeutic uses. *J Lipid Res* 59:2262–2276. doi: 10.1194/jlr.R086629
- Beutler, E. and Grabowski GA (2001) Gaucher disease. In: Scriver, C.R., Beaudet, A.L., Sly, W.S., and Valle, D., (Eds), 8th ed. McGraw-Hill, New York. 3635-3668
- Brady RO (2003) Enzyme replacement therapy: conception, chaos and culmination. *Philos Trans R Soc Lond B Biol Sci* 358:915–919. doi: 10.1098/rstb.2003.1269
- Chandrasekar B, Colby T, Emran Khan Emon A, et al (2014) Broad-range Glycosidase Activity Profiling. *Mol Cell Proteomics* 13:2787–2800. doi: 10.1074/mcp.O114.041616
- Davies G, Henrissat B (1995) Structures and mechanisms of glycosyl hydrolases. *Structure* 3:853–859. doi: [https://doi.org/10.1016/S0969-2126\(01\)00220-9](https://doi.org/10.1016/S0969-2126(01)00220-9)
- Dekker N, van Dussen L, Hollak CEM, et al (2011) Elevated plasma glucosylsphingosine in Gaucher disease: relation to phenotype, storage cell markers, and therapeutic response. *Blood* 118:e118–e127. doi: 10.1182/blood-2011-05-352971
- Desnick RJ, Brady R, Barranger J, et al (2003) Fabry Disease, an Under-Recognized

- Multisystemic Disorder: Expert Recommendations for Diagnosis, Management, and Enzyme Replacement Therapy. *Ann Intern Med* 138:338–346. doi: 10.7326/0003-4819-138-4-200302180-00014
- Ferraz MJ, Kallemeijn WW, Mirzaian M, et al (2014) Gaucher disease and Fabry disease: New markers and insights in pathophysiology for two distinct glycosphingolipidoses. *Biochim Biophys Acta - Mol Cell Biol Lipids* 1841:811–825. doi: <https://doi.org/10.1016/j.bbalip.2013.11.004>
- Ferraz MJ, Marques ARA, Appelman MD, et al (2016) Lysosomal glycosphingolipid catabolism by acid ceramidase: formation of glycosphingoid bases during deficiency of glycosidases. *FEBS Lett* 590:716–725. doi: 10.1002/1873-3468.12104
- Grille S, Zaslowski A, Thiele S, et al (2010) The functions of steryl glycosides come to those who wait: Recent advances in plants, fungi, bacteria and animals. *Prog Lipid Res* 49:262–288. doi: <https://doi.org/10.1016/j.plipres.2010.02.001>
- Hoffmann B, Schwarz M, Mehta A, Keshav S (2007) Gastrointestinal Symptoms in 342 Patients With Fabry Disease: Prevalence and Response to Enzyme Replacement Therapy. *Clin Gastroenterol Hepatol* 5:1447–1453. doi: <https://doi.org/10.1016/j.cgh.2007.08.012>
- Husaini, A.M., Morimoto, K., Chandrasekar, B., et al. (2018). Multiplex Fluorescent, Activity-Based Protein Profiling Identifies Active  $\alpha$ -Glycosidases and Other Hydrolases in Plants. *Plant Physiol* 177:24-37. doi: 10.1104/pp.18.00250.
- Jiang J, Kallemeijn WW, Wright DW, et al (2015) In vitro and in vivo comparative and competitive activity-based protein profiling of GH29  $\alpha$ -l-fucosidases. *Chem Sci* 6:2782–2789. doi: 10.1039/C4SC03739A
- Jiang J, Kuo C-L, Wu L, et al (2016) Detection of Active Mammalian GH31  $\alpha$ -Glucosidases in Health and Disease Using In-Class, Broad-Spectrum Activity-Based Probes. *ACS Cent Sci* 2:351–358. doi: 10.1021/acscentsci.6b00057
- Kallemeijn WW, Li K-Y, Witte MD, et al (2012) Novel Activity-Based Probes for Broad-Spectrum Profiling of Retaining  $\beta$ -Exoglucosidases In Situ and In Vivo. *Angew Chemie Int Ed* 51:12529–12533. doi: 10.1002/anie.201207771
- Kallemeijn WW, Witte MD, Voorn-Brouwer TM, et al (2014a) A Sensitive Gel-based Method Combining Distinct Cyclophellitol-based Probes for the Identification of Acid/Base Residues in Human Retaining  $\beta$ -Glucosidases. *J Biol Chem* 289:35351–35362.
- Kallemeijn WW, Witte MD, Wennekes T, Aerts JMFG (2014b) Chapter 4 - Mechanism-Based Inhibitors of Glycosidases: Design and Applications. In: Horton DBT-A in CC and B (ed). Academic Press, pp 297–338
- Kuo C-L, Kallemeijn WW, Lelieveld LT, et al (2019) In vivo inactivation of glycosidases by conduritol B epoxide and cyclophellitol as revealed by activity-based protein profiling. *FEBS J* 286:584–600. doi: 10.1111/febs.14744
- Kuo, C-L., van Meel, E., Kytidou, K., et al. (2018). Activity-Based Probes for Glycosidases: Profiling and Other Applications. *Methods Enzymol.* 598:217-235. doi: 10.1016/bs.mie.2017.06.039.



- Kytidou K, Beekwilder J, Artola M, et al (2018) Nicotiana benthamiana  $\alpha$ -galactosidase A1.1 can functionally complement human  $\alpha$ -galactosidase A deficiency associated with Fabry disease. *J Biol Chem* 293:10042–10058. doi: 10.1074/jbc.RA118.001774
- Kytidou K, Beenakker TJM, Westerhof LB, et al (2017) Human Alpha Galactosidases Transiently Produced in Nicotiana benthamiana Leaves: New Insights in Substrate Specificities with Relevance for Fabry Disease. *Front Plant Sci* 8:1026. doi: 10.3389/fpls.2017.01026
- Lahav D, Liu B, van den Berg RJBHN, et al (2017) A Fluorescence Polarization Activity-Based Protein Profiling Assay in the Discovery of Potent, Selective Inhibitors for Human Nonlysosomal Glucosylceramidase. *J Am Chem Soc* 139:14192–14197. doi: 10.1021/jacs.7b07352
- Li K-Y, Jiang J, Witte MD, et al (2014) Exploring functional cyclophellitol analogues as human retaining beta-glucosidase inhibitors. *Org Biomol Chem* 12:7786–7791. doi: 10.1039/C4OB01611D
- Linsmaier EM, Skoog F (1965) Organic Growth Factor Requirements of Tobacco Tissue Cultures. *Physiol Plant* 18:100–127. doi: 10.1111/j.1399-3054.1965.tb06874.x
- Marques, A.R.A., Mirzaian, M., Akiyama, H., et al. (2016a). Glucosylated cholesterol in mammalian cells and tissues: formation and degradation by multiple cellular  $\beta$ -glucosidases. *J Lipid Res.* 57:451-463. doi: 10.1194/jlr.M064923
- Marques, A.R.A., Willems, L.I., Herrera Moro, D., et al. (2016b). A Specific Activity-Based Probe to Monitor Family GH59 Galactosylceramidase, the Enzyme Deficient in Krabbe Disease. *ChemBioChem* 18:402–412. doi: 10.1002/cbic.201600561
- Nagata T, Nemoto Y, Hasezawa S (1992) Tobacco BY-2 Cell Line as the “HeLa” Cell in the Cell Biology of Higher Plants. *Int Rev Cytol* 132:1–30. doi: 10.1016/S0074-7696(08)62452-3
- Nair S, Branagan AR, Liu J, et al (2016) Clonal Immunoglobulin against Lysolipids in the Origin of Myeloma. *N Engl J Med* 374:555–561. doi: 10.1056/NEJMoa1508808
- Siebert M, Sidransky E, Westbroek W (2014) Glucocerebrosidase is shaking up the synucleinopathies. *Brain* 137:1304–1322. doi: 10.1093/brain/awu002
- Willems LI, Beenakker TJM, Murray B, et al (2014a) Synthesis of  $\alpha$ - and  $\beta$ -Galactopyranose-Configured Isomers of Cyclophellitol and Cyclophellitol Aziridine. *European J Org Chem* 2014:6044–6056. doi: 10.1002/ejoc.201402589
- Willems LI, Beenakker TJM, Murray B, et al (2014b) Potent and Selective Activity-Based Probes for GH27 Human Retaining  $\alpha$ -Galactosidases. *J Am Chem Soc* 136:11622–11625. doi: 10.1021/ja507040n
- Witte, M.D., Kallemeijn, W.W., Aten, J., et al. (2010). Ultrasensitive in situ visualization of active glucocerebrosidase molecules. *Nat Chem Biol* 6:907–913. doi: 10.1038/nchembio.466
- Witte MD, van der Marel GA, Aerts JMFG, Overkleeft HS (2011) Irreversible inhibitors and activity-based probes as research tools in chemical glycobiology. *Org Biomol Chem* 9:5908–5926. doi: 10.1039/C1OB05531C

Wu L, Jiang J, Jin Y, et al (2017) Activity-based probes for functional interrogation of retaining  $\beta$ -glucuronidases. *Nat Chem Biol* 13:867–873. doi: 10.1038/nchembio.2395

## Supplementary Material

### $\beta$ -Glucosidase profile in BY2 cell cultures over time.

Activity based probe profiling was performed for BY2 cells cultured for different days. The results reveal that  $\beta$ -glucosidases are differently expressed over time. In parallel, 4MU activities of the lysates were measured, reflecting changed  $\beta$ -glucosidase expression.

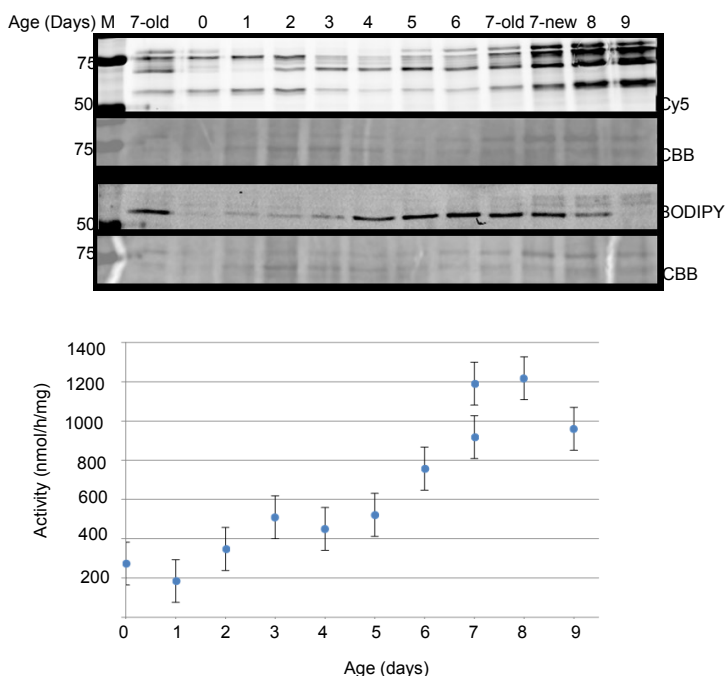


**Figure S1.** Beta-glucosidases of BY-2 cells with increasing of duration of cell culture. **A:** Detection by labeling with 0,5  $\mu$ M  $\beta$ -glucosidase ABPs containing aziridine (JJB 367) and epoxide (MDW 941) warheads (0,5 % DMSO, 2 h, pH 5.0). **B:** Detection by measurement of activity towards 4-MU  $\beta$ -D-glucopyranoside at pH 5.

### *In situ* Labelling of Cells with Activity Based Probes

The cell permeability of ABPs was examined by incubation of BY-2 cells. ABPs were added in the medium and cells were harvested after 120 minutes and lysed. Then, ABP labeling was analysed through SDS-PAGE and enzyme activity assays. ABP1 was used during *in situ* incubation; ABP2 is the one added in excess at lysis to ensure that the observed labelling with ABP1 did not happen during the preparation of lysates. As is clear from the gels in figure S2,



# Chapter 7

---

Diagnosis with activity-based probes of  
inherited glycosidase deficiencies  
using urine samples

---

*Kassiani Kytidou, Ivanna Denysiuk, Chi-Lin Kuo, Marta Artola, Herman S.  
Overkleeft, Johannes M.F.G Aerts*

*To be submitted*



## **Abstract**

Diagnosis of diseases caused by deficiencies in retaining glycosidases activities receives considerable interest because of new developments in their treatment. We here report the use of activity-based probes (ABPs) targeting retaining glycosidase to visualize active enzyme in biological materials such as cell lysates and urine samples. Proof-of-concept for diagnostic application of ABPs is presented.

## Introduction

Retaining glycosidases hydrolyze glycosidic bonds in glycoconjugates via a double displacement mechanism involving a nucleophile and acid/base catalytic residue in their catalytic pocket (Wu et al. 2019). Appropriate cyclophellitol analogues bind covalently to the catalytic nucleophile of these enzymes, as was first demonstrated for the human acid  $\beta$ -glucosidase (Atsumi et al. 1990). Using cyclophellitol as scaffold, selective activity-based probes (ABPs) toward GBA were designed. A reporter group (biotin or BODIPY) was attached to the C8 of cyclophellitol via a pentyl linker rendering ABPs allowing ultrasensitive and specific visualization of GBA *in vitro* and *in vivo* (Witte et al. 2010). Subsequently, cyclophellitol aziridine ABPs with attached reporter groups via alkyl or acyl linkers were designed reacting with multiple retaining glycosidases in the same class (Kallemeijn et al. 2012; Jiang et al. 2015a). Cyclophellitol aziridine ABPs labeling  $\alpha$ -galactosidases,  $\alpha$ -glucosidases,  $\alpha$ -fucosidase,  $\alpha$ -iduronidase,  $\beta$ -galactosidases, and  $\beta$ -glucuronidase as well as cyclophellitol ABPs labelling galactocerebrosidase have next been developed (Willems et al. 2014; Jiang et al. 2015b, 2016; Marques et al. 2016; Wu et al. 2017; Artola et al. 2018). Applications of ABPs are the quantitative detection of glycosidases in cells and tissues, as well as identification and characterization of glycosidase inhibitors by competitive ABP profiling (Lahav et al. 2017; Kuo et al. 2018; Van Meel et al. 2019).

Inherited deficiencies in retaining glycosidases with an acid pH optimum occur relatively common and form the molecular basis of several lysosomal storage disorders (LSDs)(Platt et al. 2018). Examples of such LSDs are Gaucher disease – deficiency of acid  $\beta$ -glucosidase (GBA, glucocerebrosidase, EC 3.2.1.45), Fabry disease – deficiency of  $\alpha$ -galactosidase A ( $\alpha$ GAL, EC 3.2.1.22) and Pompe disease – deficiency of acid  $\alpha$ -glucosidase (GAA, EC 3.2.1.20). Historically, diagnosis of lysosomal enzyme defects implied demonstration of reduced enzyme activities as conveniently measured with fluorogenic 4-methylumbelliferyl (MU)-glycoside substrates (Neufeld 1991). Presently, gene sequencing is used to confirm diagnosis of an inherited lysosomal glycosidase deficiency, however increasingly mutations with unknown significance are identified for several disorders (Schiffmann et al. 2016). The analysis by LC-MS/MS of accumulating metabolites during an enzyme deficiency becomes increasingly popular (Nowak et al. 2018). Our present study aims to look more closely into the value of ABPs for diagnostic purposes. Important advantages of ABPs are the selective labeling of active enzyme molecules in a complex biological sample and the additional information provided regarding the degree of proteolytic processing of lysosomal enzymes associated with their post-Golgi



maturation. In our study we analyzed lysates of cultured fibroblasts, a commonly used cell type in diagnosis, as well as urine samples. Urine is an attractive material for diagnosis because of the convenience of collection and its high content on lysosomal enzymes that constitute a major part of the total glycoprotein content allowing their enrichment with immobilized lectin Concanavalin A (Aerts et al. 1986). Already 40 years ago measurement of urinary GAA activity was employed for diagnosis of Pompe disease and later that of GBA for the diagnosis of Gaucher disease (Kokichi et al. 1977; Aerts et al. 1991).

## Results and Discussion

### **Method development.**

To develop a suitable procedure, first lysates of cultured human fibroblast known to contain lysosomal enzymes were examined by means of measurement of enzymatic activity with corresponding 4MU-glycoside substrate (Figure 1A) and ABP labeling followed by SDS-PAGE and fluorescence scanning (Witte et al. 2010; Kuo et al. 2018) (Figure 1B). Seven distinct fluorophore Cy5-equipped ABPs were used for detection of the corresponding enzymes: GBA, GAA,  $\alpha$ GAL,  $\alpha$ FUC,  $\beta$ GAL,  $\beta$ GLUR and  $\alpha$ MAN. All enzymes except  $\alpha$ FUC, present in low quantity, were successfully detected by ABP labeling (Figure 1B). The loss of the enzymatic activities after ABP labeling was checked and found to be nearly complete (Figure 1C). For most enzymes the inactivation by ABP was more than 70 % indicating after significant labelling. Only in the case of  $\alpha$ MAN, little inactivation was observed, suggesting that the enzyme activity is not due to the lysosomal  $\alpha$ -mannosidase but another of the five cellular  $\alpha$ -mannosidases (C.L. Kuo, unpublished observations). To enrich the signal of ABP-labeled lysosomal enzymes, enrichment with Concanavalin A (ConA) beads was performed (Figure 1B). The efficiency of binding to ConA beads was checked by enzyme activity measurements (Figure 1D). More than 80 % of each enzyme activity was retained on the ConA beads.

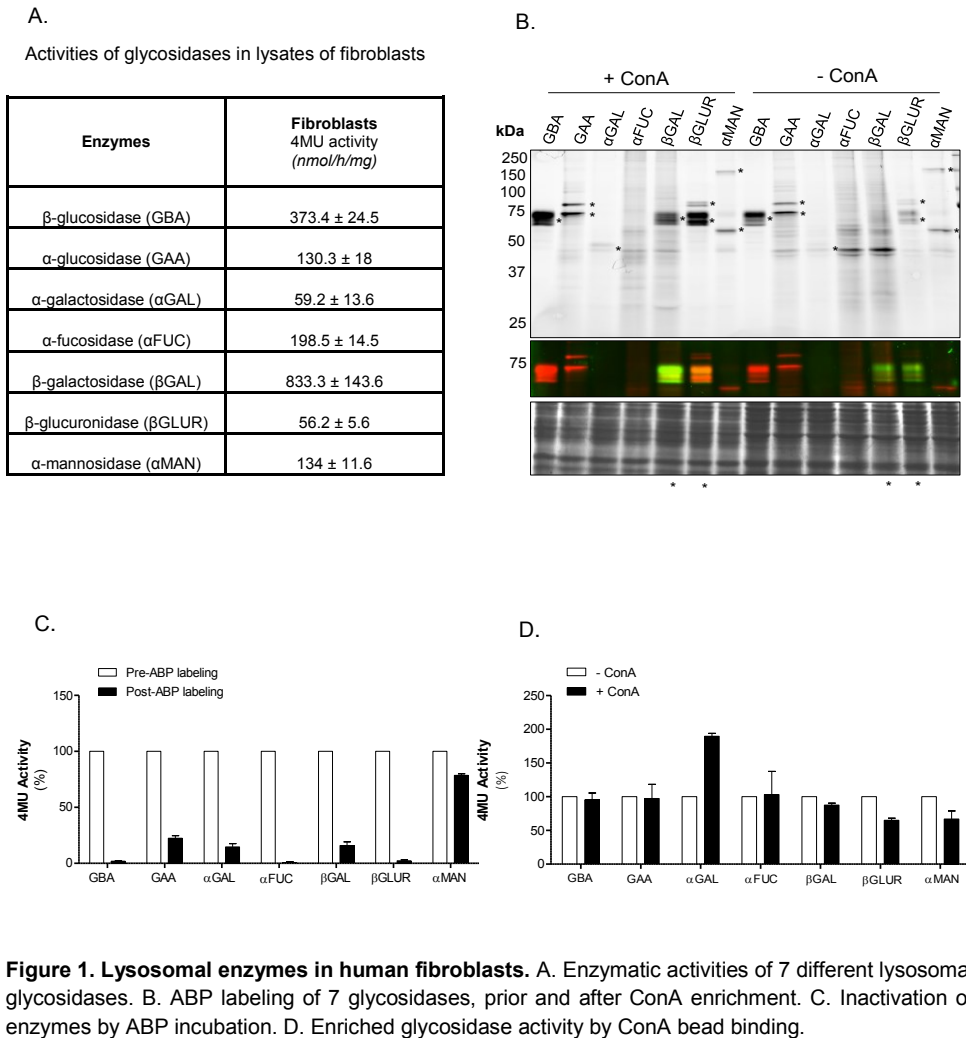


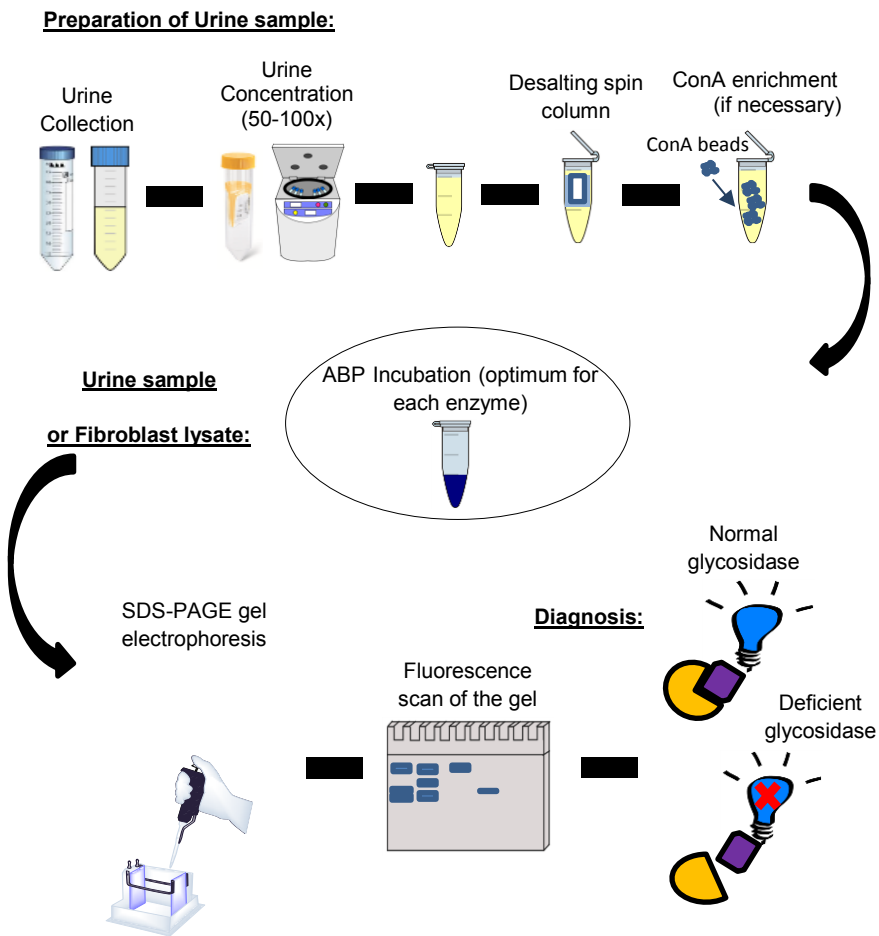
**Figure 1. Lysosomal enzymes in human fibroblasts.** A. Enzymatic activities of 7 different lysosomal glycosidases. B. ABP labeling of 7 glycosidases, prior and after ConA enrichment. C. Inactivation of enzymes by ABP incubation. D. Enriched glycosidase activity by ConA bead binding.

### ABP labeling of lysosomal enzymes in urine samples.

In freshly collected urine, the activities of various lysosomal enzymes were first determined activity measurements. The highest to lowest levels were observed for GAA,  $\beta$ GAL,  $\beta$ GLUR,  $\alpha$ GAL,  $\alpha$ FUC,  $\alpha$ MAN and GBA, respectively (Figure 2A). ABP labeling of urinary lysosomal enzymes was performed using the U-ABP method described in Scheme 1. Lysosomal enzymes in urine samples were enriched by binding to ConA beads, labeled with ABP and subjected to SDS-PAGE followed by visualization with fluorescence scanning (Figure 2B). The molecular weights of the various visualized lysosomal enzymes correspond with

the expected ones. Labeling of lysosomal enzymes in urine samples is efficient as indicated by the high degree of inactivation (Figure 2D). Enrichment of lysosomal enzymes from urine samples by ConA bead precipitation is efficient (Figure 2D). To check the need for ConA enrichment, urine samples were also analyzed without such enrichment. We noted a prominent non-specific band with the fucosidase ABP that was not seen in the ConA enriched fractions (Figure 4B). In addition, as seen in Coomassie brilliant blue staining of the gel, (Figure 4B lower panel), urine samples after ConA enrichment contain much less total protein.

**Scheme 1. Urinary Activity Based Profiling method (U-ABP)**



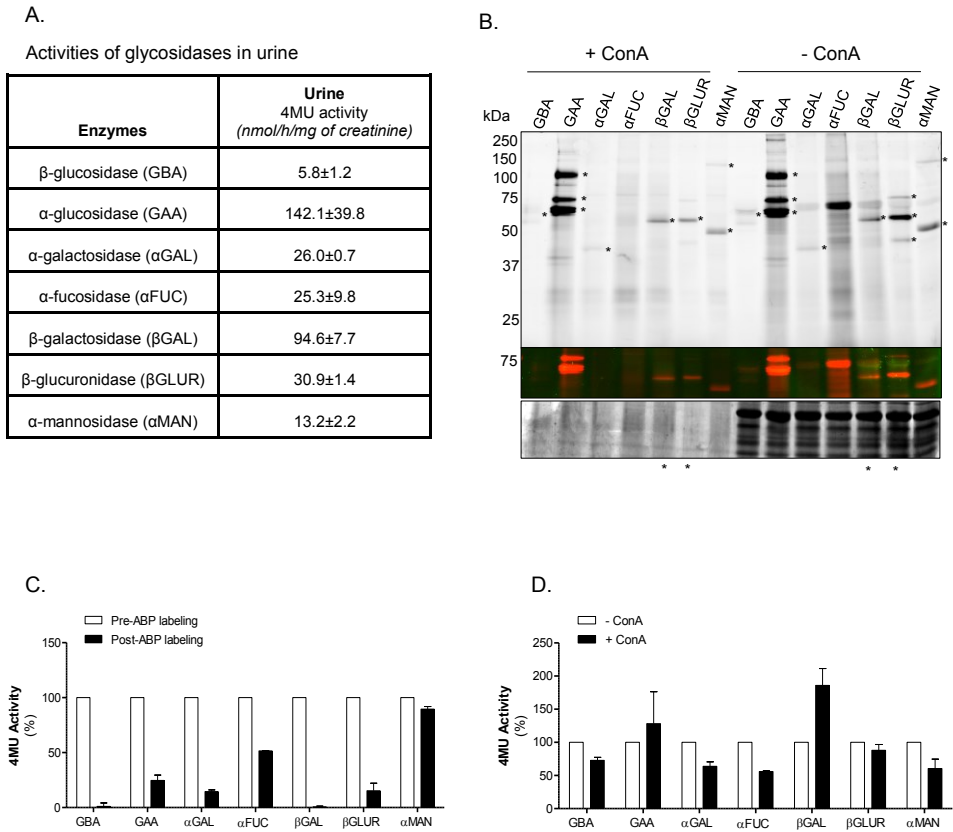


**Figure 2. Lysosomal enzymes in human urine.** A. Enzymatic activities of 7 different lysosomal glycosidases. B. ABP labeling of 7 glycosidases, prior and after ConA enrichment (U-ABP method). C. Inactivation of enzymes by ABP incubation. D. Enriched glycosidase activity by ConA bead binding.

### Diagnostic tests with ABPs.

In lysates of control and Pompe fibroblasts, GAA was labeled with JJB38Cy5 and GBA with MDW944-Bodipy. Pompe fibroblasts did not show any JJB383 labelled protein, and normal levels of MDW944 labeled GBA.

Using the U-ABP method, 3 different glycosidases in urine samples of normal individuals and type 1 Gaucher patients were labeled with corresponding fluorescent Cy5-ABPs ABPs (ME569, TB474 and JJB383, respectively). The Gaucher patients could be clearly identified based on low level of labeled GBA and concomitant prominent labeling of  $\alpha$ GAL and GAA.

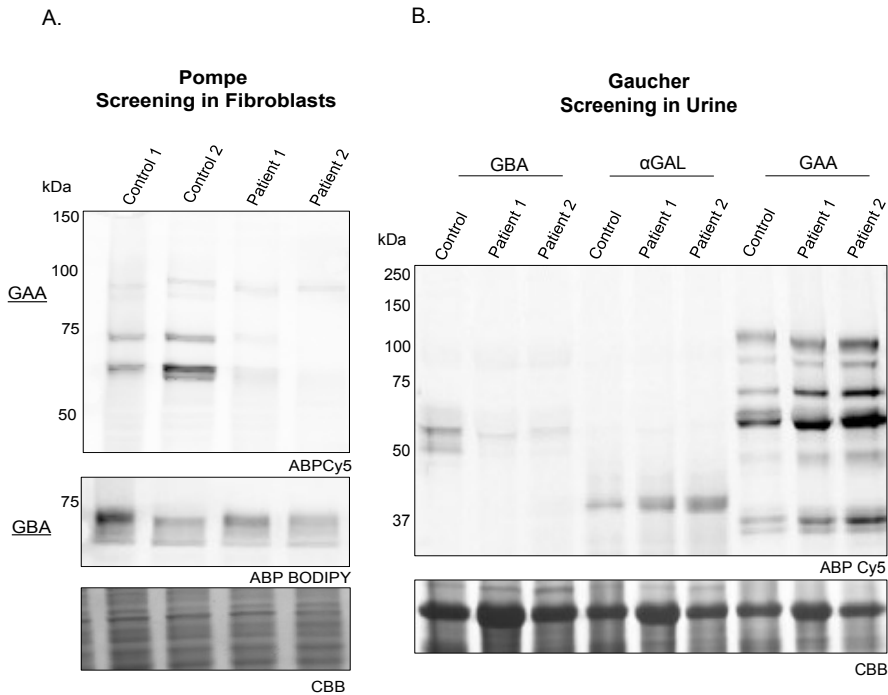


**Figure 3. Diagnostic tests with ABPs.** A. Visualization with ABP of GAA and GBA in lysates of control and Pompe disease fibroblasts. Incubation of lysate with both JJB383 (GAA) and MDW944 (GBA). B. Visualization of glycosidase in control and Gaucher urine samples using the U-ABP method. Three lysosomal glycosidases, GBA,  $\alpha$ GAL and GAA were screened using ME569, TB474 and JJB383 respectively.

Overall, the use of ABP labeling of glycosidases in lysates of cells and urine samples for diagnostic purposes holds great promise. The method is sensitive, allowing detecting of low amounts of active enzyme molecules. Western blotting is in general far less sensitive and does not provide information of active enzyme molecules but rather total enzyme protein. Activity measurements with fluorogenic substrates do not provide information on the molecular weight of the enzyme which in the case of lysosomal enzymes may give insight in endolysosomal maturation of the protein (Oude Elferink, R P et al. 1986). Extension of ABP analyses of samples of patients suffering from various glycosidase deficiencies is warranted. Moreover, with the assays in place it might be interest to also test other disease conditions on abnormalities in lysosomal glycosidases. Secondary deficiencies in lysosomal enzymes in disease conditions may have so far been overlooked as illustrated by the only recent recognition that impairment of GBA is a major risk factor for Parkinson's disease (Do et al. 2019).

## Materials and methods

**Fibroblast lysates.** Normal and Pompe human fibroblasts were grown in T-25 flasks and cultured in Dulbecco's modified Eagle's medium/Nutrient Mixture F-12 (DMEM/F-12, Sigma) media, supplemented with 10 % fetal calf serum and 1 % penicillin/streptomycin, at 37 °C with 5 % CO<sub>2</sub> in a humidified incubator. The cells were harvested when reached 80 % of confluency and lysed in ice cold lysis buffer (50 mM phosphate buffer pH 6.5, 0.1 % Triton X-100, with additional protease inhibitor) following sonication. The lysates were stored at -20 °C until further use.

**Urine samples.** Normal and Gaucher human urine was collected. Samples were concentrated 50-100 times using the Amicon® Ultra-15 Centrifugal Filter Units according to manufacturer's protocol. Next, the samples were passed through a 0.7-ml Pierce™ polyacrylamide spin desalting column 7000 MWCO (Thermo Fisher Scientific), according to the manufacturer's protocol and buffer exchanged to 150 mM Citric/Phosphate buffer (McIlvaine), pH 5.3. Samples were stored at -20 °C until further use.

**Concanavalin A enrichment.** Fibroblast lysates and urine samples were incubated for 1 or 2 h at 4 °C, while rotating with Concanavalin A-Sepharose 4B beads (ConA beads), and the protocol followed exactly as previously described (Kytidou et al. 2018). The obtained samples were immediately used for measurements of enzyme activities and ABP labeling.

**Creatinine levels and total protein measurement.** Creatinine levels of unconcentrated urine samples were determined using creatinine (3mg/dl) as standard (19). Total protein content of both fibroblast and urine samples was determined using the Micro BCA Protein Assay Reagent Kit by PIERCE with bovine serum albumin as a standard, according to the supplier's protocol.

**4MU enzymatic activities.** Activities of GBA, GAA, αGAL, αFUC, βGAL, βGLUR and αMAN were measured with the corresponding 4MU-glycoside substrate. The respective assay mixtures contained 4MU-β-D-glucopyranoside (1.25 mg/mL) at pH 5.2; 4MU-α-D-galactopyranoside (1 mg/mL) at pH 4.0; 4MU-α-D-galactopyranoside (1.5 mg/mL) at pH 4.6; 4MU-α-D-mannopyranoside at (3.4 mg/mL) pH 4.0; 4MU-β-D-glucopyranoside (0.69 mg/mL) at pH 4.8 , 4MU-α-L-fucopyranoside (0.33 mg/mL) at pH 5.5; 4MU-β-D-galactopyranoside (0.18 mg/mL) at pH4.3. The assay mixture contained 150

mM citrate-phosphate buffer at the appropriate pH supplemented with 0.1% (w/v) BSA. In the case of the GBA assay, the mixture contained also 0.1% Triton x-100 and 0.2 % taurocholic acid. Assays were performed by incubation of 25  $\mu$ L sample with 100  $\mu$ L of assay mix for 30 min to 1 h at 37 °C. The assays were stopped and released 4MU was quantified as earlier described (19).

**ABP labelling.** The following ABPs (all Cy5 labelled if not indicated differently) were used for detection of corresponding enzyme: ME569 and MDW944 (Bodipy red) labelling GBA; TB474 labelling  $\alpha$ GAL; JJB383 labelling GAA; JJB392 labelling  $\beta$ GLUR; JJB381 labelling  $\alpha$ FUC; TB652 labelling  $\beta$ GAL and TB482 labelling  $\alpha$ MAN. Fibroblast lysates and urine samples were incubated with ABPs, dissolved in 150mM McIlvaine buffer, at optimal conditions for each enzyme (20  $\mu$ L total assay volume): GBA: 250 nM ME569 at pH 5.3;  $\alpha$ GAL: 250nM TB474 at pH 4.8; GAA: 250nM JJB383 at pH 4.8;  $\beta$ GLUR: JJB392 at pH 5.3 (in the same mixture 500 nM of MDW944 for GBA1 was added to avoid cross labeling of GBA);  $\alpha$ FUC: 1  $\mu$ M JJB381 at pH4.8;  $\beta$ GAL: 1  $\mu$ M TB652 at pH 4.8 (and in the same mixture 500 nM of MDW944 for GBA1 was added to avoid cross labeling of GBA), and  $\alpha$ MAN: 1  $\mu$ M of TB482 pH 5.3. All ABP incubations were performed for 1h at 37 °C. Next, the samples were either used for activity measurements or applied to 10 % SDS-PAGE, where after the gels were scanned for fluorescence as described before (Witte et al. 2010; Jiang et al. 2016).



## References

- Aerts JMFG, Donker-Koopman WE, Koot M, et al (1986) Deficient activity of glucocerebrosidase in urine from patients with type 1 Gaucher disease. *Clin Chim Acta* 158:155–163. doi: [http://dx.doi.org/10.1016/0009-8981\(86\)90231-7](http://dx.doi.org/10.1016/0009-8981(86)90231-7)
- Aerts JMFG, Miranda MCS, de Lacerda LW, et al (1991) The identification of type 1 Gaucher disease patients, asymptomatic cases and carriers in The Netherlands using urine samples: An evaluation. *Clin Chim Acta* 203:349–361. doi: [https://doi.org/10.1016/0009-8981\(91\)90308-Y](https://doi.org/10.1016/0009-8981(91)90308-Y)
- Artola M, Kuo C-L, McMahan SA, et al (2018) New Irreversible  $\alpha$ -l-Iduronidase Inhibitors and Activity-Based Probes. *Chem – A Eur J* 24:19081–19088. doi: [10.1002/chem.201804662](https://doi.org/10.1002/chem.201804662)
- Atsumi S, Umezawa K, Iinuma H, et al (1990) Production, isolation and structure determination of a novel beta-glucosidase inhibitor, cyclophellitol, from *Phellinus* sp. *J Antibiot (Tokyo)* 43:49–53. doi: [10.7164/antibiotics.43.49](https://doi.org/10.7164/antibiotics.43.49)
- Blom D, Speijer D, Linthorst GE, et al (2003) Recombinant Enzyme Therapy for Fabry Disease: Absence of Editing of Human  $\alpha$ -Galactosidase A mRNA. *Am J Hum Genet* 72:23–31. doi: <https://doi.org/10.1086/345309>
- Do J, McKinney C, Sharma P, Sidransky E (2019) Glucocerebrosidase and its relevance to Parkinson disease. *Mol Neurodegener* 14:36. doi: [10.1186/s13024-019-0336-2](https://doi.org/10.1186/s13024-019-0336-2)
- Jiang J, Beenakker TJM, Kallemeijn WW, et al (2015a) Comparing Cyclophellitol N-Alkyl and N-Acyl Cyclophellitol Aziridines as Activity-Based Glycosidase Probes. *Chem – A Eur J* 21:10861–10869. doi: [10.1002/chem.201501313](https://doi.org/10.1002/chem.201501313)
- Jiang J, Kallemeijn WW, Wright DW, et al (2015b) In vitro and in vivo comparative and competitive activity-based protein profiling of GH29  $\alpha$ -l-fucosidases. *Chem Sci* 6:2782–2789. doi: [10.1039/C4SC03739A](https://doi.org/10.1039/C4SC03739A)
- Jiang J, Kuo C-L, Wu L, et al (2016) Detection of Active Mammalian GH31  $\alpha$ -Glucosidases in Health and Disease Using In-Class, Broad-Spectrum Activity-Based Probes. *ACS Cent Sci* 2:351–358. doi: [10.1021/acscentsci.6b00057](https://doi.org/10.1021/acscentsci.6b00057)
- Kallemeijn WW, Li K-Y, Witte MD, et al (2012) Novel Activity-Based Probes for Broad-Spectrum Profiling of Retaining  $\beta$ -Exoglucosidases In Situ and In Vivo. *Angew Chemie Int Ed* 51:12529–12533. doi: [10.1002/anie.201207771](https://doi.org/10.1002/anie.201207771)
- Kokichi S, Etsuko O, Nobuo S, et al (1977) Urinary  $\alpha$ -glucosidase analysis for the detection of the adult form of Pompe's disease. *Clin Chim Acta* 77:61–67. doi: [https://doi.org/10.1016/0009-8981\(77\)90402-8](https://doi.org/10.1016/0009-8981(77)90402-8)
- Kuo, C-L., van Meel, E., Kytidou, K., et al. (2018). Activity-Based Probes for Glycosidases: Profiling and Other Applications. *Methods Enzymol.* 598:217-235. doi: [10.1016/bs.mie.2017.06.039](https://doi.org/10.1016/bs.mie.2017.06.039).
- Kytidou K, Beekwilder J, Artola M, et al (2018) *Nicotiana benthamiana*  $\alpha$ -galactosidase A1.1 can functionally complement human  $\alpha$ -galactosidase A deficiency associated

- with Fabry disease. *J Biol Chem* 293:10042–10058. doi: 10.1074/jbc.RA118.001774
- Lahav D, Liu B, van den Berg RJBHN, et al (2017) A Fluorescence Polarization Activity-Based Protein Profiling Assay in the Discovery of Potent, Selective Inhibitors for Human Nonlysosomal Glucosylceramidase. *J Am Chem Soc* 139:14192–14197. doi: 10.1021/jacs.7b07352
- Marques, A.R.A., Willems, L.I., Herrera Moro, D., et al. (2016). A Specific Activity-Based Probe to Monitor Family GH59 Galactosylceramidase, the Enzyme Deficient in Krabbe Disease. *ChemBioChem* 18:402–412. doi: 10.1002/cbic.201600561
- Neufeld EF (1991) Lysosomal storage diseases. *Annu Rev Biochem* 60:257–280. doi: 10.1146/annurev.bi.60.070191.001353
- Nowak A, Mechtler TP, Hornemann T, et al (2018) Genotype, phenotype and disease severity reflected by serum LysoGb3 levels in patients with Fabry disease. *Mol Genet Metab* 123:148–153. doi: <https://doi.org/10.1016/j.ymgme.2017.07.002>
- Oude Elferink, R P RPJ, Van Doorn-Van Wakeren J, Hendriks T, et al (1986) Transport and processing of endocytosed lysosomal  $\alpha$ -glucosidase in cultured human skin fibroblasts. *Eur J Biochem* 158:339–344. doi: 10.1111/j.1432-1033.1986.tb09756.x
- Platt FM, d’Azzo A, Davidson BL, et al (2018) Lysosomal storage diseases. *Nat Rev Dis Prim* 4:27. doi: 10.1038/s41572-018-0025-4
- Schiffmann R, Fuller M, Clarke LA, Aerts JMFG (2016) Is it Fabry disease? *Genet Med* 18:1181–1185. doi: 10.1038/gim.2016.55
- Van Meel, E., Bos, E., van der Lienden, M.J.C., et al. (2019). Localization of active endogenous and exogenous  $\beta$ -glucocerebrosidase by correlative light- electron microscopy in human fibroblasts. *Traffic*. 20:346–356. doi: 10.1111/tra.12641
- Willems LI, Beenakker TJM, Murray B, et al (2014) Potent and Selective Activity-Based Probes for GH27 Human Retaining  $\alpha$ -Galactosidases. *J Am Chem Soc* 136:11622–11625. doi: 10.1021/ja507040n
- Witte, M.D., Kallemeijn, W.W., Aten, J., et al. (2010). Ultrasensitive in situ visualization of active glucocerebrosidase molecules. *Nat Chem Biol* 6:907–913. doi: 10.1038/nchembio.466
- Wu L, Armstrong Z, Schröder SP, et al (2019) An overview of activity-based probes for glycosidases. *Curr Opin Chem Biol* 53:25–36. doi: <https://doi.org/10.1016/j.cbpa.2019.05.030>
- Wu L, Jiang J, Jin Y, et al (2017) Activity-based probes for functional interrogation of retaining  $\beta$ -glucuronidases. *Nat Chem Biol* 13:867–873. doi: 10.1038/nchembio.2395

# Chapter 8

---

General discussion and perspectives  
for future research

---



The studies described in this thesis deal with glycosidases, in particular alpha-galactosidases. Activity-based probes are a versatile research tool in many of the investigations on glycosidases and are examined regarding diagnostic application. A specific element of the thesis investigations is the focus on plants, either as source of endogenous glycosidases as well as production platform for therapeutic human enzymes. The introductory **chapter 2** discusses also the abundant glycosylated metabolites of plants, such as flavonoids, cardiac glycosidases and phytosterols, with attention to their metabolism and the health effects of their consumption (**chapter 2**).

In this concluding chapter, the outcome of the thesis investigations is discussed and future developments are considered. Special attention is paid to enzyme replacement therapy (ERT) for Fabry disease and Gaucher disease. In addition, the use of ABPs as a future diagnostic tool for various diseases is underlined.

### **Plants as an appealing production platform.**

The use of plants as a production platform of pharmaceutical proteins has become feasible and popular. Important advantages of plant platforms are the lack of contaminations of products with animal viruses and prions (Desai et al. 2010). Furthermore, the present ease to genetically manipulate plants, the low costs of their maintenance, and high yield of recombinant protein production puts plants in a highly competitive place among other production platforms such as yeast, bacterial or mammalian cell systems. For example, grams of monoclonal antibodies (mAbs) can be rapidly produced in *Nicotiana tabacum*, illustrating how plants are particularly attractive platforms when high production of recombinant protein has to be obtained in short notice (Schähs et al. 2007; Castilho and Steinkellner 2012; Arntzen 2015). Fortuitously, plants are easily manipulated in their N-glycosylation machinery, making them very appropriate for production of therapeutic recombinant glycoproteins (Schähs et al. 2007; Castilho and Steinkellner 2012; Bosch et al. 2013). This aspect is highly relevant for the production of lysosomal enzymes that are glycoproteins with essential N-linked glycans (Storch and Braulke 2005).

### **Recombinant glycosidases for ERT of LSDs.**

Over the years, mammalian cells have mainly been used to produce recombinant lysosomal enzymes for ERT of different lysosomal storage disorders, (**chapter 2**). As envisioned by Roscoe O. Brady, targeted supplementation of macrophages with recombinant GBA1 successfully prevents, and even corrects, visceral symptoms of Gaucher patients deficient in the enzyme (Brady 2003b; Aerts and Cox 2018). The originally approved

enzyme for ERT of Gaucher disease was isolated from human placenta and engineered to have terminal N-linked glycans with terminal mannose residues to favour uptake by mannose-receptor expressing macrophages (Brady 2003b). The approach was commercialized by Genzyme Corp. and led to the registration in 1991 of Alglucerase (Ceredase®) (Ferraz et al. 2014). Subsequently, human GBA1 was recombinantly produced in Chinese hamster ovary cells (CHO), resulting in the registration of Imiglucerase (Cerezyme®; Genzyme) in 1994. Later, gene activation in cultured fibroblasts was used to recombinantly produce a competitive GBA1 enzyme, resulting in registration in 2010 of Velaglucerase (VRIV®; Shire/TKT) (Aerts et al. 2010). A few years later, Protalix managed to produce GBA1 in carrot cells and the product was named Taliglucerase (Elelyso®), registered in 2012 for treating Gaucher type 1 patients. The recombinant GBA1 enzyme is targeted into carrot plant cell vacuoles via the insertion of a specific target signal peptide at its amino acid sequence, and it contains plant specific N-linked glycosylated residues;  $\alpha$ -1,3 fucose and  $\beta$ -1,4 xylose (Shaaltiel et al. 2007). These modifications seem not to induce immune responses or interfere with GBA1 enzymatic activity and effectiveness as was shown by extensive clinical trials (Rup et al. 2017).

Following the success of ERT for type 1 Gaucher disease, the same approach was soon pursued for other lysosomal storage diseases. Among the frontrunners was Pompe disease, a disorder characterized by lysosomal glycogen storage due to deficiency of acid  $\alpha$ -glucosidase (GAA). In parallel, GAA was recombinantly produced in CHO cells and milk of transgenic animals (Geel et al. 2007). In the latter case, the GAA gene was linked to the promoter region of the casein gene that promotes high level expression in epithelial cells of the mammary gland. Despite promising data with recombinant GAA produced in rabbit milk, only recombinant human GAA was ultimately developed by Genzyme into a registered drug, Aglucosidase alfa or Myozyme/Lumizyme®) (Reuser et al. 2002). Importantly, targeting of therapeutic GAA is governed by the presence of mannose-6-phosphate moieties in its glycans and uptake and subsequent delivery to lysosomes by mannose-6-phosphate receptor (Reuser et al. 2002). More recently, cultured rice cells are explored as production platform of recombinant GAA with optimal N-glycan composition (Su et al. 2015; Choi et al. 2018).

Meanwhile, ERT products have been or are developed for several other lysosomal storage disorders: mucopolysaccharidosis type I (Hurler/Scheie disease), mucopolysaccharidosis type II (Hunter disease), Mucopolysaccharidosis type IIIA (Sanfilippo A syndrome), Mucopolysaccharidosis type IIIB (Sanfilippo B syndrome), Mucopolysaccharidosis type IVA (Morquio A syndrome),

Mucopolysaccharidosis type VI (Maroteaux-Lamy syndrome), Mucopolysaccharidosis type VII (Sly syndrome), Niemann-Pick disease type C, Alpha-Mannosidosis, Lysosomal acid lipase deficiency (Wolmann disease), Neuronal ceroid lipofuscinosis type 2, Globotriaosylceramidosis (Fabry disease), Globoid cell leukodystrophy (Krabbe disease) and Ceramidosis (Farber disease). Of note, at present gene therapy and RNA therapy approaches are actively studied for several of lysosomal storage disorders. Enzyme supplementation (either direct by infusion of recombinant enzyme or indirect by gene or RNA therapy) may induce in some patient's immune responses to the 'foreign' protein.

### **ERT of Fabry disease.**

In the case of X-linked Fabry disease (lysosomal globoside Gb3 storage due to deficiency of acid  $\alpha$ -galactosidase (GLA)), ERT is in use since 2001, when two therapeutic enzymes were approved at the same time by the EMEA, agalsidase beta (Fabrazyme® produced in CHO cells by Genzyme) and agalsidase alpha (Replagal®, produced in a human fibrosarcoma cell line by Shire). Both GLA enzymes were found to be identical in catalytic properties, nevertheless they are administrated in different doses; 0.2 mg per kg for Fabrazyme vs 1 mg per kg for Replagal (Blom et al. 2003).

ERT of Fabry disease is not as successful as for Gaucher disease (Brady 2003a). The poor clinical response is accompanied by poor correction of the lipid storage biomarker plasma lysoGb3 (Aerts et al. 2008). A major complication is the formation of neutralizing antibodies towards therapeutic enzyme in male Fabry patients impairing clinical and biomarker response (Linthorst et al. 2004). In addition to poor efficacy, the high costs of current ERT treatments of Fabry disease prompted alternative products. Protalix Biotherapeutics has managed to produce GLA in BY2 *Nicotiana tabacum* cell cultures (ProCellEx system). The enzyme (Pegunigalsidase alfa) is chemically modified with polyethylene glycol (PEG). It is currently examined in clinical trials (Schiffmann et al. 2019). Pegunigalsidase alfa shows a much higher half-life as active enzyme in blood than Replagal and Fabrazyme and its repeated infusion in Fabry patients has been found to lead to promising reductions in plasma lysoGb3 (Holida et al. 2019).

Another human GLA is currently produced in a moss cell line engineered to yield glycoproteins with high mannose N-linked glycans (Lenders and Brand 2018). This thesis reports also the production of human GLA in *Nicotiana benthamiana* plants, via agrobacteria transformations, (Kytidou et al. 2017)(**chapter 3**). In conclusion, more and more recombinant lysosomal enzymes are being produced in plant cell-based systems (He et al. 2011; Su et al. 2015).

**Alternative enzymes for Fabry ERT.**

In 2009, Sakuraba and colleagues firstly suggested the use in ERT of Fabry disease of a modified NAGA enzyme (Tajima et al. 2009). NAGA is a closely related protein to GLA that is active towards  $\alpha$ -N-acetyl-galactosiminides (Tajima et al. 2009; Tomasic et al. 2010). The proposed modification of NAGA involves substitution of alanine at position 191 into a leucine (L) and that of serine at position 188 into a glutamic acid (E). The modified NAGAEL is improved in degradation of alpha-galactosides such as the artificial 4MU- $\alpha$ GAL and natural lipid substrate Gb3 (Tajima et al. 2009). In parallel, NAGA's natural activity towards N-acetylgalactosaminides is lost. Independently, Garman and colleagues proposed the same substitutions in the active site of NAGA enzyme to improve  $\alpha$ -galactosidase activity (Tomasic et al. 2010). We have produced modified NAGAEL, as well as GLA and NAGA, in *N. benthamiana* leaves ((Kytidou et al. 2017) **chapter 3**). Our findings with the enzymes confirm that NAGAEL is improved in activity towards 4MU- $\alpha$ GAL substrate over 5 times and shows no longer activity towards the 4MU-NAGA substrate. Interestingly, the wild type enzyme is also active towards Gb3, around 10 times less than NAGAEL. NAGA and NAGAEL were found to be more stable in human plasma than GLA. NAGAEL did not cross react with antibodies in serum of male Fabry patients receiving ERT.

During expression studies in *N. benthamiana*, we noticed a prominent endogenous  $\alpha$ -galactosidase that is inactivated (and labelled) by an  $\alpha$ -galactosyl configured cyclophellitol aziridine (Willems et al. 2014). We overexpressed and purified the enzyme, named A1.1 ((Kytidou et al. 2018) **chapter 4**). The enzyme A1.1 was found to be also active towards the lipid Gb3. Incubating fibroblasts from a male Fabry patient with recombinant A1.1. led to marked reductions of Gb3 and lysoGb3. Of note, the A1.1 protein does not contain any N-linked glycans. We were able to produce crystals and elucidate the 3D structure of the enzyme (Kytidou et al. 2018). A1.1 is lacking N-linked glycans. Interestingly, the enzyme is very similar to its human homologue in overall structure, sharing 42 % amino acid sequence identity. Most importantly the active site of both enzymes is highly conserved.

A1.1 can be recombinantly produced in *N. benthamiana* at very high yields, accumulates in the apoplast, is stable and because of its homogeneity easy to purify. Considering therapeutic application of A1.1 in Fabry patients, the lack of glycans is prohibits lectin-mediated endocytosis and delivery to lysosomes. It will be rather complicated to mutagenize the enzyme in such way that synthesized N-glycans can attached to newly generated asparagine residues (Priyanka et al. 2016). The A1.1 is not neutralized by anti-human GLA antibodies of Fabry patients. Given the broad pH optimum of A1.1, it



might be considered to examine whether circulating A1.1 in the plasma is able to degrade lysoGb3 there. It is presently thought that lysoGb3 is a highly toxic agent in Fabry patients that has a negative effect on the vasculature, nociceptive neurons and podocytes (Choi et al. 2015; Sanchez-Niño et al. 2015; Aerts et al. 2017). The therapeutic potential A1.1 could be judged by AAV-9 mediated overexpression of the enzyme in liver of Fabry mice. Similarly, it might be considered to administer A1.1 (or another plant-derived  $\alpha$ -galactosidase) orally in order to lower lysoGb3 in the lumen of the intestine of Fabry patients. Fabry patients develop gastrointestinal symptoms that recently have been ascribed to a changed the gut microbiome because of the presence of lysoGb3 (Aguilera-Correa et al. 2019).

An intestinal application of a recombinant  $\alpha$ -galactosidase has earlier been conceived. The dietary supplement Beano, a fungal (*Asperigilus niger*)  $\alpha$ -galactosidase, offers relief of gastrointestinal problems after consumption of food rich in  $\alpha$ -galactosides like beans (Ganiats et al. 1994; Lettieri and Dain 1998; Levine and Weisman 2004). The enzyme also degrades 4MU- $\alpha$ GAL and is targeted by an  $\alpha$ -galactose configured ABP, (**chapter 6**). Unfortunately, the enzyme is not able to degrade Gb3.

### **Chaperone strategy for treatment of Fabry disease.**

Treatment of Fabry disease with orally administered small compound chaperones is presently investigated (Sunder-Plassmann et al. 2018; Müntze et al. 2019). Pharmacological chaperones are supposed to bind and stabilize newly formed mutant GLA. At present, PCT treatment is performed with Fabry patients with some residual endogenous  $\alpha$ GAL activity, and not for classic Fabry patients lacking the enzyme. Deoxygalactonojirimycin, (Gal-DNJ or Migalastat®, Amicus), is now approved in Europe as pharmacological chaperone (PC) for the treatment of Fabry disease (Markham 2016; Müntze et al. 2019). Migalastat binds to mutant GLAs, that are otherwise targeted for degradation, and stabilizes them, allowing delivery to lysosomes. In principle, the same chaperone approach could be considered for stabilizing recombinant GLA during ERT given the instability of the enzyme (Artola et al. 2019). For such purpose, therapeutic recombinant GLA and chaperones could be jointly infused. The synthesis and evaluation of an entire new class of inhibitors for GLA is described in **chapter 5** (Artola et al. 2019). The novel inhibitor,  $\alpha$ -cyclosulfamidate 4, ME763, shows chaperone properties like Gal-DNJ, however it is much less effective at the same dose. Interestingly, ME763 and Gal-DNJ also stabilize human GLA and NAGA as well as plant A1.1. Incubation of A1.1 with Gal-DNJ and ME763 at concentrations, 200 and 20  $\mu$ M respectively, enhances its stability during incubation in human plasma.

In conclusion, there is still an unmet need for Fabry disease. New therapeutic approaches besides existing ERTs warrant further attention, among these PCT as well as gene and RNA therapies (Liefhebber et al. 2019; Tuttolomondo and Pinto 2019; Zhu et al. 2019).

### **Human GBA and plant homologs.**

The lysosomal acid  $\beta$ -glucosidase GBA1 (EC 3.2.1.45; GH30) degrades glucosylceramide (GlcCer) to ceramide and glucose. Mutations in the GBA gene cause Gaucher disease (MIM#230800) (Ferraz et al. 2014). More recently it has been recognized that individuals with a mutant GBA allele are also at considerably increased risk for Parkinson disease (PD) (Riboldi and Di Fonzo 2019). PD is caused by progressive loss of dopaminergic neurons in the substantia nigra and its symptoms mainly include motor difficulties such as bradykinesia, resting tremor and postural instability. Non-motor symptoms in PD are depression and anxiety.

GBA1 is a 497 amino acid protein with 4 N-linked glycans that are essential for its folding, intracellular trafficking and delivery to lysosomes (Ben Bdira et al. 2018). The protein, in contrast to other lysosomal enzymes, does not acquire mannose-6-phosphate residues at its N-linked glycans for lysosomal sorting (Aerts et al. 1988). GBA1 is transported to lysosomes bound to lysosomal integral membrane protein type 2 (LIMP2) (Reczek et al. 2007; Gaspar et al. 2014). GBA1 was initially classified in the GH 5 family, a glycoside hydrolase family containing enzymes from various organisms able to metabolize GlcCer. GH5 and GH30 glycosidases are very closely related enzymes. They share an  $(\alpha/\beta)_8$  TIM-barrel domain with two, highly conserved, catalytic residues, placed between 2  $\beta$ -strands and serving as the nucleophile and acid/base. Proteins of the GH 5 and 30 families have some differences in overall structure. GH30 enzymes besides the catalytic domain a  $\beta$ -structure consisting of an immunoglobulin-like fold which is absent in GH5 enzymes.

Earlier ABPs with a cyclophellitol epoxide scaffold have been designed that specifically label GBA1, but not other human  $\beta$ -glucosidases (GBA2, GH 116 and GBA3, GH1) (Kallemeijn et al. 2012). Using such ABP, a specific protein was labelled in extracts of cultured tobacco cells. (**chapter 6**). Analysis by proteomics revealed its identity as an GH 5 glycosidase ('glucan 1,3- $\beta$ -glucosidase A, isoform X2'). The enzyme, named B56, is a soluble protein that seems to lack N-glycans based on its inability to bind to Concanavalin A beads. It shows optimal activity between pH 4.5 to 5.5 and is able to degrade the lipid substrate GlcCer with a NB-fluorophore in the acyl moiety. Modelling reveals that the catalytic residues are similarly positioned as in GBA1. Further characterization of B56 is warranted. For this purpose, the enzyme should be

overexpressed and purified. In particular, the ability of B56 to degrade natural GlcCer and its toxic metabolite glucosylsphingosine (GlcSph) should be further studied. For this purpose, B56 can be expressed in cells lacking endogenous GBA1 that accumulate GlcCer as well as GlcSph and the response in lipid abnormalities can be monitored with LC-MS/MS methods in place. The envisioned studies should reveal whether B56 has any therapeutic potential regarding Gaucher disease and other conditions with disturbed GlcCer metabolism.

### **Activity-based probes and diagnosis.**

Activity-based probes (ABPs) for various glycosidases have meanwhile been designed and characterized. Examples are ABPs labelling  $\beta$ -glucosidases  $\alpha$ -galactosidases,  $\alpha$ -glucosidases,  $\alpha$ -fucosidase,  $\alpha$ -iduronidase,  $\beta$ -galactosidases, and  $\beta$ -glucuronidase (Witte et al. 2010; Kallemeijn et al. 2012; Willems et al. 2014; Jiang et al. 2015b, a, 2016; Marques et al. 2016; Wu et al. 2017; Artola et al. 2018).

So far, ABPs have been limited used for diagnosis of LSDs (Aerts et al. 2011). A published application is the detection of active glycosidase in lysates of cells, for example the use of MDW944 to demonstrate GBA deficiency in fibroblasts of Gaucher patients (Aerts et al. 2011; Jiang et al. 2016).

In **chapter 7** the feasibility of diagnosing LSDs with fluorescent ABPs is demonstrated for cultured cells as well as urine samples. Urine is long known to be a great source of lysosomal enzymes. For example, the presence of various lysosomal enzymes in urine has been studied with activity assays and Western blot analysis already in the 90's (Aerts et al. 1991). A novel protocol for the screening of lysosomal glycosidases by ABP detection was developed for urine samples (**chapter 7**). The method is very sensitive and can be used to screen for deficiencies in  $\beta$ -glucosidase (GBA1),  $\alpha$ -galactosidase ( $\alpha$ GAL),  $\alpha$ -glucosidase (GAA),  $\alpha$ -fucosidase ( $\alpha$ FUC),  $\alpha$ -mannosidase ( $\alpha$ MAN),  $\beta$ -galactosidase ( $\beta$ GAL) and  $\beta$ -glucuronidase ( $\beta$ GLUR).

The ABP screening of urine samples from individuals not suffering from an inherited LSD may also be of potential interest. A pilot investigation was performed with urine samples of individuals with diabetes type II. It was observed that 3 out of 4 tested diabetic urines were deficient in GBA1 enzyme, based on 4MU activities and also ABP labelling. These preliminary observations should be substantiated by further studies. The preliminary observation is surprising since no link between GBA deficiency and diabetic nephropathy is reported in literature. Insulin insensitivity occurs in some Gaucher patients, but this not associated with any hyperglycemia or kidney failure as reflected by albuminuria (Langeveld et al. 2008). In view of the

findings with urine samples described above, it might be also of interest to study urine samples of individuals with Parkinson disease and Lewy Bodies regarding GBA1 enzyme deficiencies. Use of ABP urinary screenings for other disease conditions might provide clues to a not yet appreciated connection with lysosomal enzymes and impaired endolysosomal apparatus.

Another enzyme of interest to study in urine samples is heparanase (HPSE). The enzyme HPSE is responsible for the degradation of the polymer heparan sulfate (HS) into smaller oligosaccharides, present in both cell surface and the intracellular matrix. HPSE is an endo-retaining glycosidase cleaving HS moieties at internal sites of the polymeric chain. The increased activity of HPSE in blood tumour metastasis and also during tumour angiogenesis prompts the development of potent HPSE inhibitors to use as anti-cancer drugs (Shu and Santulli 2019). The enzyme is encoded by the *HPSE1* gene, and it is first synthesized as an inactive form of 65 kDa at the Golgi apparatus. From there it is destined into late endosomes, following its transport to lysosomes where it is proteolytic cleaved and activated into a heterodimer consisting of an 8 and 50 kDa molecules (Wu et al. 2015). The crystal structure of HPSE has been solved in 2015 (Wu et al. 2015). Recently, ABPs were developed to target the exo-glycosidase  $\beta$ -glucuronidase ( $\beta$ GLUR) (Wu et al. 2017). The developed ABP (JJB392) was able to label both HPSE and  $\beta$ GLUR enzymes found in human platelets and spleen. It is presently being studied with the methods developed along **chapter 7** whether HSPE levels can be studied in urine samples from diabetic and cancer patients.

A pilot investigation with JJB392 and different blood cell type lysates was performed. The same ABP was used to screen control urine samples. Both the precursor and mature HSPE could be visualized. The importance of monitoring HPSE in human urine is of great interest. Shafat et al. used a relatively insensitive ELISA type of assay to detect nanograms of active HPSE in urine of diabetic type II individuals (Shafat et al. 2011). This assay is no longer commercially available. Thus, there is a clear need for a reliable and sensitive method to measure HPSE levels in urine. We envision the use of urinary ABP screenings for monitoring HPSE levels of urines from diabetic and cancer patients. The assay might be optimized for screening large numbers of samples.

### **Concluding remarks**

This thesis deals with glycosidases used to treat lysosomal disorders caused by a deficiency in such enzymes. ABPs have proven to be valuable tools to identify glycosidases of interest cross species. Moreover, they assist detection of glycosidases and abnormalities in their levels in relation to disease. Newly identified plant glycosidases warrant further research regarding possible

therapeutic applications, a goal that drove this thesis work.

## References

- Aerts JMFG, Cox TM (2018) Roscoe O. Brady: Physician whose pioneering discoveries in lipid biochemistry revolutionized treatment and understanding of lysosomal diseases. *Blood Cells, Mol Dis* 68:4–8. doi: <https://doi.org/10.1016/j.bcmd.2016.10.030>
- Aerts JMFG, Ferraz MJ, Mirzaian M, et al (2017) Lysosomal Storage Diseases. For Better or Worse: Adapting to Defective Lysosomal Glycosphingolipid Breakdown. In eLS, John Wiley & Sons, Ltd (Ed.). doi:10.1002/9780470015902.a0027592
- Aerts JMFG, Groener JE, Kuiper S, et al (2008) Elevated globotriaosylsphingosine is a hallmark of Fabry disease. *Proc Natl Acad Sci* 105:2812–2817. doi: 10.1073/pnas.0712309105
- Aerts JMFG, Kallemeijn WW, Wegdam W, et al (2011) Biomarkers in the diagnosis of lysosomal storage disorders: proteins, lipids, and inhibitors. *J Inher Metab Dis* 34:605–619. doi: 10.1007/s10545-011-9308-6
- Aerts JMFG, Miranda MCS, de Lacerda LW, et al (1991) The identification of type 1 Gaucher disease patients, asymptomatic cases and carriers in The Netherlands using urine samples: An evaluation. *Clin Chim Acta* 203:349–361. doi: [https://doi.org/10.1016/0009-8981\(91\)90308-Y](https://doi.org/10.1016/0009-8981(91)90308-Y)
- Aerts JMFG, Schram A, Strijland A, et al (1988) Glucocerebrosidase, a lysosomal enzyme that does not undergo oligosaccharide phosphorylation. *Biochim Biophys Acta - Gen Subj* 964:303–308. doi: [https://doi.org/10.1016/0304-4165\(88\)90030-X](https://doi.org/10.1016/0304-4165(88)90030-X)
- Aerts JMFG, Yasothan U, Kirkpatrick P (2010) Velaglucerase alfa. *Nat Rev Drug Discov* 9:837–838. doi: 10.1038/nrd3311
- Aguilera-Correa J-J, Madrazo-Clemente P, Martínez-Cuesta MDC, et al (2019) Lyso-Gb3 modulates the gut microbiota and decreases butyrate production. *Sci Rep* 9:12010. doi: 10.1038/s41598-019-48426-4
- Arntzen C (2015) Plant-made pharmaceuticals: from “Edible Vaccines” to Ebola therapeutics. *Plant Biotechnol J* 13:1013–1016. doi: 10.1111/pbi.12460
- Artola M, Hedberg C, Rowland RJ, et al (2019)  $\alpha$ -d-Gal-cyclophellitol cyclosulfamidate is a Michaelis complex analog that stabilizes therapeutic lysosomal  $\alpha$ -galactosidase A in Fabry disease. *Chem Sci* 10:9233–9243. doi: 10.1039/C9SC03342D
- Artola M, Kuo C-L, McMahon SA, et al (2018) New Irreversible  $\alpha$ -l-Iduronidase Inhibitors and Activity-Based Probes. *Chemistry* 24:19081–19088. doi: 10.1002/chem.201804662
- Ben Bdira F, Artola M, Overkleeft HS, et al (2018) Distinguishing the differences in  $\beta$ -

- glycosylceramidase folds, dynamics, and actions informs therapeutic uses. *J Lipid Res* 59:2262–2276. doi: 10.1194/jlr.R086629
- Blom D, Speijer D, Linthorst GE, et al (2003) Recombinant Enzyme Therapy for Fabry Disease: Absence of Editing of Human  $\alpha$ -Galactosidase A mRNA. *Am J Hum Genet* 72:23–31. doi: <https://doi.org/10.1086/345309>
- Bosch D, Castilho A, Loos A, et al (2013) N-glycosylation of plant-produced recombinant proteins. *Curr Pharm Des* 19:5503–5512. doi: 10.2174/1381612811319310006
- Brady RO (2003a) Gaucher and Fabry diseases: from understanding pathophysiology to rational therapies. *Acta Paediatr* 92:19–24. doi: 10.1111/j.1651-2227.2003.tb00215.x
- Brady RO (2003b) Enzyme replacement therapy: conception, chaos and culmination. *Philos Trans R Soc Lond B Biol Sci* 358:915–919. doi: 10.1098/rstb.2003.1269
- Castilho A, Steinkellner H (2012) Glyco-engineering in plants to produce human-like N-glycan structures. *Biotechnol J* 7:1088–1098. doi: 10.1002/biot.201200032
- Choi H-Y, Park H, Hong JK, et al (2018) N-glycan Remodeling Using Mannosidase Inhibitors to Increase High-mannose Glycans on Acid  $\alpha$ -Glucosidase in Transgenic Rice Cell Cultures. *Sci Rep* 8:16130. doi: 10.1038/s41598-018-34438-z
- Choi L, Vernon J, Kopach O, et al (2015) The Fabry disease-associated lipid Lyso-Gb3 enhances voltage-gated calcium currents in sensory neurons and causes pain. *Neurosci Lett* 594:163–168. doi: 10.1016/j.neulet.2015.01.084
- Desai PN, Shrivastava N, Padh H (2010) Production of heterologous proteins in plants: Strategies for optimal expression. *Biotechnol Adv* 28:427–435. doi: <https://doi.org/10.1016/j.biotechadv.2010.01.005>
- Ferraz MJ, Kallemeijn WW, Mirzaian M, et al (2014) Gaucher disease and Fabry disease: New markers and insights in pathophysiology for two distinct glycosphingolipidoses. *Biochim Biophys Acta - Mol Cell Biol Lipids* 1841:811–825. doi: <https://doi.org/10.1016/j.bbalip.2013.11.004>
- Ganiats TG, Norcross WA, Halverson AL, et al (1994) Does Beano prevent gas? A double-blind crossover study of oral alpha-galactosidase to treat dietary oligosaccharide intolerance. *J Fam Pract* 39:441–445.
- Gaspar P, Kallemeijn WW, Strijland A, et al (2014) Action myoclonus-renal failure syndrome: diagnostic applications of activity-based probes and lipid analysis. *J Lipid Res* 55:138–145. doi:10.1194/jlr.M043802
- Geel TM, McLaughlin PMJ, de Leij LFMH, et al (2007) Pompe disease: Current state of treatment modalities and animal models. *Mol Genet Metab* 92:299–307. doi: <https://doi.org/10.1016/j.ymgme.2007.07.009>
- He X, Galpin JD, Tropak MB, et al (2011) Production of active human glucocerebrosidase in seeds of *Arabidopsis thaliana* complex-glycan-deficient (cgl) plants.


- Glycobiology 22:492–503. doi: 10.1093/glycob/cwr157
- Holida MD, Bernat J, Longo N, et al (2019) Once every 4 weeks - 2 mg/kg of pegunigalsidase alfa for treating Fabry disease Preliminary results of a phase 3 study. *Mol Genet Metab* 126:S73. doi: <https://doi.org/10.1016/j.ymgme.2018.12.176>
- Jiang J, Beenakker TJM, Kallemeijn WW, et al (2015a) Comparing Cyclophellitol N-Alkyl and N-Acyl Cyclophellitol Aziridines as Activity-Based Glycosidase Probes. *Chem – A Eur J* 21:10861–10869. doi: 10.1002/chem.201501313
- Jiang J, Kallemeijn WW, Wright DW, et al (2015b) In vitro and in vivo comparative and competitive activity-based protein profiling of GH29  $\alpha$ -l-fucosidases. *Chem Sci* 6:2782–2789. doi: 10.1039/C4SC03739A
- Jiang J, Kuo C-L, Wu L, et al (2016) Detection of Active Mammalian GH31  $\alpha$ -Glucosidases in Health and Disease Using In-Class, Broad-Spectrum Activity-Based Probes. *ACS Cent Sci* 2:351–358. doi: 10.1021/acscentsci.6b00057
- Kallemeijn WW, Li K-Y, Witte MD, et al (2012) Novel Activity-Based Probes for Broad-Spectrum Profiling of Retaining  $\beta$ -Exoglucosidases In Situ and In Vivo. *Angew Chemie Int Ed* 51:12529–12533. doi: 10.1002/anie.201207771
- Kytidou K, Beekwilder J, Artola M, et al (2018) *Nicotiana benthamiana*  $\alpha$ -galactosidase A1.1 can functionally complement human  $\alpha$ -galactosidase A deficiency associated with Fabry disease. *J Biol Chem* 293:10042–10058. doi: 10.1074/jbc.RA118.001774
- Kytidou K, Beenakker TJM, Westerhof LB, et al (2017) Human Alpha Galactosidases Transiently Produced in *Nicotiana benthamiana* Leaves: New Insights in Substrate Specificities with Relevance for Fabry Disease. *Front Plant Sci* 8:1026. doi: 10.3389/fpls.2017.01026
- Langeveld M, Ghauharali KJM, Sauerwein HP, et al (2008) Type I Gaucher Disease, a Glycosphingolipid Storage Disorder, Is Associated with Insulin Resistance. *J Clin Endocrinol Metab* 93:845–851. doi: 10.1210/jc.2007-1702
- Lenders M, Brand E (2018) Effects of Enzyme Replacement Therapy and Antidrug Antibodies in Patients with Fabry Disease. *J Am Soc Nephrol* 29:2265 LP – 2278. doi: 10.1681/ASN.2018030329
- Lettieri JT, Dain B (1998) Effects of Beano on the tolerability and pharmacodynamics of acarbose. *Clin Ther* 20:497–504. doi: [https://doi.org/10.1016/S0149-2918\(98\)80059-3](https://doi.org/10.1016/S0149-2918(98)80059-3)
- Levine B, Weisman S (2004) Enzyme Replacement as an Effective Treatment for the Common Symptoms of Complex Carbohydrate Intolerance. *Nutr Clin Care* 7:75–81.
- Liefhebber JMP, van der Zon T, Paerels L, et al (2019) Development of an AAV5-Based Gene Therapy for Fabry Disease. In: *Molecular Therapy*. Cell Press 50 Hampshire St, Floor 5, Cambridge, pp 442–443

- Linthorst GE, Hollak CEM, Donker-Koopman WE, et al (2004) Enzyme therapy for Fabry disease: Neutralizing antibodies toward agalsidase alpha and beta. *Kidney Int* 66:1589–1595. doi: <http://dx.doi.org/10.1111/j.1523-1755.2004.00924.x>
- Markham A (2016) Migalastat: First Global Approval. *Drugs* 76:1147–1152. doi: [10.1007/s40265-016-0607-y](https://doi.org/10.1007/s40265-016-0607-y)
- Marques ARA, Willems LI, Herrera Moro D, et al (2016) A Specific Activity-Based Probe to Monitor Family GH59 Galactosylceramidase, the Enzyme Deficient in Krabbe Disease. *ChemBioChem* 18:402–412. doi: [10.1002/cbic.201600561](https://doi.org/10.1002/cbic.201600561)
- Müntze J, Gensler D, Maniuc O, et al (2019) Oral Chaperone Therapy Migalastat for Treating Fabry Disease: Enzymatic Response and Serum Biomarker Changes After 1 Year. *Clin Pharmacol Ther* 105:1224–1233. doi: [10.1002/cpt.1321](https://doi.org/10.1002/cpt.1321)
- Priyanka P, Parsons TB, Miller A, et al (2016) Chemoenzymatic Synthesis of a Phosphorylated Glycoprotein. *Angew Chemie Int Ed* 55:5058–5061. doi: [10.1002/anie.201600817](https://doi.org/10.1002/anie.201600817)
- Reczek D, Schwake M, Schröder J, et al (2007) LIMP-2 Is a Receptor for Lysosomal Mannose-6-Phosphate-Independent Targeting of  $\beta$ -Glucocerebrosidase. *Cell* 131:770–783. doi: <https://doi.org/10.1016/j.cell.2007.10.018>
- Reuser AJJ, Van den Hout H, Bijvoet AGA, et al (2002) Enzyme therapy for Pompe disease: from science to industrial enterprise. *Eur J Pediatr* 161:S106–S111. doi: [10.1007/BF02680006](https://doi.org/10.1007/BF02680006)
- Riboldi MG, Di Fonzo BA (2019) GBA, Gaucher Disease, and Parkinson’s Disease: From Genetic to Clinic to New Therapeutic Approaches. *Cells* 8: 364. doi: <https://doi.org/10.3390/cells8040364>
- Rup B, Alon S, Amit-Cohen B-C, et al (2017) Immunogenicity of glycans on biotherapeutic drugs produced in plant expression systems—The taliglucerase alfa story. *PLoS One* 12:e0186211. doi: [10.1371/journal.pone.0186211](https://doi.org/10.1371/journal.pone.0186211)
- Sanchez-Niño MD, Carpio D, Sanz AB, et al (2015) Lyso-Gb3 activates Notch1 in human podocytes. *Hum Mol Genet* 24:5720–5732. doi: <https://doi.org/10.1093/hmg/ddv291>
- Schähs M, Strasser R, Stadlmann J, et al (2007) Production of a monoclonal antibody in plants with a humanized N-glycosylation pattern. *Plant Biotechnol J* 5:657–663. doi: [10.1111/j.1467-7652.2007.00273.x](https://doi.org/10.1111/j.1467-7652.2007.00273.x)
- Schiffmann R, Goker-Alpan O, Holida M, et al (2019) Pegunigalsidase alfa, a novel PEGylated enzyme replacement therapy for Fabry disease, provides sustained plasma concentrations and favorable pharmacodynamics: A 1-year Phase 1/2 clinical trial. *J Inher Metab Dis* 42:534–544. doi: [10.1002/jimd.12080](https://doi.org/10.1002/jimd.12080)
- Shaaltiel Y, Bartfeld D, Hashmueli S, et al (2007) Production of glucocerebrosidase with terminal mannose glycans for enzyme replacement therapy of Gaucher’s disease using a plant cell system. *Plant Biotechnol J* 5:579–590. doi: [10.1111/j.1467-7652.2007.00263.x](https://doi.org/10.1111/j.1467-7652.2007.00263.x)




- Shafat I, Ilan N, Zoabi S, et al (2011) Heparanase levels are elevated in the urine and plasma of type 2 diabetes patients and associate with blood glucose levels. *PLoS One*. doi: 10.1371/journal.pone.0017312
- Shu J, Santulli G (2019) Heparanase in health and disease: The neglected housekeeper of the cell? *Atherosclerosis* 283:124–126. doi: 10.1016/j.atherosclerosis.2019.01.017
- Storch S, Braulke T (2005) Transport of Lysosomal Enzymes BT - Lysosomes. In: Saftig P (ed). Springer US, Boston, MA, pp 17–26. doi: 10.1007/0-387-28957-7\_2
- Su J, Sherman A, Doerfler PA, et al (2015) Oral delivery of Acid Alpha Glucosidase epitopes expressed in plant chloroplasts suppresses antibody formation in treatment of Pompe mice. *Plant Biotechnol J* 13:1023–1032. doi: 10.1111/pbi.12413
- Sunder-Plassmann G, Schiffmann R, Nicholls K (2018) Migalastat for the treatment of Fabry disease. *Expert Opin Orphan Drugs* 6:301–309. doi: 10.1080/21678707.2018.1469978
- Tajima Y, Kawashima I, Tsukimura T, et al (2009) Use of a modified alpha-N-acetylgalactosaminidase in the development of enzyme replacement therapy for Fabry disease. *Am J Hum Genet* 85:569–580. doi: 10.1016/j.ajhg.2009.09.016
- Tomasic IB, Metcalf MC, Guce AI, et al (2010) Interconversion of the specificities of human lysosomal enzymes associated with Fabry and Schindler diseases. *J Biol Chem* 285:21560–21566. doi: 10.1074/jbc.M110.118588
- Tuttolomondo A, Pinto IS and A (2019) Gene Therapy of Anderson-Fabry Disease. *Curr Gene Ther*. 19:3–5. doi: 10.2174/1566523219999190415160632
- Willems LI, Beenakker TJM, Murray B, et al (2014) Potent and Selective Activity-Based Probes for GH27 Human Retaining  $\alpha$ -Galactosidases. *J Am Chem Soc* 136:11622–11625. doi: 10.1021/ja507040n
- Witte MD, Kallemeijn WW, Aten J, et al (2010) Ultrasensitive in situ visualization of active glucocerebrosidase molecules. *Nat Chem Biol* 6:907–913. doi: <https://doi.org/10.1038/nchembio.466>
- Wu L, Jiang J, Jin Y, et al (2017) Activity-based probes for functional interrogation of retaining  $\beta$ -glucuronidases. *Nat Chem Biol* 13:867–873. doi: 10.1038/nchembio.2395
- Wu L, Viola CM, Brzozowski AM, Davies GJ (2015) Structural characterization of human heparanase reveals insights into substrate recognition. *Nat Struct Mol Biol* 22:1016–1022. doi: 10.1038/nsmb.3136

Zhu X, Yin L, Theisen M, et al (2019) Systemic mRNA Therapy for the Treatment of Fabry Disease: Preclinical Studies in Wild-Type Mice, Fabry Mouse Model, and Wild-Type Non-human Primates. *Am J Hum Genet* 104:625–637. doi: <https://doi.org/10.1016/j.ajhg.2019.02.003>



**Summary**  
**Samenvatting**  
**Acknowledgements**  
**About the author**





# Summary

Lysosomal storage disorders (LSDs) are a group of over 50 discrete genetic metabolic diseases, each one caused by a deficiency in a lysosomal process. A large proportion of LSDs stems from defects in lysosomal hydrolases. One of the most common LSD is Gaucher disease, with incidence over 1 in 57000 births. It is caused by mutations in the *GBA* gene, resulting in deficient activity of glucocerebrosidase, the acid  $\beta$ -glucosidase responsible for the hydrolysis of the glycosphingolipid glucosylceramide (GlcCer) into ceramide and glucose. Fabry disease, an X-linked disorder also manifesting in female heterozygotes, is the most common LSD with an incidence of up to 1 in 3000 individuals. It is caused by deficiency of the lysosomal hydrolase  $\alpha$ -galactosidase A, which primarily cleaves terminal galactoses from globotriaosylceramide (Gb3), globotriaosylsphingosine (lysoGb3), galabiosylceramide, and blood group B, B1, and P1 antigens. Gaucher disease and Fabry disease are both multisystemic with symptoms manifesting in several organs. In Gaucher disease the enlargement of spleen and liver and hematological abnormalities are prominent whereas in Fabry disease kidney and heart are primarily affected. Both disorders show remarkable heterogeneity in nature and severity of symptoms among individual patients.

Enzyme replacement therapy (ERT) has been conceived and developed by Roscoe O. Brady as treatment for Gaucher disease and Fabry disease. ERT implies chronic, intravenous infusions of recombinant enzymes aiming to correct the deficiency in the patients. ERT is successful for treating visceral symptoms in Gaucher patients, but there are major limitations in clinical efficacy in the treatment of Fabry disease. Antibodies against the recombinant enzyme commonly develop in male Fabry patients completely lacking  $\alpha$ -galactosidase A protein. Furthermore, the presently used recombinant enzymes are intrinsically very unstable in human plasma. In this thesis, alternative recombinant enzymes for treatment of Fabry disease are discussed and special attention is paid to the potential use of plants as production platform and even as source of enzyme for treating lysosomal storage disorders.

Chapter 1 provides a general introduction and the scope of the investigations that were undertaken.

Chapter 2 describes the value of plant-derived glycoconjugates to beneficially modulate metabolism in man as well as the potential therapeutic value of plant glycosidases and the present production of therapeutic human glycosidases in plant platforms. Plants provide a convenient and highly profitable production platform of therapeutic lysosomal hydrolases. Successful

examples of this are Elelyso, produced in carrot cells for treatment of Gaucher disease, and Pegunigalsidase, produced in a tobacco cell line for treatment of Fabry disease. The recent use of smartly designed suicide inhibitors, so-called the activity-based probes (ABPs), as new tools to explore the plethora of retaining plant glucosidases is also discussed in chapter 2. Many applications of ABPs in plant science are underlined such as their use to follow metabolic processes in plants, the discovery of novel enzymes, and the identification of potential therapeutic inhibitors and chaperones.

In chapter 3, the transient production of human  $\alpha$ -galactosidases in *N. benthamiana* leaves is described. An alternative recombinant enzyme that might not suffer from antigenicity in Fabry patients is suggested. The enzyme is a modified version of the lysosomal  $\alpha$ -*N*-acetyl-galactosaminidase (NAGAL) with increased  $\alpha$ -galactosidase activity (NAGALEL). To study feasibility, in *N. benthamiana* leaves three functional lysosomal enzymes,  $\alpha$ GAL (human  $\alpha$ -galactosidase A), NAGAL and NAGALEL were transiently produced. All enzymes were produced efficiently in plant leaves, and were visualized with ABPs. In vitro studies revealed that the NAGALEL enzyme showed the desired increased activity towards 4MU- $\alpha$ -galactopyranoside substrate. Both NAGALEL and NAGAL enzymes were not neutralized by antibody-positive Fabry patient's serum, and they were significantly more stable in human plasma than  $\alpha$ GAL. Further, their ability to hydrolyse lipid substrates was tested using LS-MS/MS analysis. All enzymes were found able to degrade the lipid substrates Gb3 and lyso-Gb3 accumulating in Fabry patients. The activity towards the lipids was highest for  $\alpha$ GAL, followed by NAGALEL and finally NAGAL. It was observed that NAGALEL and to lesser extent NAGAL is able to reduce the toxic lyso-Gb3 in Fabry serum. Based on these findings, the use of NAGALEL, aiming at reduction of circulating lysoGb3, might be considered for treatment of Fabry.

In chapter 4, the identification of a novel  $\alpha$ -galactosidase from *N. benthamiana* is reported. Use of  $\alpha$ -galactose configured ABPs in *N. benthamiana* proteome resulted in the identification of a novel enzyme, named A1.1. The enzyme was found to be able to hydrolyse 4MU- $\alpha$ -galactopyranoside substrate with a comparable activity to human recombinant  $\alpha$ -galactosidase (Fabrazyme). The 3D structure of A1.1 was solved using X-ray crystallography, revealing remarkable similarities with human  $\alpha$ -galactosidases. This similarity likely explains A1.1's ability to hydrolyse Gb3 and lyso-Gb3, which are not endogenous lipids in plants. Interestingly, uptake of A1.1 by Fabry fibroblasts reduced the accumulated lipids Gb3 and lysoGb3 to normal levels. The delivery of the enzyme into cells was also studied via confocal microscopy. The easy production of A1.1 in plants, its stability over a broad pH range combined with

its capacity to degrade glycosphingolipids provides important advantages for use in ERT of Fabry disease.

In chapter 5, the challenging topic of stabilization of recombinant  $\alpha$ -galactosidases for ERT of Fabry disease is addressed. Due to the lability of recombinant enzyme preparations, a combined use of recombinant enzyme with active-site stabilizers is thought to improve the outcome of the treatment of LSDs. An already established pharmacological chaperone for  $\alpha$ -galactosidase A is 1-deoxygalactonojirimycin (Gal-DNJ, Migalastat®). Chapter 5, reports the use of newly synthesized  $\alpha$ -D-gal-cyclophellitol cyclosulfamidate 4 as a stabilizer of both human and plant derived  $\alpha$ -galactosidases. The results reveal that such stabilizers improve the stability of enzyme in human plasma and in Fabry fibroblasts. Therefore, such agents prompt great expectations for therapy of Fabry disease.

Chapter 6 reports investigations on the potential use of ABPs cross species. Studied were lysates from Bright Yellow tobacco cells (BY2) and the food supplement Beano containing a fungal (*A. niger*)  $\alpha$ -galactosidase.

The investigations with BY2 cell lysates led to the discovery of a plant  $\beta$ -glucosidase that is potently labeled by the  $\beta$ -glucose configured epoxide cyclophellitol ABP and its identity was next established by proteomics. The enzyme, here named B56, is active towards NBD-GlcCer lipid, revealing its potential use in therapy of Gaucher disease.

ABPs could be also successfully applied to label the  $\alpha$ -galactosidase from *A. niger* present in the food supplement Beano. The enzyme was found to be active towards artificial 4-methulumbelliferyl- $\alpha$ -galactoside but not towards NBD-Gb3. As Fabry patients suffer from intestinal complications, possibly induced by accumulating lysoGb3 in the intestine, future application of other  $\alpha$ GAL enzymes might be considered for diminishing such toxic agents.

In chapter 7, the potential use of ABPs for the diagnosis of LSDs is addressed. Described is a sensitive diagnostic method using cell lysates and urine samples. Seven different lysosomal hydrolases could be detected using the corresponding ABPs:  $\beta$ -glucosidase (GBA),  $\alpha$ -glucosidase (GAA),  $\alpha$ -galactosidase ( $\alpha$ GAL),  $\alpha$ -fucosidase ( $\alpha$ FUC),  $\beta$ -galactosidase ( $\beta$ GAL),  $\beta$ -glucuronidase( $\beta$ GLUR) and  $\alpha$ -mannosidase ( $\alpha$ MAN). As urine is a convenient source of lysosomal enzymes, its use in diagnosis of the diseases is proposed. A proof-of-concept for diagnostic application of ABPs is presented.

In chapter 8 the studies described in the thesis are discussed and perspectives for future research are presented.

# Samenvatting

Lysosomale stapelingsziekten (LSDs) vormen een groep van 50 discrete erfelijke stofwisselingsziekten die elk veroorzaakt worden door een specifiek defect in een lysosomaal proces. Een belangrijk deel van de LSDs betreft defecten in lysosomale hydrolasen. Een van de meest voorkomend LSDs is de ziekte van Gaucher, met een incidentie van 1 op 57.000 geboortes. Deze ziekte wordt veroorzaakt door mutaties in het *GBA* gen, resulterend in een deficiënte activiteit van glucocerebrosidase, het zure acid  $\beta$ -glucosidase dat zorg draagt voor de hydrolyse van het glycosfingolipide glucosylceramide (GlcCer) tot ceramide en glucose. De ziekte van Fabry, een X-gebonden afwijking die zich ook manifesteert in vrouwelijke heterozygoten, is de meest frequente LSD met een incidentie oplopend tot 1 in 3000 individuen. Deze aandoening wordt veroorzaakt door deficiëntie van het lysosomale  $\alpha$ -galactosidase A, een enzym dat terminale galactoses afsplitst van globotriaosylceramide (Gb3), globotriaosylsphingosine (lysoGb3), galabiosylceramide, en bloed groep B, B1, en P1 antigenen. De ziekte van Gaucher en de ziekte van Fabry zijn multi-systemisch met symptomen in verschillende organen. Bij de ziekte van Gaucher zijn vergroting van milt en lever en hematologisch afwijkingen prominent, terwijl bij de ziekte van Fabry de nier en het hart ernstig worden aangetast. Beide ziektebeelden vertonen opmerkelijke heterogeniteit in aard en ernst van symptomen bij individuele patiënten.

Enzyme replacement therapy (enzym vervangingstherapie; ERT) is bedacht en ontwikkeld door Roscoe O. Brady ter behandeling van de ziekte van Gaucher en de ziekte van Fabry. ERT impliceert herhaalde, intraveneuze infusies van recombinante enzymen met als doel het tekort hierin bij patiënten te corrigeren. ERT is zeer effectief bij de behandeling van viscerale symptomen van Gaucher patiënten, maar in veel mindere mate als behandeling voor de ziekte van Fabry. Antilichamen tegen het toegediende recombinante therapeutische enzym ontwikkelen zich doorgaans bij mannelijke Fabry patiënten zonder eigen  $\alpha$ -galactosidase A eiwit. Bovendien zijn de huidige therapeutische enzymen relatief instabiel in menselijk plasma. In dit proefschrift worden alternatieve recombinant enzymen voor de behandeling van de ziekte van Fabry beschreven. In het bijzonder wordt aandacht besteed aan het gebruik van planten als productieplatform als ook het gebruik van plant eigen enzymen voor de behandeling van lysosomale stapelingsziekten.

Hoofdstuk 1 behelst een algemene introductie en beschrijft de scope van het uitgevoerde onderzoek.



Hoofdstuk 2 beschrijft de waarde van plantaardige glycoconjugaten om het metabolisme bij te sturen. Hiernaast wordt aandacht gevestigd op de potentiële therapeutische betekenis van plantaardige glucosidasen als ook de productie van therapeutische recombinante enzymen in plant platformen. Succesvolle voorbeelden hiervan zijn Elelyso, geproduceerd in wortel cellen voor de behandeling van de ziekte van Gaucher en Pegunigalsidase, geproduceerd in een tabak cellijn voor de behandeling van de ziekte van Fabry. In het hoofdstuk worden ook beschreven activity-based probes (ABPs) waarmee retaining plant glucosidasen van planten bestudeerd kunnen worden. Diverse toepassingen voor ABPs in plant science worden bediscussieerd zoals het gebruik bij fundamenteel onderzoek aan plant metabolisme, de ontdekking van nieuwe enzymen en de identificatie van potentiële therapeutische remmers en chaperones.

In hoofdstuk 3 wordt de productie van menselijke  $\alpha$ -galactosidasen in *N. benthamiana* bladeren beschreven. Een alternatief recombinant enzym dat wellicht niet antigeen is wordt overwogen voor behandeling van de ziekte van Fabry. Het betreft een gemodificeerd lysosomaal  $\alpha$ -*N*-acetyl-galactosaminidase (NAGAL) met een verhoogde  $\alpha$ -galactosidase activiteit (NAGALEL). Om de haalbaarheid hiervan te bestuderen werden in *N. benthamiana* bladeren drie lysosomale enzymen,  $\alpha$ GAL (human  $\alpha$ -galactosidase A), NAGAL en NAGALEL geproduceerd. Alle enzymen, elk reagerend met ABP, konden met hoge opbrengst verkregen worden. In vitro studies toonden aan dat het recombinante NAGALEL enzym actief was ten opzichte van 4MU- $\alpha$ -galactopyranoside substraat. Zowel het NAGAEL als NAGAL enzym reageerde niet met neutraliserend Fabry patiënt serum. De verkregen enzymen waren significant stabiel in menselijk plasma dan  $\alpha$ GAL. Zoals gemeten met LS-MS/MS analysis, alle enzymen waren staat tot afbraak van de lipide substraten Gb3 en lyso-Gb3 die ophopen bij de ziekte van Fabry. De activiteit was het hoogst bij  $\alpha$ GAL, gevolgd door NAGALEL en tot slot NAGAL. NAGAEL en in mindere mate NAGAL bleken ook in staat het toxische lyso-Gb3 in Fabry serum af te breken. Op basis van deze bevindingen zou een gebruik van NAGALEL, met als doel circulerend lysoGb3 te verlagen, overwogen kunnen worden voor een behandeling van Fabry patiënten.

Hoofdstuk 4 beschrijft de ontdekking van een nieuw  $\alpha$ -galactosidase uit *N. benthamiana*. Met een  $\alpha$ -galactose geconfigureerd ABP werd in het proteoom van *N. benthamiana* bladeren dit enzym, genaamd A1.1, geïdentificeerd. A1.1 kan 4MU- $\alpha$ -galactopyranoside hydrolyseren met vergelijkbare activiteit aan recombinant menselijk  $\alpha$ -galactosidase (Fabrazyme). De 3D structuur van A1.1, zoals vastgesteld met X-ray kristallografie, wijst op grote overeenkomsten met menselijke  $\alpha$ -galactosidasen. Dit verklaart wellicht waarom A1.1 uitstekend in

staat is Gb3 en lyso-Gb3 te splitsen, terwijl dit geen endogene lipiden van planten zijn. De opname van A1.1 door Fabry fibroblasten leidt tot een afname van het opgehoopte Gb3 en lysoGb3. Opname van enzym door cellen kon worden bevestigd met behulp van confocal microscopy. Het gemak van de productie van A1.1 in planten, de stabiliteit van het enzym bij verschillende pH's, en het vermogen om relevante glycosfingolipiden af te breken maakt dit enzym een interessante kandidaat voor een therapie van de ziekte van Fabry.

In hoofdstuk 5 staat stabilisering van recombinant  $\alpha$ -galactosidasen centraal. Vanwege de labiliteit van recombinante enzymen wordt het gecombineerde gebruik van enzym met een active-site stabilizer overwogen. Een reeds geregistreerd 'pharmacological chaperone' voor  $\alpha$ -galactosidase A is 1-deoxygalactonojirimycin (Gal-DNJ, Migalastat®). Hoofdstuk 5 beschrijft een  $\alpha$ -D-gal-cyclophellitol cyclosulfamidate als stabilizer van menselijk en plantaardige  $\alpha$ -galactosidasen. Deze verbinding vergroot inderdaad de enzym stabiliteit in plasma en Fabry fibroblasten.

Hoofdstuk 6 beschrijft onderzoek aan het gebruik van ABPs cross species. Bestudeerd werden hiermee enzymen in lysaten van Bright Yellow tobacco cellen (BY2) en het voedingssupplement Beano welk een fungaal (*A. niger*)  $\alpha$ -galactosidase bevat.

Het onderzoek met BY2 cel-lysaten heeft geleid tot de ontdekking van een plant  $\beta$ -glucosidase dat gelabeld kan worden met een  $\beta$ -glucose geconfigureerd epoxide cyclophellitol ABP en waarvan de identiteit vervolgens met behulp van proteomics werd vastgesteld. Het enzym, vernoemd B56, splitst met hoge affiniteit NBD-GlcCer lipide, waardoor een mogelijk therapeutische toepassing voor de ziekte van Gaucher niet valt uit te sluiten.

Beschikbare ABPs kunnen ook het  $\alpha$ -galactosidase van *A. niger* in het voedingssupplement Beano labelen. Het enzym bleek actief ten opzichte van het artificiële substraat 4-methylumbelliferyl- $\alpha$ -galactoside maar niet NBD-Gb3. Fabry patiënten kunnen darmklachten ontwikkelen die wellicht veroorzaakt worden door lokaal excessief lysoGb3. Een behandeling hiervan met een geschikt  $\alpha$ GAL enzym zou overwogen kunnen worden.

In hoofdstuk7 wordt de potentiële toepassing van ABPs in de diagnostiek van LSDs behandeld. Beschreven wordt een sensitieve diagnostische methode die gebruik maakt van cel-lysaten en urinemonsters. Zeven verschillende lysosomale hydrolasen konden gedetecteerd worden met corresponderende ABPs:  $\beta$ -glucosidase (GBA),  $\alpha$ -glucosidase (GAA),  $\alpha$ -galactosidase ( $\alpha$ GAL),  $\alpha$ -fucosidase ( $\alpha$ FUC),  $\beta$ -galactosidase ( $\beta$ GAL),  $\beta$ -glucuronidase ( $\beta$ GLUR) en  $\alpha$ -mannosidase ( $\alpha$ MAN). Aangezien urine een gemakkelijk verkrijgbare bron aan lysosomale enzymen is, wordt mogelijke diagnostiek hiermee beschreven. Een proof-of-concept voor de diagnostische toepassing van ABPs wordt gepresenteerd.

In hoofdstuk 8 worden de in dit proefschrift beschreven studies bediscussieerd en wordt toekomstig onderzoek voorgesteld.

# Acknowledgements

I have so many people to thank for completing this work. First, I am grateful to my supervisor Hans Aerts. Hans, your precious guidance, valuable feedback and inspiration have shown me the true meaning of the word ‘professor’. A special thanks also to my family, friends and colleagues, who’s tremendous (moral) support, encouragement and unconditional love I will always cherish. Some claim that poets can express everything through their art. Thus, I would like to dedicate the poem Ithaka, written by a (non-ancient) Greek poet, Konstantinos P. Kavafis in 1911, to everyone that supported and helped me over this PhD “journey”.

## Ithaka

As you set out for Ithaka  
hope your road is a long one,  
full of adventure, full of discovery.  
Laistrygonians, Cyclops, angry Poseidon—don’t be afraid of them:  
you’ll never find things like that on your way  
as long as you keep your thoughts raised high,  
as long as a rare excitement  
stirs your spirit and your body. ...  
.... Hope your road is a long one.  
May there be many summer mornings when,  
with what pleasure, what joy,  
you enter harbours you’re seeing for the first time. ...  
.... and may you visit many Egyptian cities  
to learn and go on learning from their scholars.  
Keep Ithaka always in your mind.  
Arriving there is what you’re destined for.  
But don’t hurry the journey at all.  
Better if it lasts for years,

so, you're old by the time you reach the island,  
wealthy with all you've gained on the way,  
not expecting Ithaka to make you rich.  
Ithaka gave you the marvellous journey.  
Without her you wouldn't have set out.  
She has nothing left to give you now.  
And if you find her poor, Ithaka won't have fooled you.  
Wise as you will have become, so full of experience,  
you'll have understood by then what these Ithakas mean.

(Translation:  
Edmund Keeley)

*Στην μαμά μου και δασκάλα μου, Μαρία, που μου έμαθε να διαβάζω και να αγαπώ τα γράμματα και την ποίηση. Στον μπαμπά μου, Γιάννη, που μου έμαθε πάντα να κοιτώ την λεπτομέρεια σε ό,τι κάνω. Στον αδερφό μου, Γιώργο, που μου έμαθε πόσο εύκολο είναι να χαμογελάς. Στον άντρα μου, Δημήτρη, που μου έμαθε να βλέπω και από άλλες οπτικές γωνίες. Στον γιο μου, Φοίβο, που μου έμαθε τον ήχο που έχει η αγάπη. Σας ευχαριστώ, εσείς μου δείχνετε τον δρόμο.*

*Κασσιανή Κυτίδου  
Μάιος 2020*

# Curriculum Vitae

|              |   |
|--------------|---|
| 1 March 1989 | Born in Thessaloniki, Greece  |
| 2003-2006    | 3 <sup>rd</sup> General Lyceum of Thessaloniki, Greece  |
| 2006-2011    | Bachelor of Science, Molecular Biology and Genetics.<br>Dimokrition University of Thrace, Alexandroupolis, Greece                             |
| 2012-2014    | Master of Science, Plant biotechnology. Specialization plants for human health.<br>Wageningen University and Research center, the Netherlands |
| 2014-2019    | Doctor of Philosophy, Medical biochemistry.<br>Leiden University, the Netherlands   |
| 2020-Present | Junior Scientist, Adeno-associated-virus vector development.<br>Arthrogen/ MeiraGtx B.V, Amsterdam, the Netherlands                           |

# Publications

**Kytidou K.**, Beekwilder J., Artola M., Meel E. van, Wilbers R.H.P., Moolenaar G.F., Goosen N., Ferraz M.J., Katzy R., Voskamp P., Florea B.I., Hokke C.H., Overkleeft H.S., Schots A., Bosch D., Pannu N. & Aerts J.M.F.G. (2018), *Nicotiana benthamiana*  $\alpha$ -galactosidase A1.1 can functionally complement human  $\alpha$ -galactosidase A deficiency associated with Fabry disease, *Journal of Biological Chemistry* 293(26): 10042-10058.

**Kytidou K.**, Beenakker T.J.M., Westerhof L.B., Hokke C.H., Moolenaar G.F., Goosen N., Mirzaian M., Guimaraes Da Lomba Ferraz M.J., Geus M.A.R. de, Kallemeijn W.W., Overkleeft H.S., Boot R.G., Schots A., Bosch D. & Aerts J.M.F.G. (2017), Human Alpha Galactosidases Transiently Produced in *Nicotiana benthamiana* Leaves: New Insights in Substrate Specificities with Relevance for Fabry Disease, *Frontiers in Plant Science* 8: 1026.

**Kytidou K.**, Artola M., Overkleeft, H.S., & Aerts J.M.F.G. (2020), Plant Glycosides and Glycosidases: A Treasure-Trove for Therapeutics, *Frontiers in Plant Science*, 11: 357.

Kuo C.L., Meel H.M.M. van, **Kytidou K.**, Kallemeijn W.W., Witte M., Overkleeft H.S., Artola Pérez de Azanza M.E. & Aerts J.M.F.G. (2018), Activity-Based Probes for Glycosidases: Profiling and Other Applications. In: Imperiali B. (Ed.) *Chemical Glycobiology Part B. Monitoring Glycans and their Interactions. Methods in Enzymology* no. 598: Elsevier: Monograph Series. 217-235.

Artola M., Hedberg C., Rowland R.J., Raich L., **Kytidou K.**, Wu L., Schaaf A., Ferraz M.J., Marel G.A. van der, Codee J.D.C., Rovira C., Aerts J.M.F.G., Davies G.J. & Overkleeft H.S. (2019), Alpha-d-Gal-cyclophellitol cyclosulfamidate is a Michaelis complex analog that stabilizes therapeutic lysosomal alpha-galactosidase A in Fabry disease, *Chemical Science* 10(40): 9233-9243.

Aerts J.M.F.G., Guimaraes Da Lomba Ferraz M.J., Mirzaian M., Gaspar P., Oussoren S.V., Wisse P., Kuo C.L., Lelieveld L.T., **Kytidou K.**, Hazeu M.D., Boer D.E.C., Meijer R., Lienden M.J.C. van der, Herrera D., Gabriel T.L., Aten J., Overkleeft H.S., Eijk M.C. van, Boot R.G. & Rosa Alcalde Marques A. (2017), Lysosomal Storage Diseases. For Better or Worse: Adapting to Defective Lysosomal Glycosphingolipid Breakdown. In: eLS. eLS: John Wiley & Sons, Ltd.. 1-13.

Mirzaian M., Wisse P., Guimaraes da Lomba Ferraz M.J., Marques A.R., Gaspar P., Oussoren S.V., **Kytidou K.**, Codee J.D.C., Marel G.A. van der, Overkleeft H.S. & Aerts J.M.F.G. (2017), Simultaneous quantitation of sphingoid bases by UPLC-ESI-MS/MS with identical C-13-encoded internal standards, *Clinica Chimica Acta* 466: 178-184.

**Kytidou K.**, Denysiuk I., Kuo C.L., Artola M., Overkleeft H.S., Aerts J.M.F.G. Diagnosis with activity-based probes of inherited glycosidase deficiencies using urine samples. *To be submitted.*

**Kytidou K.**, Katzy R., Meel H.M.M., Voskamp P., Boot R.G., Aerts J.M.F.G. A novel  $\beta$ -glucosidase from BY2 nicotiana tobacco cell cultures with glucosylceramide hydrolytic activity. *In preparation.*